APPENDIX 9.5-A

Roberts Bank Terminal 2 Technical Report, Coastal Geomorphology Study

This page is intentionally left blank

nhc
northwest hydraulic consultants

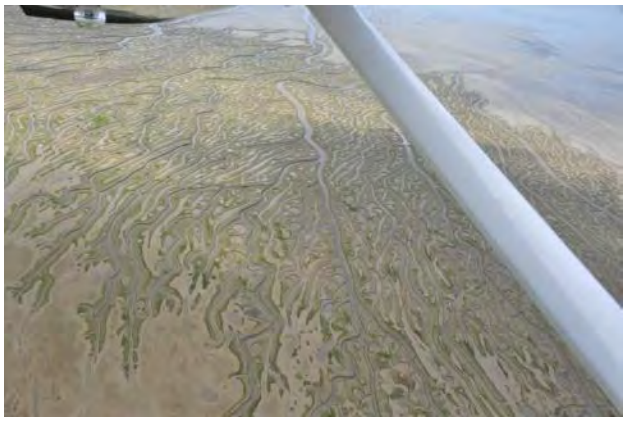

PROPOSED ROBERTS BANK TERMINAL 2
TECHNICAL REPORT
COASTAL GEOMORPHOLOGY STUDY

FINAL REPORT

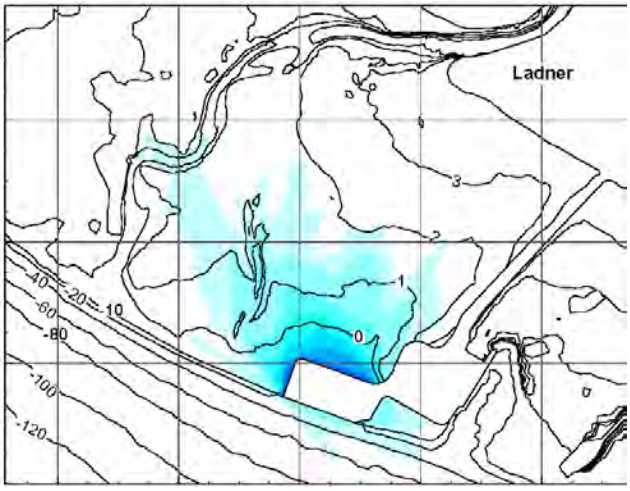

Prepared for:

PORT METRO vancouver

Port Metro Vancouver
100 The Pointe, 999 Canada Place
Vancouver, BC V6C 3T4

Prepared by:
NORTHWEST HYDRAULIC CONSULTANTS LTD.
30 Gostick Place
North Vancouver, BC V7M 3G3

March 2014
NHC 300044

TECHNICAL REPORT/TECHNICAL DATA REPORT DISCLAIMER

The Canadian Environmental Assessment Agency determined the scope of the proposed Roberts Bank Terminal 2 Project (RBT2 or the Project) and the scope of the assessment in the Final Environmental Impact Statement Guidelines (EISG) issued January 7, 2014. The scope of the Project includes the project components and physical activities to be considered in the environmental assessment. The scope of the assessment includes the factors to be considered and the scope of those factors. The Environmental Impact Statement (EIS) has been prepared in accordance with the scope of the Project and the scope of the assessment specified in the EISG. For each component of the natural or human environment considered in the EIS, the geographic scope of the assessment depends on the extent of potential effects.

At the time supporting technical studies were initiated in 2011, with the objective of ensuring adequate information would be available to inform the environmental assessment of the Project, neither the scope of the Project nor the scope of the assessment had been determined.

Therefore, the scope of supporting studies may include physical activities that are not included in the scope of the Project as determined by the Agency. Similarly, the scope of supporting studies may also include spatial areas that are not expected to be affected by the Project.

This out-of-scope information is included in the Technical Report (TR)/Technical Data Report (TDR) for each study, but may not be considered in the assessment of potential effects of the Project unless relevant for understanding the context of those effects or to assessing potential cumulative effects.

AUTHORSHIP

Report prepared by:

Derek Ray, P.Geo.
Project Manager

Edwin Wang, P.Eng.
Coastal Engineer

Charlene Menezes, P.Geo.
Geomorphologist

Apppendix D prepared by:

José Vasquez, Ph.D., P.Eng.
Senior Hydrotechnical Engineer

Joanna Glawdel, M.A.Sc., P.Eng.
Hydrotechnical Engineer

Jeffery Van Tol, E.I.T.
Water Resources Engineer

Contributing authors:

André Zimmermann, Ph.D., P.Geo – Senior Geomorphologist
Vanessa O'Connor, P.Eng. – Hydrotechnical Engineer
José Vasquez, Ph.D., P.Eng. – Senior Hydrotechnical Engineer
Sarah North, GISP – Senior GIS Analyst
Dave McLean, Ph.D., P.Eng. – Technical Editor/Reviewer

DISCLAIMER

ACKNOWLEDGEMENTS

Northwest Hydraulic Consultants Ltd. is pleased to be part of the team of professionals conducting an evaluation of environmental changes related to the Roberts Bank Terminal 2 Project. Acting as lead environmental consultant, Hemmera personnel have provided direction and support to the Coastal Geomorphology Study that was conducted by NHC. In particular, we would like to acknowledge the roles of the following people:

- Ben Wheeler – Marine Technical Director
- Ian Ponsford – Project Manager
- Pamela O'Hara – Project Manager
- Doug Bright – Technical Integration Specialist
- Carson Keever – Technical Integration Specialist
- Marina Winterbottom – Marine Invertebrate Discipline Lead
- David Gibson – Fieldwork Coordinator

We have also had the pleasure of working with members of the WorleyParsons team, the lead engineering firm, as well as providing input to the environment team. We particularly wish to acknowledge the collaborative assistance of the following:

- K. Peter Geldreich, P.Eng. – RBT2 Project Manager

EXECUTIVE SUMMARY

The Roberts Bank Terminal 2 Project (RBT2) is a proposed new three-berth container terminal that is planned to be constructed on the northwest side of the existing Roberts Bank terminals. The terminal expansion project is situated on the intertidal sand flats of Roberts Bank in the Fraser River delta. The purpose of the Coastal Geomorphology Study is to describe the changes from RBT2 on the physical landforms and coastal processes in the study area. Three methods were used to assess the physical response to the Project:

1. interpretive geomorphic studies using historical data, site observations and measurements;
2. analytical computations; and
3. numerical modelling of waves, tidal currents and sediment transport.

This coastal geomorphology study technical report and its four technical appendices summarize the physical landforms in the region, the driving forces that govern their formation and the past trends and anticipated future evolution that is expected without the Project. The main volume also summarizes results of comprehensive numerical modelling, using the TELEMAC modelling system, that was undertaken to assess the changes from the Project on tidal currents, salinity, wave climate and sedimentation patterns. The geomorphic studies and model results were interpreted to assess the post-construction changes from the Project on the coastal landforms and coastal processes. The technical appendices provide detailed information on the data sources that were utilized, the field investigations that were carried out and the numerical model studies, including its input data, schematization, calibration and validation.

The physical setting was characterized in terms of biosedimentological zones on Roberts Bank, including the existing sea dykes and causeway (anthropogenic deposits), intertidal marsh, biomat, tidal flats and delta foreslope. Ridge and runnel features, colloquially referred to as the 'mumblies', are located in the biomat zone and characterized by deep dissection of the ridge surface by the runnel channels. They are present on the upper mudflats on both sides of the Deltaport causeway as well as in Boundary Bay and play an important role in modifying patterns of tidal inundation and

emergence of the portions of Roberts Bank that have been identified as having the highest concentration of biofilm.

Sediment sampling and dating using lead (^{210}Pb) and Cesium (^{137}Cs) isotope techniques indicated the ridge and runnel complexes in the upper sections of the tidal flats are accreting on both the north and south sides of the causeway. In the absence of sea-level rise and land subsidence, the ridges associated with the ridge and runnel complexes may attain accretion rates on the order of 1 cm/year as vegetation continues to establish. The low-lying zones adjacent to the ridge and runnel complexes that have a high density of biofilm, especially those that are located inland, are also anticipated to increase in relative elevation and be colonized by vegetation communities.

The sediment supply to the southern Roberts Bank tidal flats is limited mainly to fine suspended load (silt and clay) sediments from the Fraser River plume. The amount of sand-sized sediment supplied to the flats from Canoe Passage is low. Based on the available historic data, the intertidal sand flats undergo periodic scour and fill but show no obvious trend of lowering or infilling over time.

The TELEMAC modelling system utilized in the study included three components:

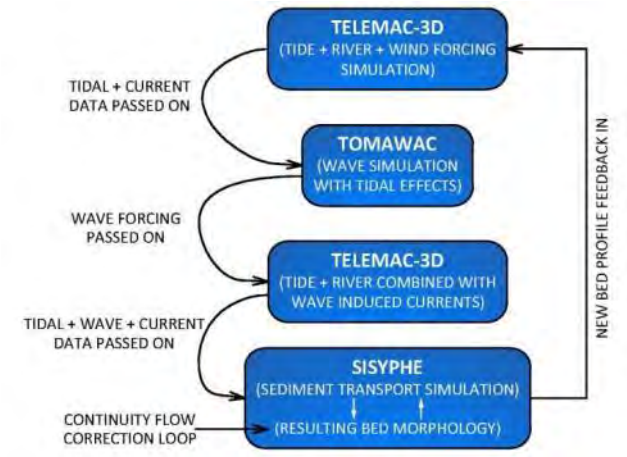

- TELEMAC-3D – A three-dimensional hydrodynamic model that solves the time-dependent Navier-Stokes equations with an evolving free surface, under the assumption of hydrostatic or non-hydrostatic pressure distribution using the finite element method.
- TOMAWAC – TOMAWAC is a third generation spectral wave model that simulates wave propagation in the coastal zone based on solving the wave action density balance equation. The model accounts for the effect of wave generation by wind, white-capping, nonlinear wave-wave interaction, refraction, shoaling and dissipation.
- SISYPHE – A sediment transport and morphodynamic model that computes separately bed-load and suspended load, and the resulting bed changes using the Exner equation.

TELEMAC-3D uses boundary conditions (Fraser River discharges plus tide levels in the Juan de Fuca Strait near Port Renfrew and Hornby Island) to compute the tidal currents (velocity and depth) around RBT2. TOMAWAC uses wind data to simulate the wave propagation and compute the significant wave height. This wave information is passed into TELEMAC-3D to incorporate its effects on the flow circulation. Local bed changes (scour and deposition) around RBT2 were computed by coupling the sediment transport and morphodynamic model SISYPHE to TELEMAC-3D and

TOMAWAC. SISYPHE uses the tide and wave information from the other two models to compute scour and deposition of the seabed. The new bed elevation computed by SISYPHE is fed back into TELEMAC-3D to re-compute the flow hydrodynamics.

Tidal currents and waves were simulated for three-month summer and winter periods using input data from 2012. The morphodynamic model was run for 1,440 model days to estimate the long-term response to the Project. The figure below summarizes the estimated physical changes from the Project based on the interpretation of the modelling results and the other geomorphic studies.

A scour zone (Zone 1) is expected to develop near the northwest edge of the proposed terminal structure due to flow acceleration around the west side of the terminal pad. General lowering in bed elevation in the primary scour zone is predicted to be approximately 0.5 m and the maximum scour elevation is expected to be to a depth of approximately -2.6 m CD, or 1.6 m below the surrounding seabed level. Eroded sediment from the scour zone will be deposited on the west side of the structure (Zone 2). The general rise in bed level in this zone was estimated to be approximately 1.0 m.

The flow acceleration and bed scour at the northwest corner is expected to increase flow exchange in a relict tidal channel (formerly draining a portion of Canoe Passage) west of the terminal (Zone 3).

Modelling of tidal currents predicted an increase in current velocity at the seaward end of the channel with the Project in place, and the morphodynamic model results indicate general bed accretion in this zone adjacent to the higher-velocity channel. Based on observation of similar channels elsewhere in the Fraser River estuary, the channel response to the accretion is expected to migrate laterally near the mouth and downcut through the accumulating sediments in order to meet base level. This channel is expected to become more active, experiencing higher flood-tide velocities, channel widening, and lateral shifting. It is unlikely that severe headcutting will be induced at the head of the channel.

The proposed terminal is predicted to locally reduce tidal currents (Zone 4) and create a local wave shadow (Zone 5) on its north side, particularly where it meets the existing terminal pad. These areas are expected to experience increased deposition of fine sediment that is currently carried in suspension (mainly silt). Nonetheless, sedimentation rates are expected to be low.

It is expected that the Project will also affect the energy and salinity environment on Roberts Bank north of the causeway (Zone 7). The proposed terminal pad will interrupt the landward movement of saline water during rising tides, causing the flow to be deflected further to the northwest. This will increase the residence time of lower salinity Fraser River water in the region shoreward of the terminal pad and immediately adjacent to the causeway. In addition, the proposed terminal configuration is predicted to modify the movement of the Fraser River plume over the tidal flats, directing more turbid water along the western end of the widened causeway. This will promote fine sediment (silt) deposition on the sand flats in and a corresponding increase in bed elevation over time near the western end of the causeway. With time, the increase in sediment accretion rates in low energy environments may enable biofilm and marsh communities to become established in a manner similar to what has been observed along the shoreline following construction of Roberts Bank causeway. The relative timing of such changes, however, is likely to be longer than observed in the higher intertidal areas south of Brunswick Point, as a result of the lower elevation of the initial bed surface in most of this area.

The ridge and runnel complex is located further from the proposed structure and will be relatively unaffected by the terminal structure. While the wind and current environment is not anticipated to be affected, the salinity may be slightly reduced and the turbidity may be slightly increased. This could result in an increased sedimentation rate within the ridge and runnel complex.

The Project is not anticipated to affect the morphology of the marsh areas, with the exception of the areas directly lost due to the widening of the causeway. Tidal currents and wave heights are small before and after the Project. Any changes in salinity that may occur are likely to be indistinguishable from the ongoing changes associated with the continued growth of Brunswick Point, accretion of the ridge and runnels and ongoing changes in the course of Canoe Passage.

The change from the expanded tug basin component of the Project (Zone 8) includes a lateral expansion to the existing pour-over channel. Formation of additional tidal channels or acceleration

in growth of existing channels is not anticipated. The expansion area will encompass an area to the immediate northwest that presently only partially drains during the higher-magnitude ebb tide events.

TABLE OF CONTENTS

LIST OF TABLES

LIST OF FIGURES

LIST OF APPENDICES

1 INTRODUCTION

1.1 PROJECT BACKGROUND

The Roberts Bank Terminal 2 Project (RBT2 or Project) is a proposed new three-berth container terminal which would provide 2.4 million TEUs (twenty-foot equivalent unit containers) of additional container shipping capacity annually. The Project is part of the Container Capacity Improvement Program (CCIP), Port Metro Vancouver's long-term strategy to deliver projects to meet anticipated growth and demand for container capacity until 2030.

Port Metro Vancouver retained Hemmera to undertake environmental studies related to the Project. This technical report describes the results of the Coastal Geomorphology Study undertaken by Northwest Hydraulic Consultants Ltd. (NHC).

1.2 SCOPE OF WORK

The purpose of the Coastal Geomorphology Study is to describe the potential changes that the proposed Project may have on the geomorphology of the study area – that is, the physical environment as well as the coastal processes that have formed, and continue to form, the physical features.

The study has been conducted at various spatial and temporal scales, ranging from the investigation of short-term changes in sediment deposition and erosion on the tidal flats at discrete locations, to consideration of landscape-scale evolution over several hundreds to thousands of years. For the purposes of the EA, the study area has been defined at two scales:

1. The local study area (LSA) includes the Roberts Bank tidal flats extending from the seaward side of the flood protection dykes along the foreshore to -60 m Chart Datum (CD) depth, and extending from the BC Ferries terminal and causeway to Canoe Passage (**Figure 1**). It represents the maximum extent of the likely zone of influence of the Project based on alterations in physical processes that are the key determinants of geomorphology.
2. The numerical model extends over a larger area in order to establish the boundary conditions, as shown in **Figure 2**, to allow for the incorporation of flow discharges from the Fraser River plus tidal and wind information in the Strait of Juan de Fuca and the Strait of Georgia.

The project components that were considered in this study include the marine terminal, the widened causeway and the expanded tug basin. Changes related to the Interim Transfer Pit, both during the construction and operations phases, are investigated by others.

Figure 1: The spatial extents of the local study area of the Coastal Geomorphology Study.

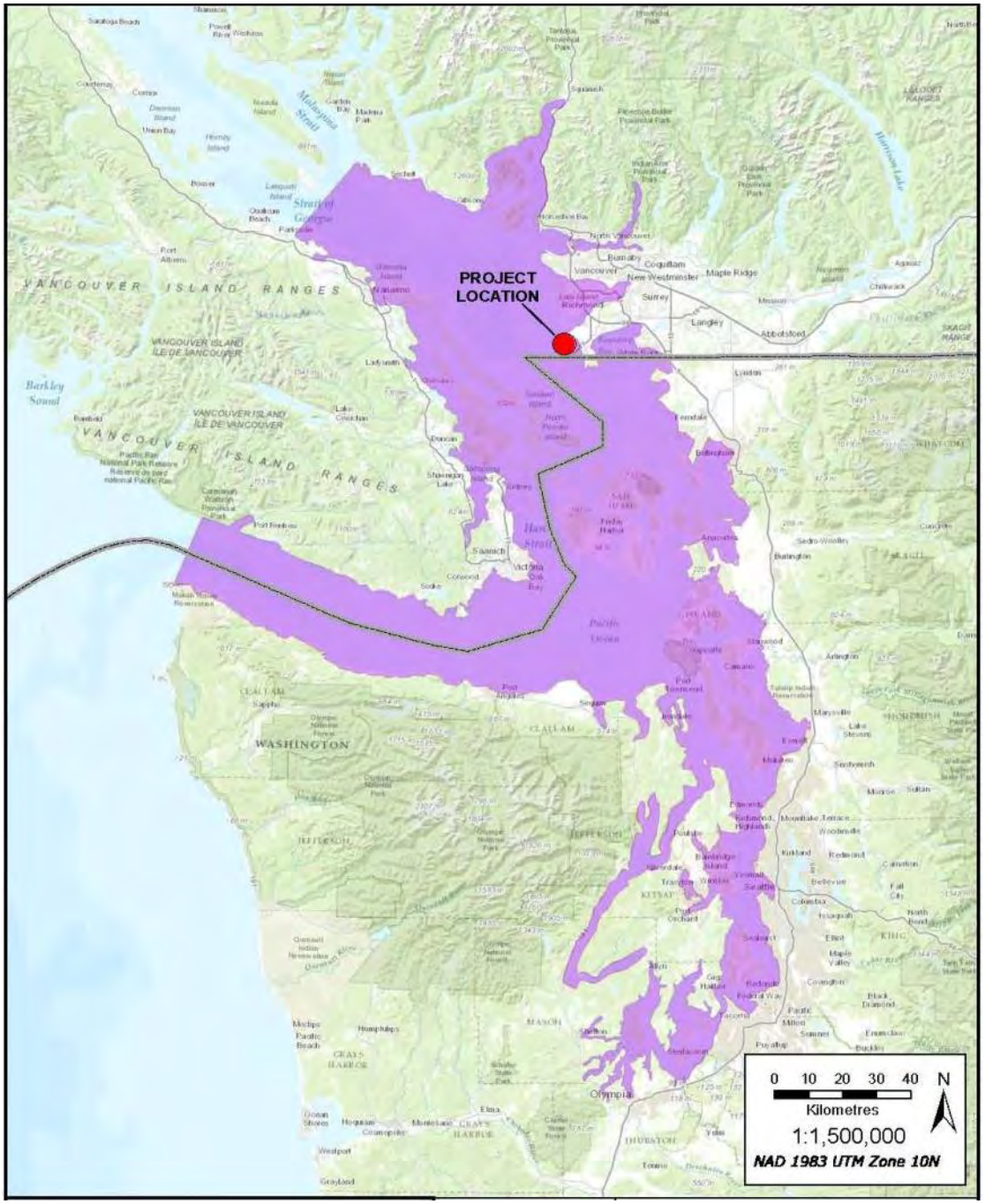

Figure 2: The spatial extents of the Coastal Geomorphology Study numerical model.

1.3 METHOD OF APPROACH

Three methods were used to assess the physical response to the proposed development:

1. Interpretive geomorphic studies using historical data, site observations and measurements;
2. Analytical methods; and,
3. Numerical modelling of waves, tidal currents and sediment transport.

Input and consensus from the scientific community on the approach to assessing changes was gathered during the Technical Advisory Group (TAG) workshops on coastal geomorphology (Compass Resource Management Ltd. 2013*a*).

The three-pronged approach seeks to provide increased confidence in the study results that may not be possible using a single study method. The same approach was adopted for a previous study of the coastal geomorphology of Roberts Bank in support of a proposed expansion to the existing Deltaport Terminal (NHC and Triton 2004). Teeter *et al*. (2001) concluded that available numerical modelling techniques were limited by present computational power as well as our understanding of the interactions between sediment and vegetation (such as eelgrass), bed sheltering and wave damping effects in very shallow water, sediment re-suspension and the mechanisms controlling drainage channel formation on tidal flats. There have been significant advances since this paper was published; both in the availability of affordable powerful computational resources as well as in the level of sophistication of numerical models. However, there continue to be limitations to the predictive ability of numerical techniques.

The major active processes that shape the Fraser River Delta and Roberts Bank tidal flat are reflected in the morphology, however, and can be qualitatively and quantitatively assessed using a range of interpretive methods including historical mapping, field observations as well as other analytical computations. These geomorphic investigations assist to overcome the limitations of available numerical models. The adopted approach integrates hydrodynamics, sedimentation, and geomorphology and focuses on developing an understanding of the long-term physical processes that drive morphological change in the Project area. Existing studies of deltaic and tidal flat geomorphology were interpreted along with observations from new field studies conducted by NHC and others to provide background information and input data. The following sections summarize the interpretive and modelling approaches, as well as the various field studies.

1.3.1 INTERPRETIVE GEOMORPHOLOGY

An interpretive geomorphology approach was taken to supplement the numerical modelling results and enable a better understanding of the morphodynamic evolution of the tidal flats. The tasks involved in this study included the following:

- Literature review – Previous field and theoretical studies were reviewed to understand the environment and driving forces at work at Roberts Bank and interpret the results of the numerical modelling in this light.

- Airphoto interpretation – Airphotos of the study site spanning the years 1932 to 2004, and orthophotos spanning the years 1995 to 2013 were analyzed. They provide insight into the planform changes that have taken place on the tidal flats since 1932 and the role of natural factors or anthropogenic developments in driving these changes.

- Bathymetric and LiDAR surveys – Bathymetric charts are available from as early as 1859 from sources that include the Great Britain Admiralty, and in later years (e.g. in 1967) from the Canadian Hydrographic Service (CHS). NHC also obtained access to bathymetric surveys

conducted in 2002 and in 2004/2005 by Public Works and Government Services Canada (PWGSC). LiDAR (Light Detection and Ranging) refers to a remote sensing technology that is used to capture high resolution imagery. LiDAR data are available for the study area for 2011. By comparing the tidal flat surface between years, vertical changes on the tidal flats over time were able to be resolved.

Data sources used to review the morphodynamic evolution of the tidal flats are summarized in **Appendix A**.

1.3.2 NUMERICAL MODELLING

The potential changes from RBT2 on tidal currents (hydrodynamics), wave climate and local seabed scour and deposition (morphodynamic) were investigated using the TELEMAC-MASCARET modelling system. Three TELEMAC models were applied to compute the various physical processes of tidal currents (TELEMAC-3D), wind-generated waves (TOMAWAC), and sediment transport (SISYPHE).

The hydrodynamic model TELEMAC-3D uses the information of flow discharges coming from the Fraser River plus the tidal information in the Juan de Fuca Strait near Port Renfrew and Hornby Island (**Figure 2**) to compute the tidal currents (velocity and depth) in the vicinity of the RBT2 footprint. The TOMAWAC model uses wind data to simulate the wave propagation and compute wave heights. This wave information is passed into TELEMAC-3D to incorporate its effects on flow circulation.

Local bed changes (scour and deposition) around RBT2 were computed by coupling the sediment transport and morphodynamic model SISYPHE to TELEMAC-3D and TOMAWAC. SISYPHE uses the tide and wave information from the other two models to compute scour and deposition of the seabed. The new bed elevation computed by SISYPHE is fed back into TELEMAC-3D to re-compute the flow hydrodynamics (**Figure 3**).

A detailed description of the TELEMAC model development and calibration is provided in **Appendix B**.

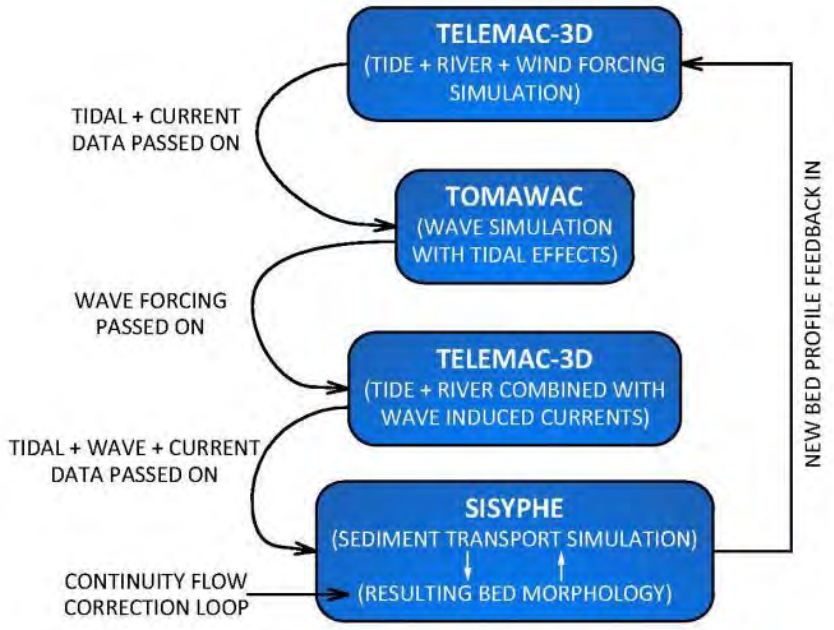

*source: Methods for medium-term prediction of the net sediment transport by waves and currents in complex coastal regions (Continental Shelf Research)

Figure 3: TELEMAC model coupling flow diagram (from Brown and Davies 2009).

A separate numerical modelling study was carried out to investigate the flow of tidal water through the semi-pervious causeway containment dyke during the construction phase. River2D was chosen for this localised investigation as it incorporates the mathematical functions that describe subsurface groundwater flow to ensure model stability for cells that go dry. This model feature was manipulated to model inundation of the area between the containment dyke and the existing causeway as well as the flow rate through the dyke on to the tidal flats during a dropping tide. Details of this model methodology, including model development, calibration, and validation using laboratory flume experiments are provided in **Appendix D**.

1.3.3 Field Investigations

Various field studies were conducted by NHC between April 2012 and August 2013 to supplement the body of existing information about the Roberts Bank area and to improve the understanding of key processes. They include:

- Measurement of channel discharge, sediment concentration, temperature and salinity in Canoe Passage, and collecting repeated bathymetric surveys along representative cross-sectional areas;
- Measurement of vertical profiles of salinity and turbidity within the water column at various locations across Roberts Bank during freshet conditions;
- Measurement of short-term erosion and deposition at various locations on the Roberts Bank tidal flats;

- Collection and radiometric dating of sediment cores from the upper tidal flats using radio isotopes (^{210}Pb and ^{137}Cs);
- Measurement of wave height and period at three locations on a transect across Roberts Bank; and
- Measurement of tidal flow in select channels in the Roberts Bank area (Canoe Passage and tidal flat channels).

Figure 4 provides a summary of the timing of field studies, including the duration of data collection. The field studies were supplemented by reconnaissance-level site visits and overflight inspections in a small fixed-wing aircraft to observe conditions at various tide stages and seasons. These field studies have been summarized in **Appendix C.**

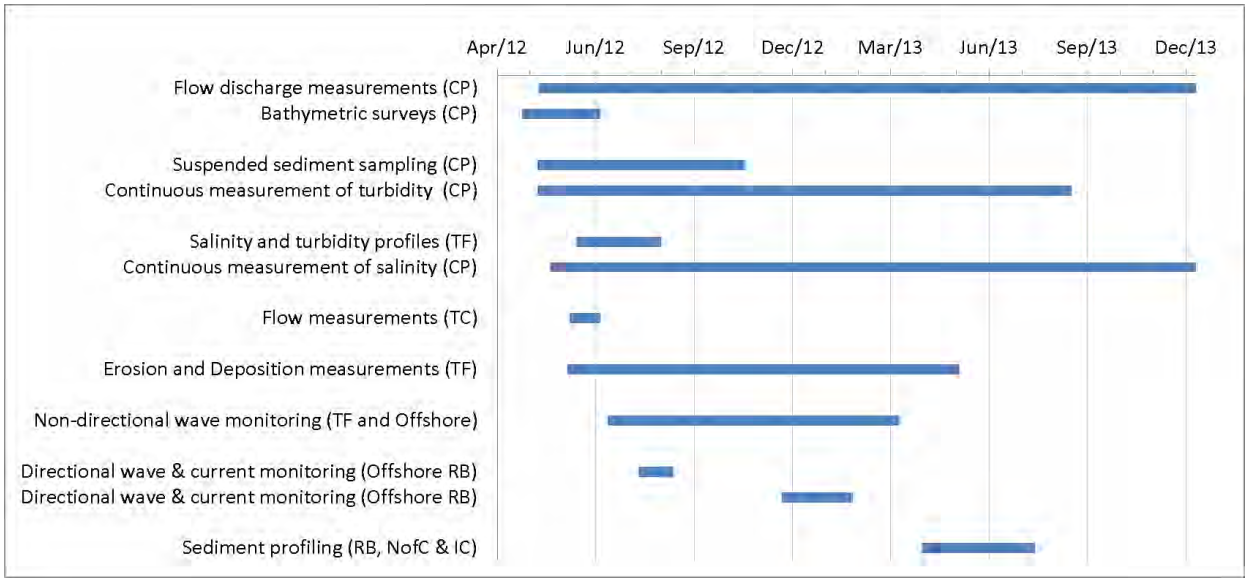

Figure 4: **Summary timeline of the field investigations and data collection.** ***CP – Canoe Passage; TF – Tidal Flats; TC – Tidal Channels; RB – Roberts Bank; NofC – North of Causeway; IC – Inter-causeway.***

1.4 REPORT OUTLINE

The results of the Coastal Geomorphology Study investigations are summarized in this main report and four appendices. Chapter 2 - *Roberts Bank Terminal 2 Project* - describes the terminal layout and configuration as well as information that was available about construction methodology. Chapter 3 - *Physical Setting* - describes the physiography and physical landforms adjacent to the Project. Chapter 4 - *Driving Forces* - summarizes the physical processes that drive the evolution of the Fraser Delta near the Project. Chapter 5 - *Morphological Changes on Roberts Bank* - summarizes the historic changes on the tidal flats and assesses the changes from earlier anthropogenic developments. Chapter 6 - *Hydrodynamic Model Analysis* - describes the predicted changes from the Project on the local current and wave characteristics. Chapter 7 - *Sediment Dynamics* - describes the predicted changes from the

Project on scour and deposition patterns on the tidal flats. Chapter 8 - *Evaluation of Project-Related Changes* - highlights potential construction-related changes on local sedimentation patterns and describes monitoring that could be implemented. Chapter 9 - *Conclusions* - summarizes the main conclusions from the study.

Four technical appendices provide supporting detailed data and analysis. Appendix A - *Data Sources* - provides a detailed compilation of the past data and reports that were used during this study. Appendix B - *Model Development* - describes the hydrodynamic modelling, including calibration and validation that was carried out to assess the impact of tides and Fraser River inflows. Appendix C - *Field Data Collection Program* - summarizes the field monitoring program that was collected in 2012 to support the geomorphic studies and numerical modelling. Appendix C also summarizes special investigations that were carried out to assess recent changes in the ridge and runnels area of the tidal flats. Appendix D - *Causeway Containment Dyke Seepage Study* - is a technical report detailing the investigations that were undertaken to quantify seepage flow through the causeway expansion containment dyke and the potential changes to geomorphology that would be related to erosion and channel formation.

2 ROBERTS BANK TERMINAL 2 PROJECT

2.1 PROJECT CONFIGURATION

A detailed description of the proposed Project has been submitted as part of the EA process. A simplified description of the Project is presented here for the purposes of identifying those components that would reasonably be expected to interact with and possibly affect coastal geomorphology. The pertinent Project components include (a) the marine terminal, (b) berth pocket, (c) tug basin expansion and (d) widened causeway (**Figure 5**).

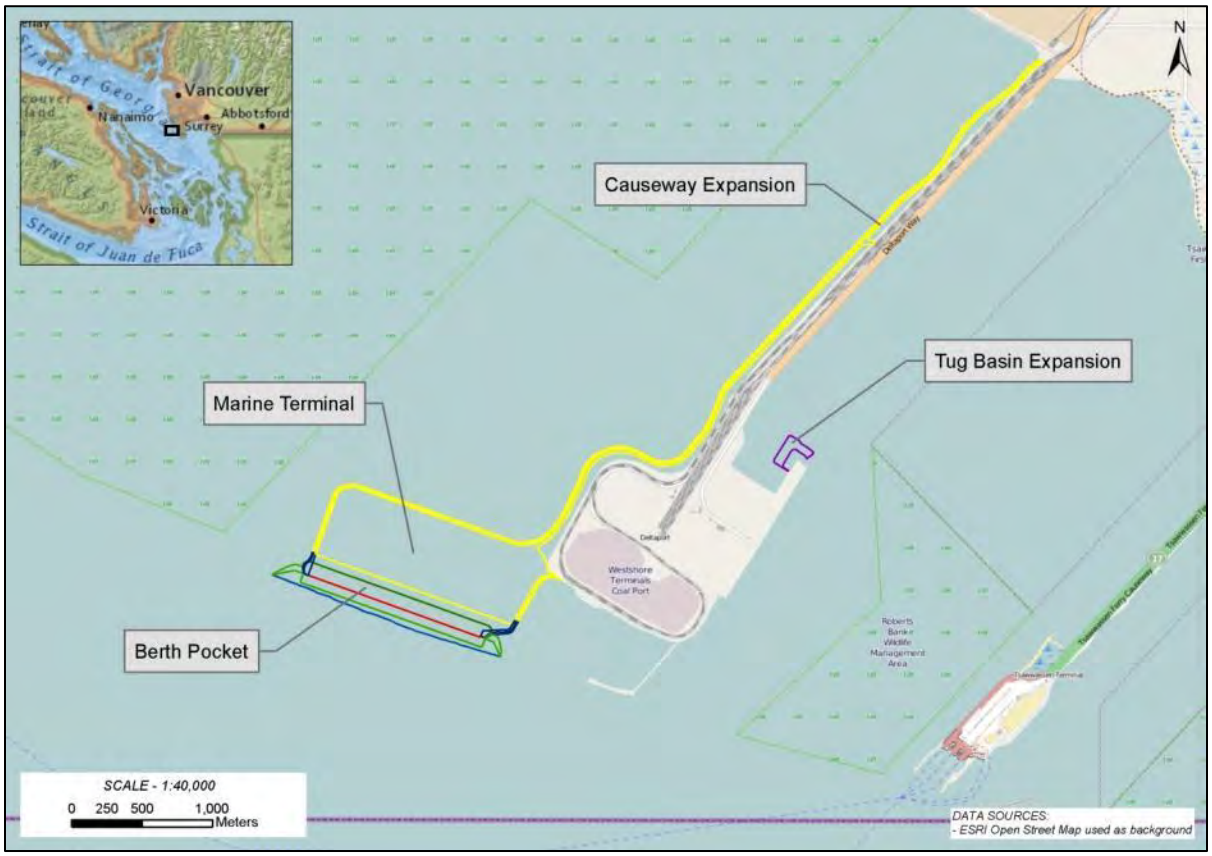

Figure 5: Schematic showing the layout of the proposed Project, from PMV (2013).

2.1.1 MARINE TERMINAL

The Project's marine terminal will be located immediately west of the existing Roberts Bank terminal facility, which is located approximately 5.5 km from the east shore end of the causeway. The terminal will be oriented parallel to the shoreline (perpendicular to the causeway) and will extend approximately 600 metres (m) further offshore than the edge of the existing terminal at Roberts Bank. The terminal will be rectangular in shape, with a berth face length of 1,300 m to accommodate the mooring of three ships, and a terminal width of 700 m to support terminal components. The terminal surface will vary from 8.75 m to 6.5 m height above mean sea level, and it will have an approximate total useable area of

108 ha. To accommodate for this space requirement, the total terminal footprint, including protected marine slopes and the three-berth wharf will be approximately 117 ha.

The berth face will be comprised of a near-vertical concrete caisson wall, while the slopes of the non-berth face edges will be protected with riprap on a 1.75H:1V slope from the top of the terminal to the seabed.

The marine terminal will be constructed almost entirely within the sub-tidal portion of Roberts Bank with only the north-east corner extending into the intertidal zone. The elevation of the seabed along the north face varies between -1.1 m CD and -2.3 m CD. The seaward south face of the terminal is approximately aligned with the existing -10 m CD contour of the delta foreslope.

2.1.2 BERTH POCKET

The berth pocket is the dredged mooring basin adjacent to the terminal wharf structure where the container ships will be berthed and moored to the wharf. The berth pocket and the associated approach and departure angles will measure approximately 1,700 m long by 62 m wide. The berth pocket will be 18.4 m deep (at lower low water level) to meet safe under-ship clearance and performance requirements for the adjacent new wharf foundation.

2.1.3 TUG BASIN EXPANSION

The existing tug basin, located in the inter-causeway, has a footprint of 1.4 ha and will be expanded by approximately 3.1 ha, for a total footprint of 4.5 ha. The expanded tug basin will be extended longitudinally (north-south) in the intertidal portion of the tidal flats between the existing Deltaport Terminal and the existing causeway. The general arrangement is shown in **Figure 6**.

The basin will be dredged to an elevation of -6.5 m CD, which is 0.5 m deeper than the existing tug basin. Crest protection will be constructed of riprap and installed around the edge of the dredged area to protect the mudflats from scouring forces and mitigate the formation of channels. The new crest protection will be tied to the pre-existing crest protection structure, but constructed with a nominal projection of approximately 0.3 m above the existing seabed, sufficient to account for settlement over time. To minimize flow diversion, pontoon floats along the dyke shoreline and gangways with a single-span piled trestle structure provide pedestrian access to the shore.

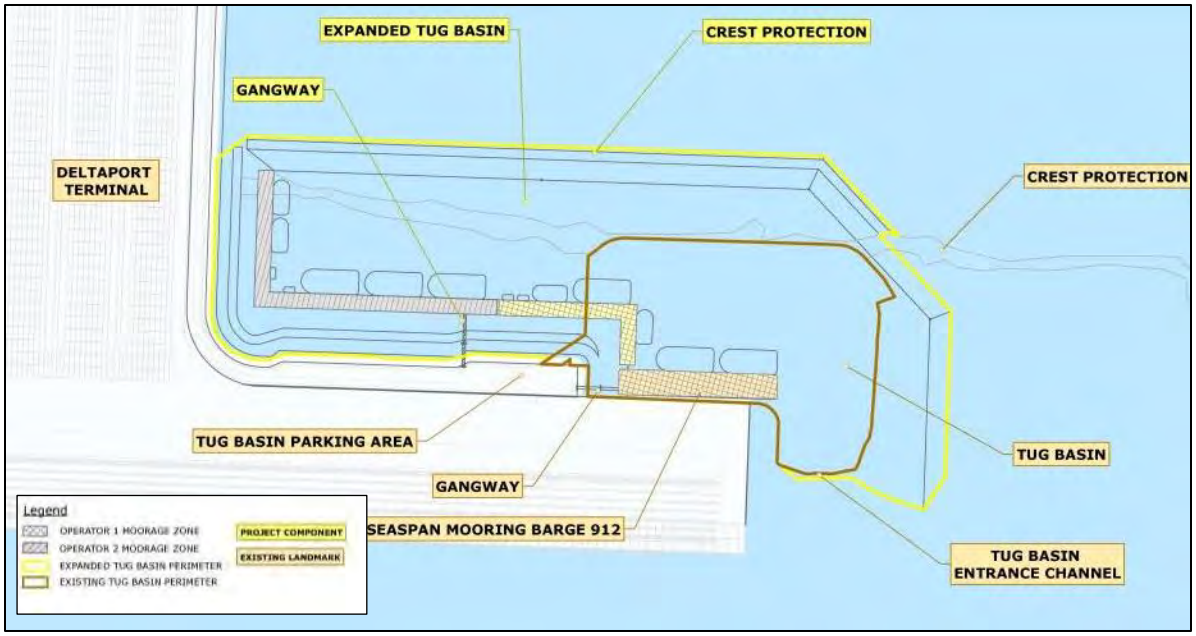

Figure 6: Schematic showing the proposed expansion to the existing tug basin in the inter-causeway adjacent to the existing Deltaport Third Berth.

2.1.4 CAUSEWAY EXPANSION

The existing causeway linking the rail network to the existing Roberts Bank terminals will be widened on the north side of the causeway, requiring an additional land area of approximately 42 ha for terminal construction and 1 ha of existing BC Rail (BCR) land for the tie-in of tracks to the existing rail network. The edge of the widened causeway will be protected with riprap at a slope of 1.75H:1V extending from the top of the causeway to the existing seabed.

2.2 CONSTRUCTION SCHEDULE

The construction phase is anticipated to span six years, and will be initiated with the placement of the terminal perimeter dykes in years 1 and 2 and by dredging of the berth pocket and caisson trench in year 2. Causeway diking will occur part-way through year 1 and in year 3. Expansion of the tug basin will occur in year 4.

The construction phase will include a number of activities that may result in short-term changes to the local tidal currents and wave patterns, or potentially changes to the seabed. These potential changes were evaluated within the Coastal Geomorphology Study. Construction changes related to the transfer and disposal of dredgeate (for example, short-term storage of dredgeate in the intermediate transfer pit and the disposal at sea of dredgeate), however, have been evaluated by others (Tetra Tech EBA 2014).

3 PHYSICAL SETTING

This chapter describes the physiography and principle landform units surrounding the Project. This section also briefly describes the geological evolution of the delta in order to provide an understanding of its recent development and controls on future evolution.

3.1 STRAIT OF GEORGIA

The Strait of Georgia occupies the inundated portion of the northwest-southeast trending Georgia Depression – part of the larger Coastal Trough that extends along the length of coastal British Columbia (Holland 1964) – that lies between the mainland and Vancouver Island. It is approximately 220 km long and 28 km wide and has an average depth of 155 m (Thomson 1981). The Strait of Georgia is linked to the Pacific Ocean on its north end by several long, narrow channels including Discovery Passage, Johnstone Strait and Queen Charlotte Strait. The southern end of the Strait of Georgia is linked to the ocean via Juan de Fuca Strait.

3.2 FRASER RIVER

The Fraser River drains 232,000 km^2 of southern British Columbia, making it the largest river on the west coast of Canada. Near Mission, 85 km from the sea, the river changes abruptly from an anabranching gravel bed to an irregularly meandering sand-bed channel. At New Westminster (35 km from the river mouth), the main channel splits into the North Arm and the Main Arm. The Main Arm diverges again around Westham Island, with Canoe Passage along the south discharging most directly to the northern Roberts Bank tidal flats.

3.3 FRASER DELTA

The contemporary Fraser River delta was formed since the most recent glaciation, beginning approximately 10,000 years ago. **Figure 7** shows the development of the delta to the present day in simplified schematic form. The Point Roberts peninsula near the southern extent of the delta is a Pleistocene uplands and former island that has become attached to more recent deltaic deposits. The initially very rapid advance of the delta front and infilling of the Fraser Valley has slowed and present day sediment inputs to the delta, particularly those areas distal to the mouth of the Main Arm, are much reduced. Inputs to southern Roberts Bank are limited to the fine fraction carried in suspension in the Fraser River plume; the tidal flats at Boundary Bay essentially receive no new sediments from the Fraser River (Kellerhals and Murray 1969).

The modern delta of the Fraser River commences near New Westminster and extends 15 to 23 km westwards in a broad delta plain encompassing Richmond, Ladner and Tsawwassen. The western margin of the delta extends into the Strait of Georgia approximately 27 km and includes Sturgeon Bank and Roberts Bank. Boundary Bay is located on the inactive southern side of the delta and extends 11.5 km.

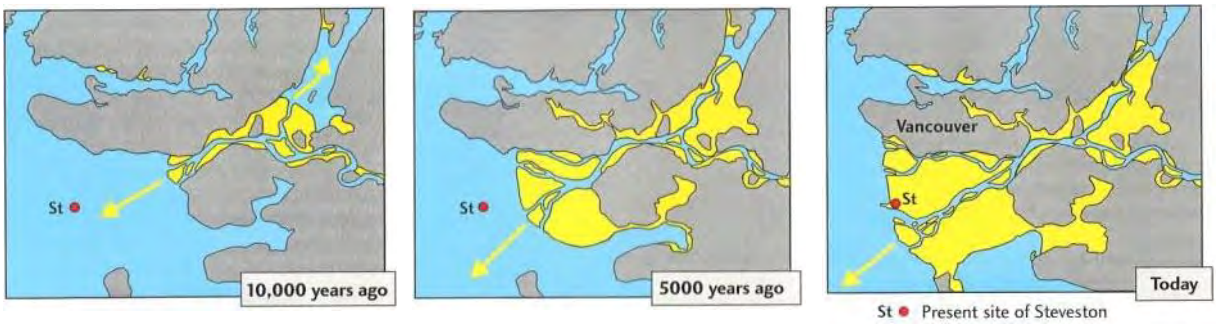

Figure 7: Growth of the Fraser delta and floodplain over the last 10,000 years (from Clague and Turner 2006).

Coleman and Wright (1975) classified deltas according to the relative importance of river, tide and wave processes. River-dominated deltas are found where rivers carry so much sediment that the deposition rate overwhelms the rate of re-working and removal due to marine processes. In river-dominant deltas, the delta shape develops as a pattern of prograding branching distributary channels, separated by marshes. The Fraser River delta is considered an example of a river-dominated delta (USACE 2002).

More generalized classification schemes have been presented to characterize the relative importance of wave energy and tides on shoreline morphology (USACE 2002). Based on these empirical methods, the large tidal range and relatively low, fetch-limited wave climate at Roberts Bank would indicate the site is strongly tide-dominated. This characterization, however, is overly simplistic, since it does not account for a number of complicating factors related to geology, topography, sediment supply and effects of adjacent fluvial processes.

3.4 BIOSEDIMENTOLOGICAL ZONATION ON ROBERTS BANK

Roberts Bank occupies the southern portion of the Fraser River delta between Point Roberts and the Fraser River Main Arm. Sea dykes, constructed to reclaim salt marsh and prevent flooding, form the boundary of the upper limit of tidal incursion, and from this boundary the delta slopes seaward towards the deep waters of the Strait of Georgia. The delta slope interacts with waves and tidal movement so that distance from shore correlates strongly with relative time of emergence/submergence, exposure to wave energy and tidal current velocity. These, in turn, correlate with sediment grain size and various ecological zones. Zonation of the tidal flats along a transect running from the top of the shore out to the edge of the tidal flats is shown in **Figure 8**. Although developed by Swinbanks (1979) to describe the tidal flats of Boundary Bay, this is generally applicable to Roberts Bank.

At Roberts Bank, the presence of the Roberts Bank causeway and the BC Ferries causeway introduces a complicating factor to this general trend, as does the input of freshwater from the Fraser River at the mouths of the Main Arm and Canoe Passage. The result is the formation of various biosedimentological zones (**Figure 9**) that have been most recently described by Hill *et al*. (2013). **Figure 8** provides a summary description of the various zones.

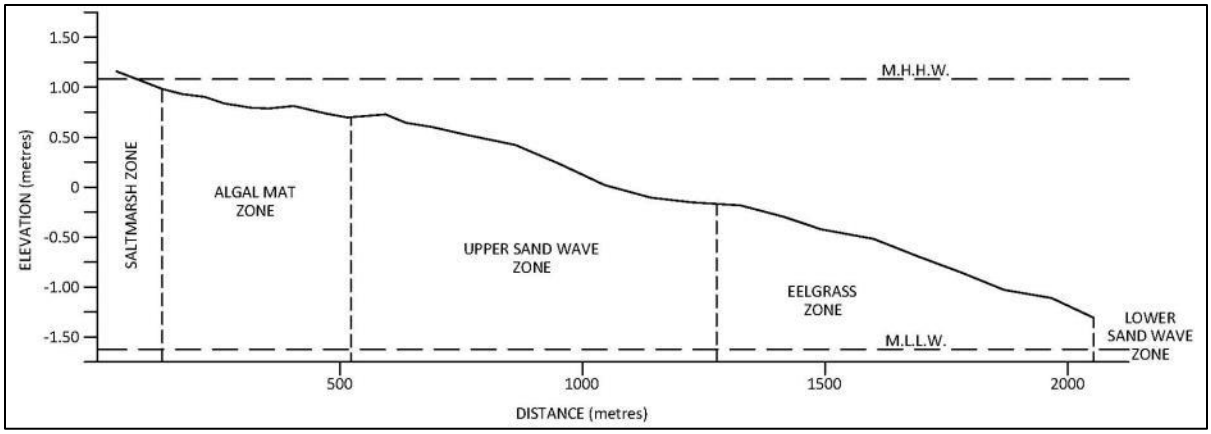

Figure 8: Zones identified on the Boundary Bay tidal flats and their corresponding elevation ranges in metres GSC (from Swinbanks 1979).

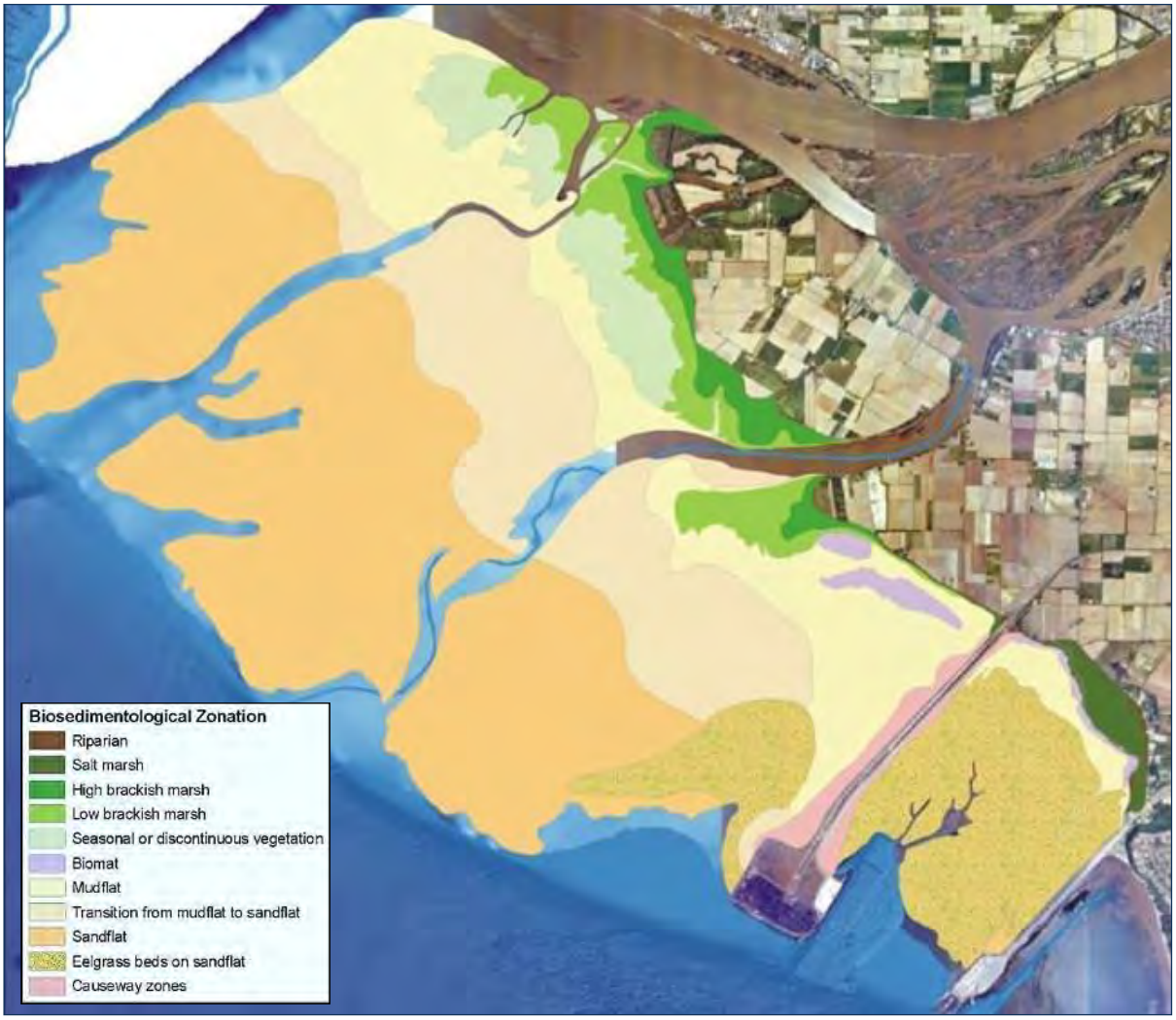

Figure 9: Biosedimentological zonation on Roberts Bank overlain on multibeam image showing the subtidal portion of the delta (from Hill *et al*. 2013).

3.4.1 SEA DYKES

Sea dykes were constructed along the shoreline of Roberts Bank as early as the late-1800s. What began as an initiative by local landowners was later adopted as government responsibility, particularly following the large Fraser River flood of 1948. The dykes were upgraded at various locations in the 1970s and 1980s (City of Delta 2013). Although the dykes along the shoreline fronting Westham Island are classified as non-standard (Delcan 2012), the presence of dykes effectively limits the inshore incursion of tidal water and reduces the drainage of tidal water from upland areas onto the tidal flats.

3.4.2 CAUSEWAY ZONES

The BC Ferries causeway was completed in 1960 and the Roberts Bank causeway was completed in 1969 (NHC and Triton 2004) to provide a barrier to waves and re-direct tidal flows. Modifications to the terminals have occurred a number of times since then, but the initial changes from the construction of the two causeways have not been significantly changed by subsequent development. **Figure 9** shows a distinct band of unique biosedimentological zonation on either side of the Roberts Bank causeway, which would typically be interpreted as being the result of interruption of sediment deposition by longshore drift. However, airphoto evidence (**Figure 10**) suggests that the construction methods employed at the time resulted in significant dispersal of sediment over the tidal flats on either side of the constructed causeway. This material has persisted to the present day in the form of an apron of material that slopes away from the causeway. The general slope of the tidal flats, on which this apron of sediment is superimposed, dips in a direction parallel to the causeway towards the Strait of Georgia.

Figure 10: 1969 airphoto showing the Roberts Bank causeway during construction.

3.4.3 INTERTIDAL MARSH

Marsh – either brackish or true salt marsh – exists as a band along most of the upper shoreline at Roberts Bank, including an intermittent fringe along portions of the Roberts Bank causeway. This band expands seaward at Brunswick Point and along the seaward edge of Westham Island in response to the effects of freshwater flows and sediment inputs from Canoe Passage. In general, marshes along the

western front of the delta are underlain by inter-bedded organic mud and sand and are dissected by creeks and contain depressions. The influx of sediment-laden water to the marshes driven by the tides results in vertical accretion due to the preferential trapping of the sediment from the water column, which is further accelerated by the accumulation of detrital material from the marsh vegetation. Tidal water draining into and out of the marshes forms a system of channels within the marsh as well as a source of water that is partially retained during a dropping tide and subsequently flows across the exposed tidal flats.

The intertidal marsh is made up of two distinct biotic communities based on their tolerance to saline conditions. Brackish marshes are more common closer to the Fraser River distributary channels, whereas salt marshes are found where inputs of freshwater are more minimal relative to seawater exposure. True salt marshes at Roberts Bank are restricted to the upper shoreline in the southern portion. A brackish marsh, such as exists at Brunswick Point, exhibits a plant community structure and associated faunal community that reflects the degree of interaction between the salt-wedge and freshwater inputs. Changes in the discharge pattern and mixing of marine and freshwater could significantly affect the marsh communities they support (GL Williams & Associates Ltd. and NHC 2009). The distribution of vegetation is also governed by elevation, which determines the extent to which plants are subject to desiccation and/or inundation.

It has been reported that dredging in the lower Fraser River had significantly altered the pattern and rate of sedimentation in the marshes at the western delta front. Williams and Hamilton (1995), focusing in on the marshes fronting Lulu Island on Sturgeon Bank, concluded that:

> *"the increased removal of sand by dredging in the Fraser River estuary has reduced sediment input and caused net erosion lowering throughout much of the sandy lower marsh."*

Subsequent studies by Hales (2000) that were more comprehensive in temporal and spatial scope showed a different trend. Fraser River marshes, both fronting marshes on Roberts Bank and south Sturgeon Bank and channel marshes near the mouth, showed an overall increase in marsh area within the study area between 1930 and 1994. According to Hales (2000):

> *"Contrary to expectations, marsh growth rates did not dramatically drop to historically low levels during or immediately following the period of extensive dredging. The most rapid period of growth coincides with the period during which the major river training structures were constructed."*

River training works likely increased the stability of the main channels, thereby allowing marsh accretion to occur without significant disturbance.

There has been some suggestion that the ragged leading edge of the marsh is an indication of its deterioration. Hales (2000) suggested that small patches of marsh now forming off the front of Westham Island are likely indicators of future areas of marsh development. As GL Williams & Associates Ltd. and NHC (2009) noted:

> *"Sediment is deposited rapidly around small patches of pioneering marsh species…increasing their elevation and rate of lateral growth. This leads to further sedimentation and the eventual establishment of the marsh."*

Perhaps the best evidence for salt marsh aggradation, as opposed to erosion, is the continued lateral growth of the marsh between 1930 and 2004.

There have been some suggestions made that geese may be contributing to the deterioration of the marsh; however, it is not known how widespread an impact this occurrence could have. Church and Hales (2007) extended their earlier work by mapping the marsh to the U.S. border for the years 1930, 1954, 1974, 1994 and 2004 (Church and Hales 2007) (**Figure 11**). This mapping indicates that in Zone 4, south of Canoe Passage, the marsh continued to increase in area between 1994 and 2004.

A more recent study of the location of the marsh leading edge was conducted at Sturgeon Bank using spacebourne radar imagery for the years 2001 to 2007 (TRE Canada 2014). The results indicate that there has been landward retreat of the leading edge along the seaward edge of Lulu Island, with the greatest losses of up to 230 m in the southern portion of Sturgeon Bank.

Temporal trends in marsh extent are also illustrated in **Section 5.2.**

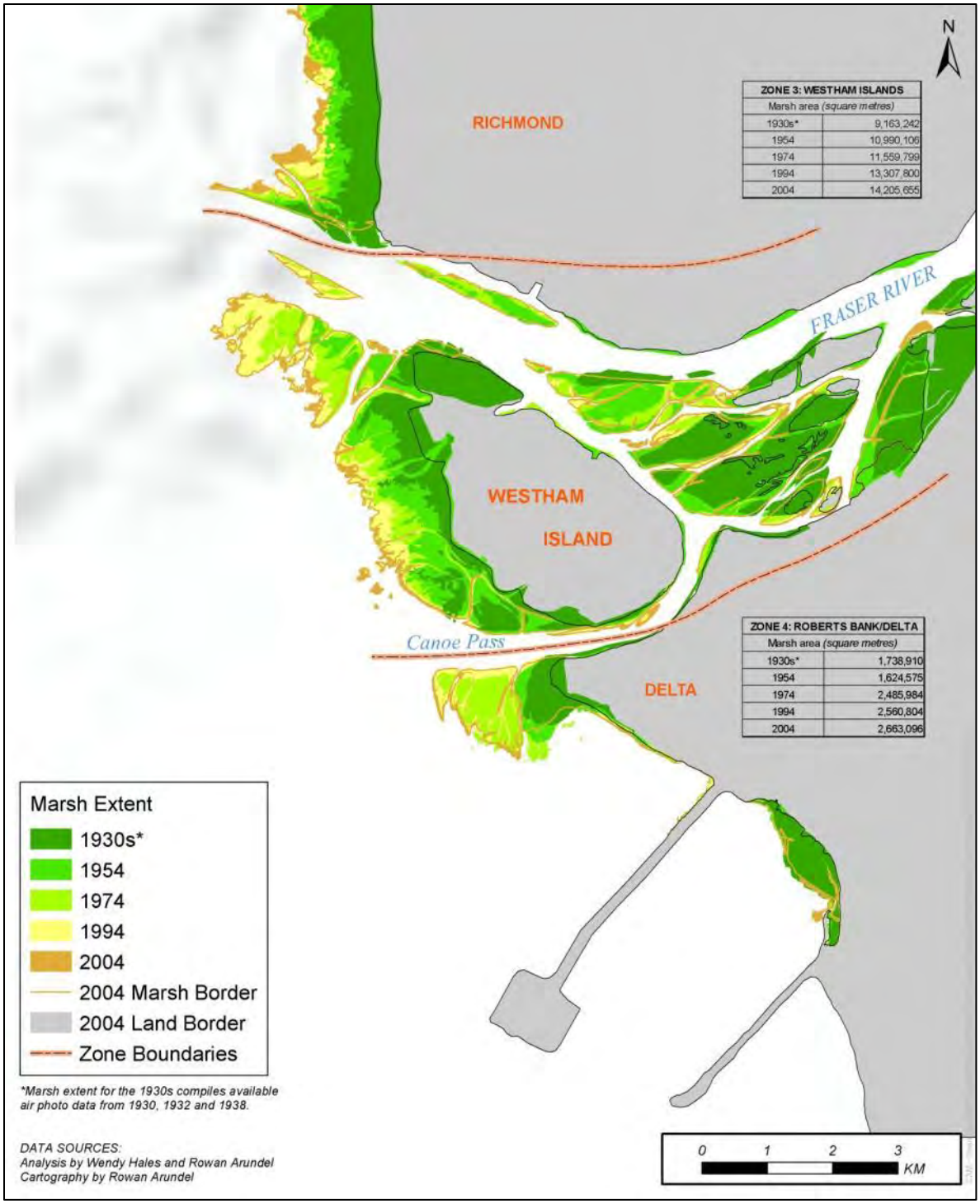

Figure 11: Fraser delta marsh development between 1930 and 2004 (from Church and Hales 2007).

3.4.4 TIDAL FLATS

Gently sloping tidal flats extend seaward from shore for a distance of up to 6 km on Sturgeon Bank and Roberts Bank. The width of the tidal flats is governed primarily by the tidal range (approximately 5 m), the wave climate and sediment characteristics.

The tidal flats represent the sub-aqueous top-set beds of the Fraser Delta (Mathews and Shepard 1962). On Roberts Bank, the zone is generally featureless except for the development of tidal channels, which typically occur either on the seaward margins of the tidal flats or on the upper tidal flats but rarely connecting between the two elevation bands. Although smaller tidal channels were present prior to anthropogenic developments and a few larger channels that were mostly remnants of former outlet channels from Canoe Passage, there are presently a number of well-developed large channels that are associated with dredging activities. Tide channels in the inter-causeway area have evolved into an extensive and complex system of shoreward-migrating tributaries, which dissect a large sand bar and drain via a large trunk channel.

Figure 12 shows the bathymetry of the Roberts Bank tidal flats. The average gradient on the tidal flats is approximately 0.0005 immediately south of Canoe Passage and 0.0011 on the north side of the causeway and in the inter-causeway area. **Figure 13** shows the hypsometry of the tidal flats on the north side of the causeway. This curve represents the area-elevation relation of the tidal flats, expressed in terms of the wetted area of the flats relative to the total area (measured from above Lowest Low Water-Large Tide (LLW-LT)). **Figure 13** shows that nearly 90% of the tidal flat is wetted when the tide level is close to mean sea level and approximately 20% is wetted at LLW (mean tide) conditions.

The tidal flats vary from medium sand through to silty sand depending on location (**Figure 14**). The lower and middle tidal flats are composed of horizontally-bedded, fine to medium grained sand, which is commonly bioturbated and contains shell fragments. These relatively clean sands grade into silty sands of the mid to upper tidal flats, with areas of fine mud in the near-shore zone.

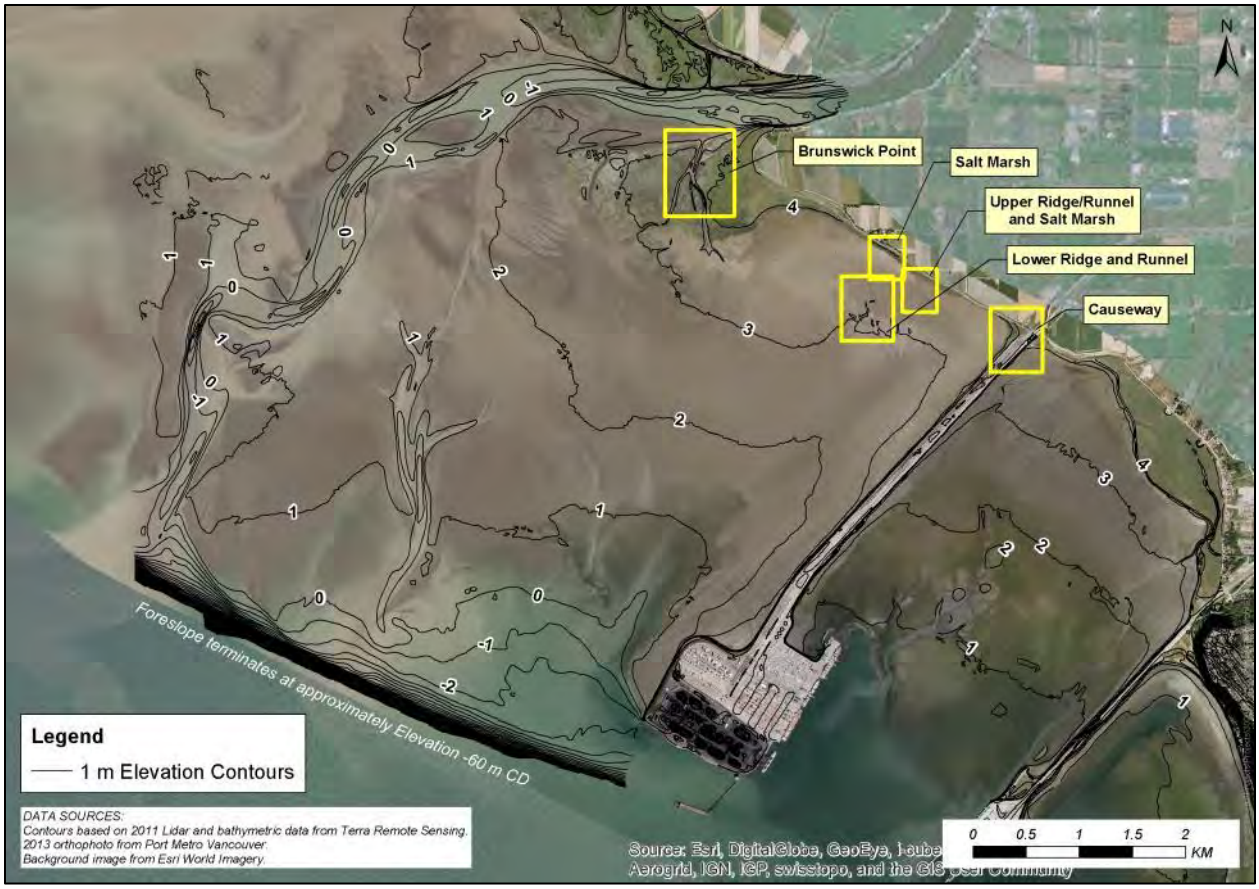

Figure 12: Bathymetry of southern Roberts Bank. Yellow boxes indicate the spatial extent of temporal airphoto comparisons that are provided in Section 5.2.

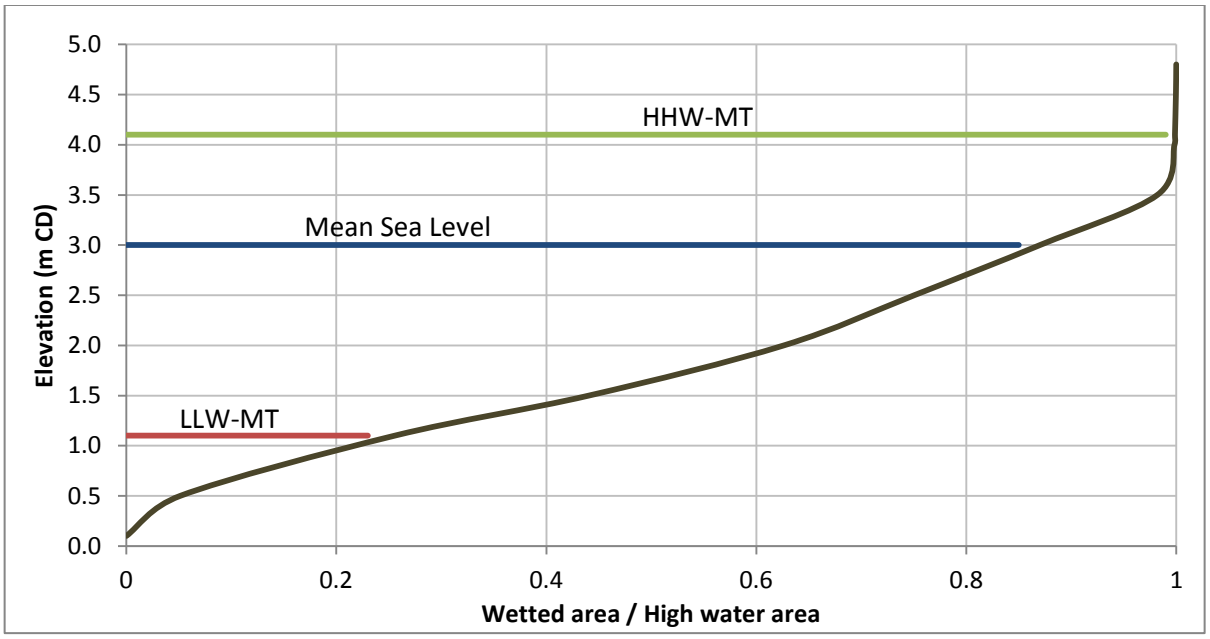

Figure 13: Hypsometry of Roberts Bank on the north side of the causeway. HHW-MT indicates the Higher High Water elevation associated with a Mean Tide and LLW-MT indicates the Lower Low Water elevation associated with a Mean Tide.

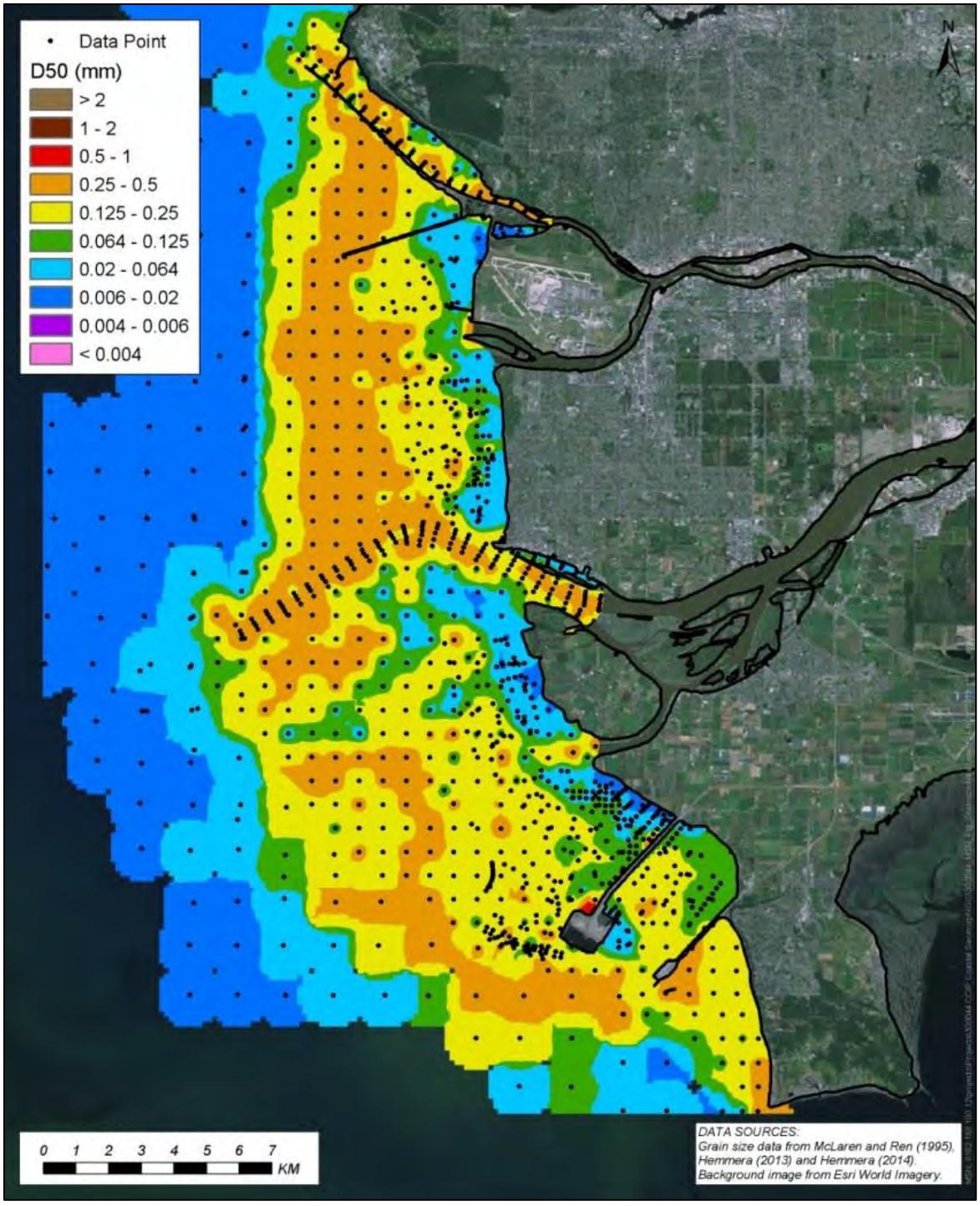

Figure 14: Surface grain size distribution of the Fraser River delta. Data are from McLaren and Ren (1995) and Hemmera (2014).

3.4.5 BIOMAT

The biomat community occurs in the upper intertidal area of Roberts Bank on the tidal flats (**Figure 9**) and coincides with a zone dominated by ridge and runnel topography, colloquially referred to as the 'mumblies'. The surface of the ridges is comprised mainly of cyanobacteria, a blue-green algae, which was verified by recent hyperspectral imagery. In the field, it is visible on the surface of the ridges but is largely absent from the ponds and runnels. Ridge and runnel topography is a common feature of tidal flats that has been described by a number of authors (e.g. Blanchard *et al*. 2000, Anibal *et al*. 2007) and was first identified in the Fraser River delta at Boundary Bay by Kellerhals and Murray (1969).

The biomat is composed of microalgae, which may act to stabilize the surface sediments of the ridges, partly through a filamentous biomass that modifies the sediment surface and, partly through the production of extra cellular polymeric substances (EPS), binds sediment particles. **Figure 8** shows that this 'algal mat' zone is restricted to approximately elevations +3.50 to +4.00 m CD (0.5 to 1.0 GSC). Accretion of the biomat zone and its role in stabilising the upper tidal flats is described in more detail in **Section 5.3.3**.

3.4.6 FORESLOPE

Figure 15 shows the characteristic steepening of the delta profile over the transition from the tidal flats into deep water. The sediments in the foreslope consist mainly of mud derived from suspended sediment in the Fraser River plume and coarser sand transported down the delta slope. Recent multibeam bathymetric surveys (**Figure 16**) confirm that the area is characterized by extensive submarine channels on the delta slope seaward of the mouth of the Main Arm channel due to gravity flows (Hill *et al*. 2008). On Sturgeon Bank, there is a sharp transition between the sands on the tidal flats and the finer grained sediment on the foreslope. The decrease in grain size with depth reflects the reduction in current and wave action from the shallow tidal flats into deep water.

Roberts Bank is generally covered with medium- to fine- grained sand extending from the tidal flats down to the foreslope. The scarcity of finer sediments above the foreslope suggests that the wave energy on the flats is sufficient to re-suspend these sediments and transport them, limiting deposition to lower-energy environments. The prevailing flood-dominated tides in the Strait of Georgia produce a net northerly transport of sediments on the foreslope in the vicinity of the Project (Luternauer and Murray 1973). The recent multibeam bathymetric surveys also confirm the occurrence of up-slope migrating sediment waves on the slope off the mouth of the Main Arm attributed to asymmetric tidal currents (Hill *et al*. 2008).

Sedimentation rates range from less than 1 to 2 cm/year over much of the Sturgeon Bank foreslope and in the Strait of Georgia. However, much higher sedimentation rates have been measured off the mouth of the main channel. Little or no sediment is being deposited today over most of the Roberts Bank slopes. Previous studies reported dunes off Roberts Bank at depths of 20 to 120 m, with net northwesterly transport. Some researchers claimed that these features were evidence of erosion of the delta front; however, these features were later interpreted to be dredged spoil that had been dumped in deep water (Hay and Company 1996).

Retrogressive slope failures and sediment-laden gravity flows have eroded the active deep valley off the mouth of the Main Arm near Sand Heads, and smaller valleys are evident off of Canoe Passage and the North Arm (Christian *et al*. 1998). There is also a large area of disturbed sediments on the southern side of Roberts Bank, termed the "Roberts Bank Failure Complex" by Luternauer *et al*. (1998). This feature was interpreted to have formed at a former river mouth in a manner similar to that occurring today off Sand Heads and is not related to present-day sedimentary processes.

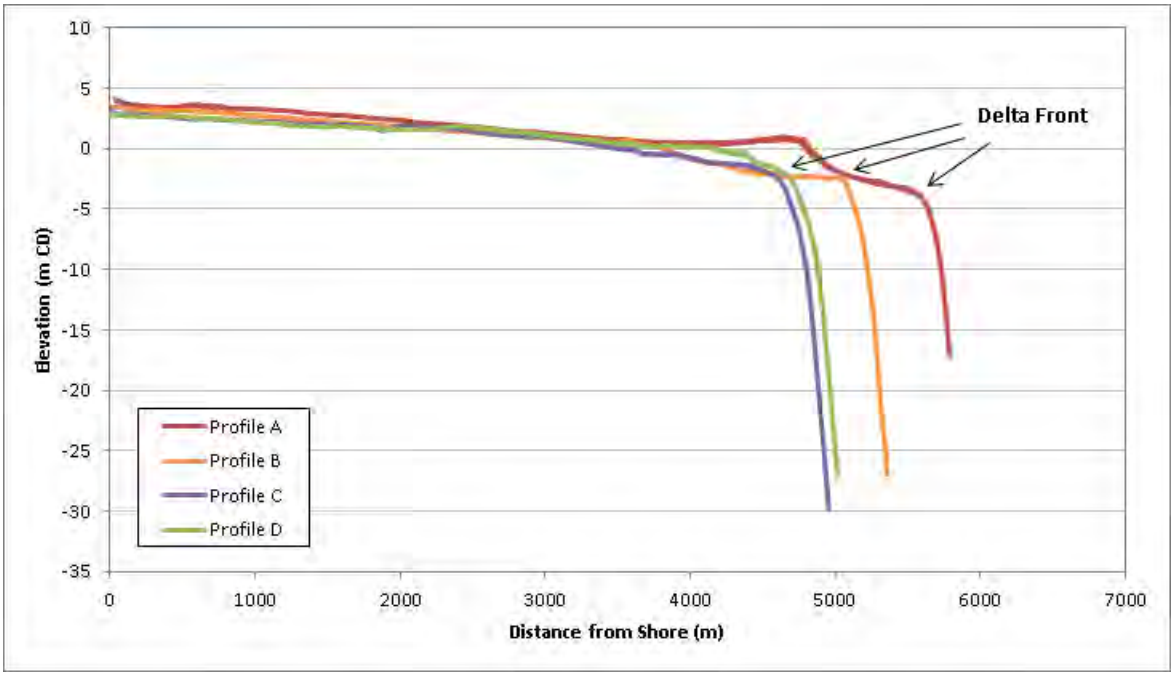

Figure 15: Profiles of Fraser River Delta, including foreslope, along four transects between Canoe Passage and Roberts Bank Causeway (extracted from 2011 Digital Elevation Model dataset). The location of transects on the tidal flats is shown in Figure 45.

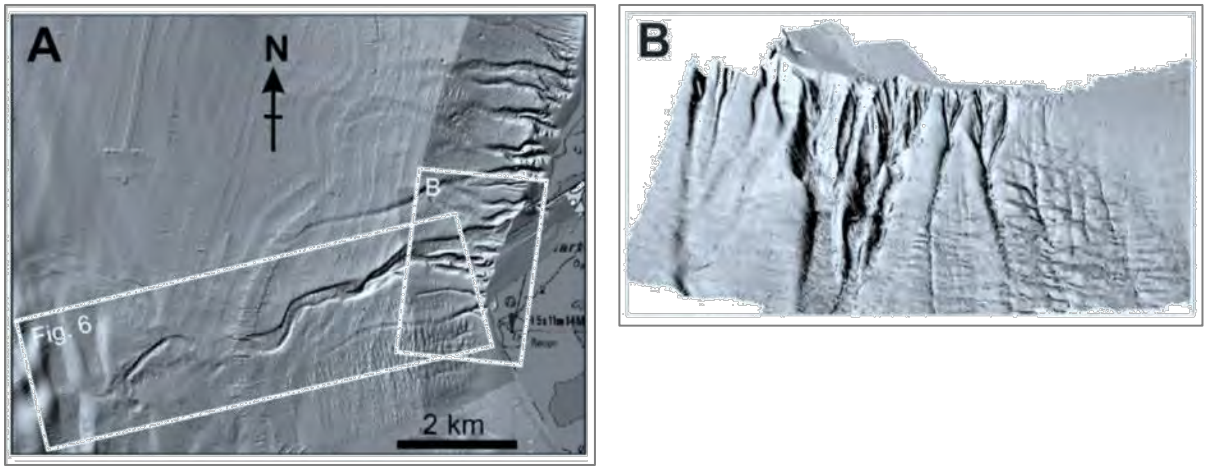

Figure 16: Recent multi-beam surveys showing (A) the extensive submarine channelling on the delta foreslope seaward of the mouth of the Fraser River main arm; and (B) 3-D rendering of the boxed area in A. From Hill *et al*. (2013).

3.5 BIOTIC COMMUNITIES

Various biotic communities have been identified at Roberts Bank and are the subject of careful investigation and effects assessment by others due to their ecological importance. A description of these ecological communities is included within this Coastal Geomorphology Study because of the strong interrelationship with sedimentary processes (e.g. biomat and intertidal marsh, described above) or because of the potential for these communities to be altered due to changes to coastal processes arising from the proposed Project. The spatial extents of the biotic communities described below do not correspond exactly with the sedimentological zones described above in **Section 3.4**.

3.5.1 BIOFILM

Biofilm is a gelatinous layer of microalgae such as diatoms and microbes that forms on substrates in shallow waters throughout the world (WorleyParsons 2012). The distribution of biofilm is dictated by a number of physical and biological factors, of which the former include light, salinity, sediment size and tidal fluctuations.

At Roberts Bank, biofilm occurs in the upper tidal flats where freshwater inputs are greater and where sediment is composed of silts and clays. **Figure 17** shows the distribution of biofilm in dark red based on 2011 hyperspectral surveys (WorleyParsons 2015). Where present, it has been found to lend stability to the sediment surface; however, the intensity of erosive forces that it can tolerate is not fully understood but is being investigated by other contributors to the EA. Higher biofilm biomass is found in a swale-like feature shoreward of the higher-elevation mumblies, which are suspected to promote quiescent conditions. The ecological importance of biofilm at Roberts Bank lies in providing a feeding ground for migrating shorebirds (WorleyParsons 2012).

Figure 17: Distribution of biofilm at Roberts Bank based on recent (2011) hyperspectral surveys analysed and mapped by (WorleyParsons 2015).

3.5.2 EELGRASS

Eelgrass at Roberts Bank occurs as continuous, dense beds in the most suitable growing areas and in sparse or patchy distributions where less optimal conditions prevail. The dominant criteria that determine habitat suitability at Roberts Bank are the extent of the Fraser River plume, wave exposure, and elevation. At the higher elevation range of its distribution, exposure time above low tide is the limiting factor due to desiccation of the plants; however, the non-native *Zostera japonica* tolerates dry conditions better than the native *Z. marina* and therefore survives at higher elevations. At the lower elevation range, down to approximately -0.5 m CD, photosynthetically available radiation (PAR) appears to be the limiting factor. As a result, the extent of the Fraser River plume, which limits the penetration of light into the water column, and wave exposure, which increases towards the seaward edge of the tidal flats, become more important. Anthropogenic features, such as the causeways and terminals, tend to deflect both waves and the plume, and therefore can alter eelgrass distribution.

The extent of eelgrass beds in the inter-causeway area increased rapidly since the completion of the Roberts Bank and BC Ferries causeways in the early 1970s (Tarbotton and Harrison 1996) due to both the deflection of the Fraser River plume from this area and the creation of a more quiescent wave environment. It was also postulated that the formation of tidal channels contributed to the overall spread of eelgrass by creating an efficient transport mechanism for the distribution of seeds and rhizomes. The extent of eelgrass – both *Z. japonica* and *Z. marina* – on the north side of the Roberts Bank causeway is shown in **Figure 18**. Compared with the extent in 1967, as mapped by Tarbotton and Harrison (1996) (prior to the construction of the Roberts Bank causeway), eelgrass has expanded into

areas that previously were exposed to high turbidity from the Fraser River plume and a more energetic wave environment.

Eelgrass and sediment are structured based on complex two-way interactions. Not only do the tidal flat surface and water column characteristics define the ability of eelgrass to become established, but eelgrass, once established, profoundly modifies the sediment and water conditions within and immediately adjacent to the beds. It creates an environment amenable to densification and lateral expansions of the species. For example, emergent eelgrass creates a much higher hydraulic roughness than bare sediment on the tidal flats; this tends to favour the retention of water long after the tide has receded. This, in turn, can improve plant survival as well as create a significant flow differential compared to areas not covered by eelgrass (e.g. NHC and Triton 2004). Researchers have noted the moderating influence of eelgrass in areas exposed to large waves and high tidal velocities and made linkages with the survival of eelgrass and accretion rates (Stevens and Lacy 2011) as well as the seasonal effect due to growth and senescence (Hansen and Reidenbach 2013).

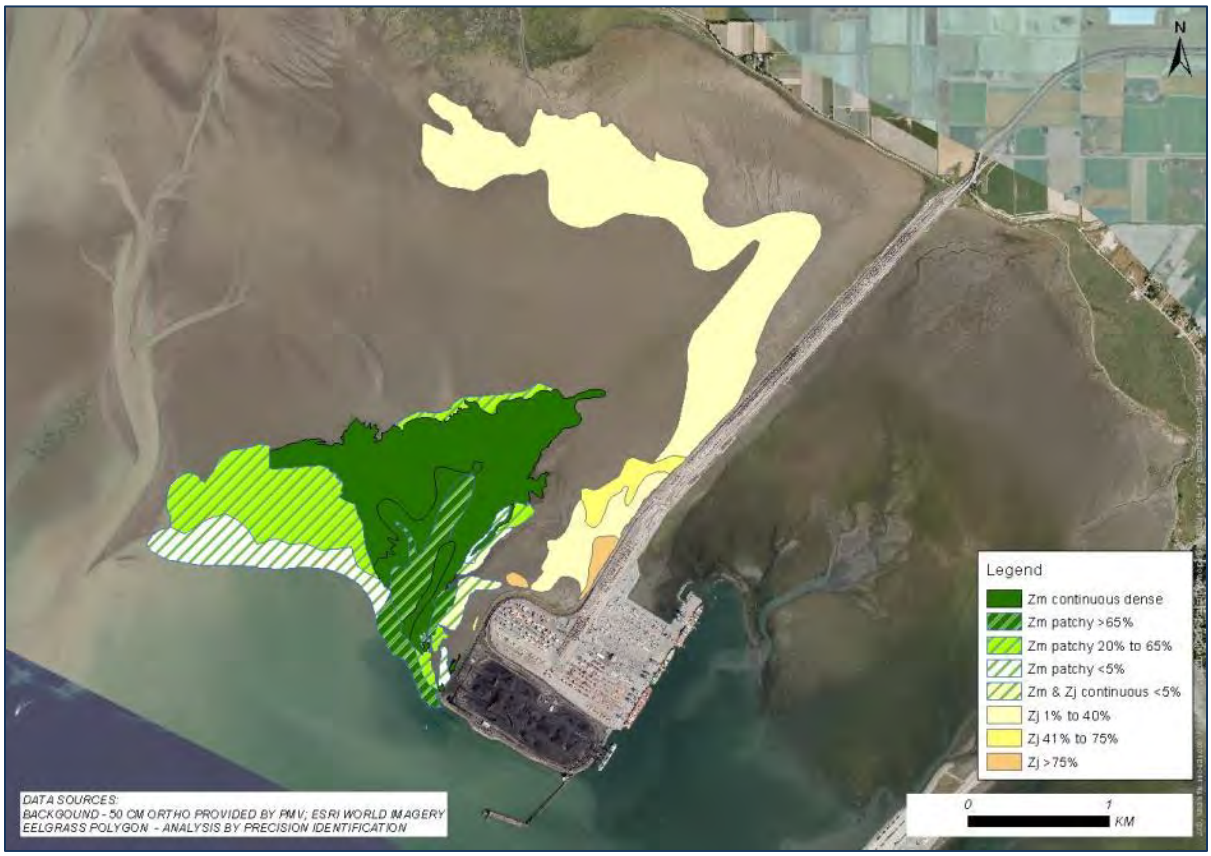

Figure 18: Extent of eelgrass at Roberts Bank on the north side of the Roberts Bank causeway (based on mapping by Precision Identification 2008).

4 DRIVING FORCES

This chapter summarizes the external drivers of long-term morphology and sedimentology near the Project site. The morphology and evolution of the tidal flats is governed primarily by the following four macroscale factors:

- Tidal currents
- Waves
- Fraser River discharge and sediment supply
- Tectonics (subsidence)

Climate change can substantially modify some of these factors and therefore has been described separately in this chapter.

4.1 TIDES

Tidal fluctuations in the Strait of Georgia are driven by forcing and resonance with the tide cycles of the Pacific Ocean, which are predominantly mixed, having two highs and two lows of unequal height in a lunar day. The tidal range near Tsawwassen is up to 5 m Chart Datum (CD), and the mean tidal height is +3.0 m CD. **Table 1** summarizes tidal statistics at Tsawwassen as reported by WorleyParsons (2013).

Table 1: Water levels in the Strait of Georgia near Tsawwassen. Values reported by WorleyParsons (2013).

Tide Level (Chart Datum)	Mean Tide	Large Tide	Extreme Tide*
Higher High Water	4.1	4.8	5.4
Lower Low Water	1.1	0.1	-
Mean Water Level	3.0	3.0	-0.2

*Projected 50-year recurrence interval

In the central Strait of Georgia, the tidal stream is predominantly northwest to north during the flooding tide and south to southeast during the ebbing tide. There are two main components to the tidal currents in the vicinity of the Project. In deeper water, the tide floods towards the northwest parallel to the front of the delta foreslope, while during the ebb tide, the flow is towards the southeast. Over shallower portions of the study area, the flow follows the direction of the slope as the water moves onto and off the tidal flats.

The maximum flood velocity typically occurs two to four hours before high water, while the maximum ebb velocity occurs two to four hours before low water. The maximum speed of the currents offshore from the terminal typically reaches 0.6 m/s during flooding and ebbing conditions.

Tides vary during the lunar month in response to equilibrium between solar and lunar forces to produce spring tides, with neap tides occurring during the first and last quarter of the moon phase. The moon's perigee results in seasonal variation in magnitude of the spring and neap tides. Tidal amplitude (the difference between high and low tide) is plotted in **Figure 19** based on predicted tides at Tsawwassen

for 2012 to illustrate the seasonal variation. The summer months of April to July and the winter months of October to December (and January) are periods of the greatest tidal amplitude, with values exceeding 4.0 m CD during most of the months in these two periods. The intervening periods of lower maximum tidal amplitude – February and March, and August and September – also show longer periods of time when tidal amplitude is less than 2.5 m.

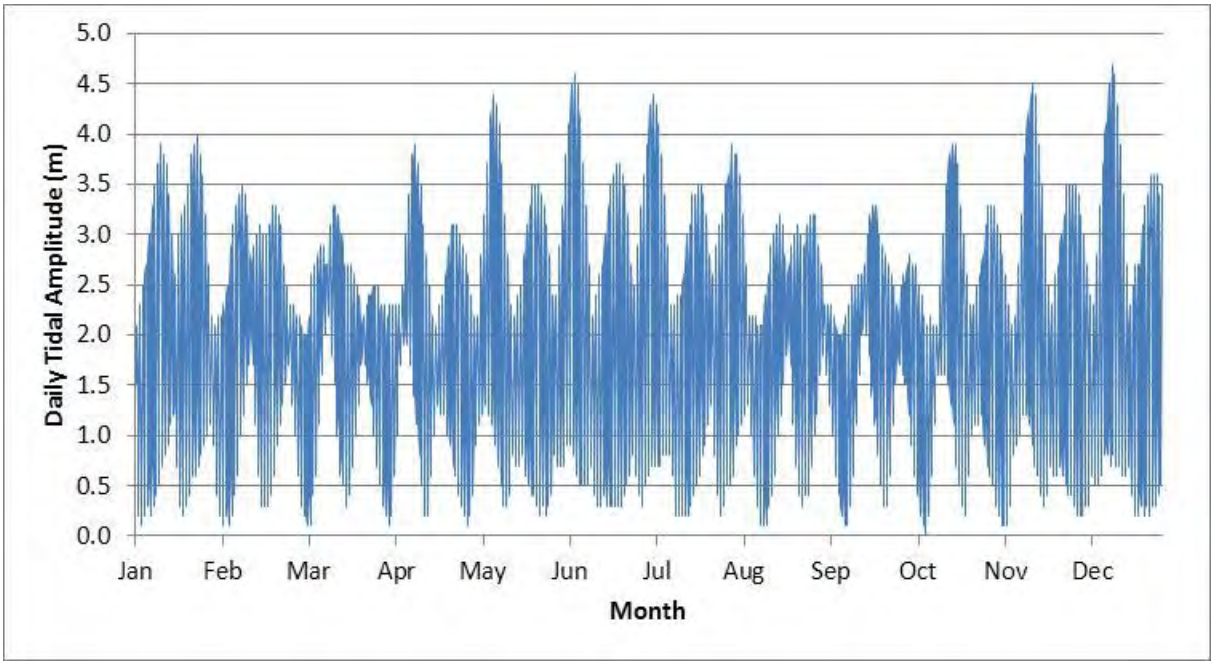

Figure 19: Tidal amplitude calculated based on the Tsawwassen gauge for 2012.

A 19-year lunar cycle is superimposed on the monthly and seasonal lunar tide cycles; this results in inter-annual variation in the height of the higher and lower tidal cycles. For instance, the average level of lower low water varies by approximately 25 cm (Bell Dawson 1923). McKinnell and Crawford (2007) reported that 2006 and other years (1988, 1969) separated by 18.6 years coincide with maximum diurnal and minimum semidiurnal tides. Diurnal inequalities attain their greatest value coincident with a maximum lunar declination (Warburg 1922).

The "diurnal inequality index", which describes the relative difference between higher high water and lower low water, has been calculated for each year from 1983 to 2013 using Point Atkinson (CHS Station #7795) hourly water level data and plotted against the height of the summer seasonal minimum tide (**Figure 20**) and the summer seasonal maximum tide (**Figure 21**). These plots support the concept that diurnal inequality would have been at a maximum in 1988, minimum in 1997 and at a maximum again in 2006. More importantly, there is also a correlation of this index specifically with the maximum summer tidal range and an inverse correlation with the minimum summer tide height. The 2012 tidal year, which was used as a representative input year for the numerical modelling, has a near-neutral diurnal inequality index value of -0.2 (compared to a maximum potential value of -1.0/1.0). At present the long-term cycle is in a period of increasing minimum summer tide levels, and the index provides context for present and future long-term tidal fluctuations at Roberts Bank.

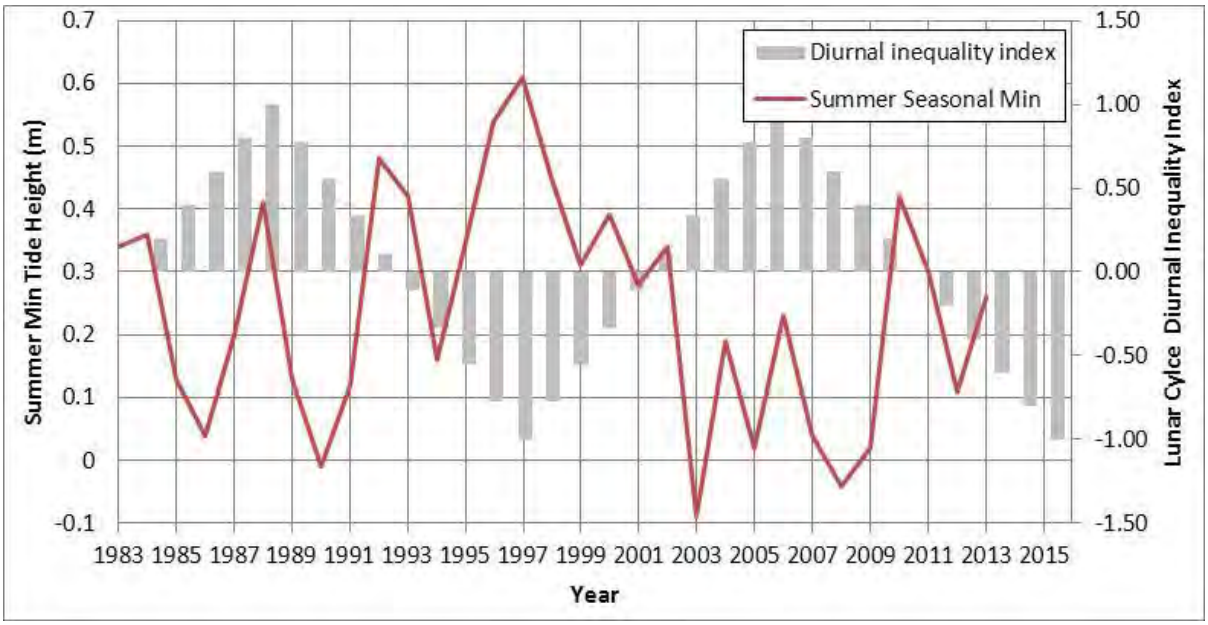

Figure 20: Minimum predicted summer tide height at Point Atkinson (1983-2016).

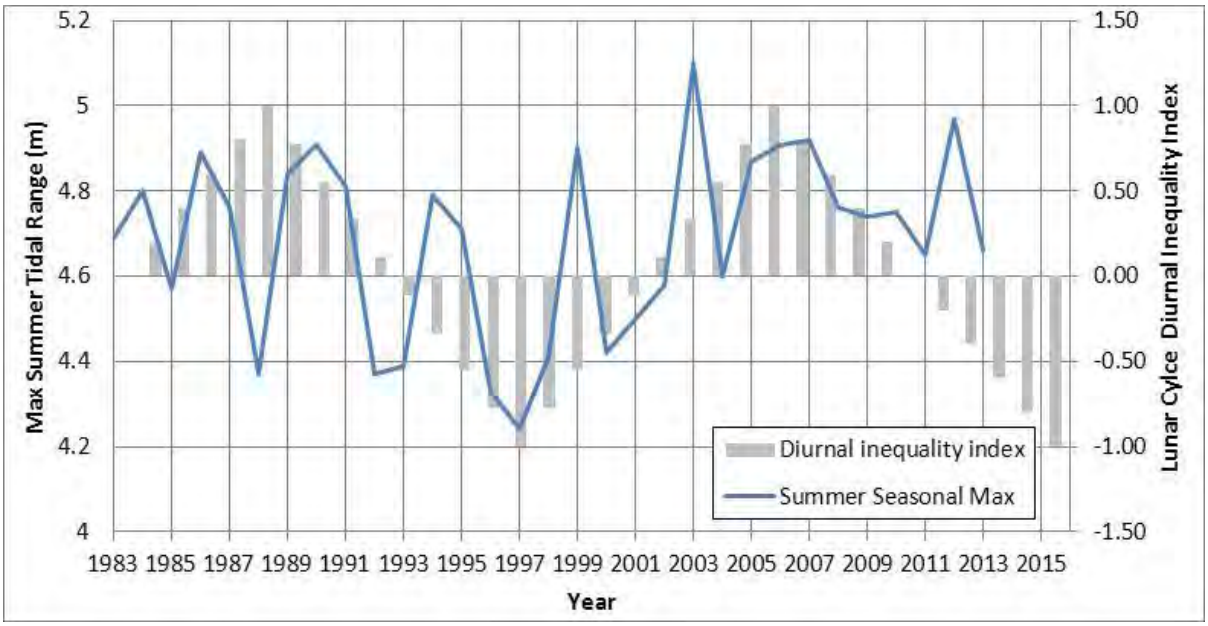

Figure 21: Maximum predicted summer tide height at Point Atkinson (1983-2016).

While the diurnal inequality index has implications for inter-annual variation in the maximum velocities generated during large tidal swings, the actual difference would be quite small compared to the absolute velocity. However, emergence time on the lower and higher elevations on the tidal flats could potentially alter the distribution of certain species or ecosystems that are sensitive to desiccation and exposure to light.

4.2 FRASER RIVER

4.2.1 DISCHARGE REGIME

The Fraser River has a snowmelt-dominated flow regime, with the discharge typically rising in April, peaking between May and July and then receding during the autumn and winter months (**Figure 22**). Based on the flow gauge at Hope (WSC 08MF005), the average peak flow is about 7,000 m^3/s in June and the average low is approximately 850 m^3/s in March. Representative discharges at Mission are as follows:

- long-term mean: 3,340 m^3/s
- mean annual flood: 9,580 m^3/s
- flood of record (1894): 20,000 m^3/s

The river is tidally-affected as far upstream as Mission, 85 km above the ocean. Below New Westminster, the river splits into the Main Arm, Annacis Channel and the North Arm (**Figure 23**).

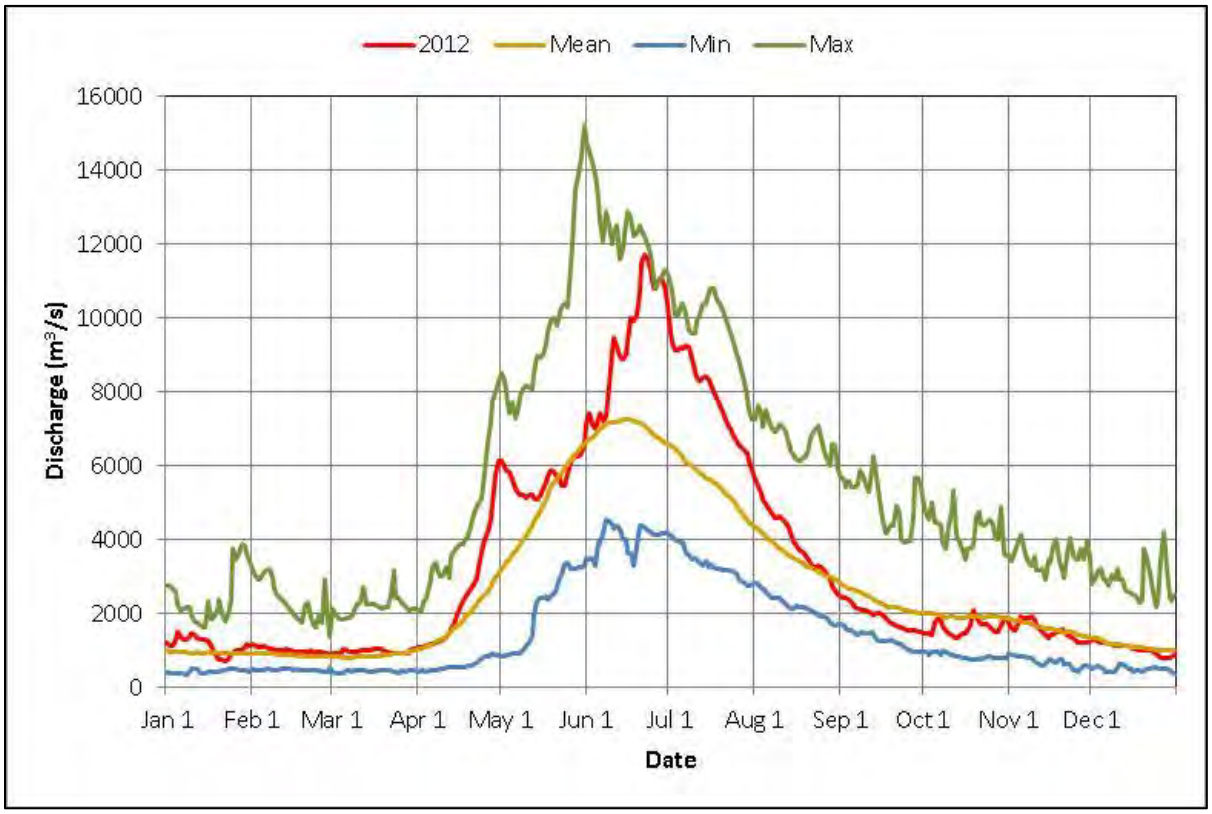

Figure 22: Annual hydrographs of Fraser River at Hope. Data from Water Survey of Canada 2014.

Figure 23: Distribution of flow in distributary channels as measured by PWGSC in 2005 and 2006. Measurements upstream of Km 25 are from freshet conditions in 2005 and down river data are from a single day of flow measurements in January 2006.

The Main Arm divides again just below Deas Island (18 km upstream from the ocean), with a portion of flow diverted into Ladner Reach and then again into Canoe Passage. Estimates of the flow splits in the various branches have changed over time due to the effects of river training and dredging. Accurate estimation of the flow splits is complicated by the tidal influence on the flow. Early results (Keane 1957) were reported in Water Survey of Canada (1970) and indicated that the Main Arm conveyed 90% of the flow below New Westminster, 10% of the flow into Ladner Reach and 5% of the flow through Canoe Passage.

By 1981, PWGSC reported that the amount of flow carried by the North Arm was 15%, with the remaining 85% carried by the Main Arm. In May-June 2005, PWGSC conducted ADCP[1] discharge measurements at several branches of the river in support of flood modelling investigations (NHC 2006). Those measurements indicated that the North Arm carried 10% of the flow at New Westminster, and the flow in the Main Arm just downstream of Annacis Island was 90% of the flow at New Westminster. An additional day of measurements during winter conditions suggested that the flow in Canoe Passage

[1] Acoustic Doppler Current Profiler

was 5.3% of the total flow at New Westminster. A more accurate assessment is possible by comparing daily flows measured at Canoe Passage in 2012-2013 with the total flow of the Fraser River. To determine the total discharge into the Strait of Georgia, the flow at Hope (WSC 08MF005) can be used if downstream inflows are accounted for, or model results from the Fraser River MIKE11 model (NHC 2008) for the period spanning January 1st, 2012 to May 31st, 2013 can be used. The results from both approaches are shown in **Figure 24** and indicate that Canoe Passage conveys 8% of the Fraser River discharge, a relatively small amount compared to other distributaries.

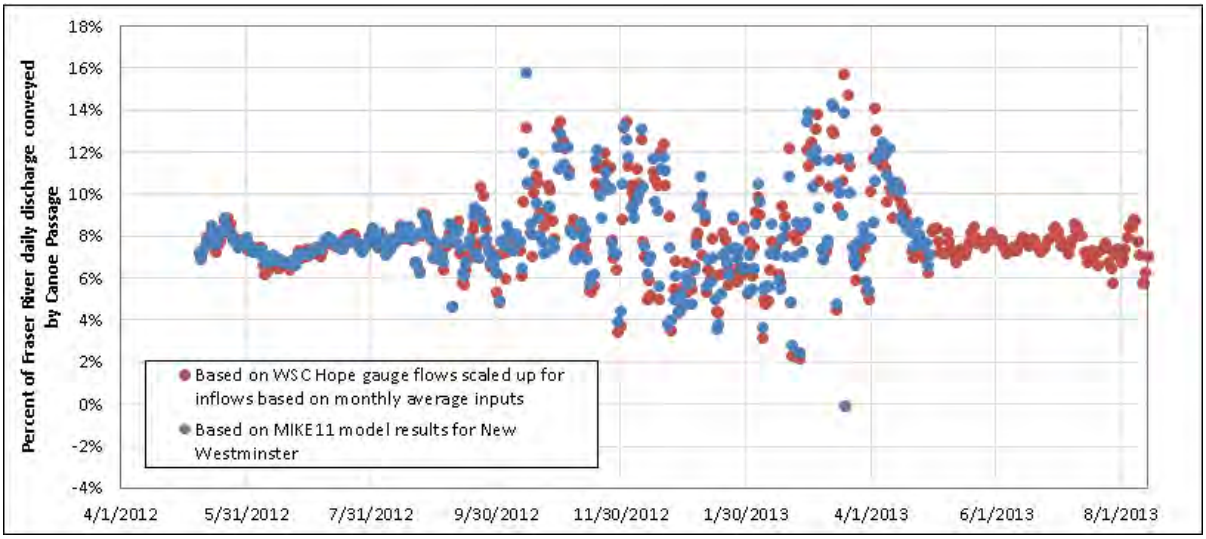

Figure 24: Percent of daily discharge in Fraser River conveyed through Canoe Passage.

4.2.2 SEDIMENT LOADS

During the freshet period (May to July), freshwater from the Fraser River discharges as a jet from the mouth near Steveston into the Strait of Georgia. This less dense water spreads over a portion of the strait as a brackish silt-laden layer with a thickness of up to 10 m. The momentum of the river directs the current in a south-westerly direction. During freshet conditions and low tides, the currents reach up to 2.5 m/s near the river mouth and typically 1 m/s during mean tide conditions.

Sediment loads on the lower Fraser River were measured by Water Survey of Canada at Hope, Agassiz and Mission during the period 1965 to 1986. Based on that data, the total suspended load averaged 17.3 million tonnes/year (range 12.3 million to 31.0 million), with the load consisting of 35% sand, 50% silt and 15% clay (McLean and Tassone 1988, McLean *et al*. 1999). The suspended bed-material load[2] averaged 2.8 million tonnes/year (range from 9.0 million to 1.2 million). The criteria for distinguishing

[2] Bed-material load is that part of the total sediment load of a river which is composed of particle sizes present in appreciable quantities in the shifting portions of the bed.

suspended bed-material load from wash load[3] was based on the Einstein (1950) definition and involved collecting bed samples in the main channel between Mission and Sand Heads and determining the principal sand size classes that form the actively transported channel sediments. A grain size of 0.18 mm was used to distinguish the bed load from the wash load material. Suspended sediment was measured during the 2010 freshet period and the general patterns of sediment transport with respect to discharge and relative composition by grain size that were previously observed were confirmed (Attard et al. 2014). The 2010 sediment budget was found to be in the lower range of historically measured annual suspended sediment loads.

Bed load[4] sampling measurements at Mission and Port Mann indicate that the bed load was less than 5% of the total bed-material load. There are no reliable, long-term sediment transport measurements in the estuary, although considerable effort was made to measure loads at Port Mann during the 1960s (the tidally-varying flow conditions made it impractical to determine transport rates reliably). An estimate of the annual bed material load between Mission and the river mouth at Sand Heads was made by McLean and Tassone (1988) using a sediment budget approach, based on measurements at Mission, observed changes in channel topography, and dredging volume records. That analysis indicated that the annual bed material load delivered to the mouth of the river at Sand Heads was roughly 30% of the load at Mission during the period 1972 to 1997. As Water Survey of Canada discontinued its program of systematic sediment transport measurements on the lower Fraser River over 25 years ago, it is unclear whether these estimates are representative of present or future conditions.

It is not known whether there are any historic sediment transport measurements in Ladner Reach or Canoe Passage. An approximation of sediment transport through Canoe Passage can be made by assuming the fraction of the sediment load will be the same as the flow split (about 8%). This assumption results in a total load of 1.38 million tonnes/year and a bed material load of 220,000 (sand >0.18 mm) tonnes/year. A considerable effort was made to monitor flow and suspended sediment concentration in Canoe Passage throughout 2012 and 2013 as part of this study (**Appendix C**). The annual suspended load in Canoe Passage was estimated to be approximately 930,000 tonnes in 2012 and 460,000 tonnes in 2013, with the sand fraction (>0.063 mm) amounting to 65,000 and 32,500 tonnes in 2012 and 2013 respectively (**Table 2**). The 2012 freshet was a large event, having a return period of 20 years (at Hope gauge 08MF005), and it is assumed that the transport rate in 2012 was substantially higher than the long-term average load. The 2013 freshet had a daily peak flow with a return period of about five years but was quite short in duration. These results suggest that the contemporary sediment load is less than what the historical load scaled to Canoe Passage would imply. Considering the reduced entrance velocities and higher elevation channel entrances associated with the distributaries that lead to Canoe Passage, it is not surprising that Canoe Passage transports less sediment than estimates based on the flow split would suggest. These results demonstrate that the amount of sand available to be supplied to the tidal flats from Canoe Passage is very small in most years.

[3] Wash load is that part of the total sediment load of a river which is composed of particle sizes finer than those generally found in shifting portions of the bed.

[4] Bed load refers to the sediment that is transported along the streambed by sliding, rolling or bouncing.

Table 2: Annual suspended sediment load in Canoe Passage based on 2012 and 2013 measurements.

Year	Suspended Load Tonnes/yr	Sand Load (>0.063 mm) Tonnes/yr
2012	935,000	65,000
2013	465,000	32,000

River training works that were installed beginning in the early 1900s prevent the Main Arm from migrating across the tidal flats to distribute coarse sediments. As a result, the coarse sediment transported through the lower reaches of the Main Arm discharges into deep water off the channel mouth and avalanches down the delta front. There is thought to be little or no delivery of coarse sediment to the Roberts Bank tidal flats further to the south.

The sediments that make up the tidal flats between Canoe Passage and the Roberts Bank causeway mainly consist of non-cohesive sand and silt; cohesive (silty-clay) sediments are limited to the upper portion of the tidal flats. Compared to the volume of sand stored in tidal flats, the net sand transport flux onto the tidal flats (amount of ongoing annual deposition) is believed to be very low.

The fine silt and clay sediments carried in the freshwater that is discharged from the Fraser River spread as a plume out into the Strait of Georgia, reaching as far as the Gulf Islands (**Figure 25**). Sedimentation rates over the tidal flats of Roberts Bank appear to be entirely dependent on the material that is delivered from the plume as there is no obvious mechanism for the coarser sediments to be transported shoreward once deposited in deeper water.

Figure 25: Portion of 1999 Landsat image of the Strait of Georgia showing the extents of the Fraser River plume during a summer ebbing tide.

4.2.3 SALINITY

Lower density freshwater from the Fraser River discharges into the saline waters of the Strait of Georgia in the form of a sediment-laden plume (**Figure 25** and described above). The lower density freshwater from the river initially floats on the surface but to some extent mixes vertically over time due to tidal currents and waves. The areal extent of the plume is dependent on river discharge, tidal currents, and wind. The plume extends across the Strait of Georgia during high discharge periods and is more localised during winter low-flow periods.

The moderating influence of freshwater from the river can have a profound effect on biotic communities, including the composition of salt marsh plants (GL Williams & Associates Ltd. and NHC 2009). Depending on the proximity to one of the Fraser River distributary channels, the effect can be nearly continuous, or can vary on a daily or seasonal basis. Physical structures, such as the Roberts Bank and BC Ferries causeways can influence the extent of this influence by diverting the plume; for instance, the plume is believed to be excluded from the inter-causeway portion of Roberts Bank.

Field data collection during 2012 included measuring vertical profiles of turbidity and salinity at Roberts Bank during the freshet during various dropping and rising tides. The sample locations are shown in **Figure 26**. The results, presented and described in **Appendix C**, demonstrate a distinct boundary between the sediment-laden fresh water near the surface and the relatively clear saline water at depth.

A sample of the measurements that were collected on June 14, 2012 is presented in **Figure 27**. Limited vertical mixing was found to occur over time as depths decreased (because of the dropping tide) but was found to be almost complete at the shallowest site (T5). Vertically-integrated values of average salinity at Roberts Bank are presented as part of the model results in **Section 6.3**.

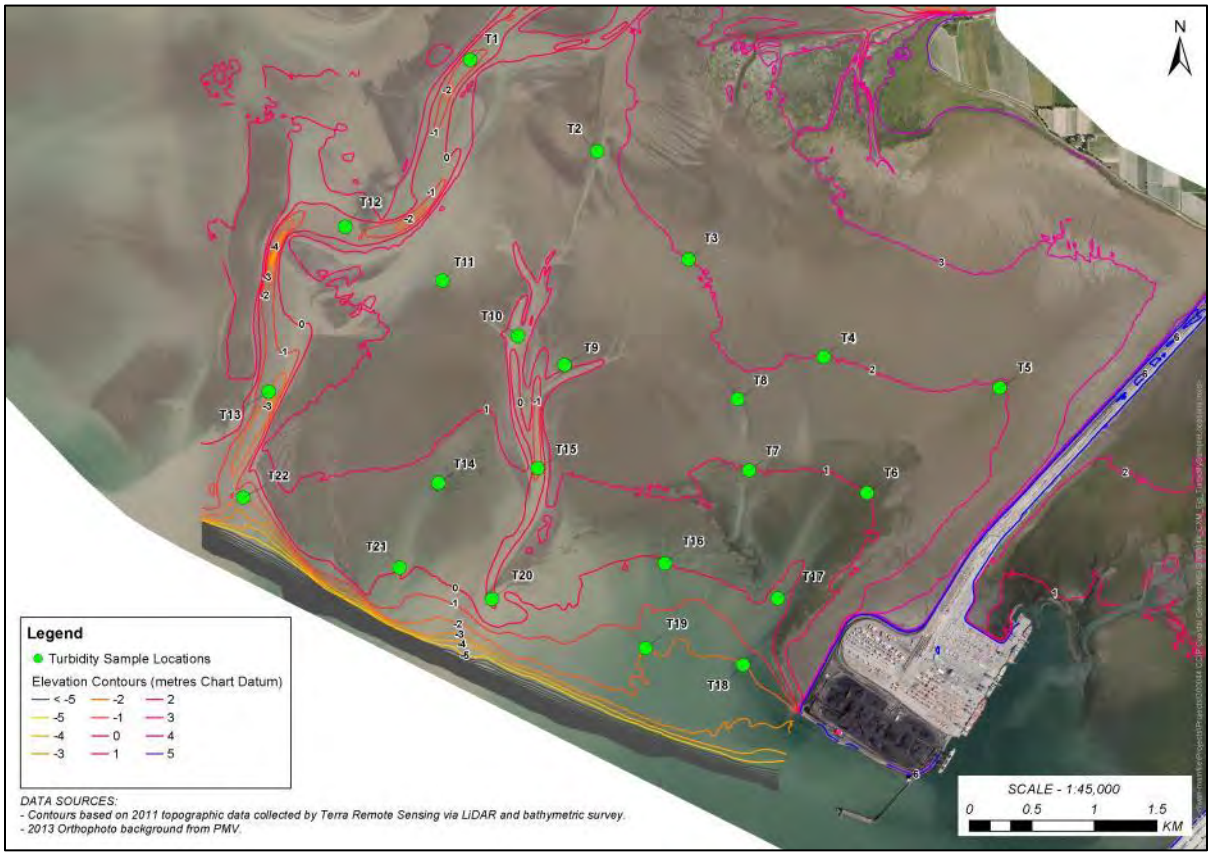

Figure 26: Turbidity and salinity sampling locations on Roberts Bank.

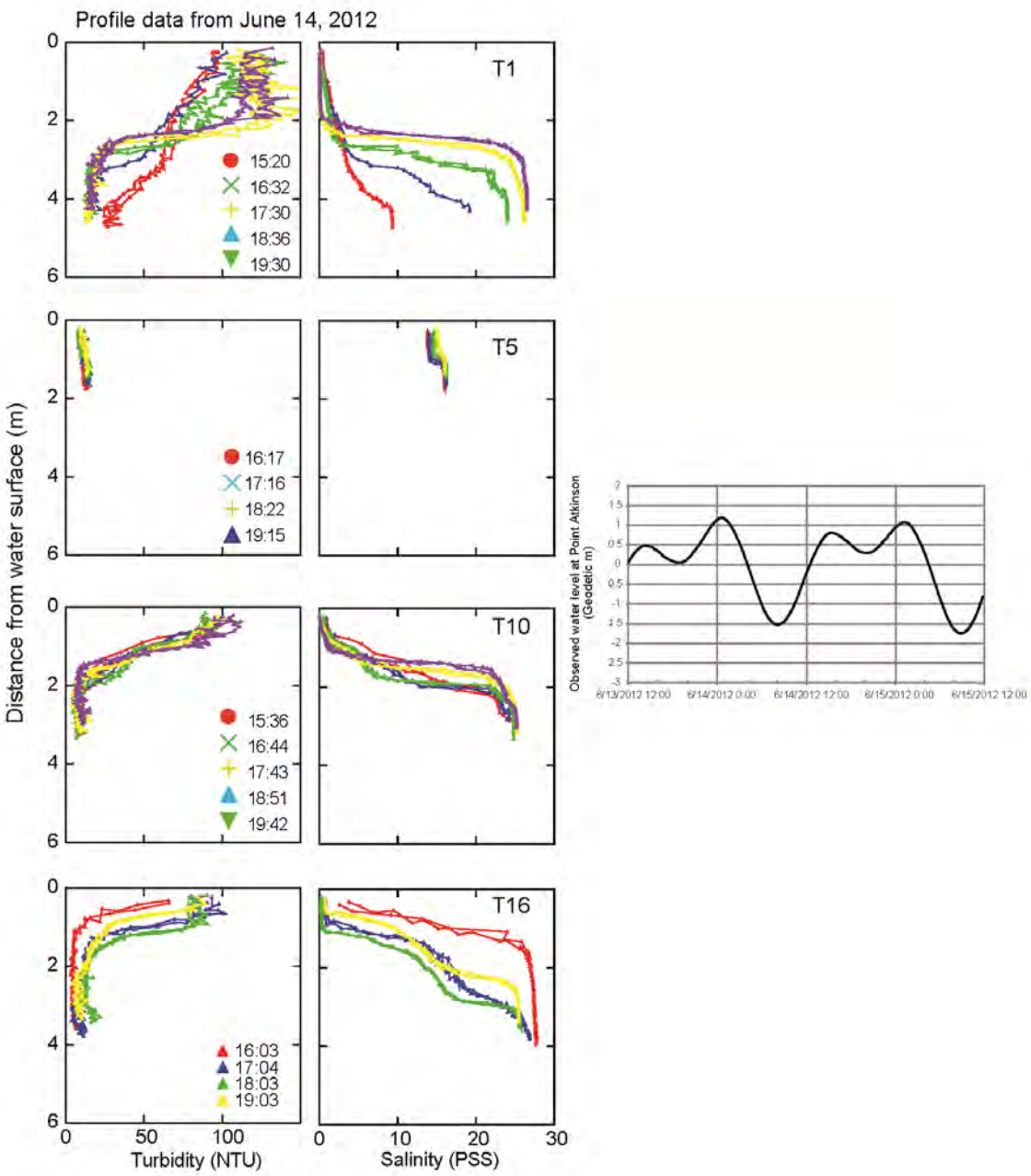

Figure 27: **Turbidity and salinity profiles collected on June 14th, 2012 at select locations across the Roberts Bank tidal flats. The tide curve during the period of measurement is also shown.**

4.3 WAVES

The immediate study area is exposed to open water wind-generated waves from the northwest, west, southwest, south and southeast directions. Wind speed and direction have been recorded at several stations in the region. The wind rose shown in **Figure 28** is derived from hourly records at Sand Heads

(1991 to 2013). Winds most frequently blow from the northwest and southeast and are the dominant driving force for wave generation, both in terms of frequency of occurrence and maximum wind speeds.

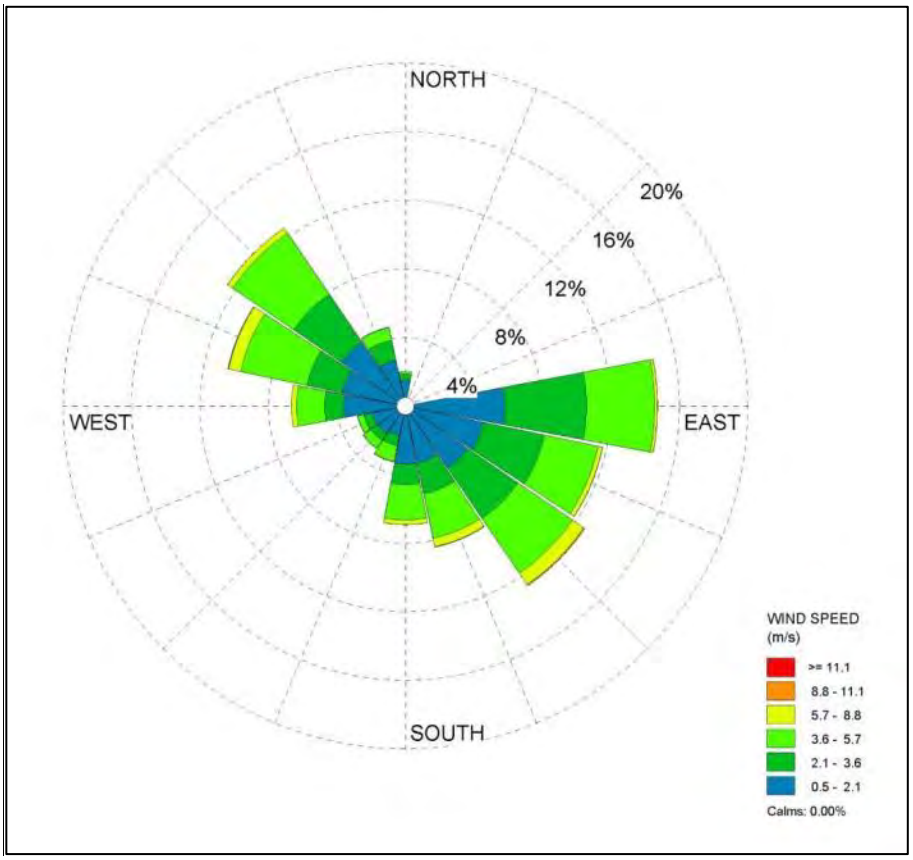

Figure 28: Wind rose for Roberts Bank based on wind data measured at Sand Heads from 1991 to 2013.

The height of waves propagated in deeper waters and arriving at the study area is a function of wind speed, duration of time that the wind has blown, and the distance over which the wind acts on the water (fetch). The largest offshore waves are generated from the southeast (SE), south (S) and northwest (NW) directions. Deep water wave hindcasting predicts that the significant wave height exceeds 2.0 m for a total period of 105 hours/year on average (approximately four days per year). Waves from the SE and S directions account for 100 hours/year of the total duration, while the remaining 5 hours/year are from NW waves.

Table 3 compares the significant wave height (H_s) and peak wave period (T_p) for a specified frequency of occurrence (12 hours/year). Waves from the SE are substantially larger for a similar frequency of occurrence and indicate that waves, like currents, will tend to move sediment northward. Prior to the construction of the causeways, waves would have transported sand from Point Roberts northward onto the delta.

Table 3: Wave conditions at Roberts Bank for an exceedance frequency of 12 hours/year.

Direction	H_s (m)	T_p (sec)
SE	2.5	7.5
S	1.5	6.2
W	1.4	5.8
NW	1.8	6.4

As waves enter the shallower waters of the tidal flats, there is a greater interaction between the base of the wave and the bed. Basal friction results in a decrease in wave height that is a function of initial wave height and water depth (or tide stage). Wave height decay is at a minimum during very high tide stages but results in very small waves arriving at the upper shoreline.

4.4 TECTONICS AND DELTA SUBSIDENCE

The land surface of the Fraser River delta is subsiding due to settling and compaction of the recently deposited sediments. Subsidence rates vary across the delta because of the variations in the depositional history, thickness of sediments across the delta, and thickness of the underlying Pleistocene unit (Hunter and Christian 2001).

An ongoing study by Hill *et al*. (2013) at Roberts Bank employed InSAR[5] technology to detect surface movement over several years, with the capability of resolving movements on the order of about 1 mm/year. Rates of uplift or subsidence were mapped across Metro Vancouver (**Figure 29**) and show that the Holocene delta in the municipalities of Richmond and Delta is subsiding at rates from 0 to 3 mm/year. Subsidence was noted to be occurring more rapidly (2 to 3 mm/year) in areas where fill has been added to facilitate relatively recent construction, such as the Roberts Bank terminals and BC Ferries terminal.

[5] Interferometric Synthetic Aperture Radar

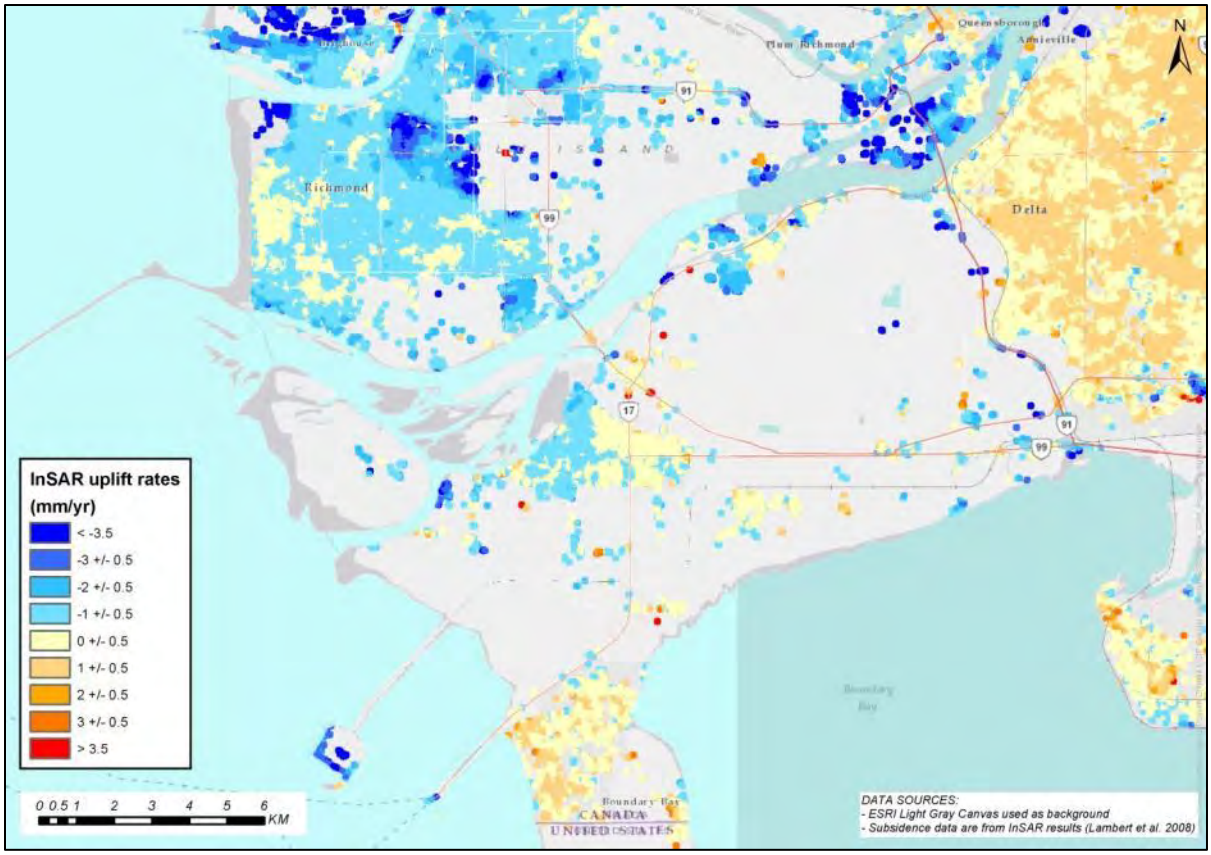

Figure 29: Uplift and subsidence rates across the western part of Metro Vancouver (various sources - from Hill *et al*. 2013).

Based on these values, the potential subsidence of the tidal flats in the general vicinity of the Project will be on the order of 0.1 to 0.15 m over a 50-year horizon. Construction of the elevated land mass, including pre-loading, to form the Project will likely result in additional localised subsidence, which is not accounted for here.

4.5 CLIMATE CHANGE

Climate change could appreciably change four of the macroscale factors that influence Roberts Bank: i) sea level, ii) Fraser River discharge, iii) Fraser River sediment loads, and iv) wave climate. It is important, therefore, to evaluate the current state of knowledge about these processes.

4.5.1 ASSUMPTIONS

Although estimates of timing and magnitude vary, it is generally accepted within the scientific community that anthropogenic impacts on the earth's atmosphere will have a profound impact on global climatic conditions. Globally, climate change is expected to result in changes to synoptic weather patterns, increase the frequency and intensity of storms, alter current trends in summer and winter temperature extremes, and increase the volume of water in the world's oceans (IPCC 2013). Predictions of global trends do not necessarily downscale to local conditions.

The following factors have been considered as potential effects on the driving forces for this geomorphic assessment:

a) sea level rise,

b) changes to the magnitude and frequency of storm events in the Strait of Georgia, and

c) changes to the flow regime and sediment inputs from Fraser River.

4.5.2 CHANGES TO SEA LEVEL AND WAVE CLIMATE

Based on worldwide tide gauge records, global sea level has risen more than 0.2 m since the late 19th century (Thomson *et al*. 2008). The rate of sea level rise is expected to be considerably greater in the 21st century. However, projections of sea level rise are highly uncertain.

Estimates of local sea level rise are determined by combining eustatic ocean level changes as well as isostatic changes of the coastline caused by subsidence or uplift. As described in **Section 4.4**, the rate of subsidence on portions of the Fraser Delta is approximately 2-3 mm/year. In 2008, Fisheries and Oceans Canada published forecasts of relative sea level rise for the year 2100 on the Fraser Delta for three scenarios (Thomson *et al*. 2008):

- Low estimate: 0.35 m
- Medium estimate: 0.50 m
- Extreme high estimate: 1.20 m

The relative sea level rise values are referenced to the year 2000 and incorporate the effects of both rising ocean levels and land subsidence.

In January 2011, the Province of BC adopted a rate of sea level rise of 0.5 m by the year 2050 and 1.0 m by the year 2100 (10 mm/year) for the purposes of planning for coastal flooding throughout British Columbia (Ausenco-Sandwell 2011). The assumed sea level rise relation is shown in **Figure 30**, and the estimate for 2050 coincides with the medium scenario in Thomson *et al.* (2008). Based on the terms of reference for this study, the time frame for assessing the Project is 50 years from its completion date in 2023. The relative sea level rise that is predicted to occur within that timeframe based on the median projection shown in **Figure 30** is approximately 0.5 m. In reality, a 0.5 m relative sea level rise may occur before (or after) the Project horizon year, and that estimate was adopted in the analysis of future conditions within this study.

There is more uncertainty about the effect of climate change on storm magnitude and frequency than its effect on sea level. Although there is an accepted popular assumption that storms will become stronger and more frequent in the future, the analysis conducted in support of the Provincial guidelines for coastal flooding concluded that there was no statistically significant indication that the existing storm population would not "provide a reasonable model for the expected storm population in the future" (Ausenco-Sandwell 2011). Given the lack of strong science indicating otherwise, the assumption has been made that storm conditions will remain constant within the time horizon of this study.

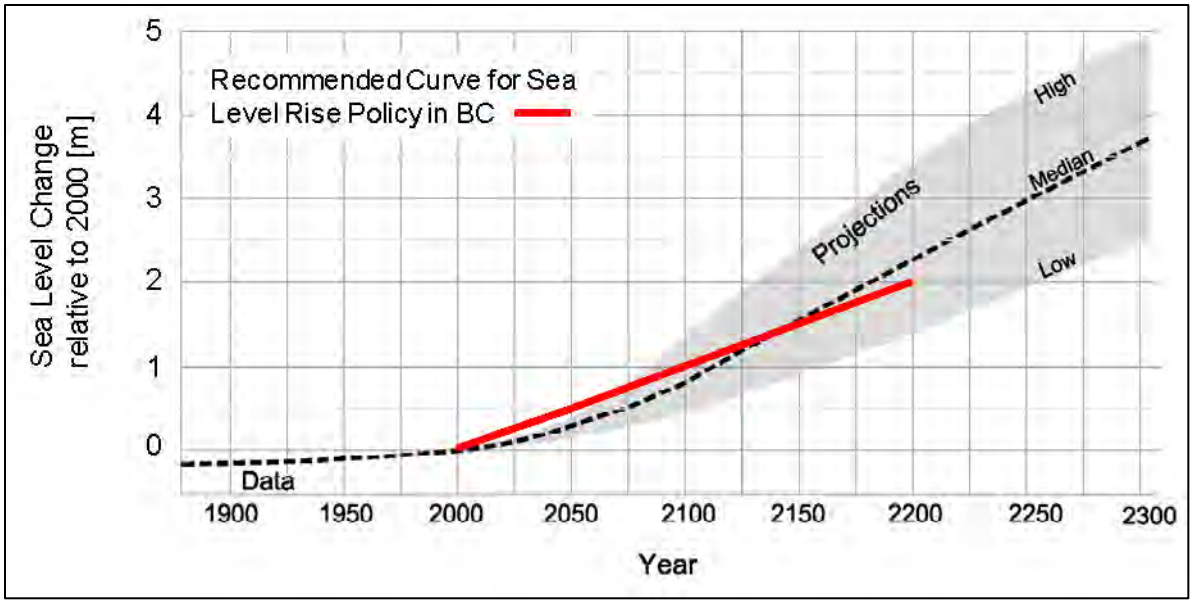

Figure 30: Projected sea level rise used in BC Ministry of Environment Climate Change Adaptation Guidelines (Ausenco-Sandwell 2011).

4.5.3 CHANGES TO FRASER RIVER FLOWS AND SEDIMENT LOADS

The Fraser River basin encompasses a wide range of climatic and physiographic regions. The hydrologic response of Fraser River to future climate change will be complex and, given the large drainage area, this response could potentially be largely self-moderating. Limited scientific studies have been conducted on the influence of past land development and resource extraction influences within the Fraser River watershed on sediment transport and the associated geomorphic responses down-river: for instance, those brought about by widespread placer mining in the mid-nineteenth century (Nelson and Church 2012). However, accurate predictions of future trends in sediment yield related to climate change have not been studied. Given the likelihood that the climate change signal would be very difficult to identify in such a large watershed, the assumption has been made that Fraser River discharge and sediment yield will remain constant within the time horizon adopted for this study.

5 MORPHOLOGICAL CHANGES ON ROBERTS BANK

This chapter summarizes trends in sedimentology and morphological change on the tidal flats over the last century and describes the response of the tidal flats to past developments, including anthropogenic changes. Understanding the long-term response of the physical environment to past disturbance and interventions is critical for assessing the future conditions near the Project site. The assessment is based on a review of past research conducted over the last several decades by the Geological Survey of Canada, other government agencies and academic researchers, as well from other site-specific field and office studies conducted as part of this study.

5.1 OVERVIEW OF ANTHROPOGENIC DEVELOPMENTS

The configuration of the delta prior to major engineering modifications is illustrated from the early navigation charts that date back to 1859-1860 when HMS *Plumper* surveyed the Fraser River and offshore delta areas (**Figure 31**).

Information on the early history of diking and river training comes from reports by Morton (1949) and Sinclair (1961). Efforts to control the mouth of the river began in 1886 with the building of brush mattresses and rock jetties to close side channels breaking out from the main channel through Sand Heads (Morton 1949). Between 1886 and 1893, a 4 km-long training wall was constructed about two kilometres south of the present main channel to confine the flow as it spilled across the northern portion of Roberts Bank. This was followed by the construction of a second structure on the north side of the channel from 1889 to 1892. A low-level berm was in place at Westham Island by the 1880s; however, it was overtopped or failed during the 1894 flood.

Figure 31: Chart of the Fraser River delta from 1860 surveyed by Great Britain Admiralty (Library and Archives Canada[6]).

More extensive development started in 1910. The Steveston North Jetty was built in stages from 1911 to 1932 and the South Jetty was constructed between 1930 and 1932. The training wall at Woodward Island was constructed in 1925-26 while the first Albion Jetty was constructed in 1935. As a result of these structures, the channel in the estuary was significantly narrowed and deepened in comparison to conditions that existed in 1894. The channelized section of river was also extended approximately nine kilometres seaward, mainly as a result of the Steveston North Jetty. The Kirkland Island Bifurcation was completed more recently in 1949, dividing the flow between the Main Arm and Ladner Reach. The general location of these works is shown in **Figure 32**.

[6] http://www.bac-lac.gc.ca/eng/Pages/home.aspx

Figure 32: Historic training works installed at the mouth of the Fraser River.

The history of dykes is less well-documented. Sea dykes were first constructed in the 1800s in the Fraser River delta. By the time of the second largest flood of record in 1948, dykes had been constructed along much of the lower Fraser River (Fraser Basin Management Board 1994). However, the dykes failed during this flood at a number of locations throughout the lower valley. Dyke upgrades were undertaken following the 1948 flood and in 1968 the Fraser River Flood Control Program was established, which ensured further upgrading and expansion of dykes until 1995, when the agreement terminated. This extensive diking program has resulted in the river being confined to a relatively narrow strip of the delta compared to historical conditions, particularly downstream of Mission.

Development on the tidal flats for transportation and shipping occurred more recently. The BC Ferries terminal and causeway were constructed between 1958 and 1960. Construction of the Roberts Bank causeway and terminal began in the early 1960s and finished in 1969. The terminal was expanded between 1979 and 1982 by dredging a ship-turning basin on the flats. In response to the subsequent formation of a network of tidal channels, a crest protection structure was built in 1981 to arrest this development. Dredging near the BC Ferries terminal also initiated channel development, following which a spur was constructed in the early 1990s. More recently, the Deltaport terminal was expanded to include a third berth; its construction began in 2007 and was completed in 2009.

5.2 PLANFORM CHANGES

Planform refers to the shape of features as seen from above and are interpreted from aerial photographs and orthophotos. The largest planform changes on the tidal flats occurred in the 19th

century and early decades of the 20th century when the Fraser River was channelized and trained by a series of jetties west of Steveston. A comparison of the 1860 channel configuration (**Figure 31**) with its contemporary alignment (**Figure 32**) shows the main channel used to pass through Ladner Reach (bringing more water into Canoe Passage). The outlet of the main arm flowed in a wide, relatively shallow channel across Roberts Bank well south of its existing route. The supply of sand to the southern portion of Roberts Bank was probably considerably higher in the 1860s than during the last 80 or more years.

Planform changes on the Roberts Bank tidal flats near the Project were assessed through an analysis of airphotos and orthophotos available for different time periods. The photos examined provide a comprehensive history that spans the period from 1932 to 2013. The imagery has been collected at a variety of scales, with the greatest detail of the area between Canoe Passage and the causeway in the pre-digital imagery era presented in the 1949, 1963, 1979 and 1995 photos. Many of the photos were rectified by NHC to reveal changes in planform; certain features were also mapped in successive photo years for comparison.

Some key changes in planform are discussed below and outlined in **Figure 33** through **Figure 38**. An index map showing the location of the airphoto comparisons is shown in **Figure 12**. The alignment of Canoe Passage across the tidal flats was mapped from airphotos and shows distinct changes over time (**Figure 33**). In 1938, the channel made an unusually sharp turn southwards immediately upon reaching the sand flats (**Figure 34**); the bend is substantially sharper than typical river bends in alluvial material. While it is not known how this bend came about, it is speculated that a large storm with winds from the northwest may have pushed the outlet of Canoe Passage south as part of the along-shore movement of sediment. Large storms occurred in both October 1934 and January 1935. The 1949 imagery shows Canoe Passage flowing southward across the tidal flats, with its position roughly corresponding to that of the existing relict tidal channel. Between 1949 and 1971 the channel changed its alignment to flow further east, a similar path to the present-day. Since 1971, the alignment of the channel has changed very little; however, ongoing lateral shifting near the mouth of Canoe Passage at the delta front has caused periodic channel incision and erosion. Monitoring by NHC in 2012 showed no channel change during the freshet period.

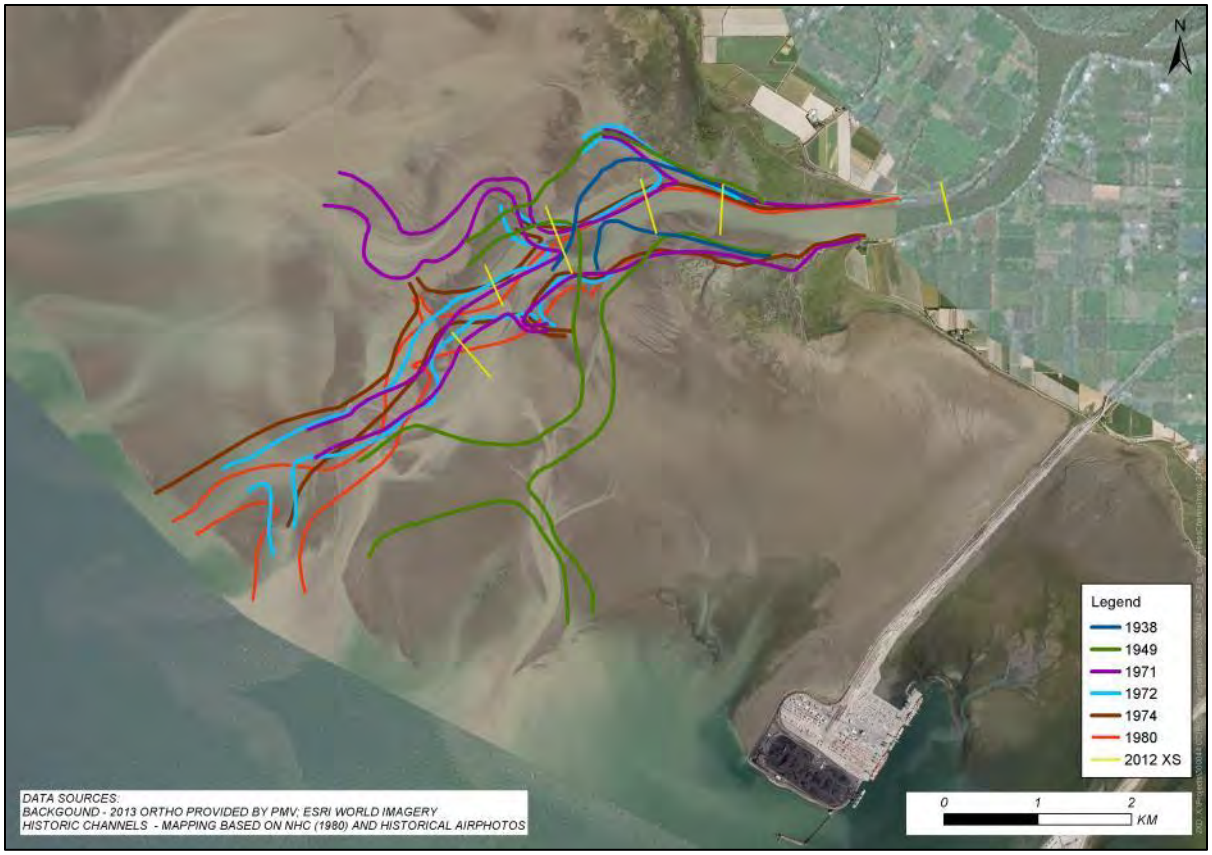

Figure 33: Observed alignments of Canoe Passage across Roberts Bank over the past 74 years.

Striations visible on the tidal flats in the 1949, 1959 and 1963 photos may be indicative of the fact that the tidal flats historically drained in a northwest to southeast direction. Construction of the BC Ferries causeway in 1960 and the Roberts Bank causeway in 1969 are thought to have altered the direction of flow. The response, observed in the 1979 photos, has been to drain in a north-south direction, parallel to the causeways but modified due to local topographic controls. In addition to altering the direction of dominant tidal flow, the Roberts Bank causeway altered local topography, particularly where it meets the shoreline, and has allowed a zone of saltmarsh to establish along the fringes of the causeway (**Figure 35**).

Figure 34: Airphoto from 1938 showing the abrupt bend in Canoe Passage towards the south.

Further north, the general direction of the channels has remained the same (**Figure 36**), but the exact location of the channels has continued to change over time. The salt marsh has expanded seaward and the area of relatively uniform elevation (presently an area of high biofilm productivity) between the ridge and runnels and the uplands has also expanded seaward. Some of the channels associated with the runnels on the shore side of the complex have developed a sinuous channel pattern after initially being straighter. Overall, the impression is that the runnels have become more developed with time, but differences in image resolution confound the interpretation.

Figure 37 shows the changes that occurred to a sharp bend in a runnel complex and demonstrates that the channels can migrate laterally. Since 1979, this particular bend has stabilized and the channel is no longer adjusting laterally. However, at the seaward side of the ridge and runnel complex, where the

channels drain on to the sand flats, lateral channel migration has occurred in the last decade. Based on **Figure 36** and **Figure 37**, it appears that once the ridge and runnel complex reaches a certain rugosity (i.e., elevational difference between the tops of the mounds and the adjacent runnels), lateral migration of the channels is reduced, since recent lateral migration is only occurring at the seaward and inland margins of the ridge and runnel complex. Nonetheless, the main distributaries through the ridge and runnel area tend to persist over years and decades, suggesting that while lateral channel migration is part of the dynamic equilibrium in this area of the Roberts Bank mudflat, the rate of discernible change occurs over a period greater than across seasons or individual years.

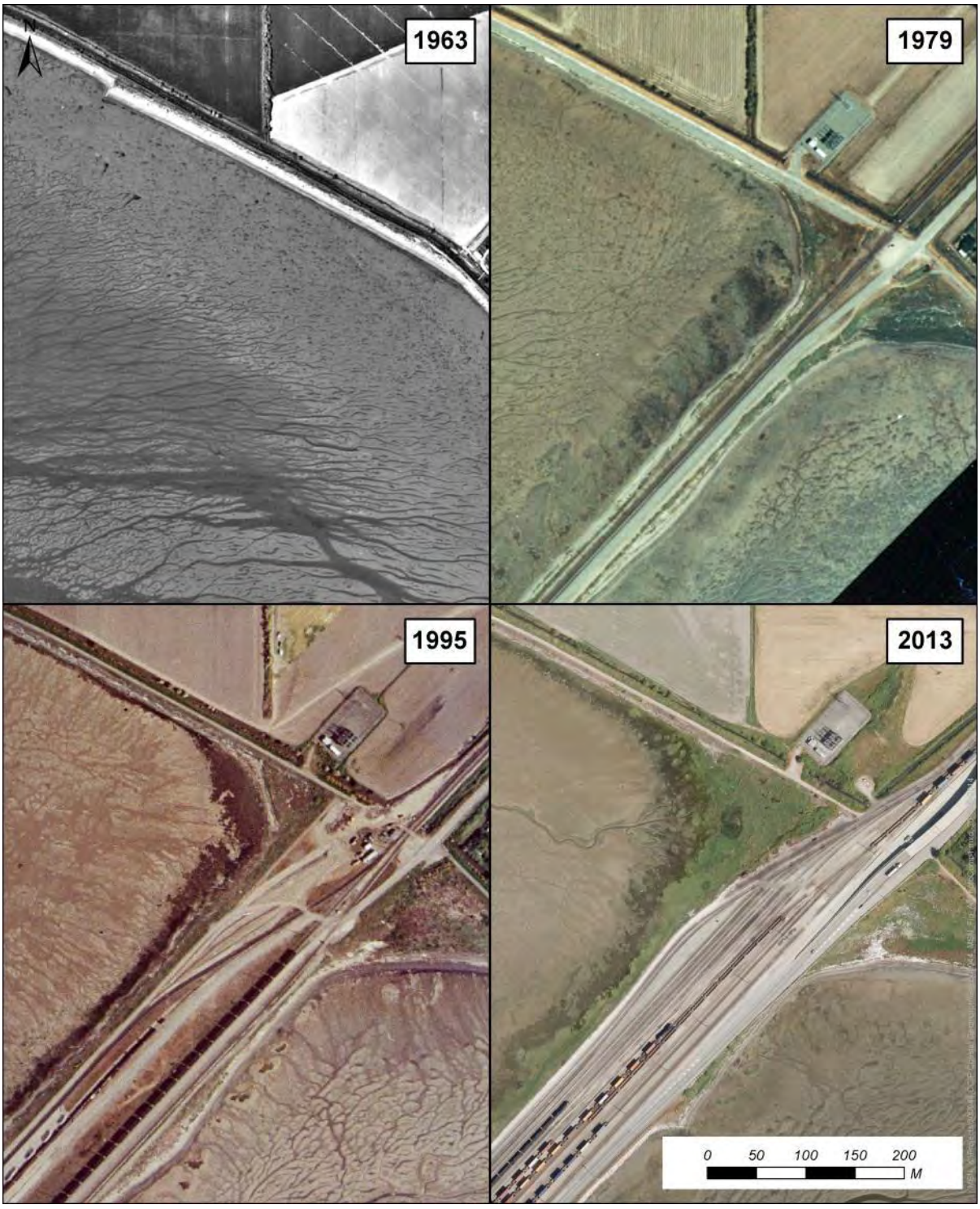

Figure 35: Planform changes on the tidal flats immediately adjacent to the Roberts Bank causeway where it intersects the shore.

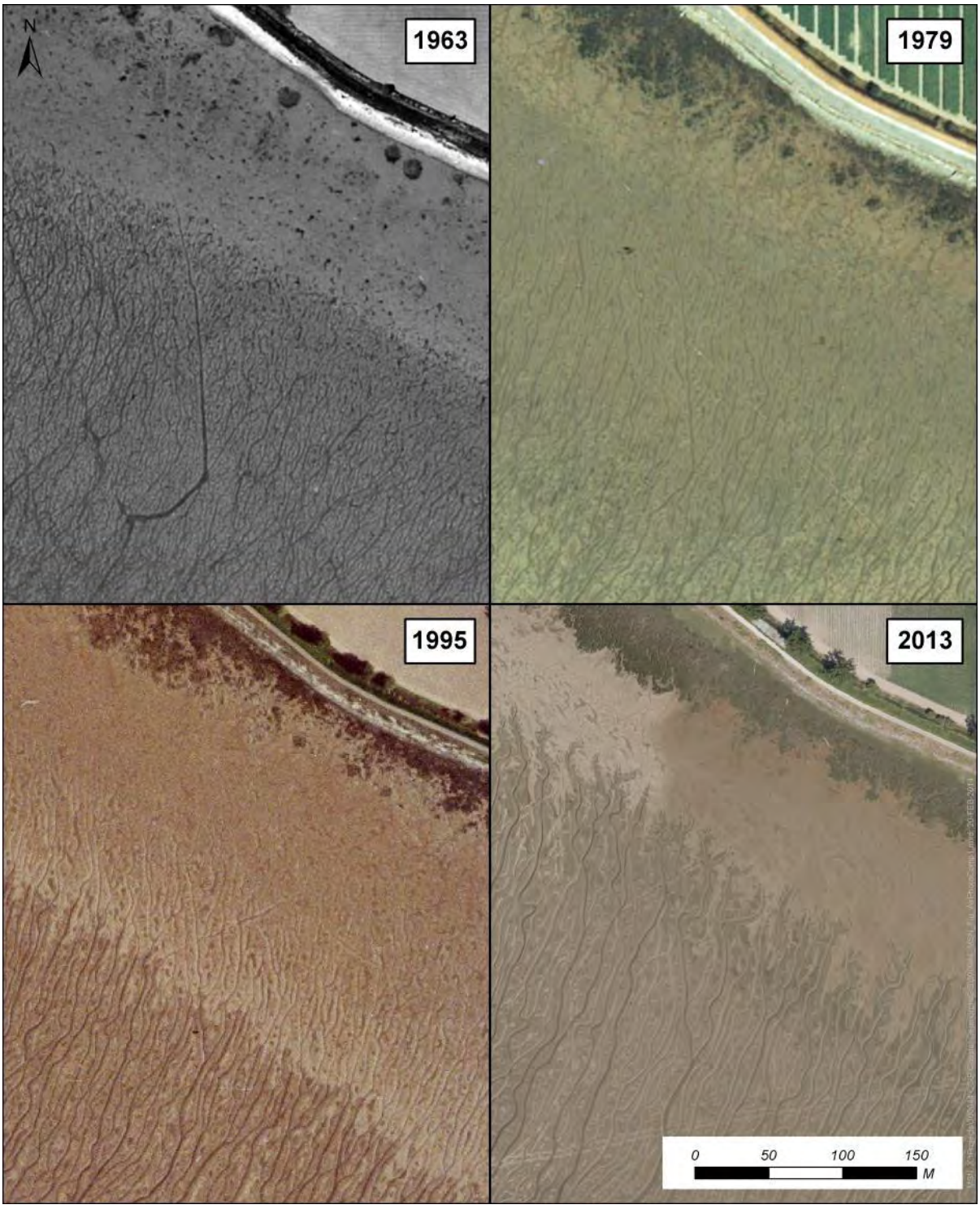

Figure 36: Planform changes at the head of the tidal flats near the ridge and runnel complex.

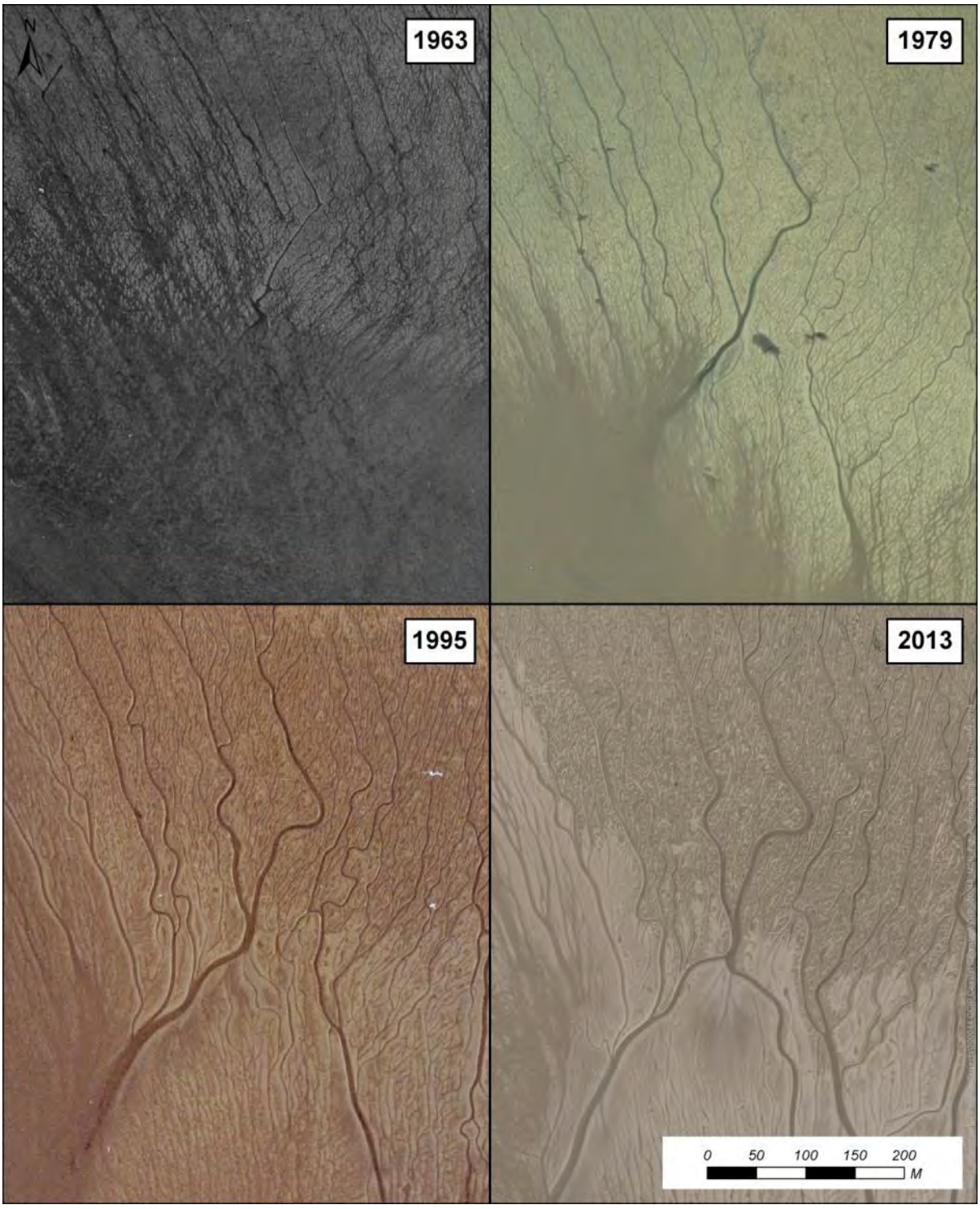

Figure 37: Planform changes on the lower ridge and runnel complex. Note that a portion of the 1979 photo is covered by water.

Increases in the extent of intertidal marsh have also been observed in the airphotos (**Figure 38**). For the area north of the Roberts Bank causeway, Hales (2000) noted lateral marsh growth between 1932 and 1994 and Williams and Hamilton (1995) noted seaward marsh progradation from the 1960s to present.

A comparison between the 1963 airphoto and the 1995 airphoto is instructive. The 1963 airphoto shows isolated clumps of vegetation in the marsh at Brunswick Point. In the 1995 photo, the areas between those clumps have filled in and vegetation cover is much denser. In the inter-causeway area marsh, Luternauer (1976) had noted based on ground photos that construction of the Roberts Bank causeway appeared to contribute to its apparent retreat, but the construction of a dyke along the seaward edge of the marsh, which is visible in the 1981 photo, appears to have stabilized this.

Although not visible in airphotos, areal changes on the delta front have also occurred and are discussed in **Section 5.5**.

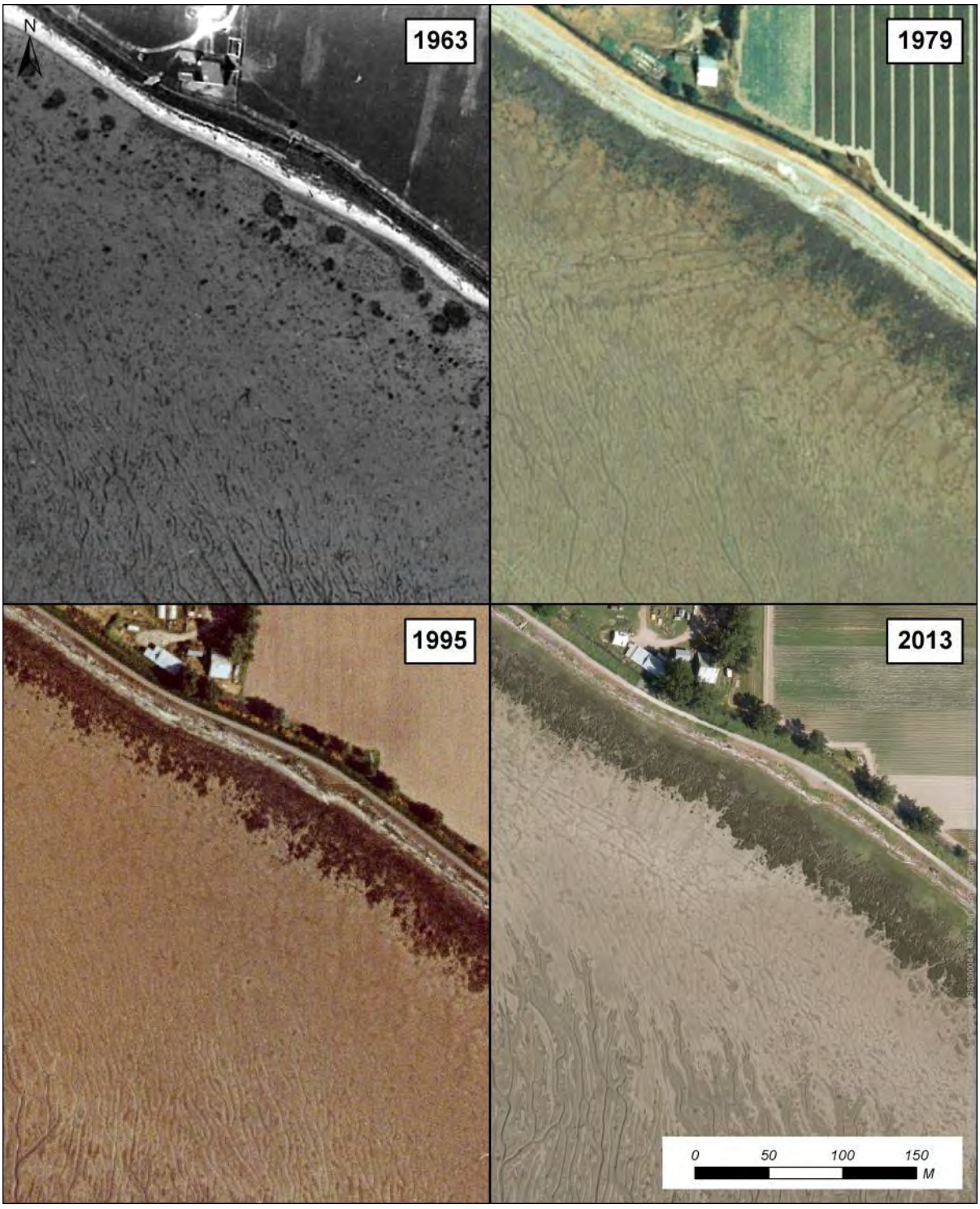

Figure 38: Planform changes showing the lateral expansion (seaward) of the salt marsh.

5.3 VERTICAL CHANGES – MARSH, MUDFLAT AND SAND FLAT

5.3.1 MARSH

The stability of the upper and lower marshes at and near Brunswick Point near Canoe Passage has been the subject of scientific debate. Williams and Hamilton (1995) found a decrease in sedimentation rates at Sturgeon Bank from the 1954-64 period to the 1964-1996 period. This was interpreted as indicative of an eroding marsh caused by a reduction in sediment inputs resulting from dredging activities in the Fraser River. The area of study in Hales (2000) was more relevant to the Project LSA, encompassing both Brunswick Marsh and Westham Island. This study found that vertical marsh growth rates in the study area were 0.80 g/cm^2/year and were greatest between 1910 and 1954 and slowed from 1954 to 1996. The hypothesis presented in that study suggested that marshes grow laterally by colonizing small patches that gradually connect, followed by subsequent vertical growth. The average rate of vertical marsh accretion, as reported by Hales (2000), was 1.18 cm/year.

5.3.2 MUDFLAT AND SAND FLAT

In 1967, the Canadian Hydrographic Service (CHS) surveyed the area extending across the tidal flats from the Canada-U.S. border north to the mouth of the Fraser River main arm, and seaward beyond the delta front to the deep ocean. In 2002, PMV (then Vancouver Port Authority) completed a bathymetric survey, this time covering the areas south and west of the causeway. It was compiled in digital format and combined with published CHS charts to produce a digital elevation surface. In 2011, LiDAR (Light Detection and Ranging) was used to survey the tidal flats of Roberts Bank between the Roberts Bank causeway and Canoe Passage in detail, and additional bathymetric surveys were conducted in the sub-tidal portions at the shoreward margin of the tidal flats.

The various topographic and hydrographic surveys each represent a 'snapshot' in time that describe the position of particular features and elevations on the tidal flats. The surveys can be overlain in GIS to evaluate change over time; however, there are challenges with respect to correcting for vertical datum and horizontal position. Relative horizontal position is possibly the largest source of error when comparing older surveys to more recent data, both because older surveys do not always report the geoid model that is used to represent the curving earth's surface on a planar chart, and because older survey techniques were less precise with respect to determining horizontal position. As elevations change with horizontal position, there is the potential for apparent changes to be only attributable to elevation measurements taken at different locations.

The 1967 dataset contained discrepancies in elevation units and had more uncertainty than the newer datasets. As such, it required more interpretation, but elevations were considered to be accurate within ±0.3 m. Taken together with the 2011 surface, an approximate comparison of bed level changes on the tidal flats is obtained over a period of four decades. **Figure 39** shows that the upper to middle tidal flats were relatively stable over that time span, displaying between 0 and 0.25 m of deposition in some areas and erosion in others, magnitudes of change that are within the accuracy of the survey. Brunswick Marsh is shown as having undergone deposition and the Canoe Passage outlet channel and relict channels exhibit erosion. The largest change occurs along the edge of the foreslope, displaying between 2 m and 25 m of deposition; however, these changes are suspect and may represent differences in

positioning on those steeply sloping land surfaces. Data from chemical analysis (PCB and ^{210}Pb) of sediments at the berth pocket dredge footprint indicate very little, if any, deposition near the top of the foreslope. Surface sediments were found to be 60 years old or older suggesting erosion and loss of more recently deposited sediments (Hemmera 2014).

Anthropogenic changes associated with past projects are also apparent on the tidal flats. Sediment deposited on either side of the Roberts Bank causeway and on the north side of the Roberts Bank terminals has resulted in a bed level rise of between 1 m and 5 m. This rise is partly associated with the original construction of the causeway (see **Section 3.4.2**) and also with discharge of dredge spoil on to the tidal flats during construction of Deltaport Pods 2 and 3 between 1981 and 1984 (Tarbotton and Harrison 1996). The elevational change does not represent net sediment deposition from littoral transport along the foreshore. In addition, an area off of the southwest corner of the existing terminal may have been dredged to result in 0.75 m to 1.5 m of apparent erosion.

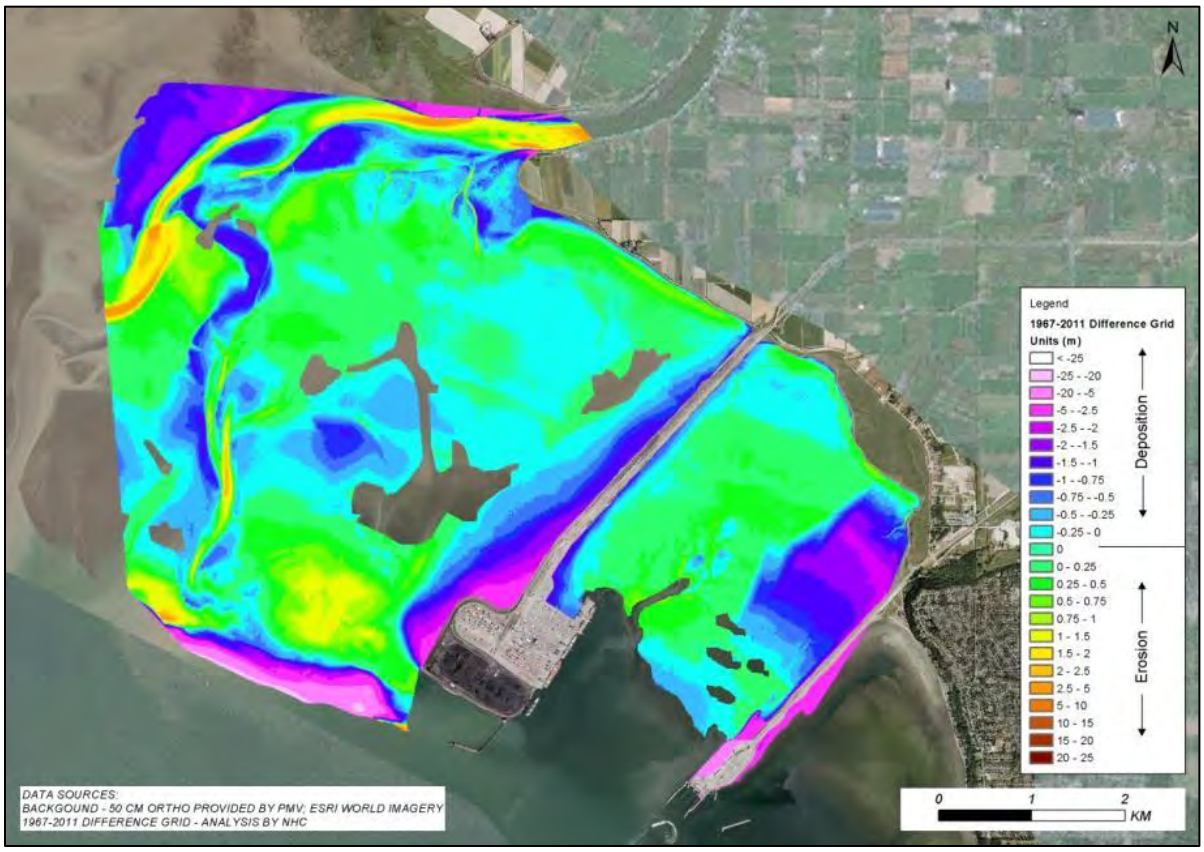

Figure 39: Topographic changes on the tidal flats from 1967 to 2011.

The portion of the Roberts Bank tidal flats between the north side of the Roberts Bank causeway and Canoe Passage (Brunswick Point) has remained relatively stable over the last decade. A comparison of LiDAR surveys from 2002 and 2011 shows vertical changes, both of accretion and erosion, of less than 0.25 m over much of the tidal flats (**Figure 40**), which is within the survey accuracy of 0.3 m. The relict channel south of the outlet of Canoe Passage has experienced a greater change, on the order of 1 m. The alternating spatial pattern of erosion and deposition suggests that the channel has undergone some shifting in the intervening period. Similar to the area to the north of the causeway, portions of the tidal

flats in the inter-causeway area that lie outside of the direct influence of the tidal channels have also seen little change (< 0.25 m) at the decadal time span.

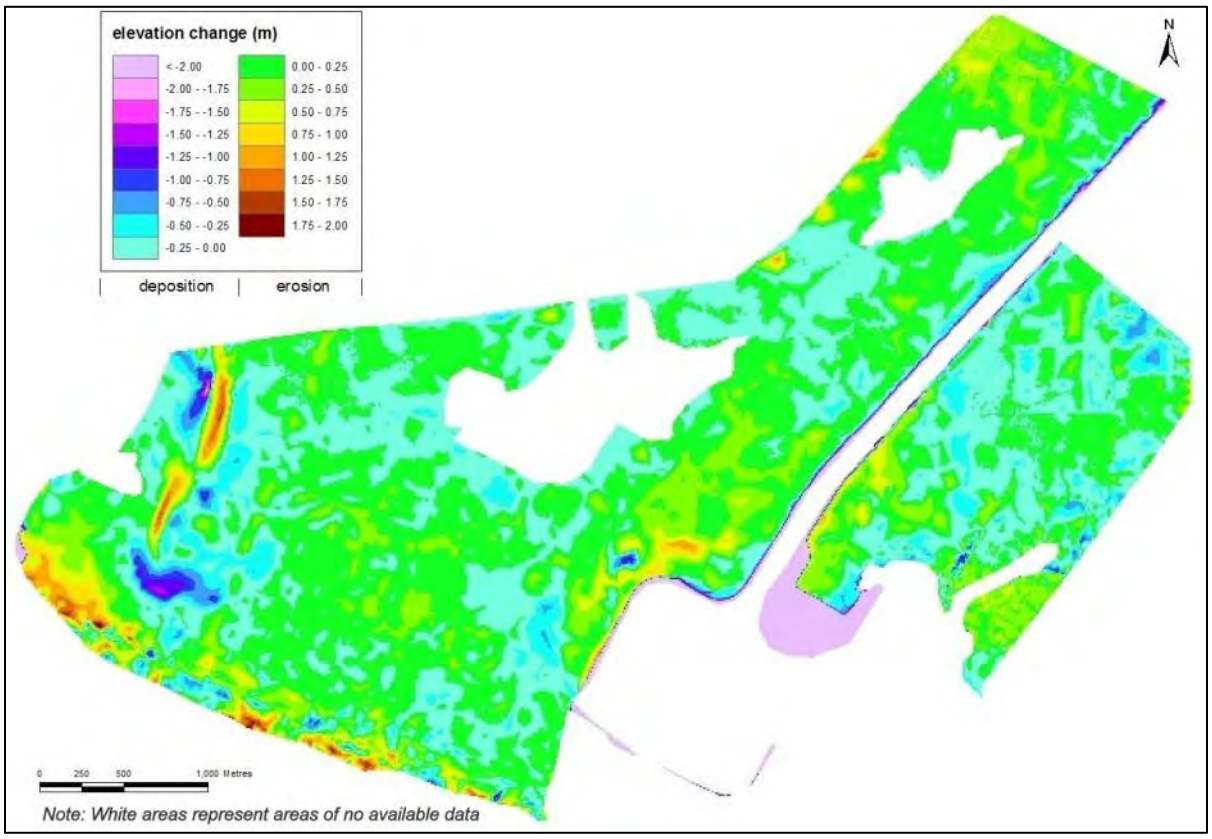

Figure 40: Topographic changes on the tidal flats from 2002 to 2011 based on LiDAR and bathymetric data.

Shorter-term vertical changes on the tidal flats have been assessed at various locations as part of this study and by others using Depth of Disturbance (DoD) rods. The DoD rods typically consist of a metal washer placed on the sediment surface and referenced to a rod that is pushed into the sediment to the point of refusal. Repeated manual measurements of the vertical distance between the top of the rod and the sediment surface and/or the washer can be compared to evaluate maximum erosion and net deposition between measurements. The method is shown schematically in **Figure 41**, which was used as part of the Deltaport Third Berth (DP3) AMS[7] monitoring (see for example Hemmera *et al*. 2012) as well as field investigations in support of the present study. Similar instruments were deployed on Roberts Bank by Hill *et al*. (2013) across four transects in 2003 and 2004. The ideal precision of the method is the level of accuracy at which measurements can be made (on the order of millimetres) but the practically achievable level of imprecision can be as high as a centimetre or more depending on how firm the sediments are. For instance, in very loose muddy sediments, the washer has been observed to sink under its own weight resulting in a false measurement of net erosion.

[7] Deltaport Third Berth Adaptive Management Strategy

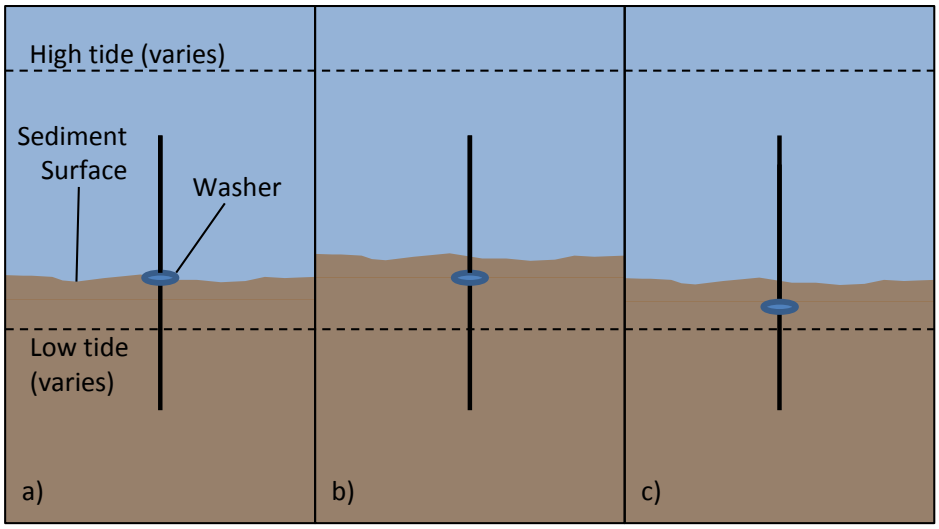

Figure 41: Schematic illustrating DoD rod monitoring: a) shows initial installation, b) shows subsequent deposition, and c) shows erosion with subsequent deposition.

The DoD rods that were monitored in support of the present investigation were installed along three loops to the north of the Roberts Bank causeway. The monitoring program lasted from June 2012 to May 2013 and, as such, encompassed a large 2012 freshet event. Thirty rods were used to measure change in the upper (numbered U1-U10), middle (M1-M10) and lower (L1-L10) tidal flats.

Large mats of algae and seaweed were observed to be wrapped around the DoD rods during monitoring visits, likely enhancing the trapping of sediment, and thereby confounding elevation changes. Care was taken to collect measurements after removing the mat, but even with the presence of the mats, the results are instructive. **Table 4** shows that measured changes (including accretion and loss) were on the order of 4-5 cm for the lower flats, 2-3 cm for the middle flats and 1-2 cm for the upper flats. This trend toward smaller elevation changes higher up the tidal flats is consistent both with the observed results of the bathymetric and LiDAR comparisons and with the general shoreward gradient associated with dissipating wave and tidal current energy.

Table 4: Statistics associated with change in DoD Rod elevations measured on different parts of the tidal flats.

	ELEVATION CHANGE (cm)				
	LOWER FLATS	MIDDLE FLATS	UPPER FLATS		
			Ridge	Runnel	Biofilm
Maximum	4.7	3.0	0.8	8.4	2.5
Minimum	-5.0	-2.7	-0.4	-0.9	-1.1
Average	-0.4	0.0	0.1	2.0	0.2
Summer average	0.0	0.2	0.2	2.5	
Winter average	-1.3	-0.3	0.1	1.3	

These results are in general agreement with those of Hill *et al*. (2013) for data collected between June 2003 and April 2004, which also observed a seasonal trend. In the middle and lower flats, there was a slight preference observed in the DoD rod data towards more deposition in the summer and more erosion in the winter. The effect of the storm period is more noticeable in the lower flats, where the relatively high negative average value indicates erosion. The average change (**Table 4**) suggests little positive or negative change in the tidal flat surface between June 2012 and May 2013.

5.3.3 RIDGE AND RUNNEL COMPLEX

The ridge and runnel complex corresponds to the biomat biosedimentological zone described in **Section 3.4.5**. The feature is present on the upper mudflats on both sides of the Roberts Bank causeway as well as in Boundary Bay (Kellerhals and Murray 1969) and appears to play an important role in modifying patterns of tidal inundation and emergence of the portions of Roberts Bank that have been identified as having the highest concentration of biofilm (see **Figure 17**) as well as moderating the wave climate in this region.

A recent reference to this feature as being a relict marsh surface (FSM Management Group Inc. and Hatch Ltd. 2012) is inconsistent with field observations of geomorphic processes and existing conceptual models of delta formation. A variety of observations, field measurements and analysis of sediment cores that are presented below indicates that the ridge and runnel complex is an accreting sedimentary feature that has shown significant vertical and horizontal expansion in recent decades. This model of mudflat building has very different implications for the overall health of the various ecosystems on the tidal flats as opposed to general loss of elevation on the upper tidal flats that would be implicit if it were in fact a relict marsh surface. It is therefore very important to determine which of these models more accurately represents the evolution.

The conceptual model that is advanced in this study describes accretion of the ridge and runnel complex caused by the presence of the biomat on the ridge surface. Biomat is comprised mainly of cyanobacteria, a blue-green algae that imparts a high degree of stability to the fine sediments, as well as a much higher hydraulic roughness. Fine sediments are preferentially collected from the water column onto the rough surface, which leads to more rapid accretion where the biomat is present as compared to the bare sediments. The cyanobacterial mats and bacteria that cohabit this environment produce exocellular polymeric substances (EPS) or mucilage (Ladakis *et al.* 2006), which binds sediment particles but is water-soluble and is therefore absent from the runnels and surface depressions where standing water is present for long periods. At the micro-scale, the biomat forms polygonal forms in the sediment surface, which are themselves separated by small flow paths between the polygons that favour dissolution of the EPS (**Figure 42**).

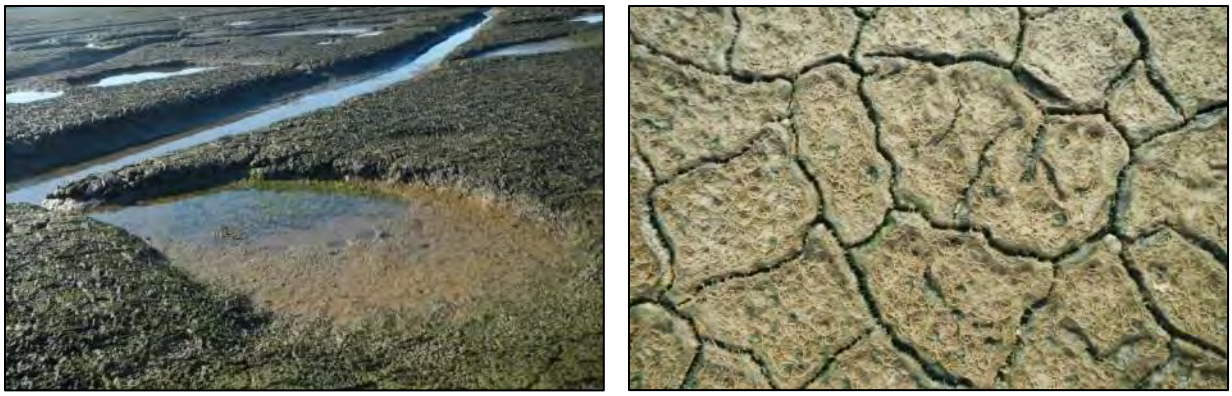

Figure 42: Overview of the ridge and runnel complex illustrating the effect of standing water in the shallow pools and runnels that inhibit biomat growth (left) and close-up of the biomat surface showing the polygonal form and surface roughness imparted by the biomat (right). Both photos were taken in July and August of 2012.

Observations and interpretation made in the field are supported by quantitative measurements at six of the DoD rods that were located in the ridge and runnel system. Three pairs of DoD rods – one of each pair situated on the ridge and another in the runnel – were installed in the mumblies area: U3 and U4; U5 and U6; and U7 and U8. All rods experienced net deposition on average, with those in the runnels experiencing more deposition than on the ridges. The DoD rods located on the tops of the ridges provided a stable site to observe the striking seasonal growth and decay of the biomat, which grew up around the washer over the summer months, extending up to half a centimetre above the bottom of the washer. The seasonal growth and decay of the blue-green algal mats was also described by Kellerhals and Murray (1969) in Boundary Bay. Throughout the winter, the sediment on the ridges is brown but as the summer progresses, it gets noticeably greener in response to the increase in algal biomass.

The ridge and runnel complex in the inter-causeway area appears to be less robust at present than in the area north of the Roberts Bank causeway. The biomat on the ridge surface shows the same polygonal forms as on the north side of the causeway, but spacing between the forms is much larger and the edges are much softer. Erosion and undercutting of the edges of the polygonal forms is evident. Similarly, the runnels are less distinct and lack the steep sides seen on the north side of the causeway (**Figure 43**). The deterioration of the ridge and runnel features in the inter-causeway area is interpreted to be due to the reduced delivery of fine sediments in the water column, mainly because the Fraser River plume is routinely excluded from the inter-causeway area.

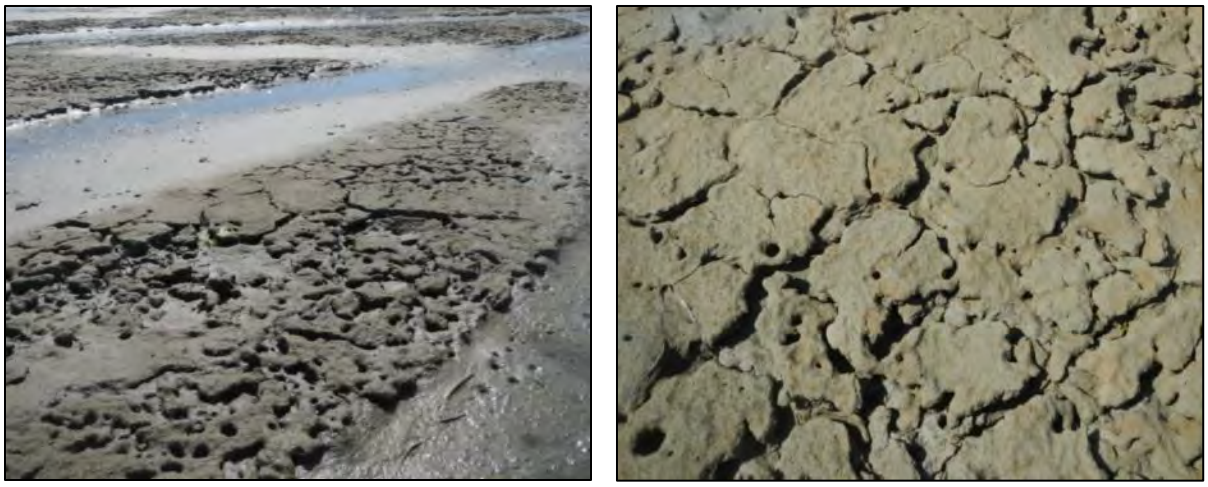

Figure 43: Overview of biomat in the inter-causeway area (left) and close-up showing soft edges and wide spaces between polygonal forms (right). Photos taken April 24, 2013.

To further increase confidence in the theory that the ridge and runnel complex is an accreting environment, sediment samples were collected from both the north side of the causeway and in the inter-causeway area. In each of these areas, one pit was excavated and sediment samples were collected at small intervals down-profile. This sampling method was chosen so as to avoid the issue of compression of sediment associated with core collection (similar to methods employed by Johannessen *et al.* (2008*a*) in their study). The specific dating techniques applied, in this case ^{137}Cs and ^{210}Pb, are commonly used for dating marine sediments in the region (Lavelle *et al.* 1986, Williams and Hamilton 1995, Johannessen *et al.* 2008*b*), and they provide two independent means of assessing sediment accumulation rates.

Based on three site visits that included soil pits, collection of cores and subsequent radiometric dating of sediments located both within the inter-causeway area and north of the causeway, an improved understanding of the sediment accumulation pattern at the ridge and runnel complex was attained. In particular, it was observed that the bases of the runnels are primarily sand, while the ridges are composed of a finer-grained mud. Samples from the ridges show that the sand continues under the ridges at an elevation similar to the elevation at which it is found under the runnels. The radiometric data suggest that the mud that makes up the ridges was deposited since the construction of the causeways and at a relatively constant rate. Since the construction of the causeways, the rate of sedimentation within the inter-causeway area has been about 5 mm/year. North of the causeway, the sedimentation rate has been about 6.4 mm/year. The sediment accumulation rates are moderated by subsidence rates that have been estimated to be between 1 and 3 mm/year for the uplands adjacent to Roberts Bank (Hill *et al.* 2013). Bioturbation appears to be more active north of the causeway and/or the sedimentation rate has recently increased in the area north of the causeway.

Looking ahead, sedimentation rates on the north side of the causeway may increase dramatically if lower salt marsh plants continue to colonize the area as the reduced velocities associated with vegetation will promote sediment accretion (**Figure 44**). This theory is consistent with the results of the

2004 Fraser Delta Marsh Mapping Project and the related earlier work by Hales (2000) that constructed the recent history of marsh development at the mouth of the Fraser River delta.

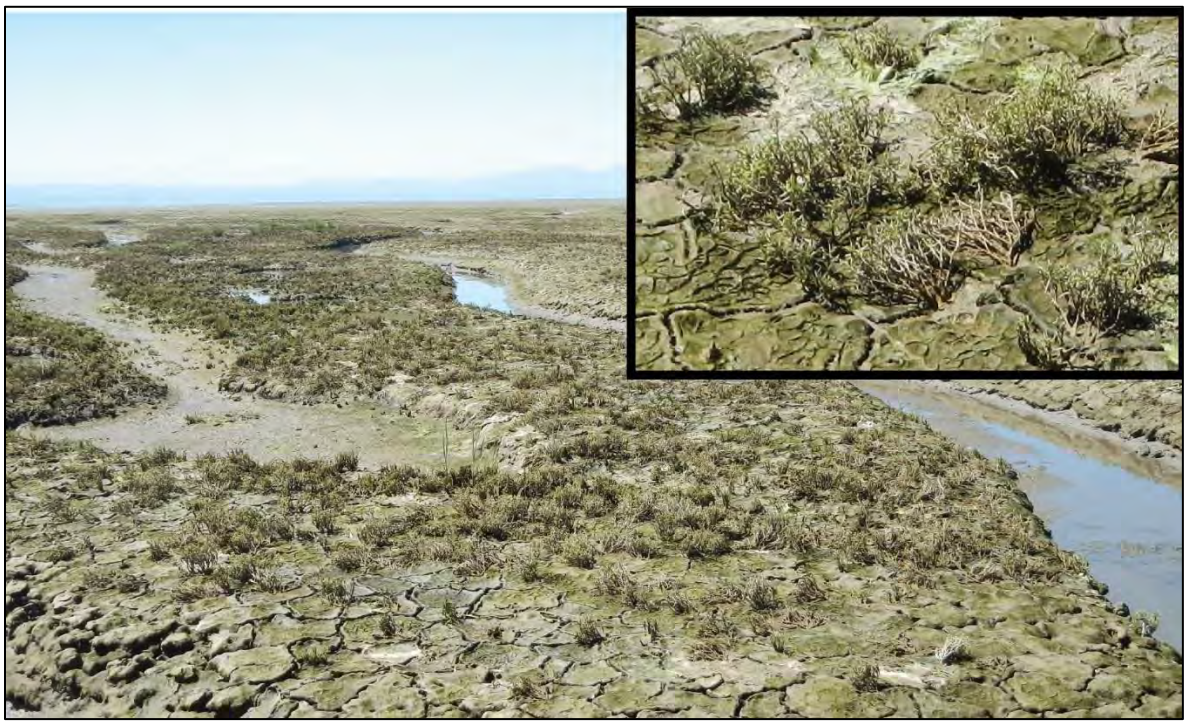

Figure 44: Salt marsh plants occupying the higher elevations of the eastern portion of the mumblies. Photo taken on August 6, 2013.

5.3.4 TIDAL FLAT PROFILES

When averaged over long time scales, tidal flat morphology typically approaches a dynamic equilibrium with the external forcing from waves and tidal currents (Friedrichs 2011). Convex-up profiles are associated with increased sediment supply, increased bioaggregation/adhesion, and external forcing by faster-rising tides whereas concave-up profiles are related to decreased sediment supply, increased bioturbation, and external forcing by faster-falling tides. Furthermore, dominance by tides tends to favour convex-up profiles whereas dominance by waves tends to favour concave-up tidal flat profiles (Friedrichs 2011).

Four profiles from north of the causeway and one from the inter-causeway region were extracted from the 2011 LiDAR and Bathymetric DEM[8] (see **Figure 45** and **Figure 46**). Profiles A and B show a slightly convex-up shape across the main portion of the tidal flats. Profile A is affected by the existing port structure and the sediment that was introduced to the tidal flats during the initial causeway construction. This profile also shows the variable bed elevation associated with the ridge and runnel complex between 500 and 800 metres from the uplands. Profiles C and D are weakly concave-up but

[8] Digital Elevation Model

only in the upper portion of the profile (the portions below approximately 2 m CD were truncated because of the presence of channels). These profile shapes are consistent with higher sediment supply and sediment adhesion, as referenced by Friedrichs (2011). In contrast, the Inter-causeway profile is strongly concave-up, which is consistent with a portion of Roberts Bank that has received little, or no, new sediment since the causeways were constructed.

Figure 45: Planimetric map showing the locations of elevation profiles extracted from the 2011 LiDAR data.

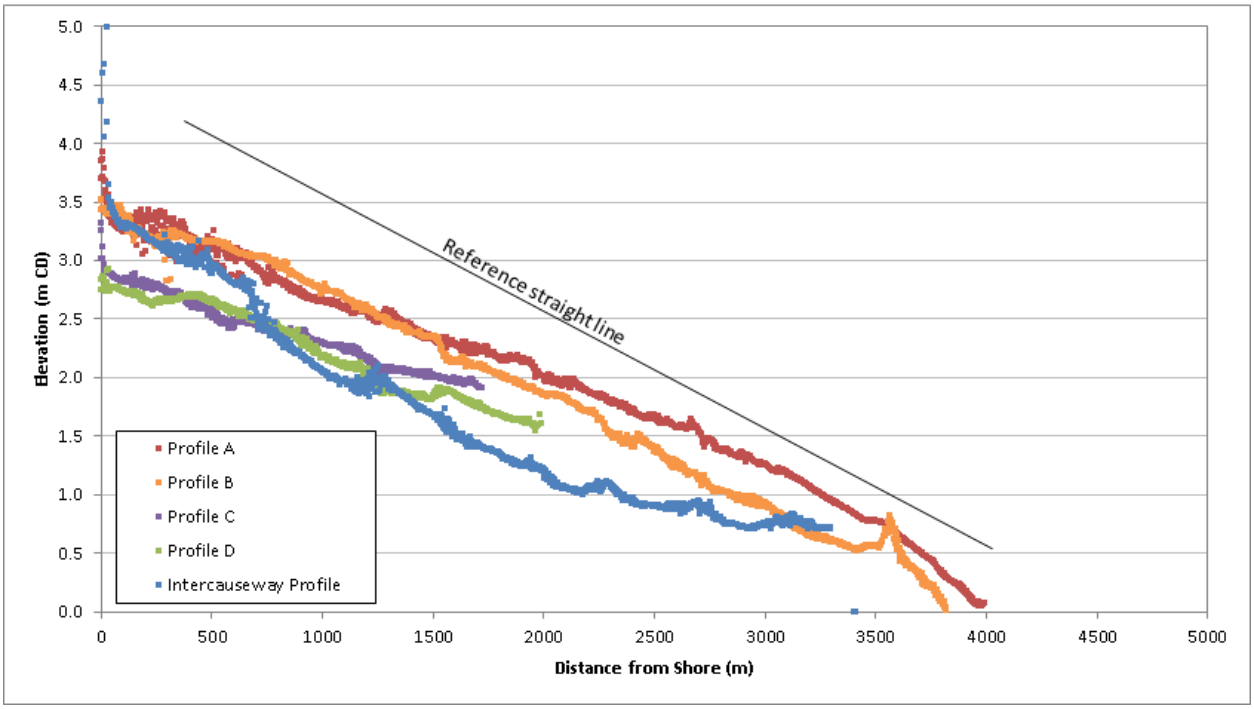

Figure 46: Profiles across intertidal portion of Roberts Bank based on 2011 LiDAR data and bathymetry survey.

5.4 SEDIMENTOLOGICAL CHANGES

Sedimentological data at Roberts Bank has been compiled from various sources over the past few decades. Some of these include:

- Luternauer (1976) – collected over 600 samples in 1975 during the pre-freshet winter season and the post-freshet summer season. Unfortunately, the complete data set has been lost (Hill 2013), and only a subset of the data is accessible via the published manuscripts;
- McLaren and Ren (1995) – collected 1,484 surface samples between February 9th and April 7th, 1993 across the delta and in the distributaries of the Fraser River; and
- Hemmera (2014) – collected 493 samples between April 19th and September 25th, 2012. The samples were collected around the Project footprint and across Roberts Bank and Sturgeon bank. An additional 30 samples were collected in 2013 near the Project area.

The Luternauer (1976) study suggests that grain size changes seasonally off the Main Arm of the Fraser, but less so on the upper slopes. With respect to anthropogenic change, the study noted that the extent to which Roberts Bank causeway, which was completely constructed by 1969, contributed to the poor sorting of sediments northwest of the causeway could not be defined because virtually nothing is known of pre-causeway sediment distribution. It is possible, however, to compare sediment size on the tidal flats from seven years later, in 1976, to present-day conditions. The samples collected by McLaren and Ren (1995) may not be ideal for comparison as they were simple surface grab samples. Temporal trends

are summarized in **Figure 47**, **Figure 48** and **Figure 49**. Overall, it is difficult to detect any general patterns as there are relatively few samples that are close enough in space to show a clear pattern of grain size change. While the McLaren and Ren (1995) data suggest that the percent sand has reduced in the vicinity of the causeways, the 2012 data do not support the same conclusion. In the vicinity of Canoe Passage, the changes in grain size are most likely attributed to changes in channel planform, and again, no general conclusions are possible. In summary, the temporal sequence of grain size sampling programs does not clearly demonstrate that a change in grain size has occurred across any one feature of the delta. There are some areas, especially on the north side of the causeway, where fining may have occurred, but with only one 1974 sample point (Point 138 in **Figure 47**), it is not possible to make general conclusions about changes in grain size.

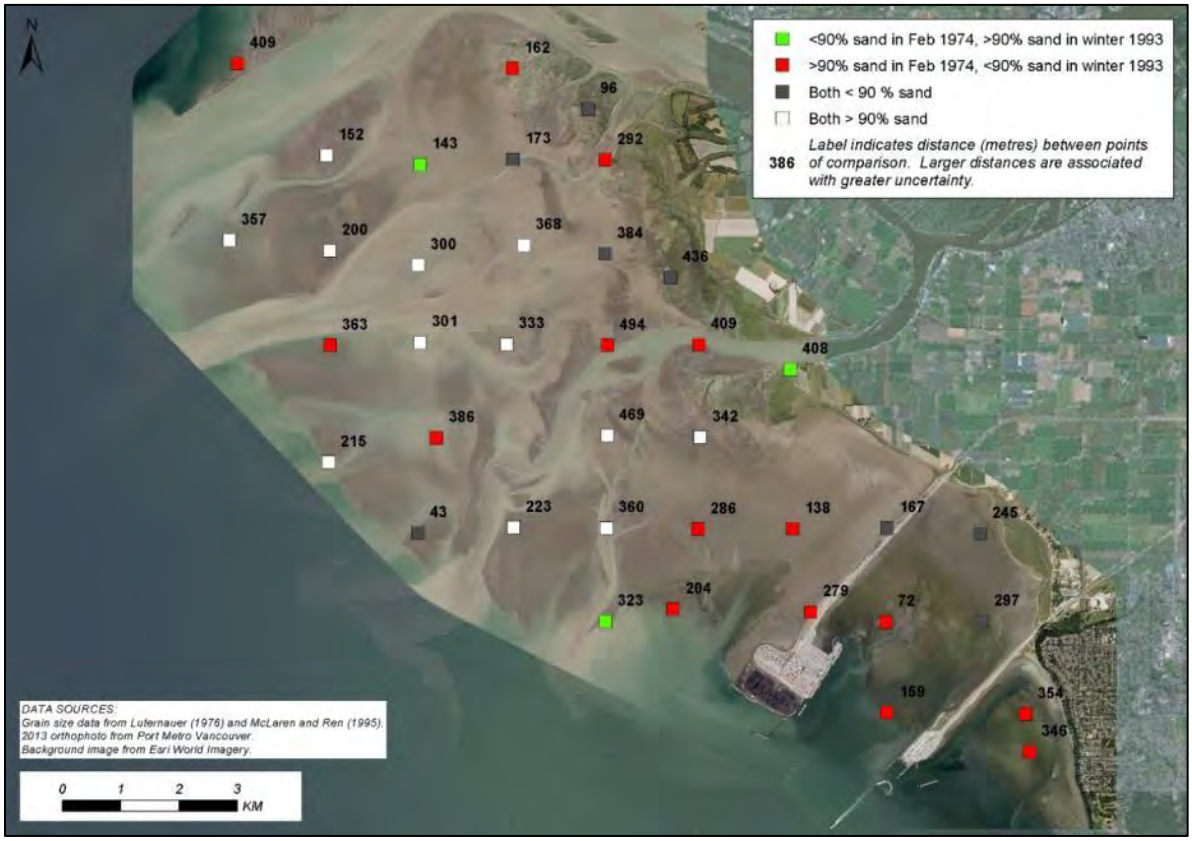

Figure 47: Change in percent sand from 1974 to 1993 based on results from Luternauer (1976) and McLaren and Ren (1995).

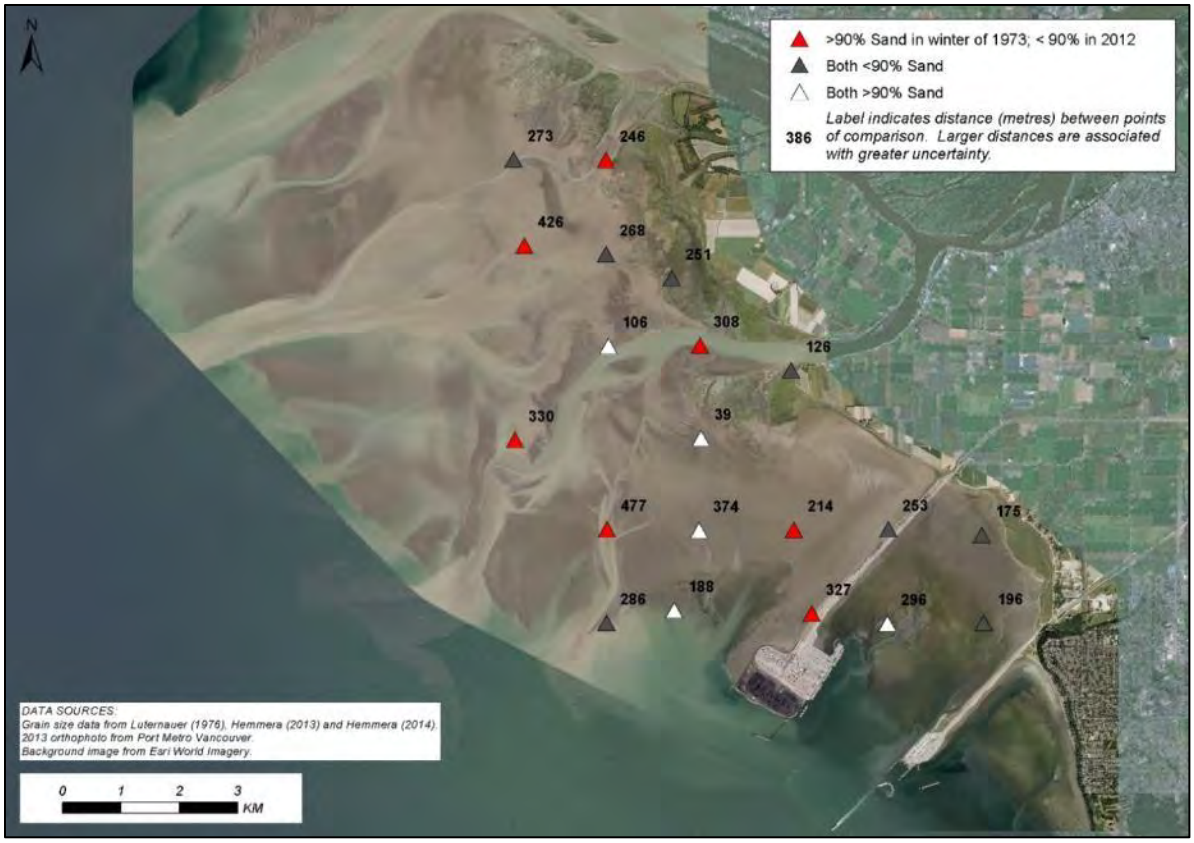

Figure 48: Change in percent sand from 1974 to 2012 based on results from Luternauer (1976) and Hemmera (2014).

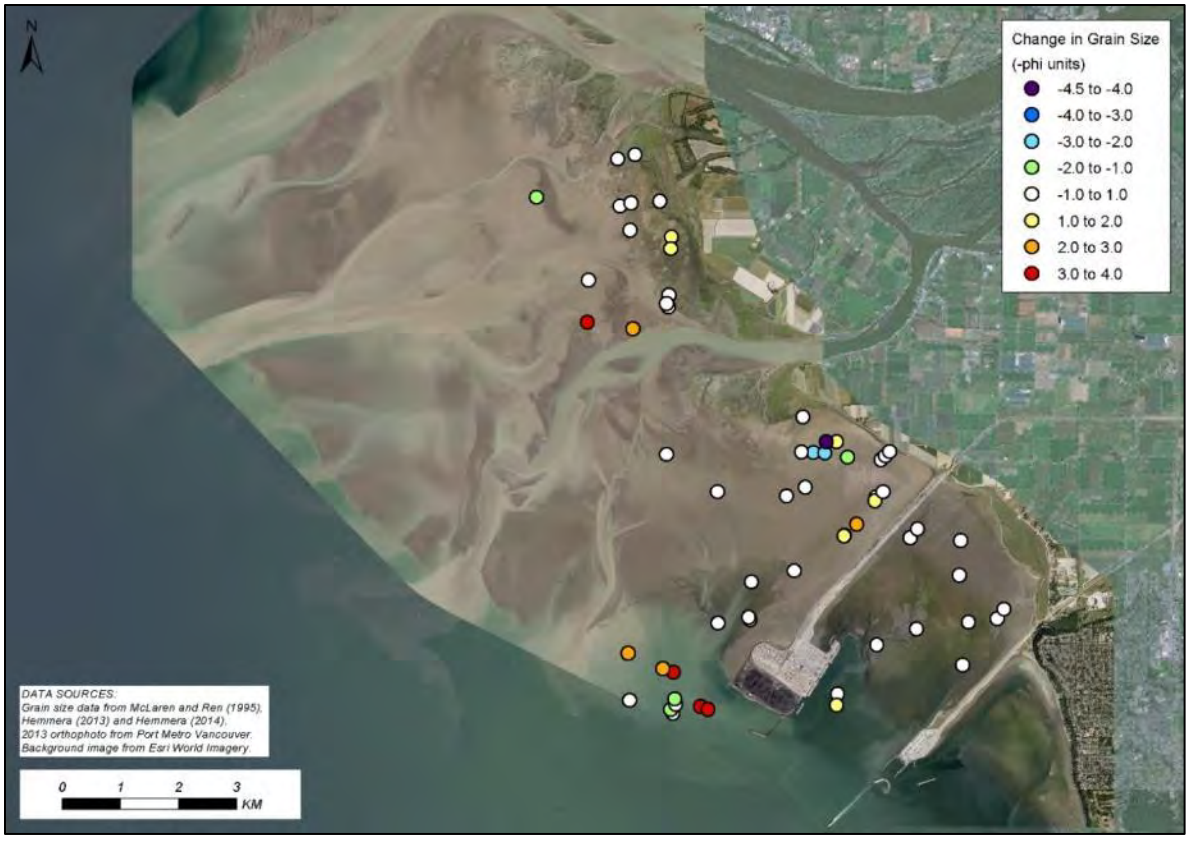

Figure 49: Increase in median sediment grain size (D_{50}) from 1993 to 2012/2013 based on data from McLaren and Ren (1995) and Hemmera (2014).

5.5 DELTA FORESLOPE CHANGES

Stewart and Tassone (1989) carried out a comprehensive assessment of the delta foreslope along both Roberts Bank and Sturgeon Bank for the period between 1929 and 1985 by digitizing selected elevation contours from the available historic sounding charts. Their results showed that the delta foreslope advanced approximately 100 to 240 m in the zone from Sand Heads to midway to the international boundary. There is an alternating pattern of advance and retreat of the delta from the midway point to Westshore Terminals, south of which there is general retreat.

The pattern from the midway point (which roughly corresponds to where the outlet of Canoe Passage would intersect with the delta edge) to Westshore Terminals is consistent with the comparison of LiDAR surfaces between 2002 and 2011 (**Figure 40**). The density of data points in both of these years' datasets is high enough (10 m resolution for 2011; 10-20 m resolution for 2002) that the changes are relatively accurately represented. In the intervening period, the edge of the delta foreslope displayed a pattern of erosion interspersed with smaller areas of deposition. At sufficiently large magnitudes, these changes are expressed laterally as retreat and advance of the delta foreslope respectively.

Multibeam imagery collected for a study by Hill *et al.* (2008) provides an explanation for what is observed on the edge of the delta foreslope. **Figure 16** shows a three-dimensional surface of the delta

foreslope seaward of the mouth of the Main Arm. The submarine channels that are present at the head of the delta foreslope and the adjacent higher elevation sediments reflect localised erosion and deposition that is mainly driven by punctuated episodes of foreslope sediment deposition and localised down-slope lateral transport via smaller- to larger-scale turbidity currents.

The 1967 to 2011 survey comparison (**Figure 39**) does not reflect the same alternating pattern. This is likely because the 1967 elevation surface is compiled from elevation contours that vary in spacing from 5 m to 50 m, increasing downslope. The comparison instead shows a depositing foreslope, which can also be interpreted as a net advancement of the delta over the 44-year period.

5.6 SUMMARY OF OBSERVED TRENDS AND IMPLICATIONS FOR FUTURE CONDITIONS

Before attempting to understand the changes from the proposed Project on Roberts Bank, it is necessary to understand what has happened in the recent history and where the physical environment is tending in the future. The following two sections outline the key changes and trends for both the inter-causeway area and the area on the north side of the Roberts Bank causeway. These trends are also used to make informed assessments of projected ongoing changes on the flats without the Project.

Prior to the construction of the BC Ferries causeway, a small amount of sand was supplied to Roberts Bank from Point Roberts via both northward-dominated tidal currents and winds from the southeast. Fraser River bed material load was only moved south via channel avulsions. Thus, the Roberts Bank sand flats were maintained by the erosion of Point Roberts or re-working of Fraser River sediments deposited by previous avulsions. While finer suspended sediments (silt/clay) carried by the Fraser River plume would have moved south across the flats during falling tides, these sediments were unlikely to be deposited due to the high energy tide and wave environment that was present.

Since the construction of the two causeways, the dominantly northward tidal- and wave-forcing has been greatly reduced and the supply of Point Roberts sand to the Roberts Bank sand flats has been eliminated. The Point Roberts sands that migrate north are intercepted by tidal channels that dissect the tidal flats and are then moved offshore where they move northward, but only along the deeper portion of the Strait of Georgia. As a result, there does not appear to be a contemporary mechanism for supplying sand to the Roberts Bank sand flats over the long-term. In response to continued sea level rise and subsidence, and the elimination of Point Roberts sand inputs, water depths over the sand flats are anticipated to increase with time. Given the current state of knowledge, the rate of increase is unknown, but at a minimum is likely to equal sea level rise plus subsidence.

Finer sediments that can remain in suspension within the Fraser River plume continue to be supplied to the area on the north side of the Roberts Bank causeway, but the supply rate has been greatly reduced or eliminated in the inter-causeway area. The difference in fine sediment supply has resulted in distinct evolution histories and trajectories that are discussed individually below.

5.6.1 NORTH SIDE OF CAUSEWAY

The sediment sampling conducted in the ridge and runnel complexes demonstrated that these features are accreting and are distinct from the sands that predate the construction of the causeways and underlie the ridges and runnels. At present, the ridge and runnel complex on the north side of the causeway has attained an elevation of nearly 3.5 m CD (Profile A in **Figure 46**), which is higher than the marsh areas on Brunswick Point (see profiles C and D in **Figure 46**). Marsh plants that have begun to establish on certain portions of the ridge and runnel complex (**Figure 44**) will presumably continue to colonize the higher areas.

In the absence of sea level rise and land subsidence, the ridges associated with the ridge and runnel complexes may attain accretion rates on the order of 1 cm/year as vegetation continues to establish (based on results of Hales 2000). While the ridges accrete, the main runnels will likely be preserved as they will continue to convey flow to and from the inland areas. The low-lying zones adjacent to the ridge and runnel complexes that have a high density of biofilm, especially those that are located inland, are also anticipated to increase in elevation and be colonized by vegetation communities.

There is sufficient uncertainty in the rate and timing of sea level rise, sediment accretion and subsidence that it is not possible to predict precisely what the change in relative sea level will be for the ridge and runnels over the next few decades. The mean sea level rise for the next hundred years, plus the land subsidence rates are similar in magnitude to the sediment accretion rate, suggesting that it is possible that vertical development of the ridges may keep pace with sea level rise for the next 50 years or so. However, if sea level rise does not increase significantly in the next decade or two as projected (**Figure 30**), increased marsh growth and accompanying sedimentation may significantly change the ridge and runnel complex.

Hill *et al.* (2013) estimated 13 m and 36 m of shoreline retreat in the absence of sediment accretion, using 0.23 m and 0.62 m of sea level rise respectively, and 4 m and 12 m of retreat for the outer edge of the sand flat based on these two sea level rise scenarios. Hill *et al.* (2013) also projected a 45-63% reduction in mudflat area and also erosion of the marsh due to coastal squeeze by 2100. The study authors acknowledged a low level of confidence in these predictions due to possible mitigation by sedimentation and marsh accretion over the same time period. Clearly, sediment accretion is an important factor in maintaining the marsh and ridge/runnel features.

The continued accretion of the ridge and runnel complex in the absence of a mechanism for sand delivery to the lower sand flats presents a developing disequilibrium: it is anticipated that the upper mudflats will continue to accrete while the lower sand flats will remain unchanged or subside. This disequilibrium will progressively result in an increase in wave and tidal energy delivered further onto the sand flats that may result in waves moving sands from the upper flats to the lower flats.

The potential exists for Canoe Passage to avulse (shift its main channel) towards the south across the Roberts Bank tidal flats, similar to what is shown in **Figure 34**. If this were to occur, there would be a significant increase in the supply of sand to the middle and northern portion of northern Roberts Bank. Such a shift would alter prevailing habitat and water quality, particularly in terms of salinity and

sediment supply. Even following an avulsion, it appears unlikely that Canoe Passage could supply sand to the portion of Roberts Bank immediately north of the causeway. At the 100- to 1,000-year time scale, it appears that there is a deficiency in sand supply to the outer portion of Roberts Bank immediately north of the causeway.

Other potentially more extreme changes have been described in previous studies, including an avulsion of the Fraser River Main Arm near Kirkland-Woodward Island into Canoe Passage (McLaren and Ren 1995). Given the status of the existing training walls and ongoing maintenance dredging program on the Main Arm of the river, the risk of such a change appears to be extremely small.

5.6.2 INTER-CAUSEWAY REGION

In contrast to the area north of the causeway, the inter-causeway region receives very little suspended sediment from the Fraser River plume. As a result, the ridge and runnel complex is accreting at a slower rate and the profile across the flats has developed a strongly concave-up profile. During the sediment sampling on the ridge and runnel complex, silts were not easily mobilized, unlike the area north of the causeway, and field observations suggest sediment may not be accumulating at the site. Within the limitations of the dating techniques, it is not possible to determine whether the top of the surface is actively accreting or if accretion ceased a number of years earlier. If the ridge and runnel complex is currently accreting, the rate is expected to be especially low and largely maintained by the re-working of sediments already within the inter-causeway area.

Over the long-term, the accretion rate is likely to be reduced and the relative sea level rise within the inter-causeway area will increase on account of eustatic and isostatic effects. Along with relative sea level rise, it is anticipated that continued re-working of the sand and mud flats will occur as waves are able to migrate further inland. A modest increase in the supply of fine sediment from the Fraser River plume would likely increase sedimentation in the area as sediment supply is likely the main factor limiting accretion. It is anticipated that the large system of tidal channels and associated sand lobe formation caused by dredging of the ship turning basin will persist, but the overall rate of change will slowly diminish with time as relative sea level increases.

6 HYDRODYNAMIC MODEL ANALYSIS

NHC conducted numerical modelling analysis using the TELEMAC SYSTEM, a suite of finite element computer programs developed by the Laboratoire National d'Hydraulique et Environnement (LNHE), a department of Electricité de France's Research and Development Division, to evaluate changes in tidal currents, wave climate, salinity and seabed evolution associated with the Project. The TELEMAC SYSTEM is a modelling tool recognized throughout the world, having over 4,000 registered users including BC Hydro, Hydro-Quebec and Canadian Coast Guard[9]. Due to its origin, the TELEMAC SYSTEM is used by many French design offices as well as French state organizations. In addition, a large number of universities, engineering schools and research centres use TELEMAC.

TELEMAC programs utilized in the study include:

- TELEMAC3D – A three-dimensional hydrodynamic model that solves the time-dependent Navier-Stokes equations with an evolving free surface, under the assumption of hydrostatic or non-hydrostatic pressure distribution using the finite element method.
- TOMAWAC – A third-order spectral wave model based on the wave action density balance equation that simulates wave propagation in the coastal zone. The model accounts for the effect of wave generation by wind, white-capping, nonlinear wave-wave interaction, refraction, shoaling and dissipation.
- SISYPHE – A sediment transport and morphodynamic model that computes bed load and suspended load separately, and the resulting bed changes using the Exner equation.

6.1 MODELLING METHODOLOGY

The TELEMAC model grid used for the study extends from Ballenas Island at its north boundary to Port Renfrew at its west boundary (**Figure 50**). The model also includes the Fraser River up to Kilometre 36, immediately upstream of New Westminster. These extents were developed with due consideration given to the need to balance the size of the model, and hence computation time, with the need to provide accurate tide and wave conditions at the Project site.

The model grid contains approximately 28,000 nodes, 51,000 elements and 11 levels in the vertical dimension. The element lengths vary from approximately 3,000 m in the Strait of Georgia to about 25 m in the vicinity of the Project. The model bathymetry was derived using the following distinct datasets:

1. In the Port and surrounding areas, 2011 bathymetric surveys and LiDAR were used.
2. In the Fraser River, 2004 PWGSC bathymetric surveys and 2005 Fraser Basin Council LiDAR were used.
3. In Puget Sound, the Strait of Georgia and Juan de Fuca Strait, the dataset is comprised of CHS bathymetry data, as well as data from other sources (see **Appendix B**).

[9] TELEMAC is used by the Canadian Coast Guard to forecast available water depths for vessels navigating the Fraser River South Arm Channel (see http://www2.pac.dfo-mpo.gc.ca/ for more details).

The model simulation utilized the 2012 environmental conditions (water level, Fraser River flow and wind forcings). This period was selected because the wind and wave climate is similar to that of a typical wind and wave climate experienced in the Strait of Georgia, its relatively large freshet flow and the availability of current and wave data to validate the model. The relatively large magnitude of the 2012 freshet (estimated at 25-year return period) provides a usefull contrast to the low-flow periods during the late-winter and early-spring for comparison of the potential changes resulting from the Project.

Tidal levels at the open boundaries (Ballenas Island and Port Renfrew) were obtained using the WebTide Tidal Prediction model (Department of Fisheries and Oceans 2005) based on Foreman (2000). Inflows to the Fraser River at New Westminster were obtained from the hydraulic model of the Fraser River that uses the MIKE11 one-dimensional hydrodynamic software developed by the Danish Hydraulic Institute. NHC developed the Fraser River MIKE11 model for Fraser Basin Council in 2006 (NHC 2006) and updated it for BC Ministry of Environment two years later (NHC 2008). Details on model development, calibration, and validation are provided in **Appendix B**.

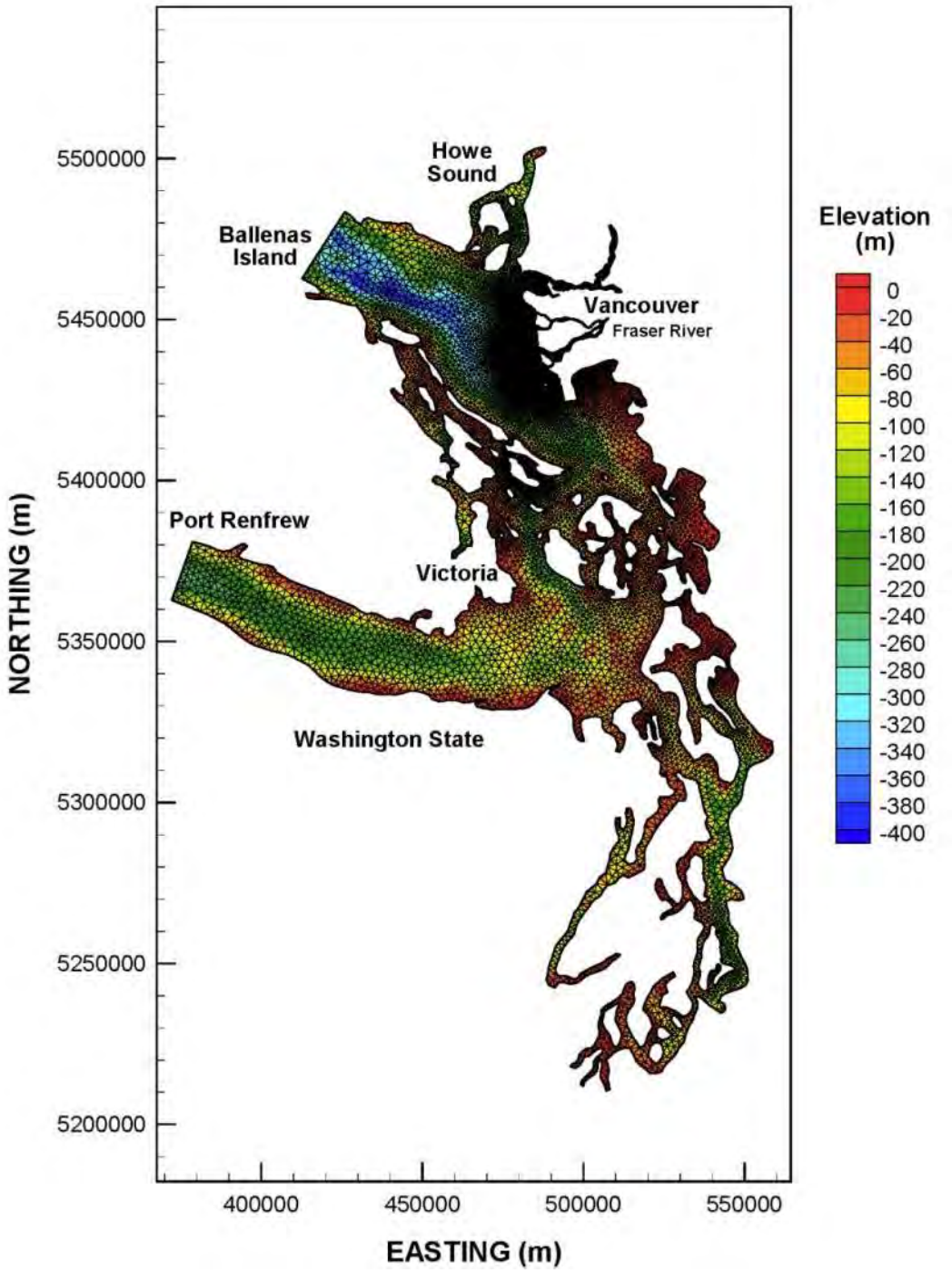

Figure 50: TELEMAC model mesh.

To account for wind stress acting at the water surface and wind-generated waves in the Strait of Georgia, hourly wind data were obtained from four Meteorological Service of Canada (MSC) stations (Pam Rocks, Race Rocks, Sand Heads, and Victoria), the Environment Canada Halibut Bank wave buoy and four US National Oceanic and Atmospheric Administration (NOAA) stations (Cherry Point, Port Townsend, Smith Island and West Point). The locations of these stations are shown in **Figure 51**.

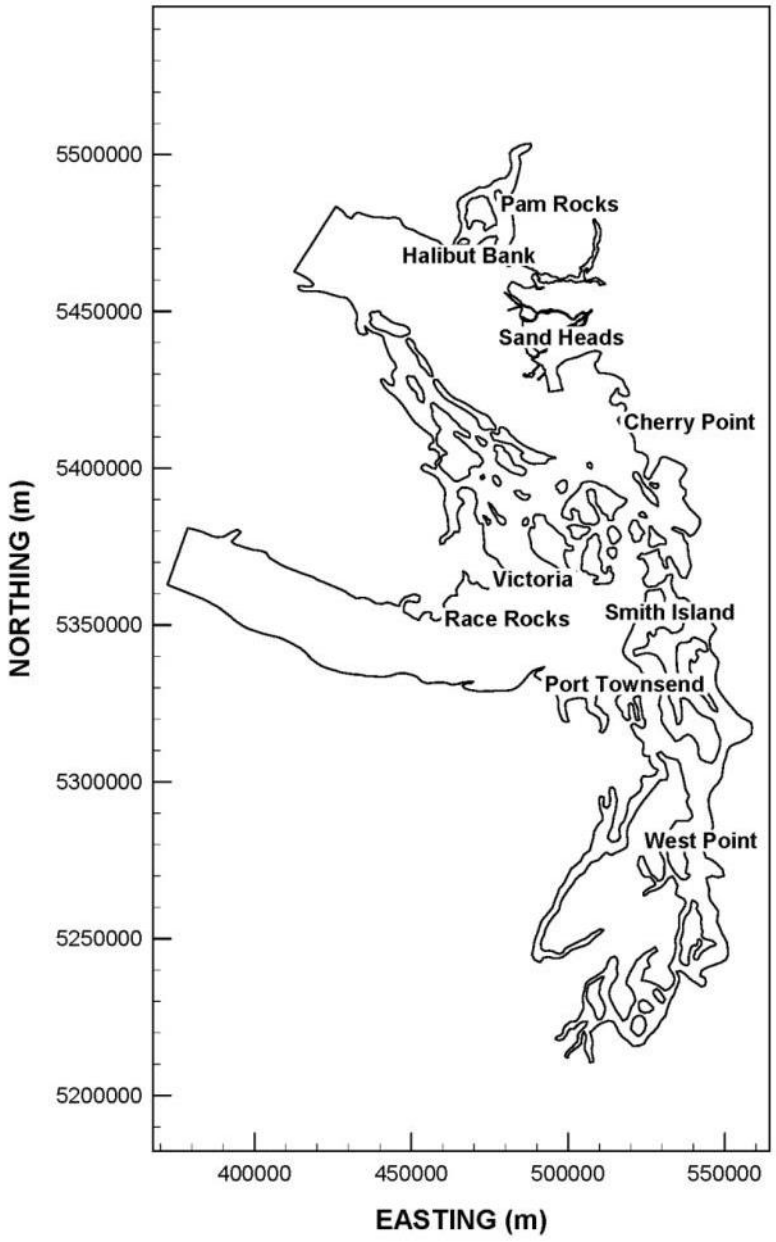

Figure 51: Location of wind stations in the model area.

Three complimentary numerical modelling approaches were used to gain the knowledge necessary to evaluate the potential impact of the Project on the coastal processes:

1. Hydrodynamic-wave modelling to evaluate potential changes to waves and currents on the tidal flats.

   The hydrodynamic model TELEMAC-3D uses wind data and the outflow discharge from the Fraser River plus the tidal information in the Juan de Fuca Strait near Ballenas Island and Port Renfrew to compute the tidal currents around the Project. The TOMAWAC model uses wind

data to simulate wave propagation and compute significant wave height. This wave information is passed into TELEMAC-3D to incorporate the effects on the flow circulation.

2. Salinity modelling to evaluate potential changes to the distribution of and mixing of fresh Fraser River water with the saline water of the Strait of Georgia on the tidal flats.

   The hydrodynamic model TELEMAC-3D uses wind data and outflow discharge from the Fraser River plus the tidal information in the Juan de Fuca Strait near Ballenas Island and Port Renfrew to compute the tidal currents around the Project. The wave effect is not considered as it does not have a significant impact on the overall salinity transport process. Salinity monitoring data collected by Fisheries and Oceans Canada[10] were used to initialize the salinity field and applied at the open boundaries.

3. Morphodynamic modelling to evaluate sediment transport and potential changes to the surface of the tidal flats. These modelling results are described in Chapter 7.

Only the modelling methodology and results are presented in this section. Further details on the development, calibration and validation of the numerical models can be found in **Appendix B**.

6.1.1 MODELLING SCENARIOS

The modelling exercise considered three different temporal scenarios:

- Existing conditions;
- Expected conditions;
- Future conditions with the Project;

The characterisation of existing conditions was reflective of the year 2012. The model studies used wind, tide, and Fraser River flow data from 2012 as inputs to the numerical model. This allowed the model results to be directly compared to the field data that were collected primarily in 2012 for this assessment. The year 2012 was typical in terms of storm frequency and intensity but was above average for discharge from the Fraser River. Most of this above-average discharge occurred in late spring and early summer. The effects of high Fraser River freshet flows on the Project area were compared to periods of similar tides during the late fall and early winter when the Fraser River discharge is typical of winter lower flow conditions. The geomorphic system is dynamic but rates of change are sufficiently small that the existing conditions that are described based on the 2012 field data can be expected to persist through to Project commencement.

The predictions of Project-related changes were based on the construction and operation phases of the Project. For comparison purposes, potential future changes in coastal geomorphology associated with the Project were compared against existing conditions in 2012 in the case of waves and ocean currents. In the case of morphodynamic evolution, comparisons are made to the expected conditions case; the reason for this is that the Roberts Bank ecosystem is a dynamic environment with ongoing processes

[10] http://www.pac.dfo-mpo.gc.ca/science/oceans/

and influences. As a result, it is necessary to compare future conditions with the Project, to the same future year without the Project (referred to as expected conditions) to understand the nature of the morphodynamic changes that may be caused by the Project.

To determine the influence of sea level rise on wave predictions, the existing condition is compared to the expected conditions and future conditions with Project cases, and the future conditions with the Project case is also compared to the future conditions with the Project case and sea-level rise. This approach isolates the changes related to sea-level rise from the Project-related changes.

6.2 OCEAN CIRCULATION

Ocean circulation is mainly driven by the tides, but there is a component of the currents that is modified by wind and waves. The hydrodynamic model incorporates both wind and tidal forcing to calculate currents but in the following discussion, no distinction is made between the two components. The local change from the proposed terminal on tidal current patterns was assessed by comparing the hydrodynamic-wave model simulations of existing conditions and future conditions with Project. Three analyses were conducted, including:

1. Spatial analysis using velocity distribution at selected tide stages on a spring tide cycle.
2. Temporal statistical analysis displayed on a current rose at selected locations on the tidal flats.
3. Spatial and temporal statistical analysis using the 50th percentile velocity and displayed on a map.

6.2.1 SPATIAL ANALYSIS - VELOCITY DISTRIBUTION ON SELECTED TIDAL STAGE ON MAY 7, 2012

The following discussion is based on a tide cycle occurring on May 7, 2012 as shown in **Figure 52** – a typical large tidal swing. **Figure 53** and **Figure 54** show the spatial distribution of ocean currents during the flood tide at 3:00 a.m. for the existing conditions and future conditions with Project scenarios respectively. The colour coding indicates the surface flow velocity in metres per second and the vectors represent current direction and magnitude. Points A10, B05, B03 and D01 shown on the figures indicate the selected locations for current rose analysis (discussed in the next section).

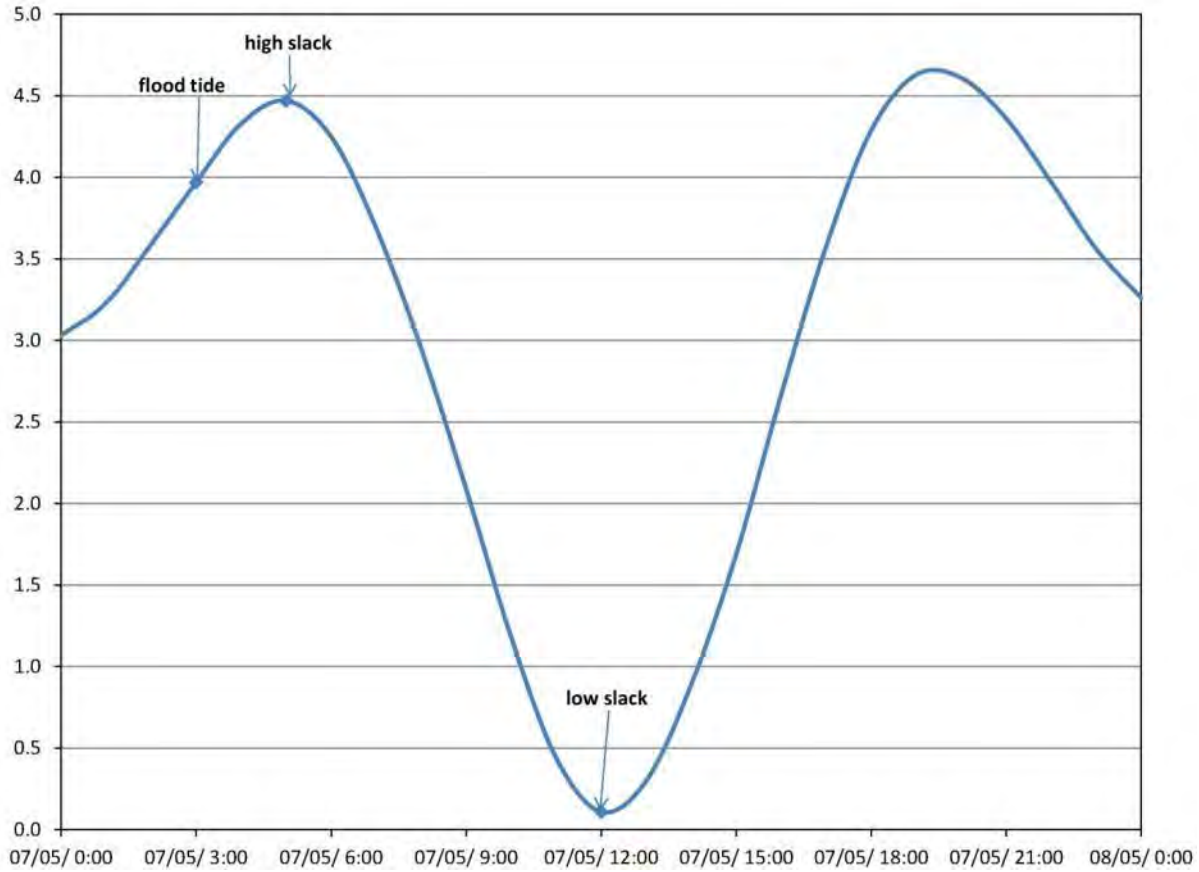

Figure 52: Tide height on May 7, 2012 based on observed water levels at Point Atkinson (#7795).

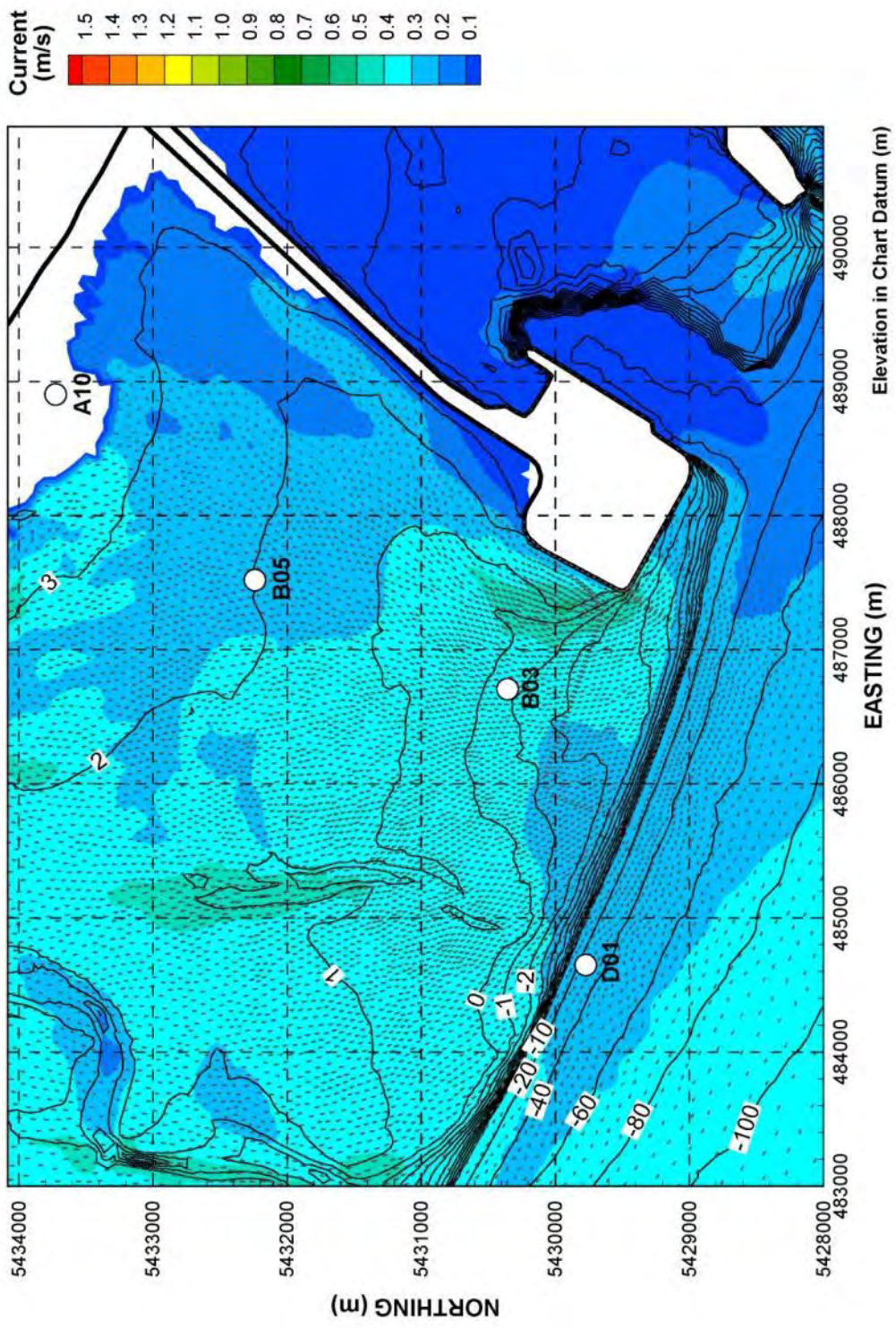

Figure 53: Current velocities associated with a flood tide on May 7, 2012 under existing conditions.

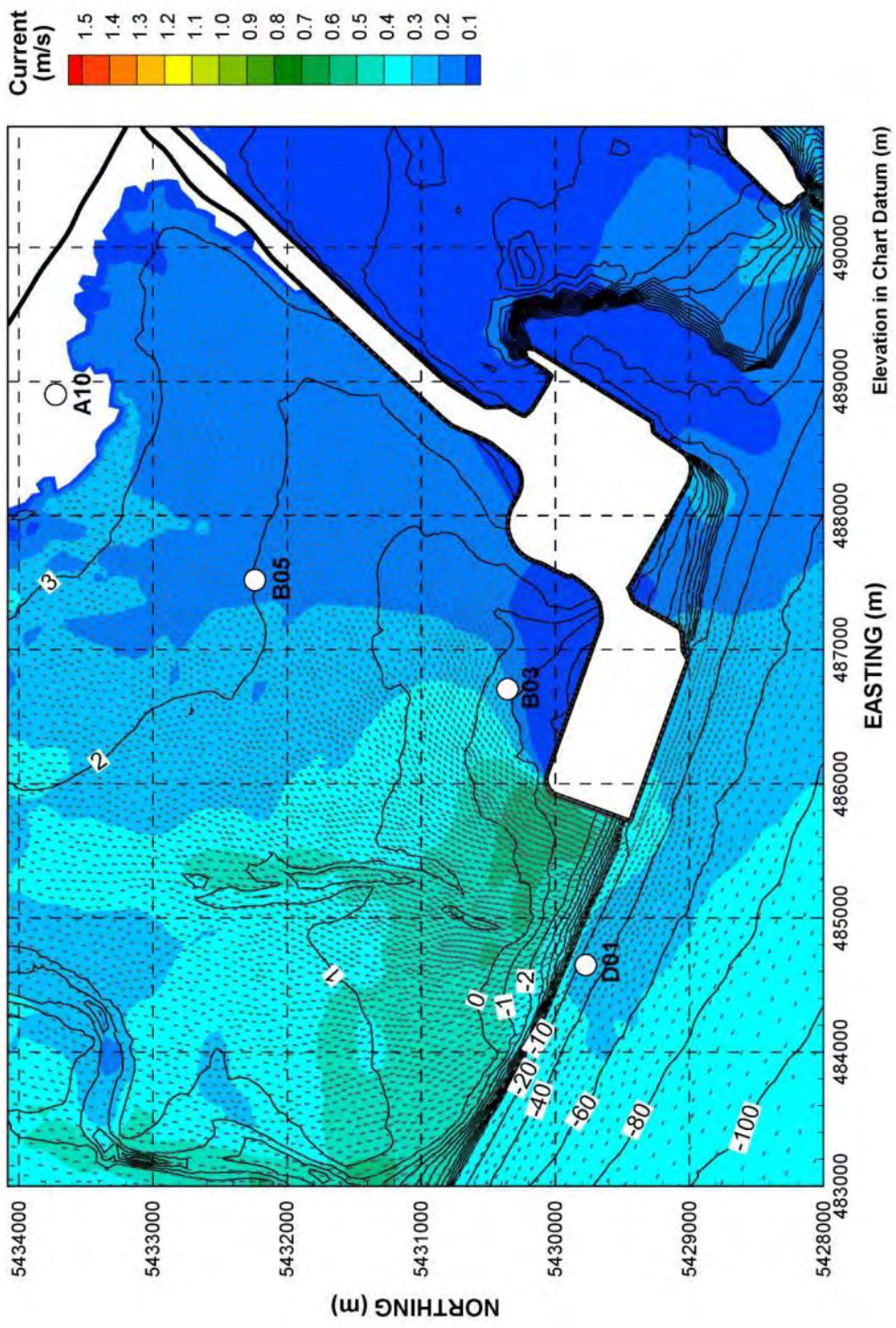

Figure 54: Current velocities associated with a flood tide on May 7, 2012 under future conditions with Project.

The general pattern of ocean circulation in the vicinity of the Project is similar to that in the deep waters of the Strait of Georgia: tidal currents flood to the northwest and ebb to the southeast. This dominant flow pattern, which is parallel to the delta foreslope, is altered by interaction with the shallower areas of the tidal flats such that flow direction is dominantly onshore-offshore in relation to the rising and falling tide respectively. Under existing (without Project) conditions, there is a moderate acceleration of flow at the southwest corner of the Roberts Bank terminals as the rising tide sweeps onshore and around the structure (**Figure 53**).

The Project will extend the existing structural control of the Deltaport terminal on ocean currents. During the flood tide, the proposed terminal will interrupt the existing shoreward movement of water, causing the flow to be deflected further to the northwest and accelerated around the western end of the terminal (**Figure 54**). This zone of flow acceleration occurs mainly between the -2.0 m and +0.5 m CD contour and overlaps with the seaward end of a tidal channel that is presently minimally active. A zone of flow separation and recirculation is predicted off of the northwest corner of the proposed terminal. This is likely to sweep sediment around the corner and deposit it along the north side of the proposed terminal. The addition of the terminal is also predicted to reduce velocities near the elbow at the connection point with the west face of the existing Westshore Terminals. It is likely that sediment will tend to deposit in this region. A second recirculating back-eddy was found to form in the corner between the south face of the Westshore Terminals and the east side of the proposed terminal face. The seaward extent of the back-eddy is predicted to reach EL -5.0 m CD. It is likely that sediment will tend to deposit in this region due to the velocity change but would likely be offset by increase in wave energy relating to wave reflection from the terminal side (see **Section 6.4**).

Figure 55 and **Figure 56** show the current velocities and current pattern near the time of low slack water at 12:00 p.m. (see **Figure 52**) on the same date for existing conditions and future conditions with Project respectively.

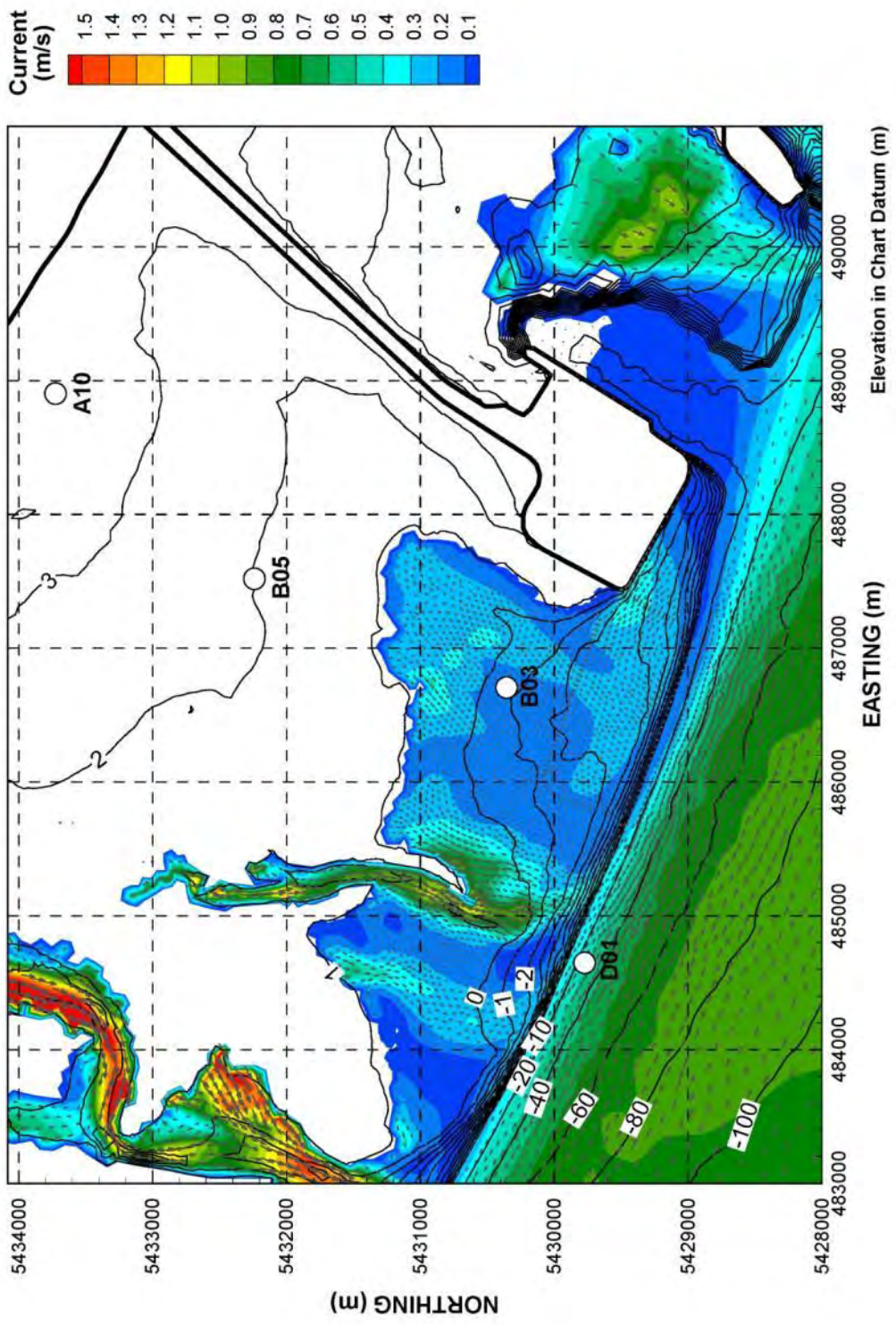

Figure 55: Current velocities associated with an ebb tide on May 7, 2012 under existing conditions.

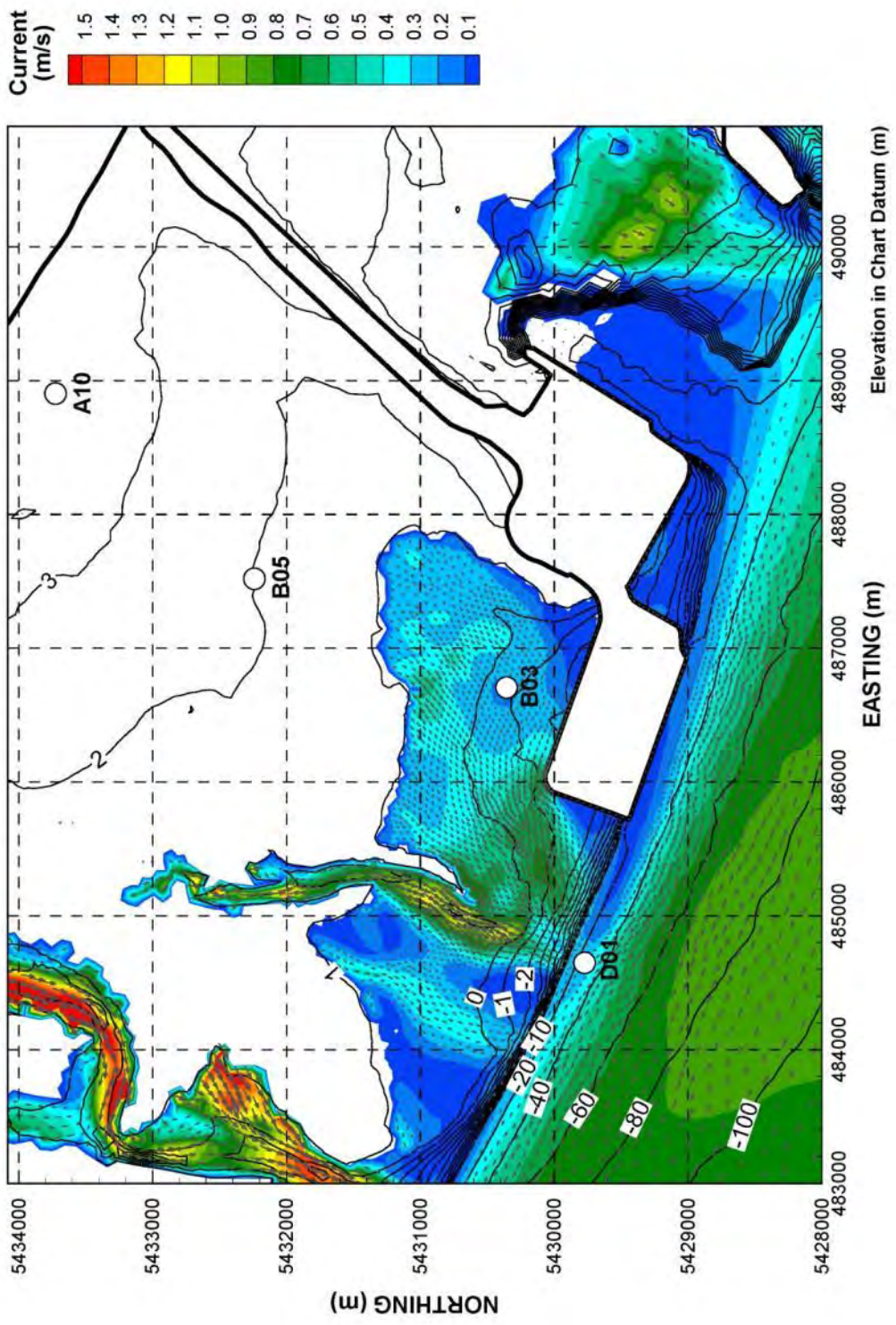

Figure 56: Current velocities associated with an ebb tide on May 7, 2012 under future conditions with Project.

During ebbing tide conditions, the proposed terminal would interrupt the existing seaward movement of water, causing the flow to be deflected and accelerated around the western face of the terminal. This zone of increased current velocity occurs mainly between the +0.0 m to -2.0 m CD contour. The westward edge of the zone of increased current velocity coincides with the seaward end of an existing tidal channel on the flats to the west of the terminal. Sediment mobilization is more likely to occur in this zone with the Project in place than under the existing conditions scenario.

There is a zone of flow separation and recirculation, creating a back-eddy near the southwest corner of the proposed terminal, and it is likely that sediment will tend to deposit in this region during low slack water condition.

The proposed terminal would decrease the tidal current velocity in the elbow formed by the connection point with the western face of the existing Westshore Terminals. The decrease in velocity is evident from the model results on both the landward and seaward sides of the terminal. A stagnant low-velocity zone would develop along the east face of the proposed terminal. A small back-eddy would form in the corner, similar to the situation that develops during the slack tide. Thus, it is likely that sediment will deposit in this region to a greater extent than under the existing conditions scenario.

6.2.2 Temporal Statistical Analysis - Current Rose at Selected Locations

The spatial representations of currents in the vicinity of the proposed Project presented in **Section 6.2.1** provide a 'snapshot' of conditions during a typical large tidal exchange. The local change from the Project on ocean currents can be further illustrated using a current rose, which provides a statistical representation of conditions in 2012 at a single location. The current rose indicates current velocity, frequency of occurrence, and direction (direction toward which the prevailing current flows). Current roses were prepared for Locations D1, B3, B5 and A10 (as shown in **Figure 53** to **Figure 56**) for the existing conditions and future conditions with Project scenarios (**Figure 57** to **Figure 60**).

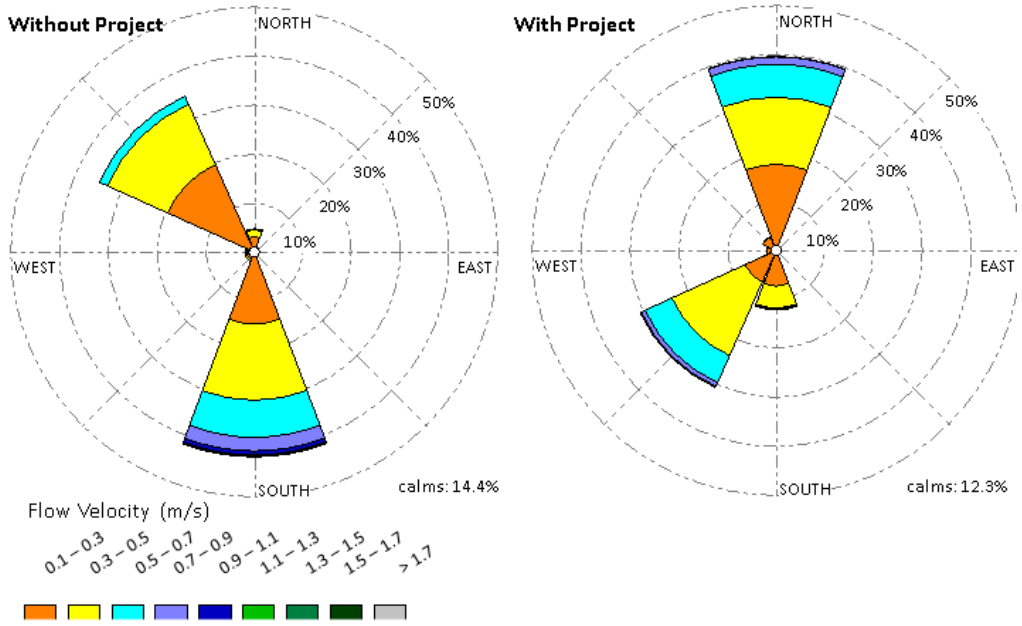

Figure 57: Current velocity statistics for the January 1 to December 31, 2012 period for existing conditions (left) and future conditions with Project (right) at reference location D1.

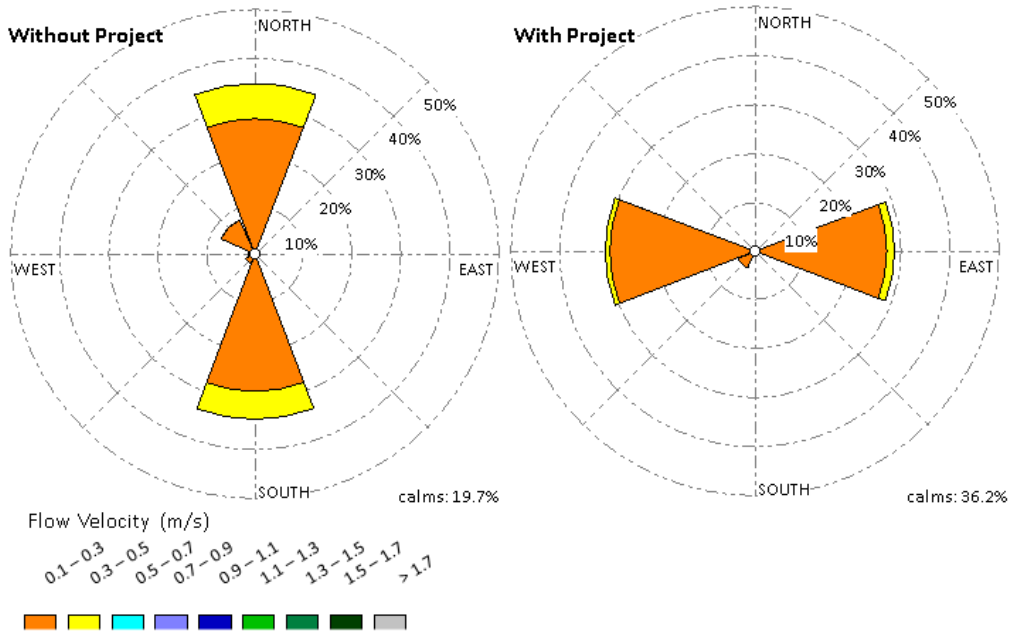

Figure 58: Current velocity statistics for the January 1 to December 31, 2012 period for existing conditions (left) and future conditions with Project (right) at reference location B3.

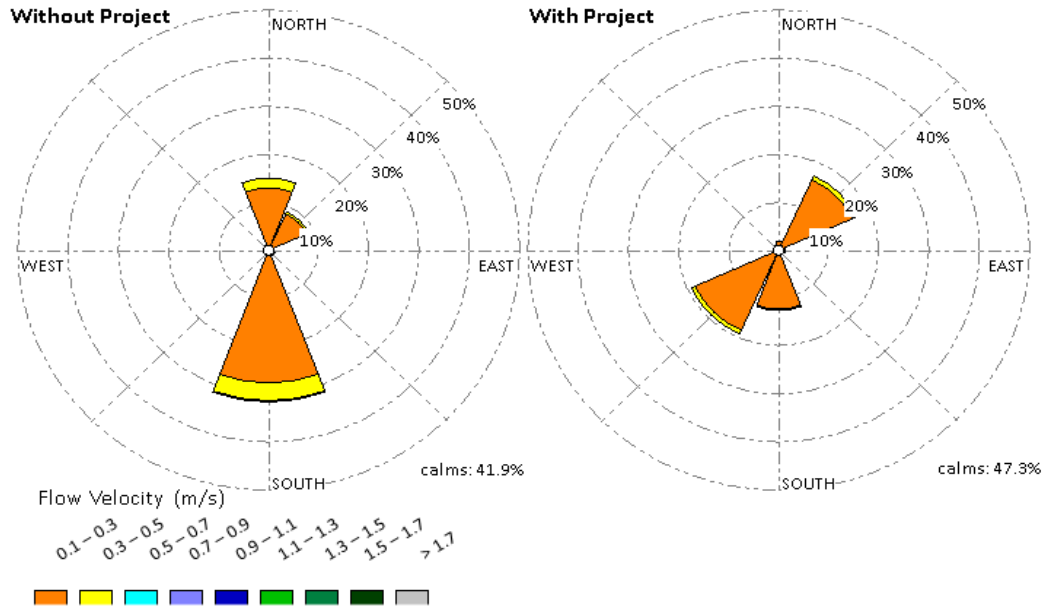

Figure 59: Current velocity statistics for the January 1 to December 31, 2012 period for existing conditions (left) and future conditions with Project (right) at reference location B5.

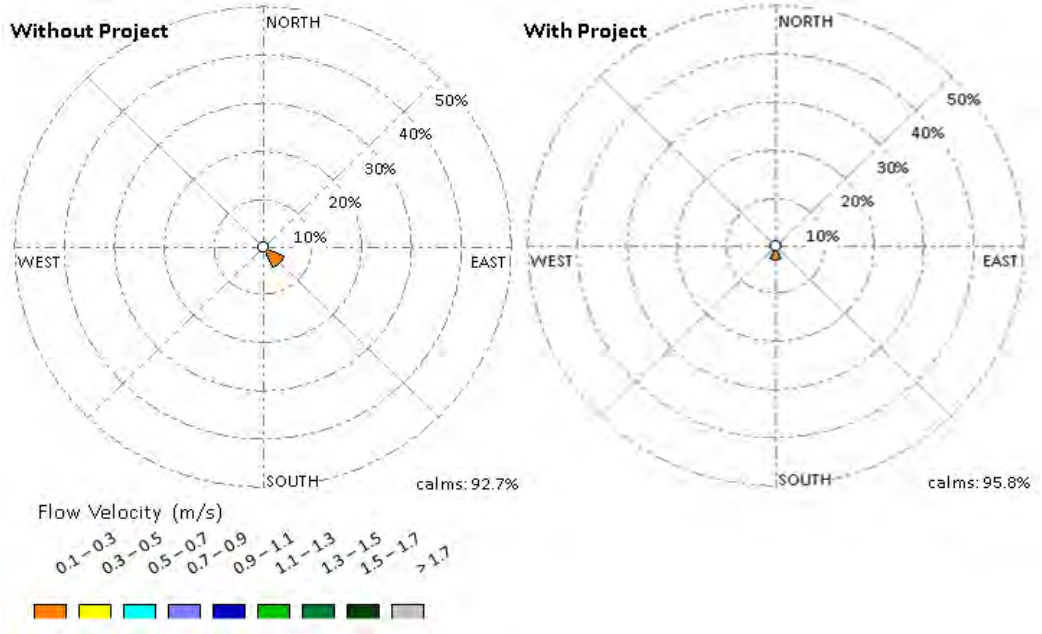

Figure 60: Current velocity statistics for the January 1 to December 31, 2012 period for existing conditions (left) and future conditions with Project (right) at reference location A10.

Location D1 (**Figure 57**) is situated in the deeper water of the delta foreslope. Under existing (without Project) conditions, the predominant current directions are to the northwest during the flood tide and to the south during the ebb tide, with the ebb tide currents occurring slightly more frequently and with slightly higher velocity due to the momentum of the water draining off of the tidal flats. With the

Project in place, the predominant current directions are predicted to shift from northwest to north and from south to southwest. **Figure 57** also shows a change in current magnitude. Under existing conditions, the maximum flood velocity to the northwest is found to be between 0.5 and 0.7 m/s. With the Project in place, the maximum flood velocity in the northerly direction is predicted to increase to between 0.7 and 0.9 m/s. Under existing conditions, the maximum velocity to the south is found to be between 0.9 and 1.1 m/s. With the Project in place, the predicted maximum velocity to the southwest reduced to between 0.7 and 0.9 m/s. The resulting asymmetrical tidal current, with the flood tide being more dominant, is likely to promote net onshore sediment transport.

At Location B3 (**Figure 58**), situated north of the proposed terminal approximately on the -1 m CD contour, the predominant current directions are to the north during flood tide and to the south during ebb tide under existing conditions. With the Project in place, the predicted predominant current directions change from north to east and from south to west, reflecting a reorientation of the offshore-onshore currents to compensate for the Project footprint. **Figure 58** shows that a reduction in current velocity is predicted. Under existing conditions, current velocities in the 0.3 to 0.5 m/s range occurs 13% of the time. With the Project in place, currents in this velocity range occur only 3% of the time, with a subtle asymmetry to the east versus west current directions that would favour movement of fine sediment towards the existing Deltaport Terminal.

At Location B5 (**Figure 59**), positioned at about +2 m CD on the foreshore, the predominant current directions are to the north during flood tide and to the south during ebb tide under existing conditions. With the Project in place, the predicted predominant current directions shift from north to northeast and from south to southwest. Similar to B3, there is an anticipated reduction in current velocity at B5 with the Project in place.

At Location A10 (**Figure 60**), which occurs on the upper foreshore, current velocities less than 0.1 m/s occur 93% of the time under existing conditions. With the Project in place, the proportion of occurrence of current velocities less than 0.1 m/s is predicted to increase by three percentage points to 96%. At this location, current velocities are essentially very small under both scenarios.

6.2.3 Spatial and Temporal Statistical Analysis – 50th Percentile Velocity Map

The 'snapshot' spatial representation of currents presented in **Section 6.2.1** and the at-a-location statistical representation of currents presented in **Section 6.2.2** provide a summary of the hydrodynamic changes as a result of the Project. Another way to illustrate the potential hydrodynamic changes from the Project is by comparing the 50th percentile current maps under the existing conditions and future conditions with Project scenarios.

The 50th percentile value is a statistical representation computed based on hourly modelled velocities during the period of interest. It is a useful way to illustrate the general hydrodynamic effects. Fifty percent of the time, velocities are higher than that value at a given location, and 50% of the time, they are lower. Slack periods, as well as periods during which there is no current because the model element is dry, are accounted for as a value of zero is recorded in these cases. Assigning zero current values for the hours that emergent cells are dry reflects the fact the smaller influence of tidal currents at higher

elevations on the tidal flats. Failing to include these values in the case of currents would skew the results of the 50th percentile value.

Figure 61 and **Figure 62** show the 50th percentile velocities during the freshet period (May to July) for the existing conditions and future conditions with Project scenarios respectively. **Figure 63** and **Figure 64** show the 50th percentile velocities for the non-freshet (October to December) for the existing conditions and future conditions with Project scenarios respectively.

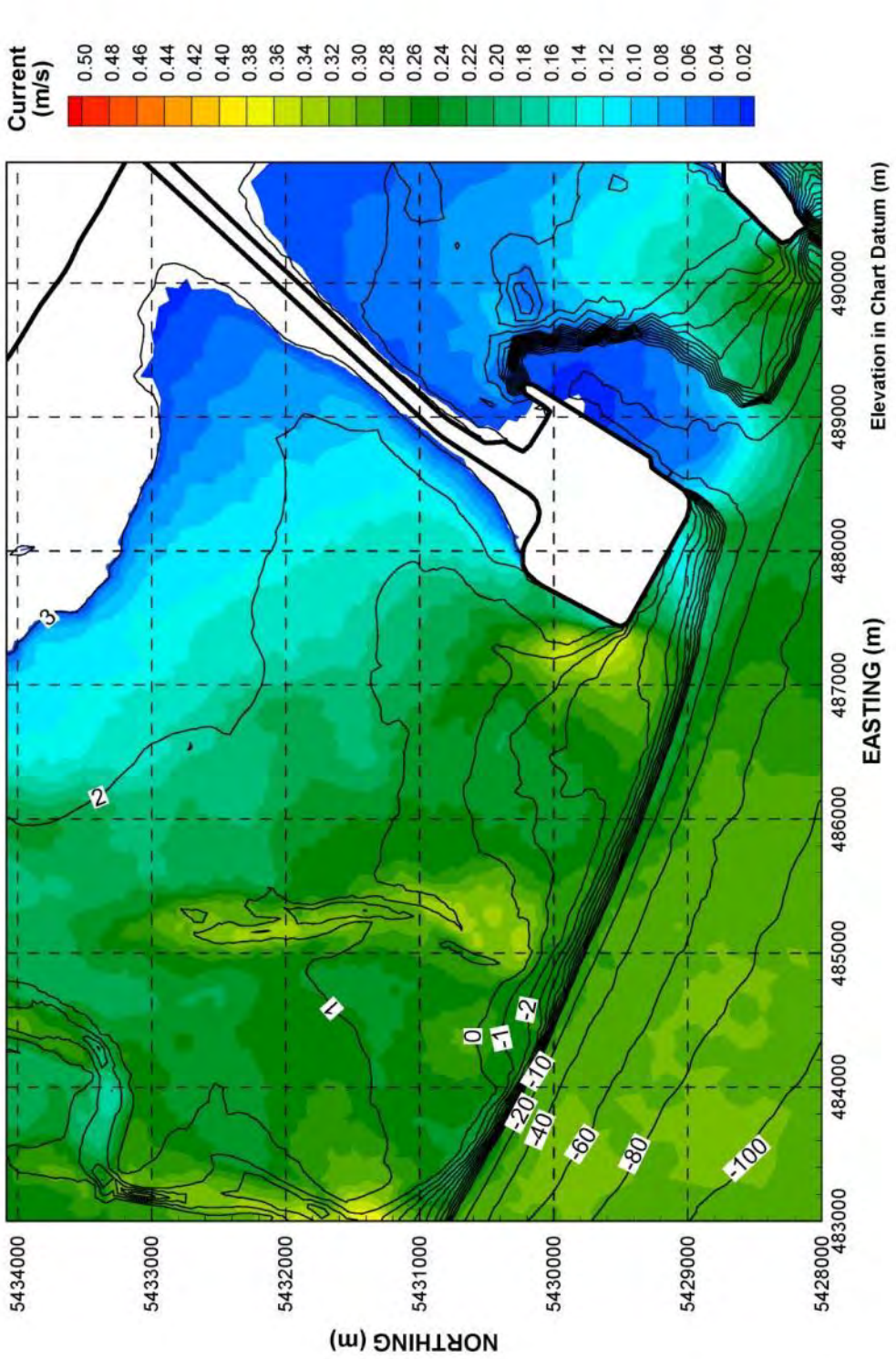

Figure 61: **50**th **percentile current velocities associated with the freshet period (May to July) under existing conditions.**

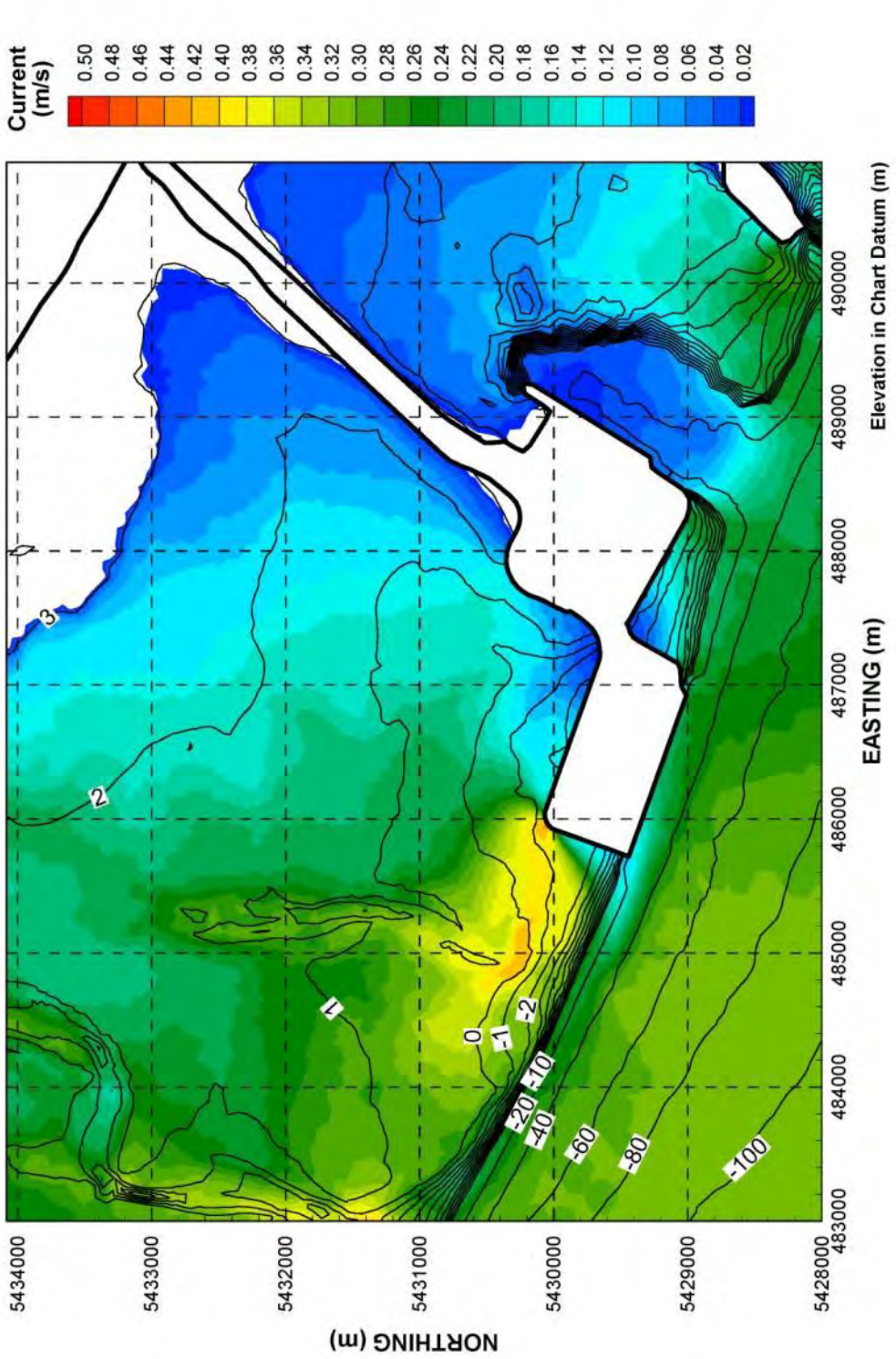

Figure 62: 50th percentile current velocities associated with the freshet period (May to July) under future conditions with Project.

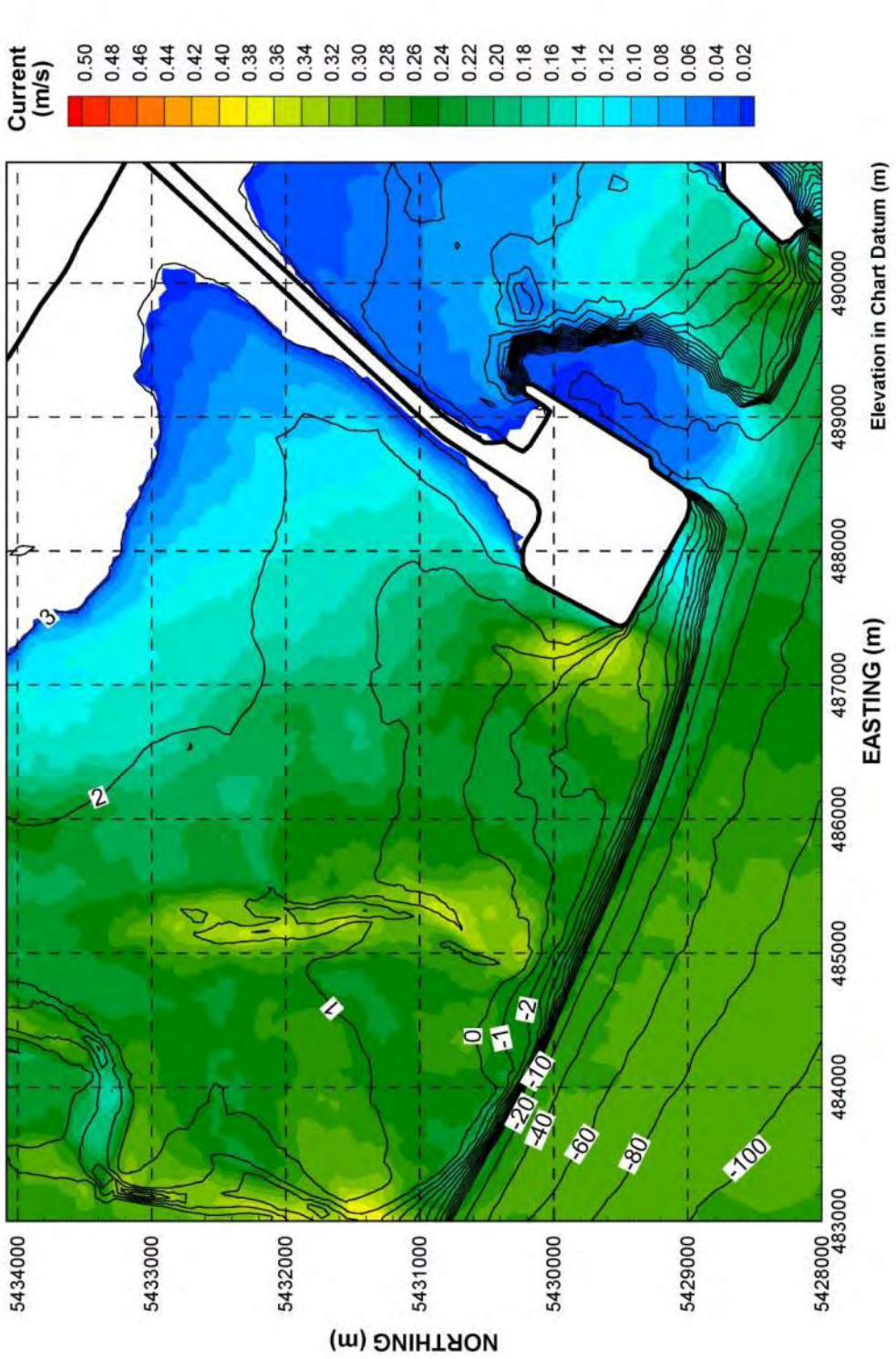

Figure 63: **50th percentile current velocities associated with the non-freshet period (October to December) under existing conditions.**

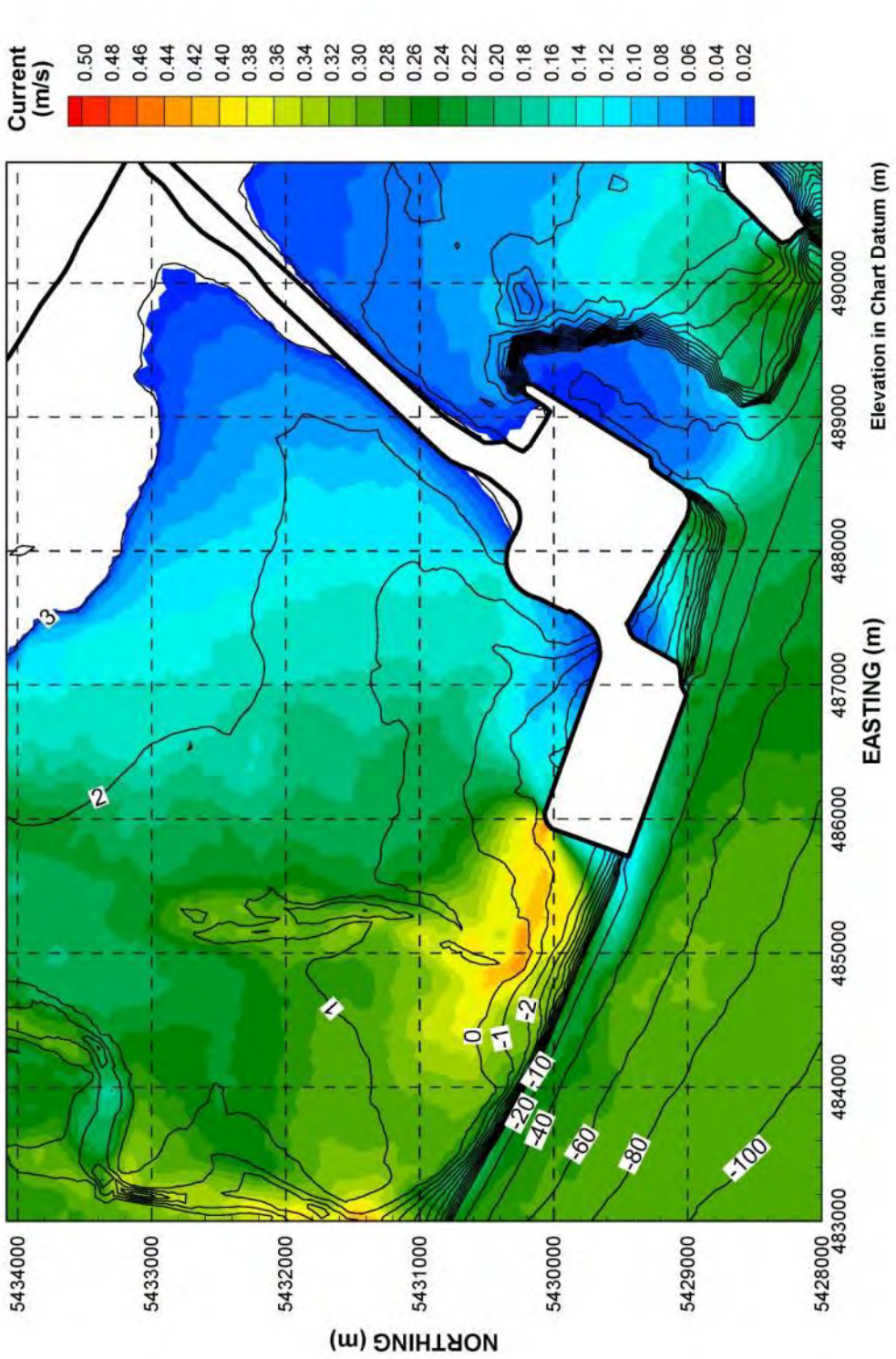

Figure 64: **50th percentile current velocities associated with the non-freshet period (October to December) under future conditions with Project.**

Under existing conditions, there are two areas of generally higher velocities on the tidal flats: the zone at the southwest corner of the Roberts Bank terminals and the zone within the relict channel. With the Project in place, flow acceleration along the western edge of the proposed terminal is evident (**Figure 62** and **Figure 64**) in the form of a field of higher velocities that extend from the northwest corner of the Project across the tidal flats to the existing tidal channel. Low velocity zones exist in the shallow areas adjacent to the causeway and along the upper shoreline. With the Project in place, low velocity areas would be created on both the seaward and shoreward sides of where the proposed terminal connects with the Roberts Bank terminals. The 50th percentile current velocities are slightly higher during the non-freshet period than during the freshet period, which is likely due to the larger tidal swing and smaller Fraser River discharge outside of the freshet.

The potential change from the Project on currents can be assessed more directly by mapping the difference between 50th percentile currents calculated for the existing conditions and future conditions with Project scenarios. **Figure 65** and **Figure 66** show the difference in the predicted 50th percentile current for the freshet and non-freshet periods respectively. The results map uses a neutral colour (white) to indicate currents that are nearly zero as well as areas that are outside the model domain, namely dry land, the terminals and the causeway.

The results summarized in **Figure 65** and **Figure 66** show that the flow acceleration around the western end of the proposed terminal would result in an increase in the 50th percentile current velocity by approximately 0.1 m/s over an area measuring about 2 km by 2 km. It is likely that this region will experience increased sediment mobilization. The velocity reduction in the elbow formed near the connection point between the proposed terminal and existing Westshore Terminals is about 0.3 m/s. The 50th percentile velocity in the foreshore shoreward of the proposed terminal is predicted to be approximately 0.05 m/s slower.

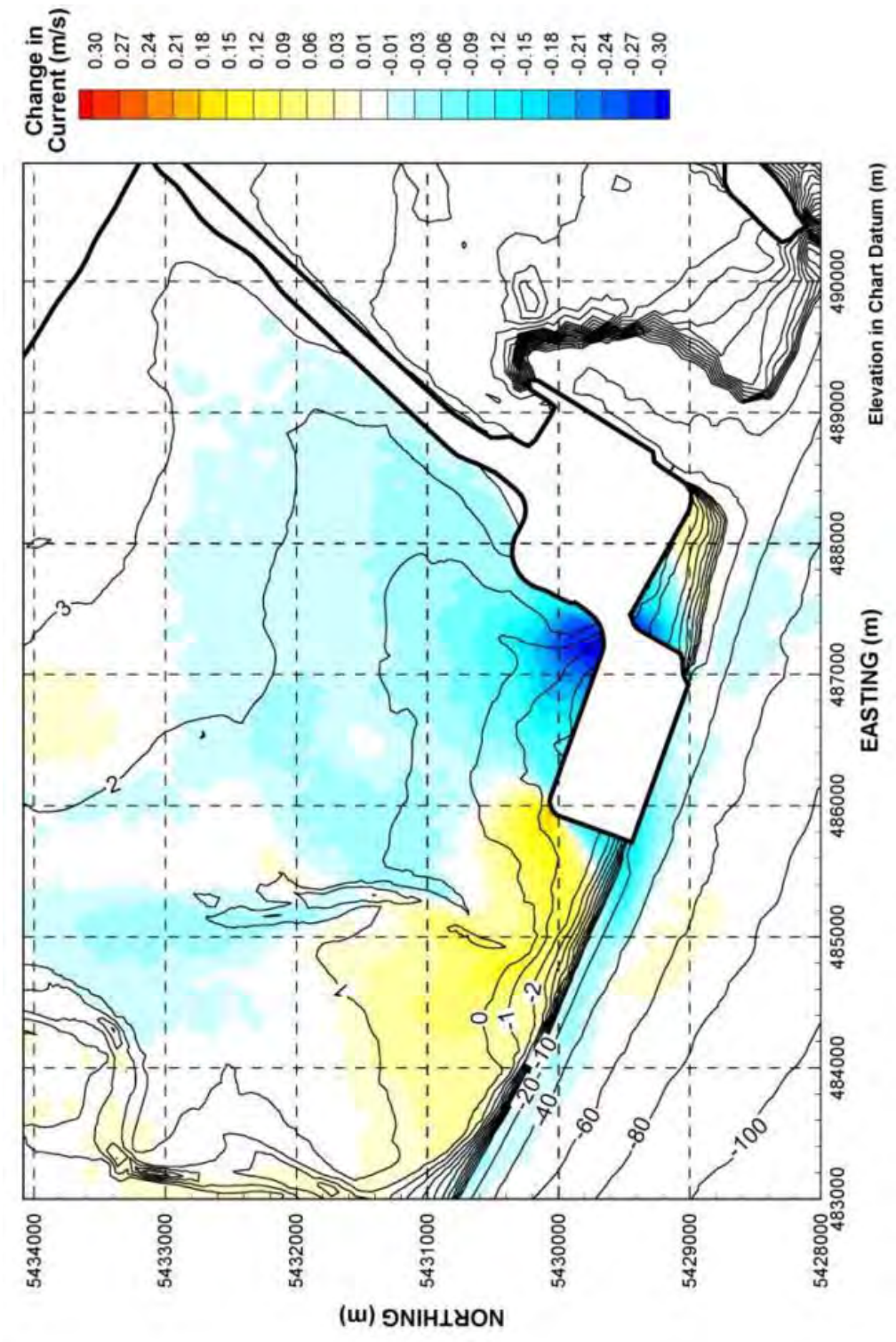

Figure 65: Predicted change in 50th percentile current velocities associated with the Project footprint (future conditions with the Project compared to existing conditions) – freshet period (May to July).

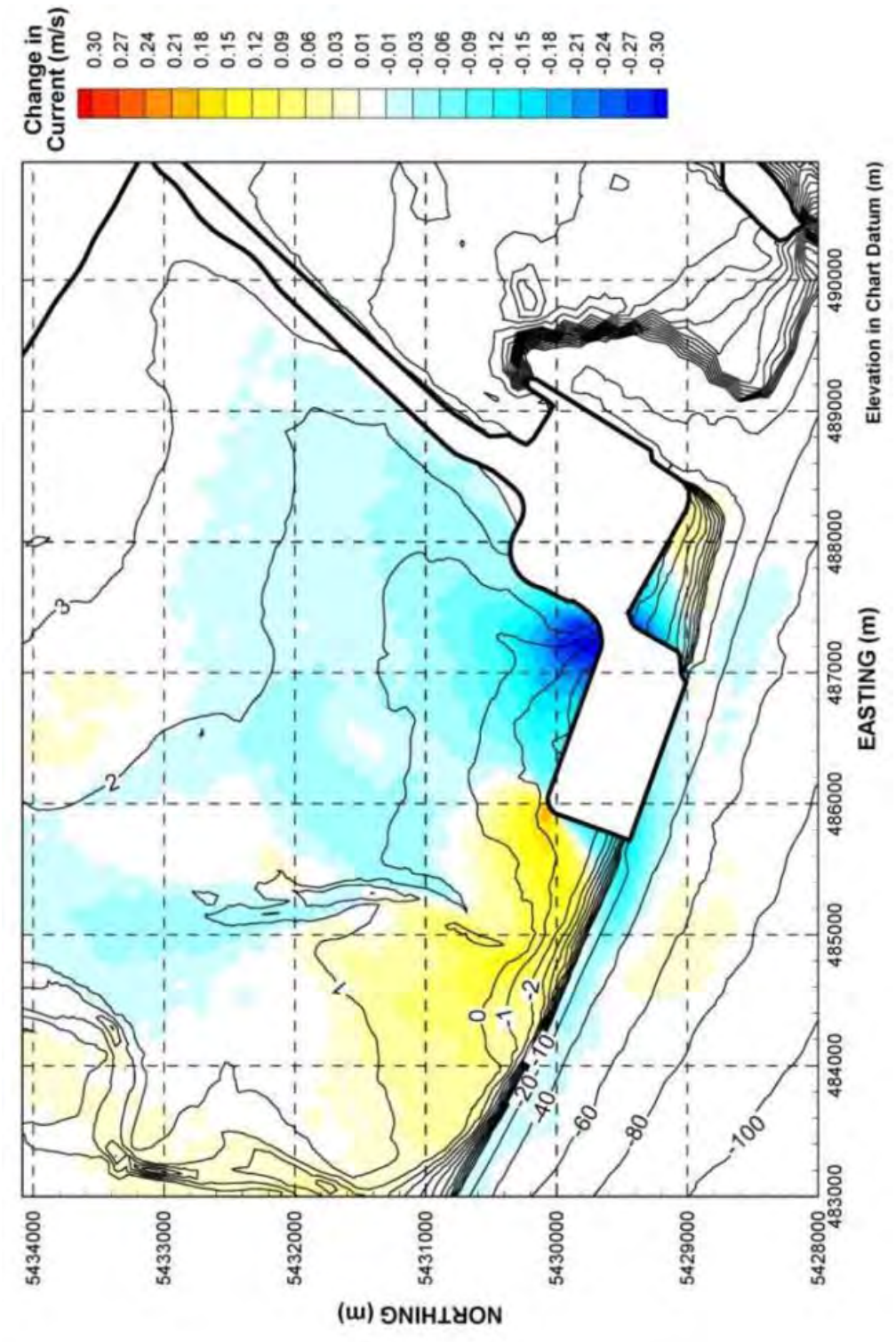

Figure 66: **Predicted change in 50th percentile current velocities associated with the Project footprint (future conditions with the Project compared to existing conditions) – non-freshet period (October to December).**

6.3 SALINITY

The general process that results in variations in salinity in the vicinity of the Project due to mixing of saline water from the Strait of Georgia with freshwater from the Fraser River is described in **Section 4.2.3**. Salinity is computed by the TELEMAC model by assessing the relative quantity of water from these two sources. The hydrodynamic model computes the flows in three dimensions but the vertical layers do not represent field conditions with sufficient accuracy to make predictions of salinity at various depths in the water column, particularly in the shallower areas on the tidal flats. Model results are therefore reported as vertically-integrated values.

The local change from the proposed terminal on salinity was assessed by comparing the hydrodynamic model simulations of existing and future with Project scenarios. Three analyses of the model output were conducted:

1. Spatial analysis of salinity distribution at selected tide stages during a spring tide cycle;
2. At-a-Station hourly variation in salinity; and
3. Spatial and temporal statistical analysis using 50th percentile salinity, displayed on a map.

6.3.1 SALINITY DISTRIBUTION AT SELECTED SPRING TIDE STAGES

The following discussion is based on the tide cycle occurring on May 7, 2012 as shown in **Figure 52**. **Figure 67** and **Figure 68** show the modelled salinity distribution near high slack tide at 5:00 a.m. on May 7 under existing conditions and the future conditions with Project scenarios respectively. The colour coding indicates the salinity in PSU (practical salt units: equivalent to g/kg, or parts per thousand ($^{o}/_{oo}$)). The selected condition represents a typical high tide during the Fraser River freshet period to illustrate the extent of mixing that occurs.

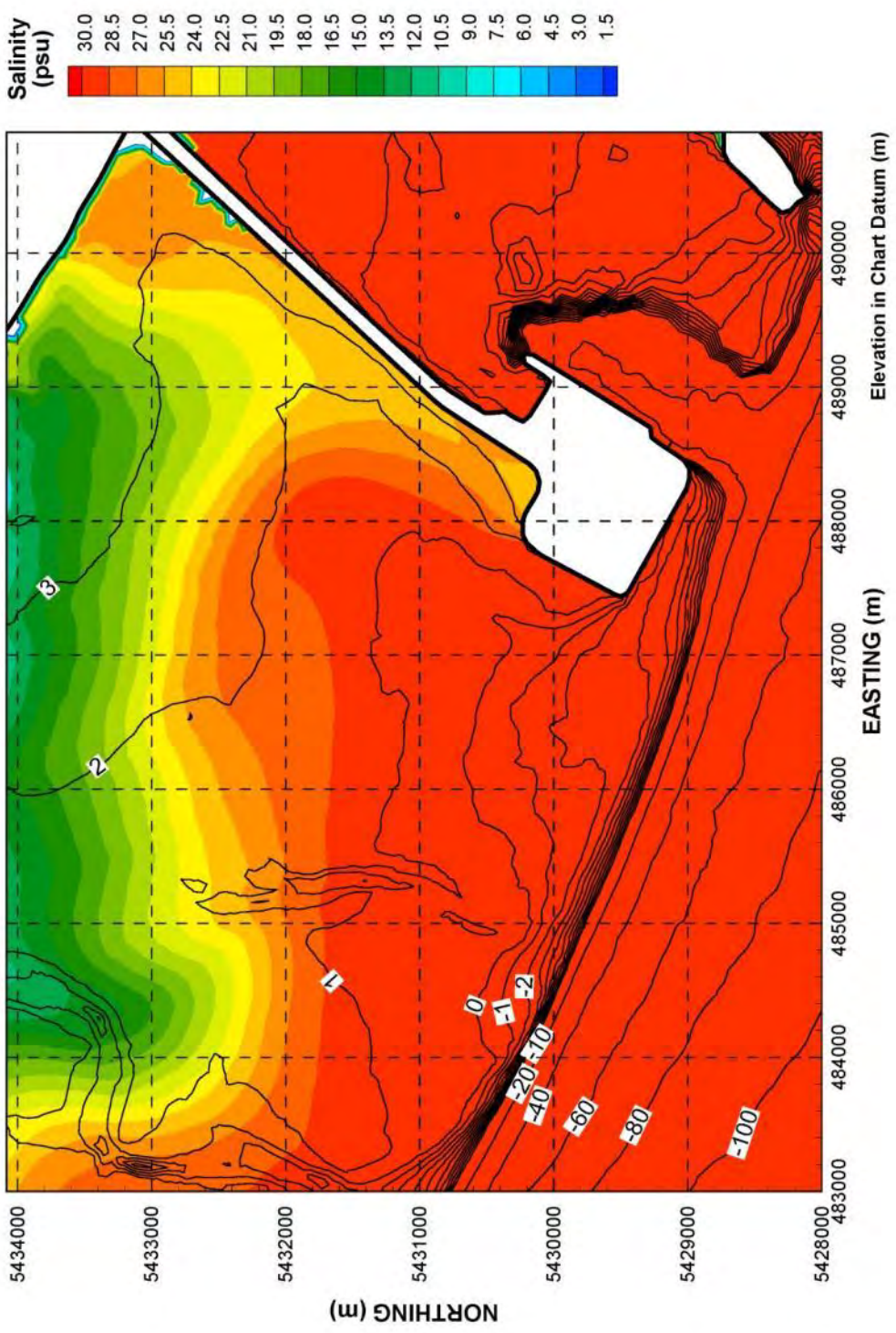

Figure 67: Salinities associated with a high slack tide on May 7, 2012 under existing conditions.

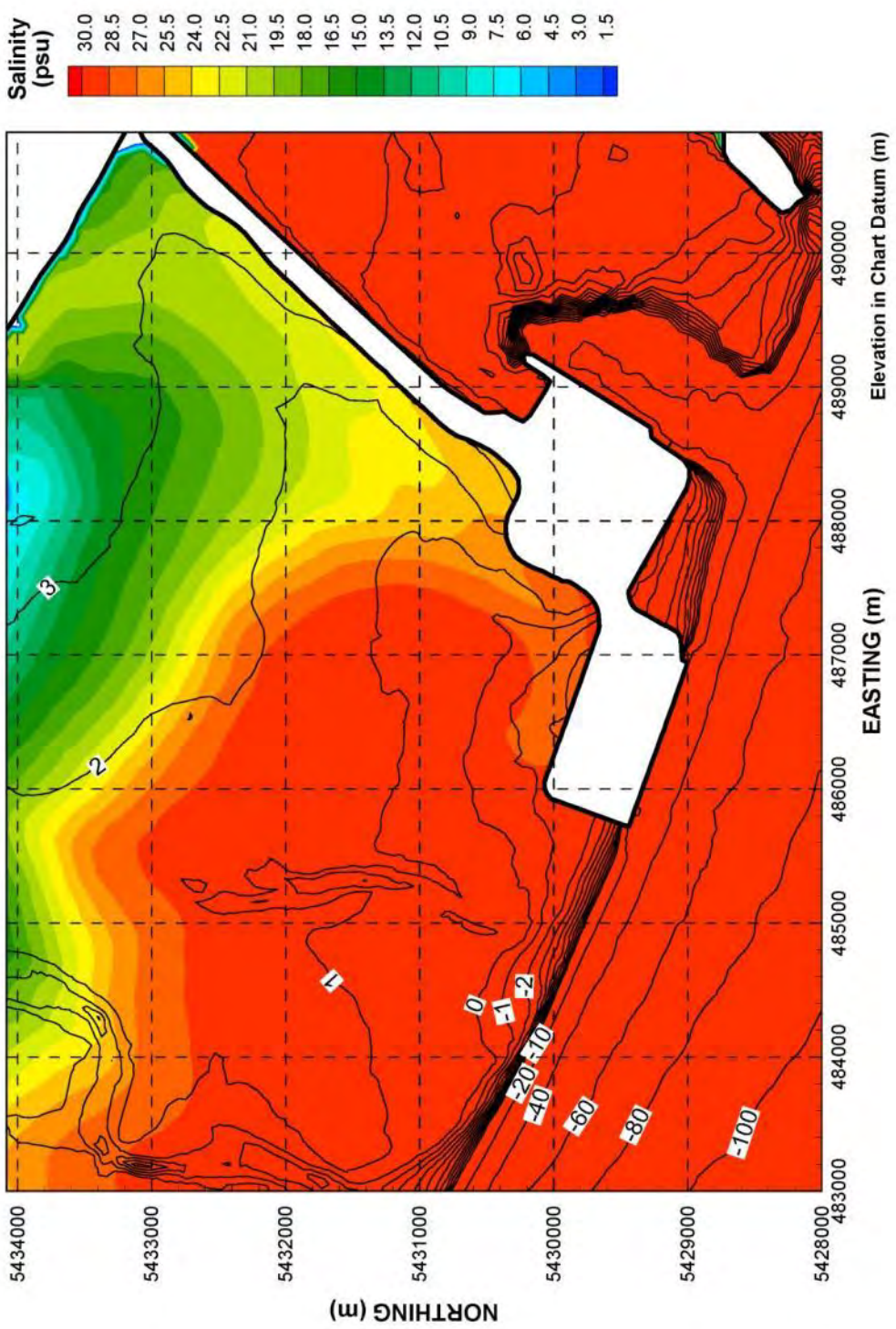

Figure 68: Salinities associated with a high slack tide on May 7, 2012 under future conditions with Project.

Under existing conditions, during a rising tide, saline water from the Strait of Georgia floods onto the tidal flats and displaces brackish water that is generated by the mixing with freshwater draining from Canoe Passage. At high slack tide, an area of slightly reduced salinity is retained along the north side of the causeway, but a broader area of brackish water persists on the upper tidal flats between Canoe Passage and the causeway (**Figure 67**). In this zone, salinity decreases towards the outlet of Canoe Passage, reflecting proximity to the source of the freshwater input.

During the rising tide, the proposed terminal would interrupt the shoreward movement of seawater causing the flow to be deflected further to the northwest and resulting in onshore currents moving parallel to shore across the tidal flats to flood the area shoreward of the structure. This flow diversion would result in a change in the overall pattern of tidal currents during a rising tide, from an onshore-directed pattern to a clockwise flow pattern (compare **Figure 53** to **Figure 54**). The result is that the more saline water would flow onshore in the region north of the terminal and fresher water would flow into the region along the causeway (**Figure 68**). Under existing conditions (**Figure 67**), the modelled salinity along the causeway varies between 24 and 26 PSU at high slack. With the proposed terminal in place, modelled salinity along the causeway is reduced to between 16 and 24 PSU at high slack tide.

Figure 69 and **Figure 70** show the salinity distribution at low slack water at 12:00 p.m. on May 7, 2012 under existing conditions and the future with Project scenario respectively. The timing of the model output relative to the daily tide cycle is shown in **Figure 52**. This condition was chosen to represent a typical low tide during the freshet and to demonstrate the retention of freshwater at the seaward limit of the tidal flats at low tide. Under existing conditions, freshwater from Canoe Passage spreads south and east over the tidal flats as the tide drops. Initially, the less dense freshwater is retained as a distinct layer floating above the saline water from the Strait of Georgia, but over time there is vertical mixing of the two water masses. As the tide drops further, the tidal flats emerge and freshwater is retained along the seaward margin of the tidal flats (**Figure 69**).

During the ebb tide, the proposed terminal represents a physical barrier to the seaward movement of water, forcing flow to move parallel to the shoreward end of the terminal when draining seaward. This modification to the flow pattern will divert the more saline water from the shoreline zone in to the region shoreward of the proposed terminal prior to retreat, as well as change the direction of ebb flow off the tidal flats. A zone of more saline water is created where previously it consisted almost entirely of freshwater (**Figure 70**), although this change is not dominant, as seen from the plots of 50th percentile salinity values below.

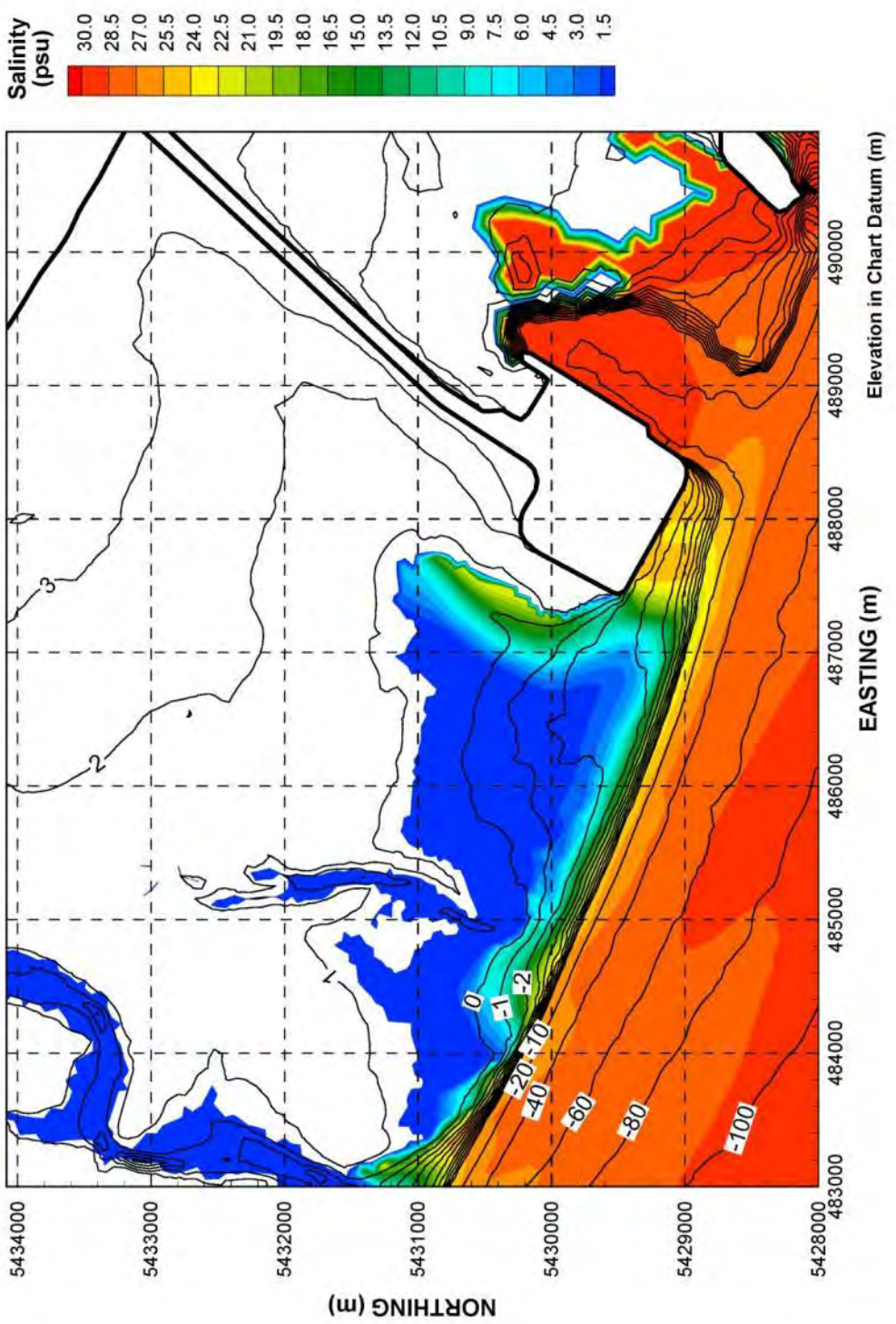

Figure 69: Salinities associated with an ebb tide on May 7, 2012 under existing conditions.

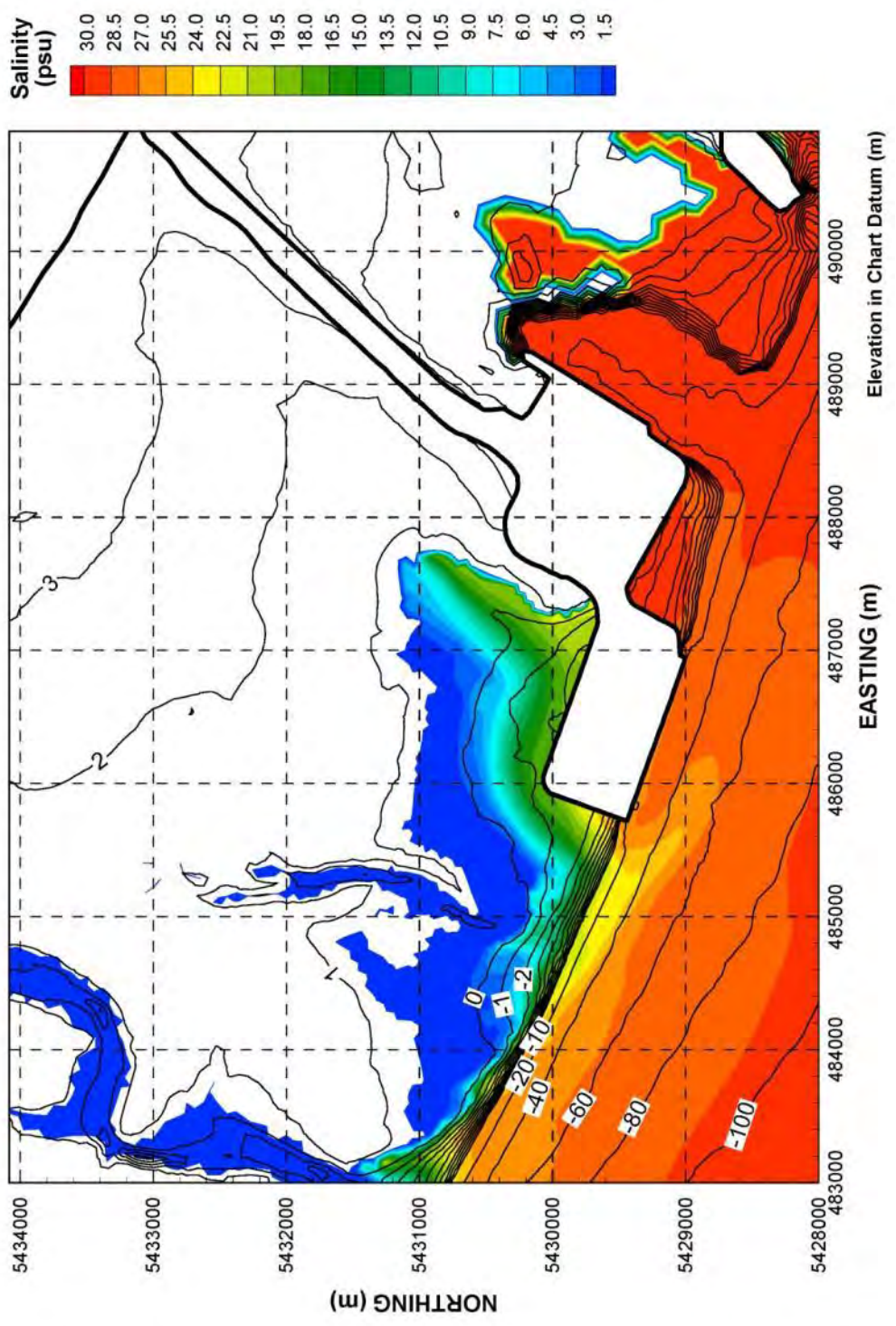

Figure 70: **Salinities associated with an ebb tide on May 7, 2012 under future conditions with Project.**

6.3.2 AT-A-STATION HOURLY VARIATION IN SALINITY

The salinity values presented in **Section 6.3.1** for selected tide stages show the spatial variation but do not describe change over time, while the 50th percentile values presented in **Section 6.3.3** integrate numerous time steps but don't describe short-term time-steps. The TELEMAC model results can be used to describe daily variation in salinity values at various locations.

Hourly values of salinity were extracted from the model at two locations (shown in **Figure 71**), for both the existing conditions and the future with Project. For the period June 11 to June 24, 2012, the existing conditions hourly variation in salinity ranges from below 5 PSU to over 25 PSU at T5, often in a single day but the variability at this location is smaller overall with the Project in place and declines over time during this period (**Figure 72**). At T6, which is approximately 1.3 km further seaward, the existing conditions daily range is slightly greater, reflecting higher exposer to the Fraser River plume, which flows towards the southeast during the dropping tide (**Figure 73**). The future with Project salinity values at T6 show that there is a slightly reduced salinity range for this period but the effect is less pronounced than at T5.

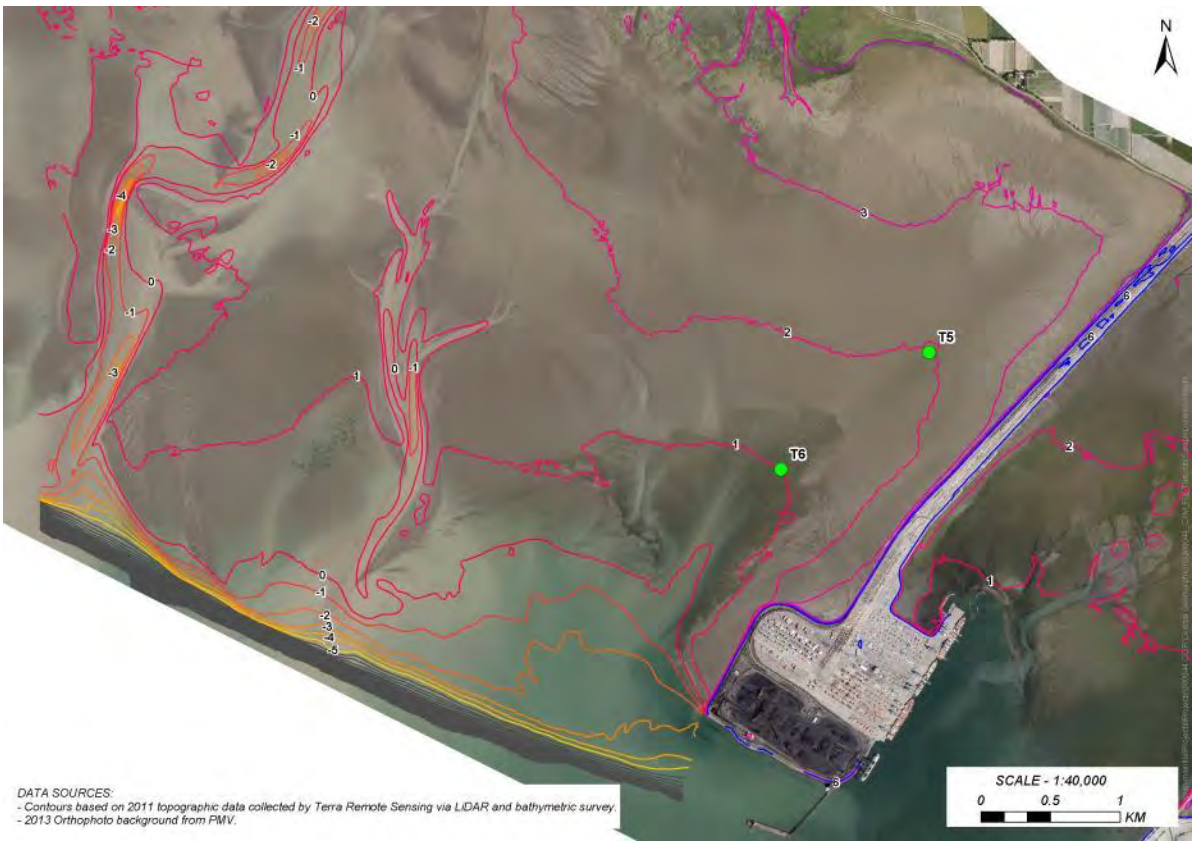

Figure 71: Location of hourly salinity values: Station T5 and Station T6.

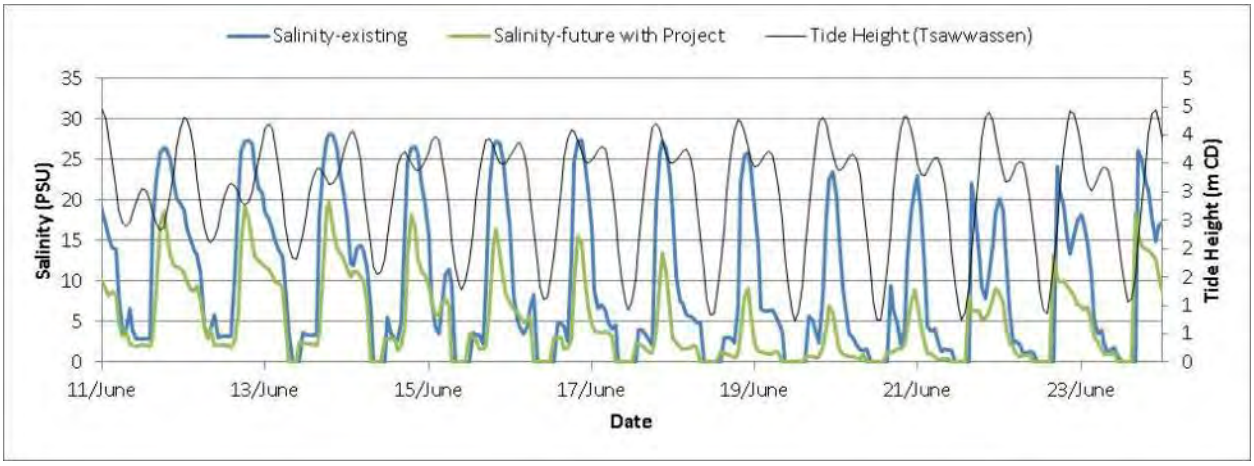

Figure 72: Hourly variation in salinity and tide height at Station T5 for the period June 11 to June 24, 2012 based on TELEMAC model results.

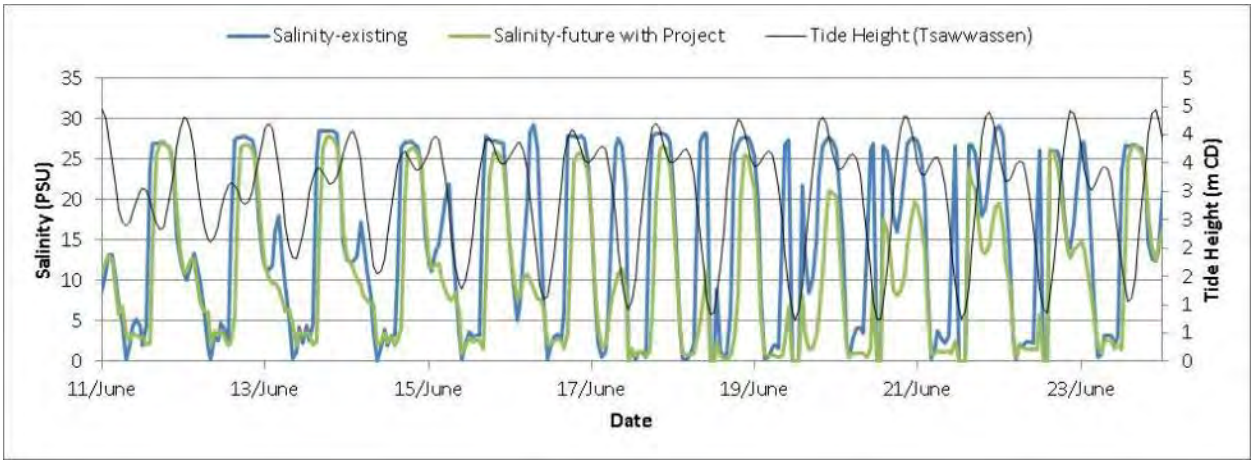

Figure 73: Hourly variation in salinity and tide height at Station T6 for the period June 11 to June 24, 2012 based on TELEMAC model results.

6.3.3 50TH PERCENTILE SALINITY MAP

The snapshot spatial representation of salinity presented in **Section 6.3.1** provides a description of the effect of the Project on the mixing of freshwater from Canoe Passage with saline water in the Strait of Georgia during freshet conditions and a large tidal exchange. Another way to illustrate the potential change from the Project on salinity is by comparing the 50th percentile salinity maps under the existing conditions and future conditions with Project scenarios.

The 50th percentile value is a statistical representation computed based on hourly modelled salinity values during the period of interest. Fifty-percent of the time, salinities are higher than that value at a given location, and 50% of the time, they are lower. It is a useful way to illustrate the general change from the Project on salinity under the full range of water levels and Canoe Passage discharges during the

freshet and non-freshet periods as it focuses on the average salinity. In contrast to the way emergent areas are treated for tidal currents and waves (for a discussion see **Section 6.2.3** and **Section 6.4.3** respectively), emergent areas cannot be assigned a zero value for salinity because this value indicates freshwater rather than the absence of water. In order to calculate the 50th percentile salinity values, the periods of time when areas are dry are not considered in the statistic.

The 50th percentile salinity maps are presented for the existing conditions and future conditions with Project scenarios for the freshet period (May to July – **Figure 74** and **Figure 75**) and for the non-freshet period (October to December – **Figure 76** and **Figure 77**).

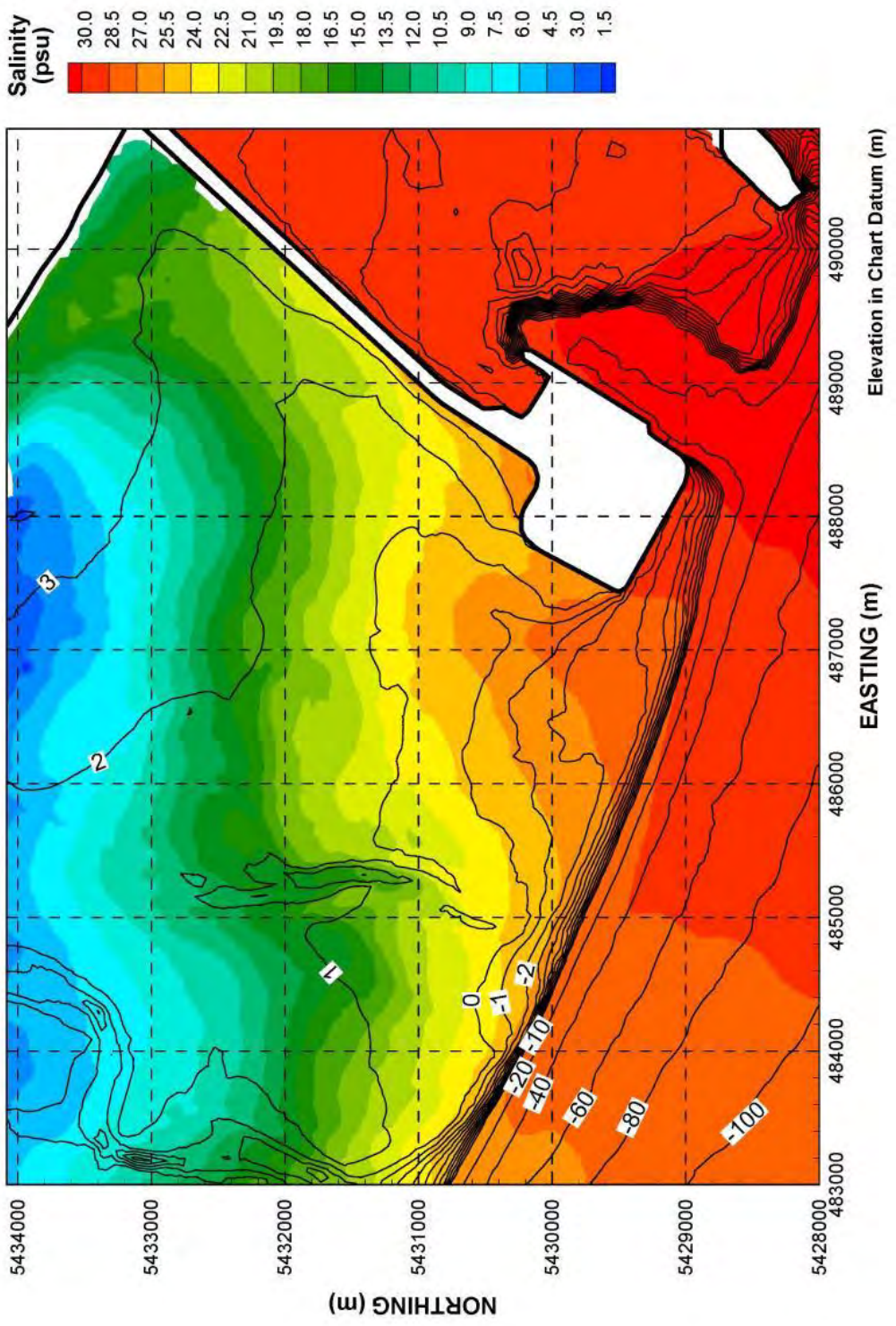

Figure 74: **50th percentile salinities associated with the freshet period (May to July) under existing conditions.**

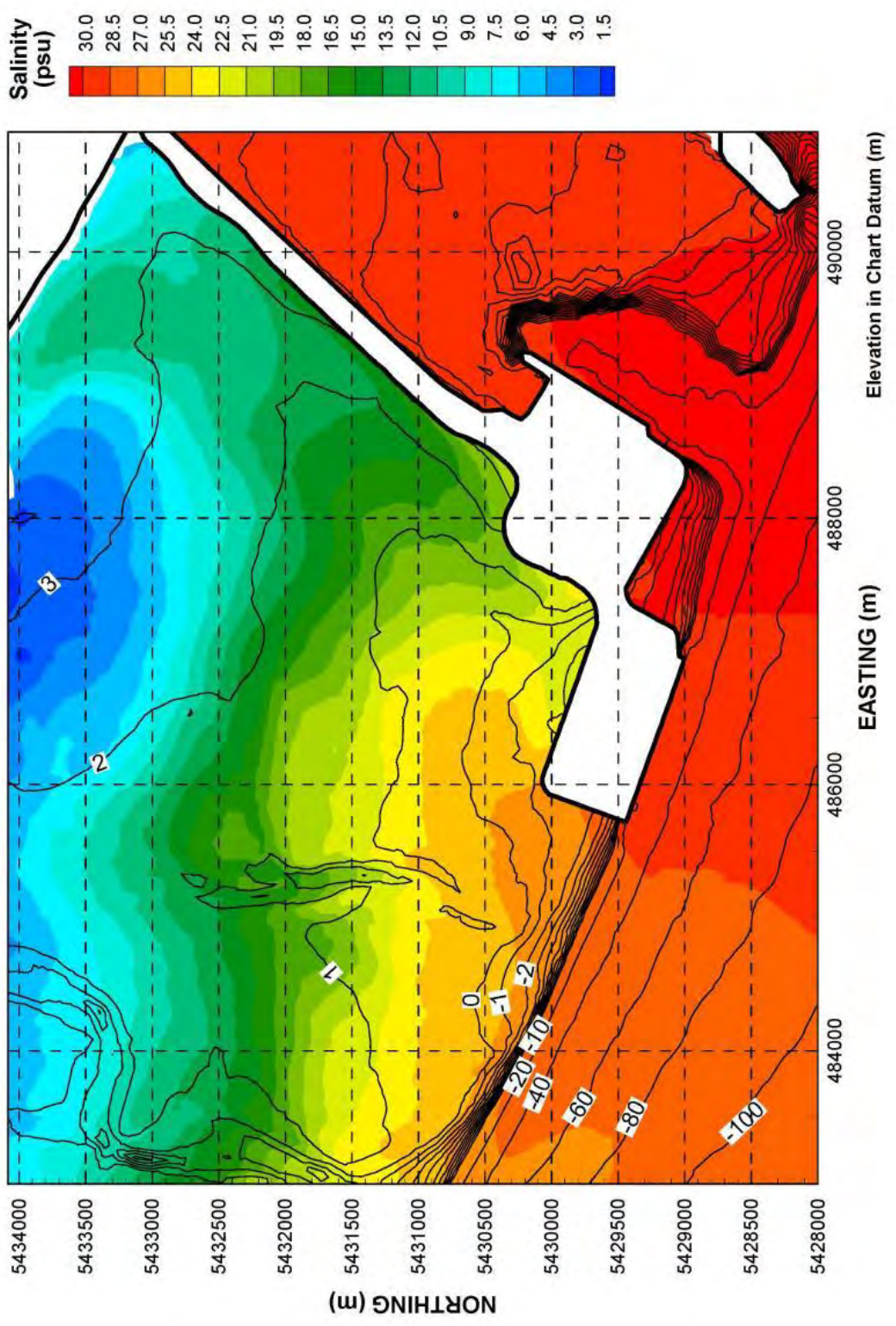

Figure 75: **50th percentile salinities associated with the freshet period (May to July) under future conditions with Project.**

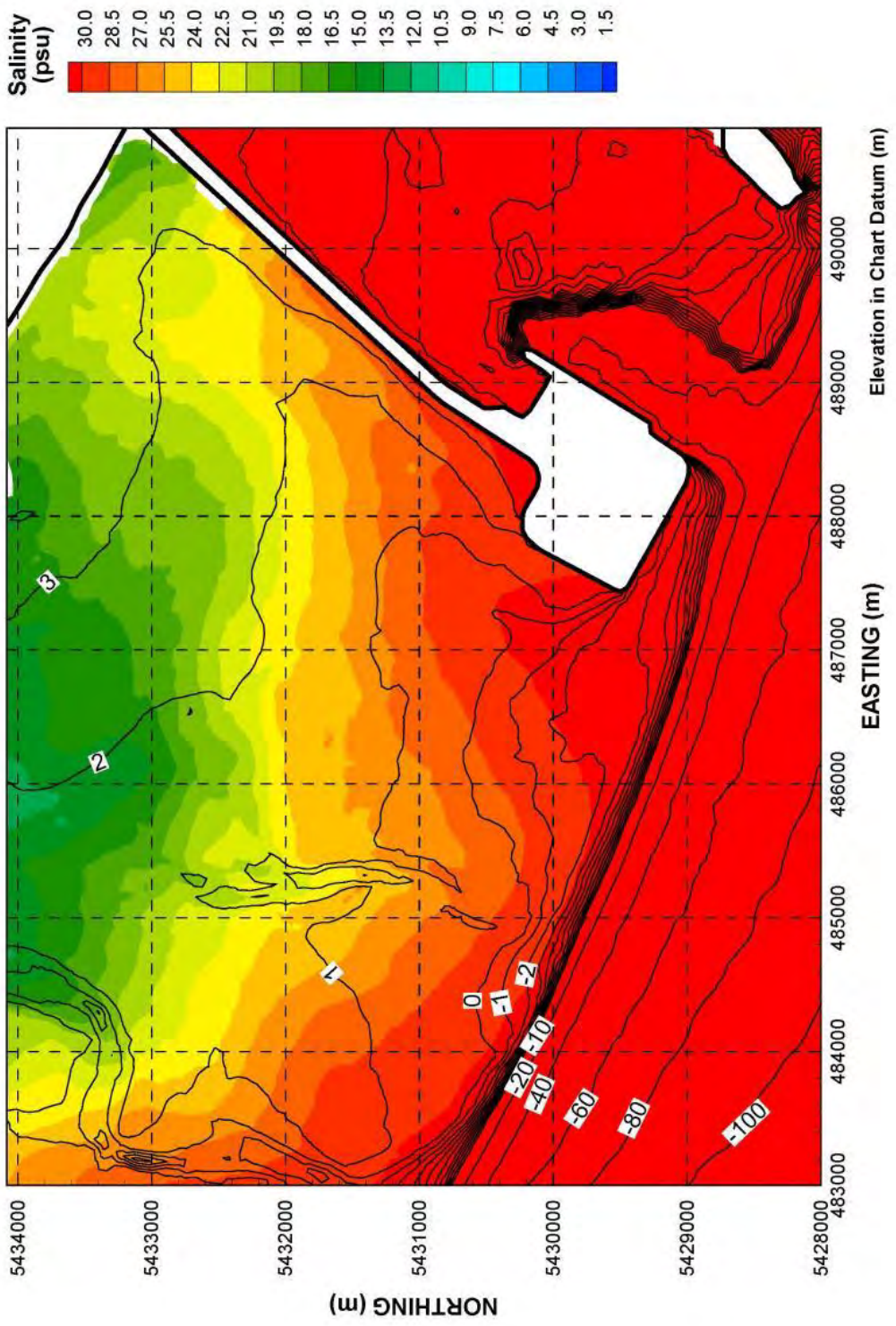

Figure 76: **50th percentile salinities associated with the non-freshet period (October to December) under existing conditions.**

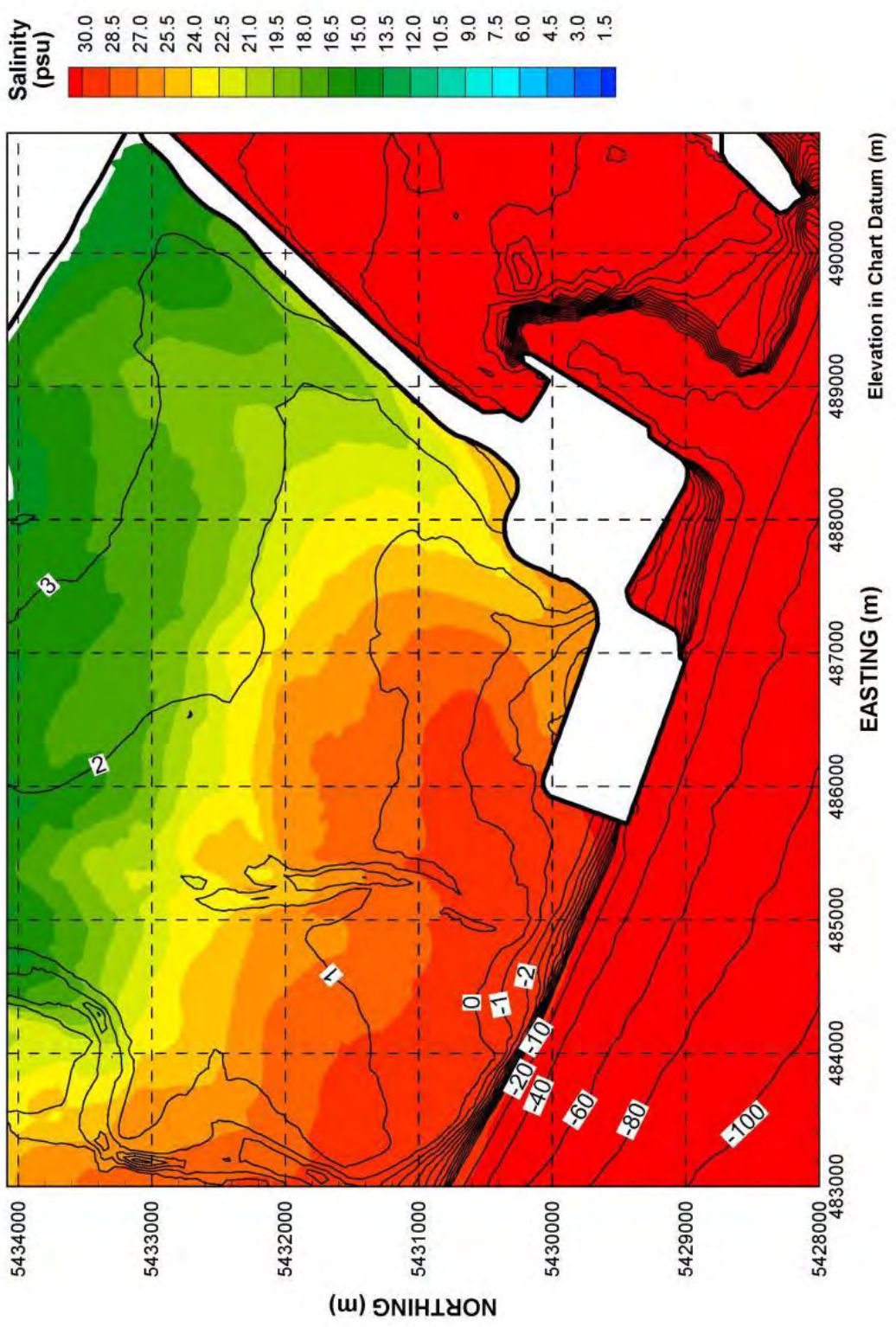

Figure 77: **50th percentile salinities associated with the non-freshet period (October to December) under future conditions with Project.**

The influence of the Fraser River freshet on the 50th percentile salinity values is apparent. Under existing conditions, salinity during the freshet period shows a nearly uniform gradient from almost entirely freshwater emanating from the Fraser River to saline water from the Strait of Georgia in the vicinity of the existing terminal (**Figure 74**). During the non-freshet period, a gradient exists but with higher salinity across Roberts Bank when the Fraser River flows decline in the later Fall (**Figure 76**). Near the Canoe Passage outlet, salinity is as high as 19 PSU, reflecting the much smaller volume of freshwater mixing over the tidal flats. With the Project in place, there is a greater retention of freshwater across the tidal flats, particularly along the causeway. This is true for both the freshet period (**Figure 75**) as well as the non-freshet period (**Figure 77**), the main difference being in the relative influence of freshwater, which is dependent on discharge from Canoe Passage.

The potential change from the Project on salinity distribution on the tidal flat is further illustrated by mapping the difference between 50th percentile salinity values for the existing conditions and future conditions with Project scenarios for the two periods, as shown in **Figure 78** and **Figure 79**. Difference values that are close to zero are shown using a neutral colour (white), indicating no change. This colour is also used within the Project footprint to indicate the exclusion of this area from the modelled flows.

With the Project in place, local current patterns during the rising tide are modified such that they shift flow further towards the northwest before moving onto the tidal flats. The result is that on average there is a decrease in along the north side of the Roberts Bank causeway extending 2 to 3 km and an increase in salinity in the area of the outer tidal flats between the Canoe Passage outlet and the Project. **Figure 78** shows that the both the magnitude and extent of the change are greatest during the freshet months of May through July and smaller during the non-freshet months of October through December (**Figure 79**). The maximum change in salinity based on the 50th percentile value is -8 and +4 PSU during the freshet and -7 and +4 during the non-freshet period.

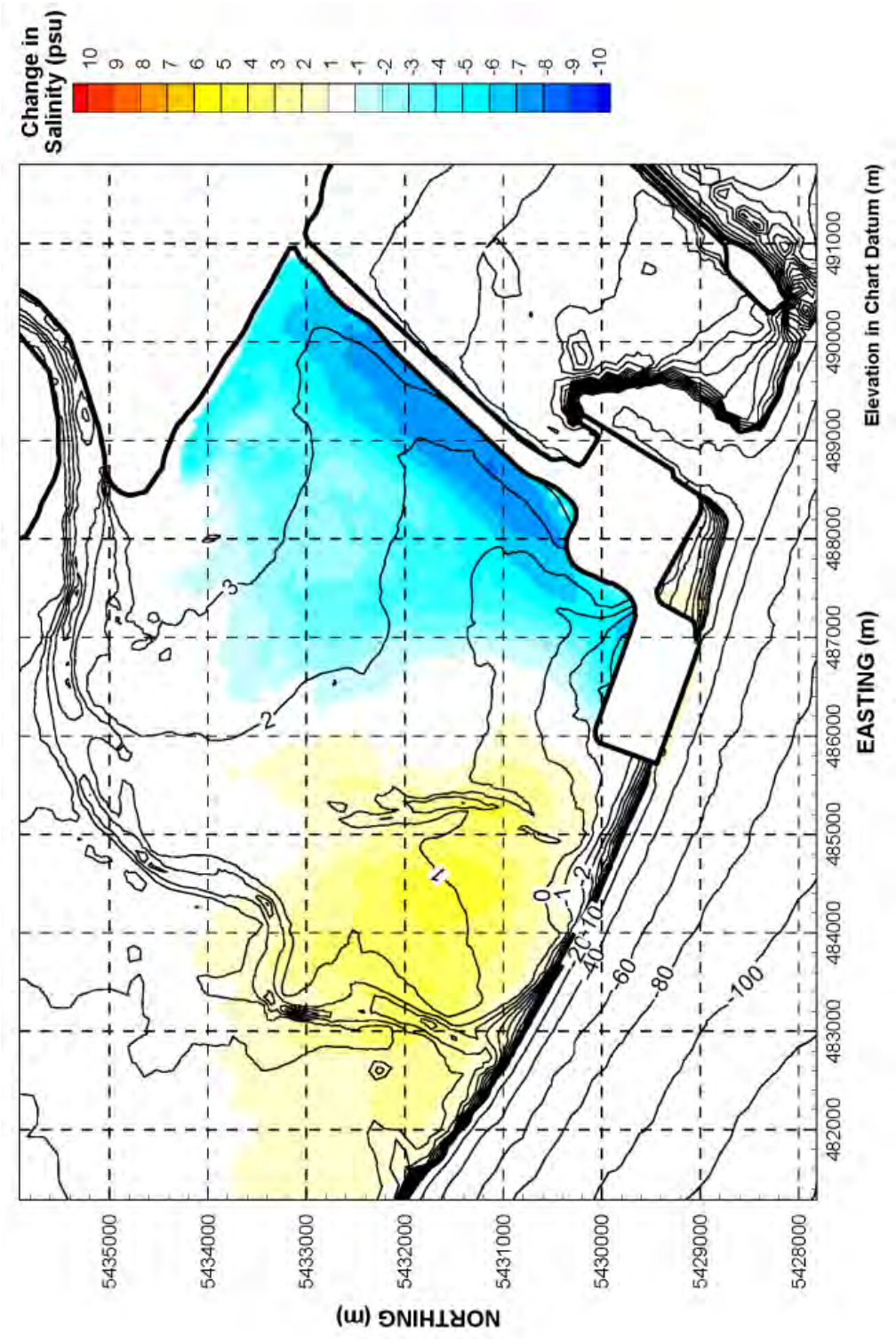

Figure 78: Predicted change in 50th percentile salinity associated with the Project footprint (existing conditions compared to future with Project) – freshet period (May to July).

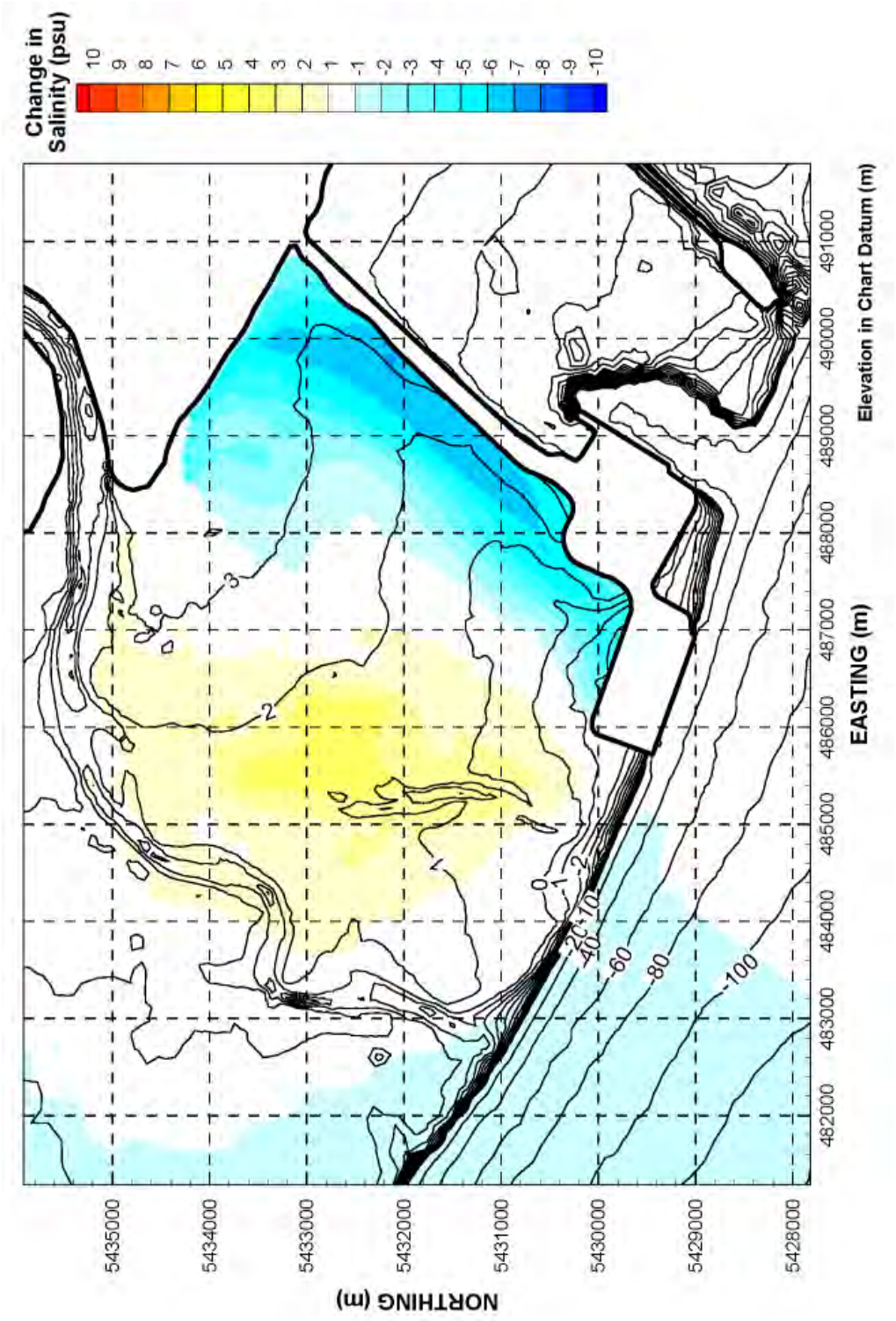

Figure 79: Predicted change in 50th percentile salinity associated with the Project footprint (existing conditions compared to future with Project) – non-freshet period (October to December).

6.3.4 PREDICTED CHANGES IN SALINITY AT THE SEDIMENT-WATER INTERFACE

As noted, the modelled salinity has been expressed as a vertically-integrated average value at each model node. Field measurements presented in **Section 4.2.3** and **Appendix C** describe the vertical distribution of salinity and turbidity. These results (**Figure 27**) indicate that the freshwater from Canoe Passage remains stratified above the saline water of the Strait of Georgia during large portions of the dropping tide and that vertical mixing occurs slowly over time and does not fully mix except in shallower waters. As a result, the vertically-integrated model results will tend to over-predict the exposure of the water-sediment interface to fresher water, both in terms of the magnitude of salinity but also in terms of exposure time, particularly in the deeper portions of Roberts Bank.

6.4 WAVE CLIMATE

A description of the synoptic wave climate and the transformation of incident deep-water waves as they interact with the tidal flats is included in **Section 4.3**. The change to the local wave climate from the proposed terminal was assessed by comparing the hydrodynamic-wave model simulations existing conditions and future conditions with Project. Three analyses of the model results were conducted:

1. Spatial analysis of wave distribution at selected storm events;
2. Temporal statistical analysis displayed on a wave rose at selected locations on the tidal flat; and
3. Spatial and temporal statistical analysis using the 50th percentile wave height, displayed on a map.

6.4.1 SPATIAL ANALYSIS - WAVE DISTRIBUTION DURING SELECTED STORM EVENTS

Prevailing winds in the Strait of Georgia are primarily from the northwest direction in the summer and from the southeast direction in the winter, corresponding to the orientation of the long axis of the Strait. **Figure 80** and **Figure 81** show the modelled wave heights during a northwesterly storm event on May 18, 2012 for the existing conditions and future conditions with Project scenarios respectively, at a water level of +4.1 m CD. **Figure 82** and **Figure 83** show the modelled wave heights during a southeasterly storm event on December 19, 2012 for the existing conditions and future conditions with Project scenarios respectively, at a water level of +4.8 m CD. The colour coding indicates the wave height in metres. Locations D01, B03, B05, and A10, B05 shown on these figures represent the selected locations for wave rose analysis (to be discussed in the next section).

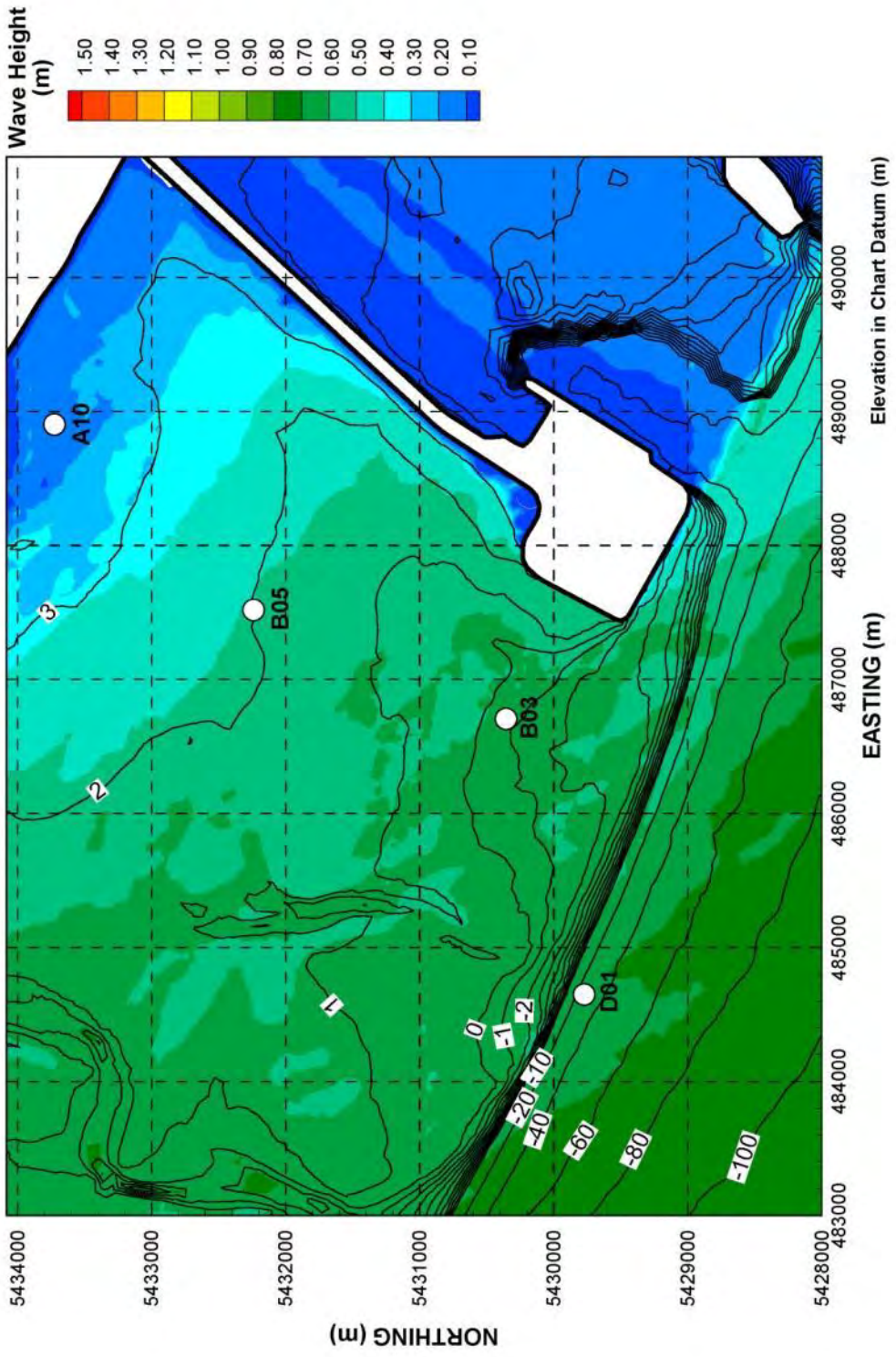

Figure 80: Wave heights associated with a northwesterly storm on May 18, 2012 under existing conditions.

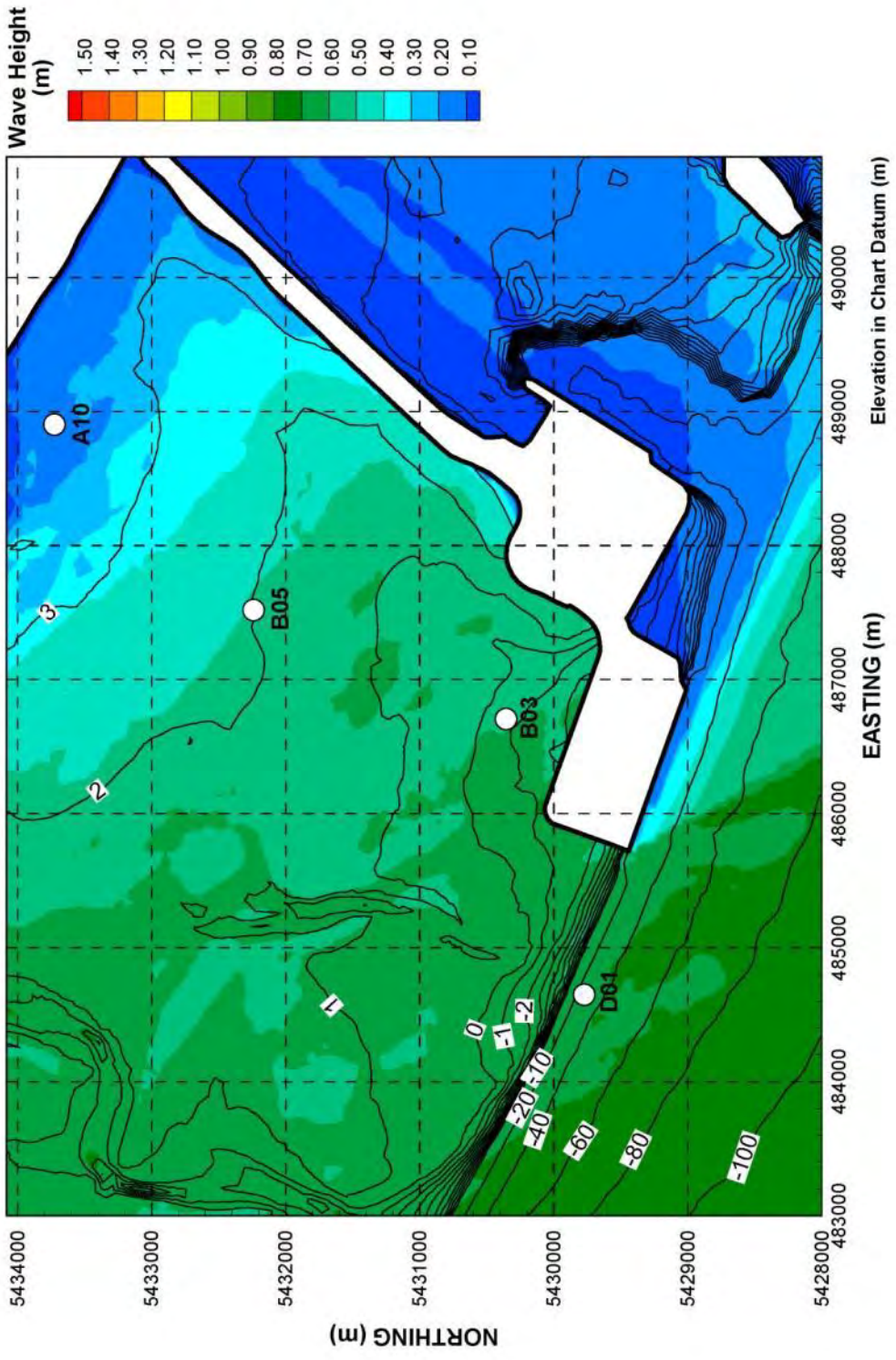

Figure 81: Wave heights associated with a northwesterly storm on May 18, 2012 under future conditions with Project.

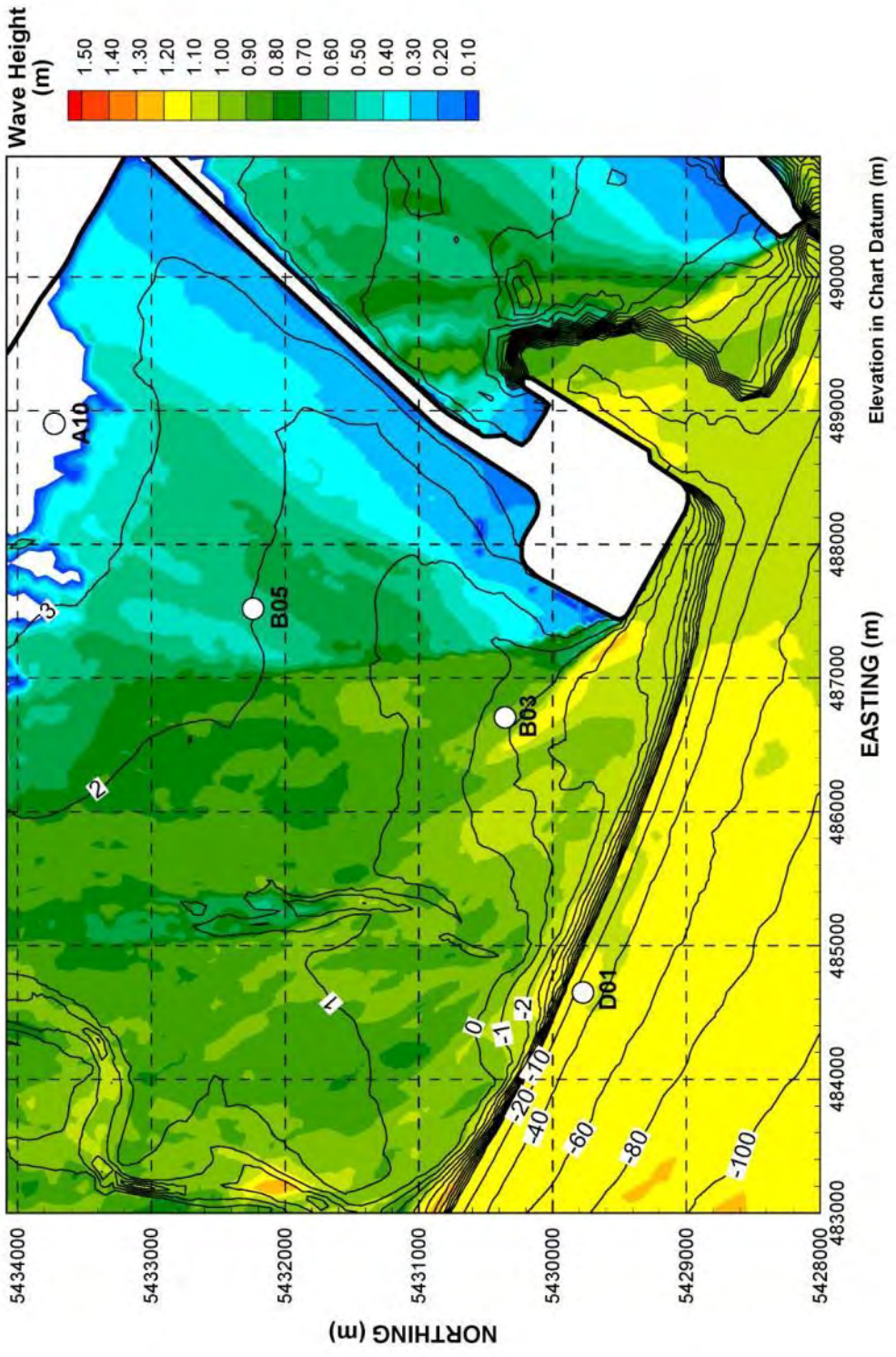

Figure 82: Wave heights associated with a southeasterly storm on December 19, 2012 under existing conditions.

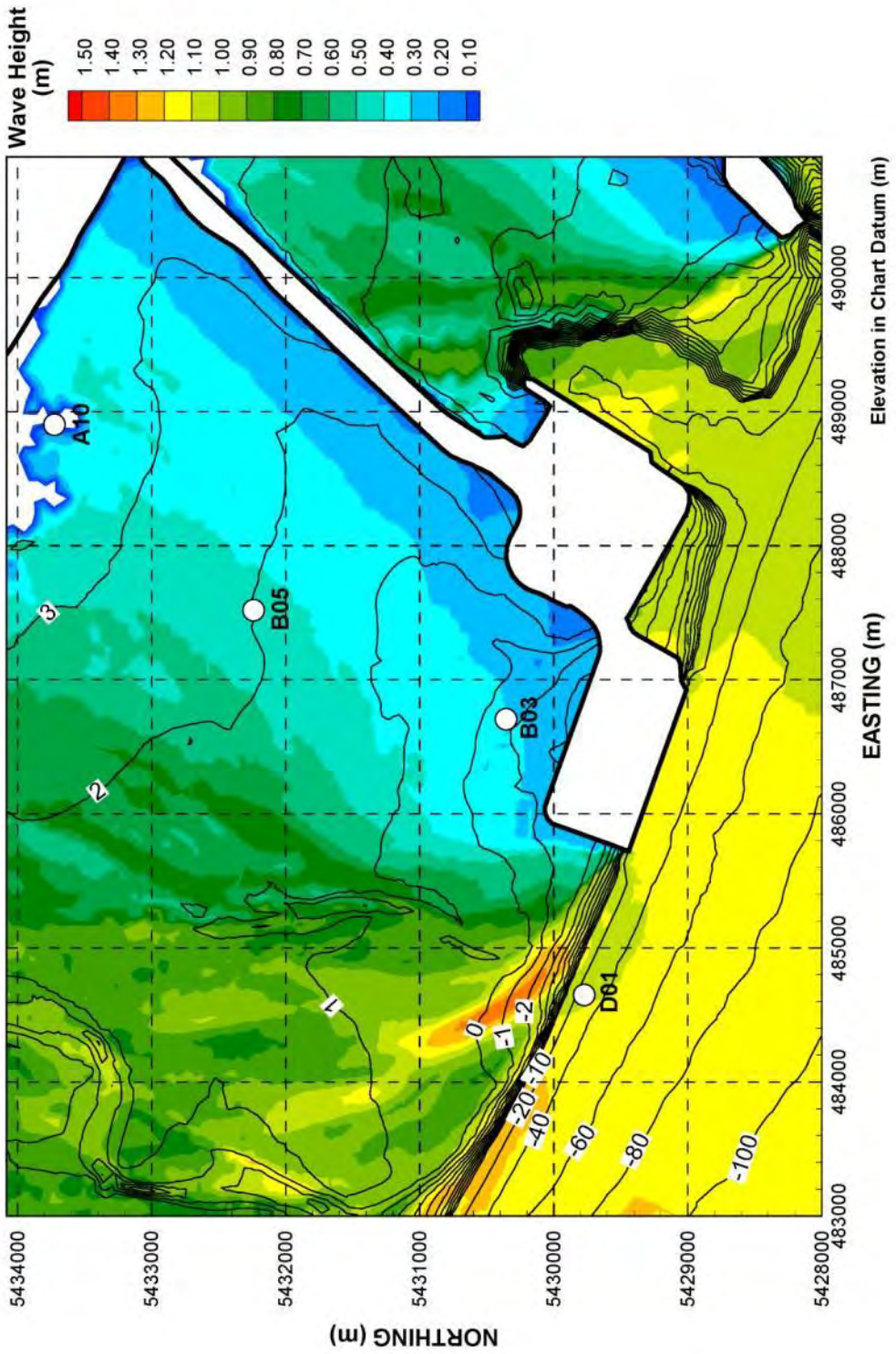

Figure 83: Wave heights associated with a southeasterly storm on December 19, 2012 under future conditions with Project.

As expected, the TELEMAC model results indicate that wave heights decrease in the shoreward direction, but onshore wave height decay is also a function of wind direction. During the northwesterly storm on May 18, 2012, maximum wave heights in the offshore waters reached 0.8 m and were as small as 0.1 m in nearshore areas (**Figure 80**). Onshore wave height decay during this storm closely follows the elevation contours, but there is also a reduction in wave height as waves travel over the tidal flats along the contour lines. In contrast, during the southeasterly storm on December 19, 2012, offshore wave heights were as high as 1.3 m and wave heights decline in response to waves moving onshore into shallower water (**Figure 82**), although there is a strong shadowing influence from the existing Roberts Bank causeway and terminal.

The Project will create an additional wave shadow effect. During a northwesterly storm the wave shadow extends to the southeast of the proposed terminal (**Figure 81**), while during a southeast storm the wave shadow extends to the northwest of the terminal (**Figure 83**). Higher onshore current velocities created by the proposed terminal also result in an increase in localised wave height in the vicinity of Location D01 (**Figure 83**).

Figure 84 shows the differences in waves based on the existing conditions and future conditions with Project model results for the southeast storm on December 19, 2012. The results map uses a neutral colour (white) to indicate wave heights that are nearly zero as well as areas that are outside the model domain, namely dry land, the terminals and the causeway.

The wave shadow effect is greatest in the areas closest to the proposed terminal. Wave heights are up to 0.8 m lower immediately shoreward of the terminal. The effect is less pronounced further onshore such that in the areas along the causeway and above the +3 m CD elevation contour, wave heights are reduced by less than 0.1 m. Wave heights are predicted to be slightly higher across localized areas due to the influence of the Project, which in most cases is related to an increase in the velocity of onshore currents.

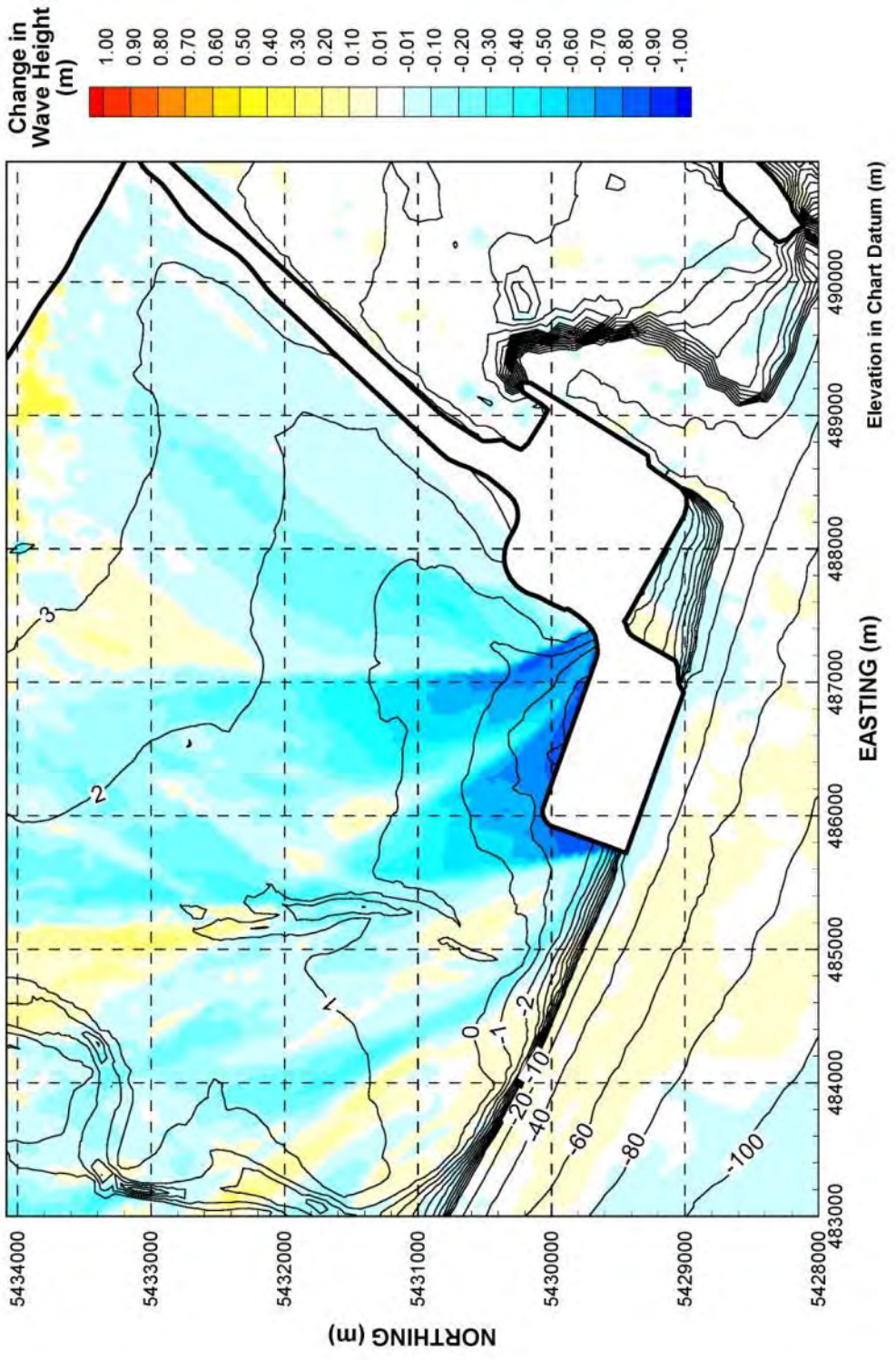

Figure 84: **Predicted change in wave heights associated with the Project footprint (future conditions with the Project compared to existing conditions) – southeasterly storm on December 19, 2012.**

6.4.2 TEMPORAL STATISTICAL ANALYSIS – WAVE ROSE

The spatial representation of wave heights in the vicinity of the proposed terminal presented in **Section 6.4.1** provides a snapshot of conditions during two typical storms (from the northwest and southeast) to illustrate the relative change from the Project. The local change from the proposed terminal on the wave climate in 2012 can be further illustrated using a wave rose, which is a statistical graphic representation of the annual wave climate at a specified location. The wave rose indicates wave height, frequency of occurrence and direction (direction from which the wave is coming). Wave roses were produced for Locations D01, B03, B05 and A10 (as shown in **Figure 80** to **Figure 83**) for the existing conditions and future conditions with Project scenarios (**Figure 85** to **Figure 88**).

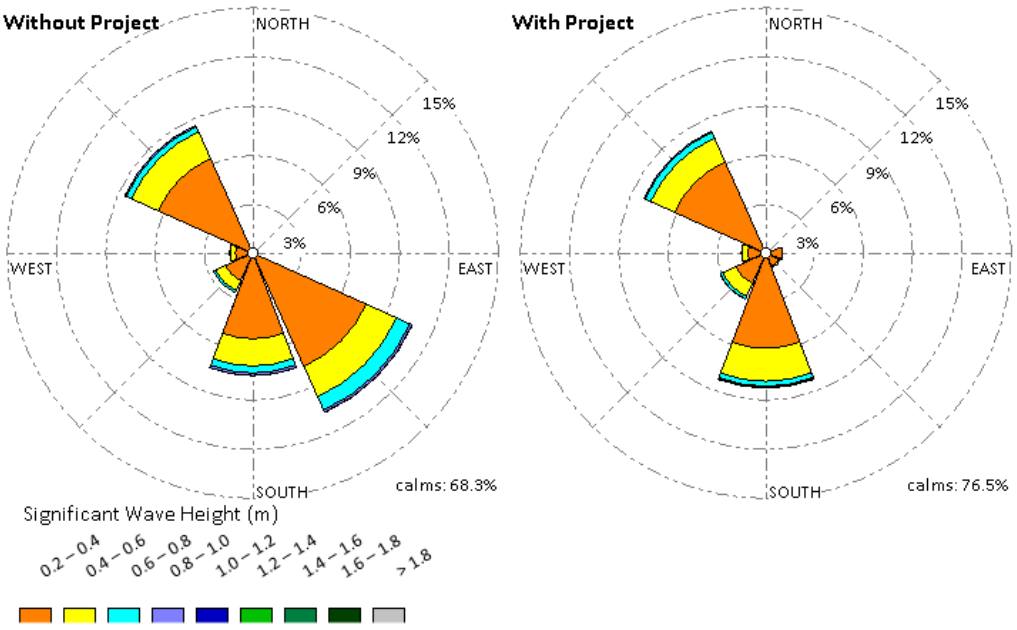

Figure 85: Wave statistics for the January 1 to December 31, 2012 period for existing conditions (left) and future conditions with Project (right) at reference location D01.

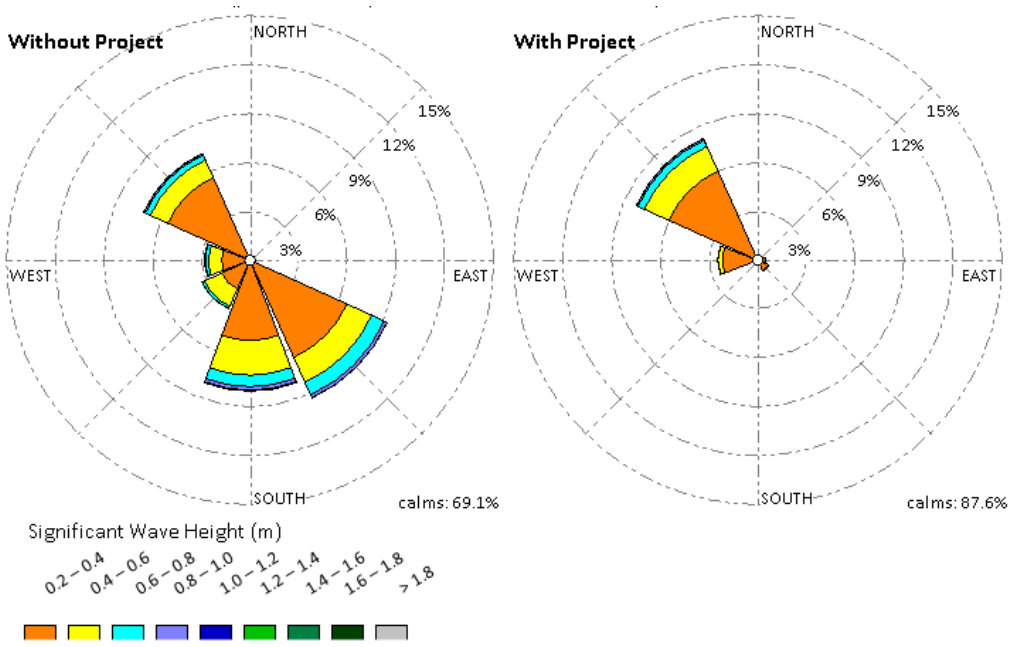

Figure 86: Wave statistics for the January 1 to December 31, 2012 period for existing conditions (left) and future conditions with Project (right) at reference location B03.

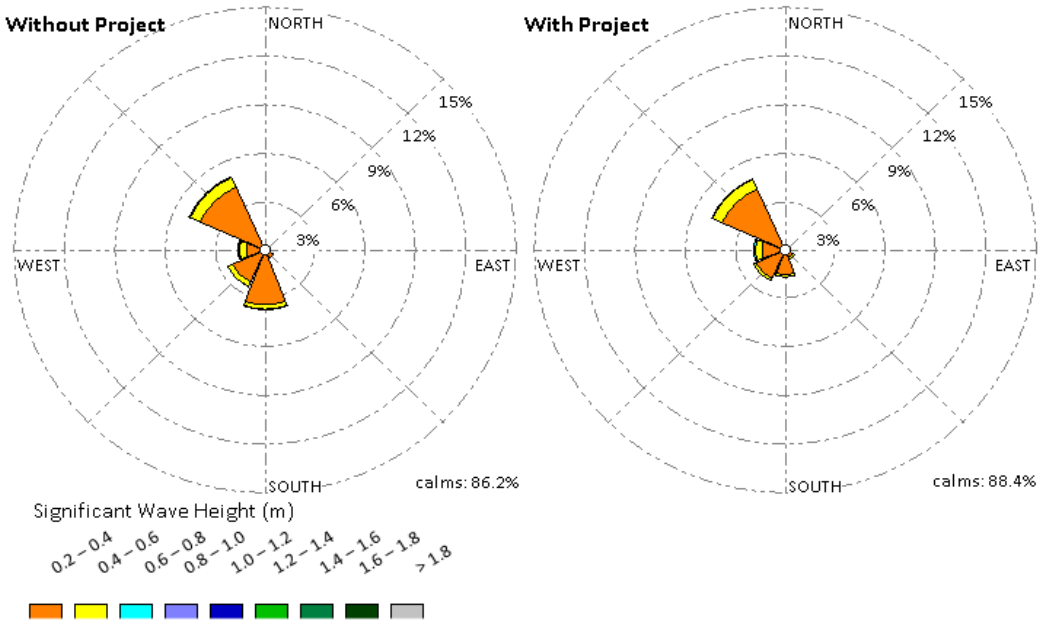

Figure 87: Wave statistics for the January 1 to December 31, 2012 period for existing conditions (left) and future conditions with Project (right) at reference location B05.

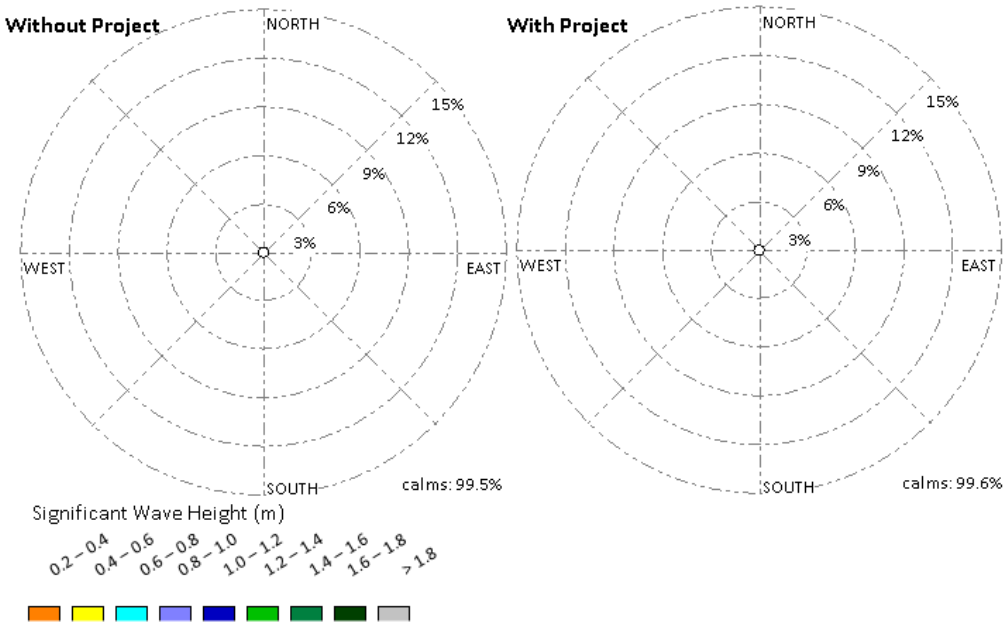

Figure 88: Wave statistics for the January 1 to December 31, 2012 period for existing conditions (left) and future conditions with Project (right) at reference location A10.

At Location D01, which is located in deeper water on the delta foreslope, the predominant wave directions are from the northwest and southeast under existing conditions (without Project), with a secondary component of the waves coming from the south (**Figure 85**). With the Project in place, the location is predicted to experience similar northwesterly and southerly wave conditions. However, due to the sheltering effect of the proposed terminal, southeasterly waves at the location will be virtually eliminated.

At Location B03, which is located shoreward of the proposed terminal, the predominant wave directions are from the northwest, south and southeast under existing conditions (**Figure 86**). With the Project in place, the location is forecasted to experience similar northwesterly wave conditions. However, due to the sheltering effect of the proposed terminal, the location will experience almost no southerly or southeasterly waves. The percentage of calm periods (consisting of waves less than 0.2 m in height) is predicted to increase from 69% to 88% under the future conditions with Project scenario.

At Location B05, which is located at elevation +2 m CD on the tidal flats, the predominant wave directions are from the northwest and south (**Figure 87**). Similar to Location B3, the location is expected to experience fewer southerly waves due to the sheltering effect created by the proposed terminal, but the relative effect is not as pronounced since waves are generally small at this location. As this location is above mean water level (and therefore does not experience waves when the water level is lower than the mean) and as the existing terminal already provides some sheltering, calm conditions are predicted to increase slightly from 86% to 88% under the future conditions with Project scenario.

At Location A10, in the upper foreshore, the wave climate under existing conditions is similar to that predicted with the Project (**Figure 88**). The change from the Project is not important at this location because waves are generally very small or non-existent.

6.4.3 SPATIAL AND TEMPORAL STATISTICAL ANALYSIS – 50TH PERCENTILE WAVE MAP

The snapshot spatial representation of wave heights presented in **Section 6.4.1** and the at-a-point statistical representation of currents presented in **Section 6.4.2** provide a summary of the changes from the Project on the wave climate. Another way to illustrate the potential changes from the Project on waves is by comparing the 50th percentile wave height maps under existing conditions and future conditions with Project scenarios.

The 50th percentile value is a statistical representation computed based on hourly modelled wave heights during the period of interest. Fifty-percent of the time, wave heights are higher than that value at a given location and 50% of the time, they are lower. Mapping 50th percentile values is a useful way to illustrate the general changes from the Project on waves under the full range of water levels over an extended period of time as it focuses on the average condition. Calm periods, as well as periods when there are no waves because the model element is dry, are accounted for as a value of zero is recorded. Similar to the way the 50th percentile currents are calculated for emergent areas, zero values are assigned for emergent areas of the tidal flat in the case of waves to reflect the reduced influence of waves at higher elevations on the tidal flats, both in terms of wave height and the reduced time that higher elevations are exposed to the geomorphic influence of this process.

Fiftieth percentile wave height maps were generated for the existing conditions and future conditions with Project scenarios for two separate periods: the summer northwesterly wind-dominant period (May to July – **Figure 89** and **Figure 90**), and for the winter southeasterly wind-dominant period (October to December – **Figure 91** and **Figure 92**)Figure 89. Difference plots for the two periods are shown in **Figure 93** and **Figure 94**. The results map uses a neutral colour (white) to indicate wave heights that are nearly zero as well as areas that are outside the model domain, namely dry land, the terminals and the causeway.

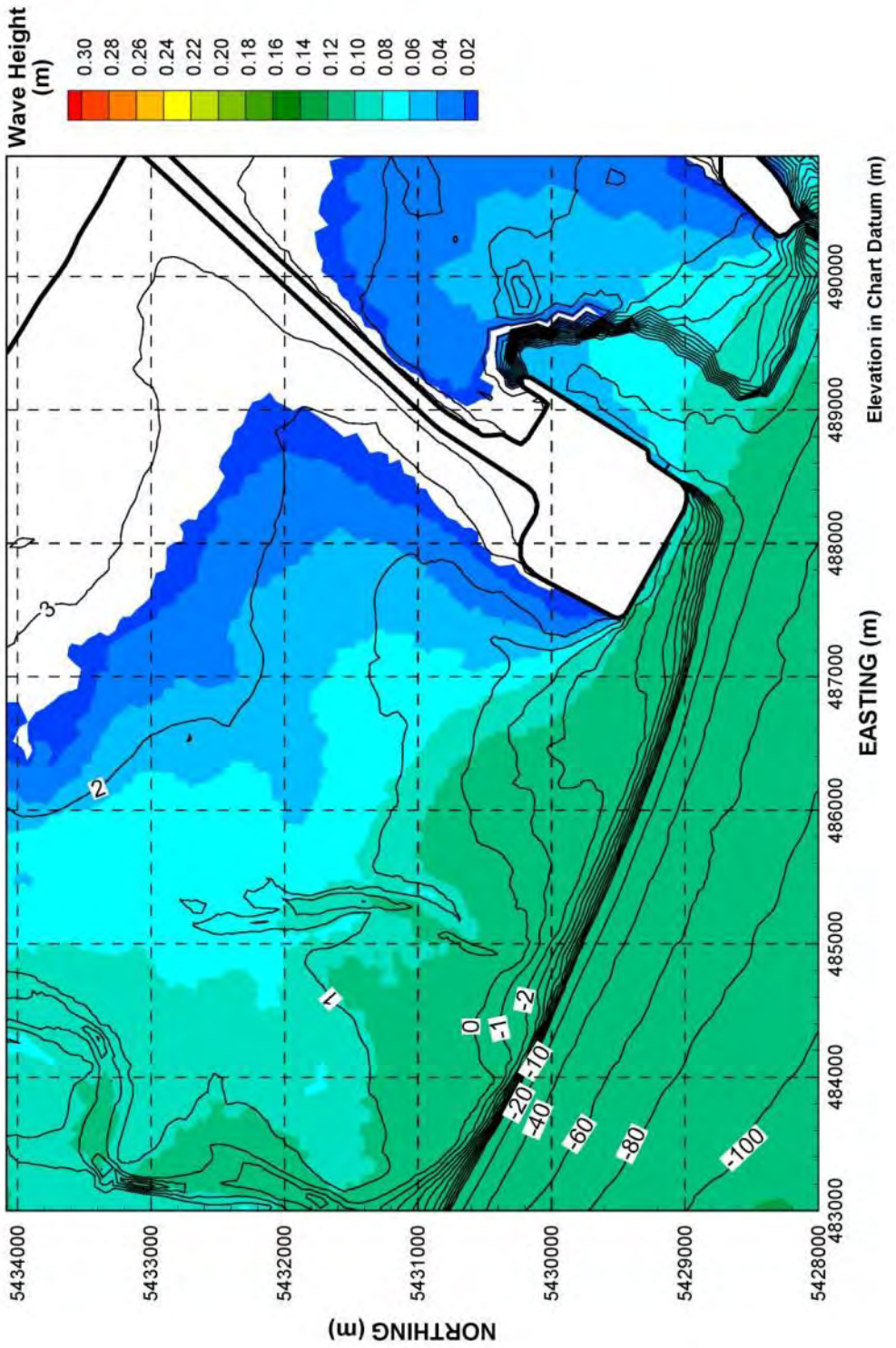

Figure 89: **50th percentile wave heights associated with the summer season (May to July) under existing conditions.**

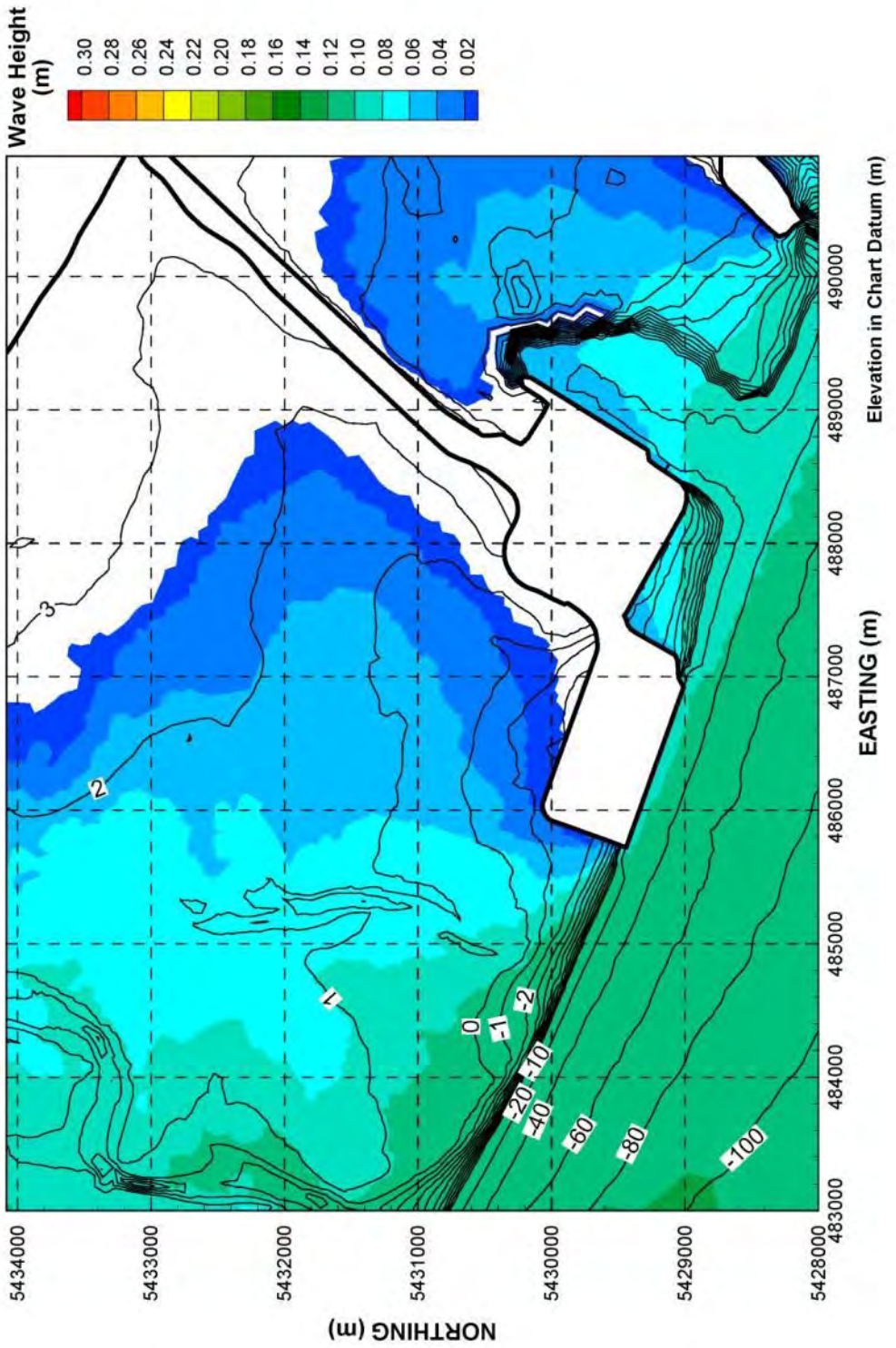

Figure 90: **50th percentile wave heights associated with the summer season (May to July) under future conditions with Project.**

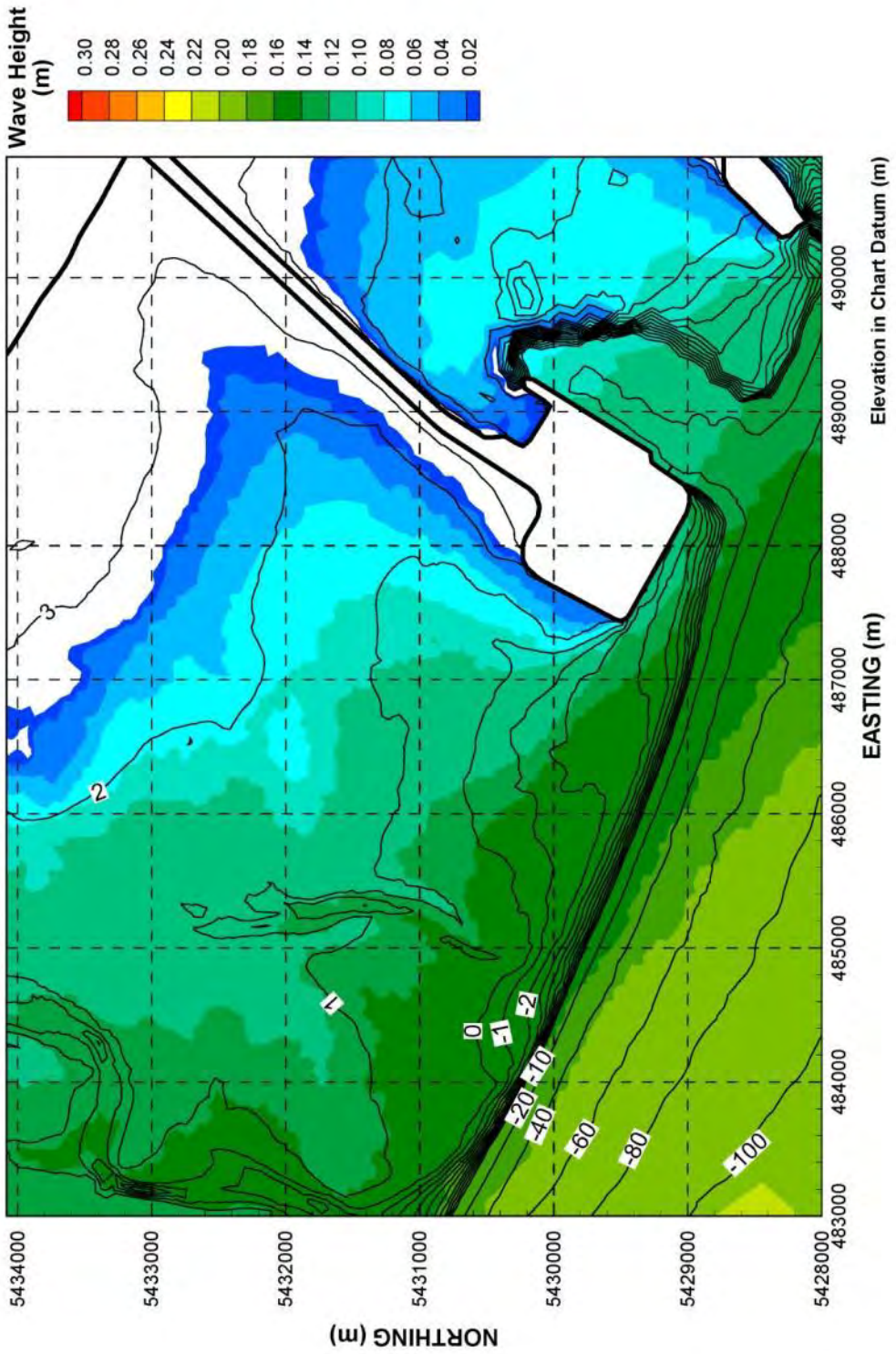

Figure 91: **50th percentile wave heights associated with the winter season (October to December) under existing conditions.**

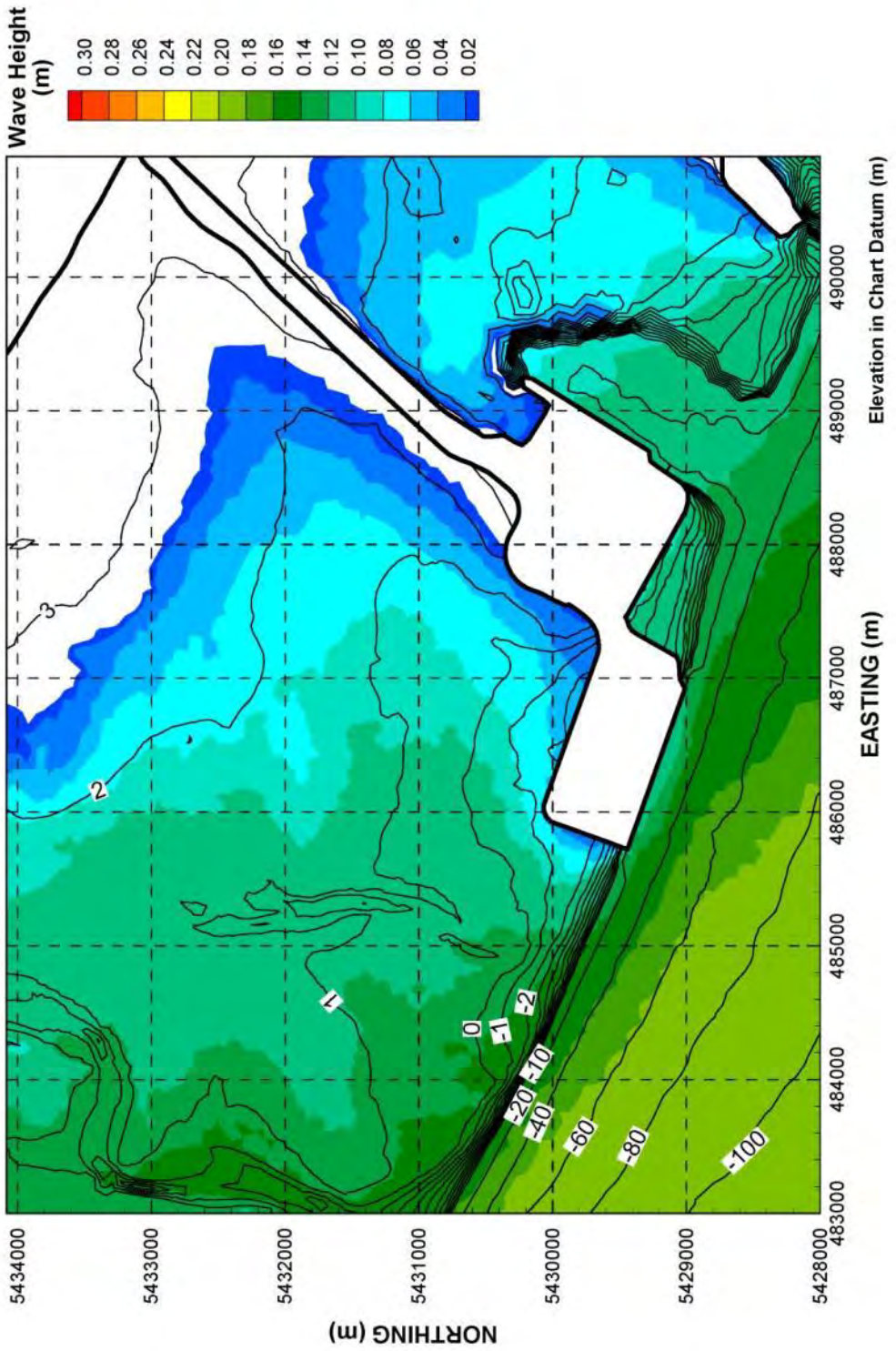

Figure 92: **50th percentile wave heights associated with the winter season (October to December) under future conditions with Project.**

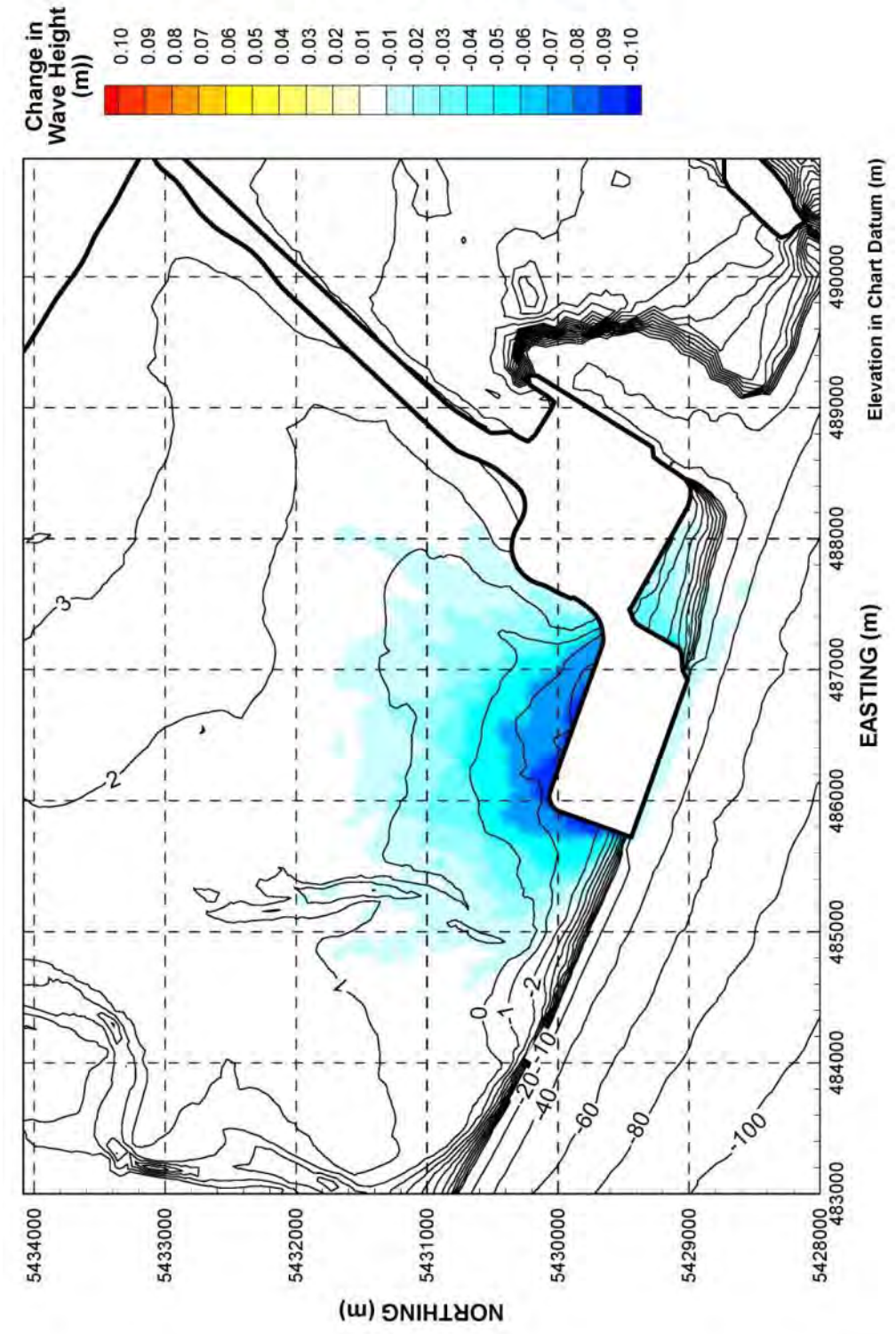

Figure 93: Predicted change in 50th percentile wave height associated with the Project footprint (future conditions with the Project compared to existing conditions) – summer season May to July).

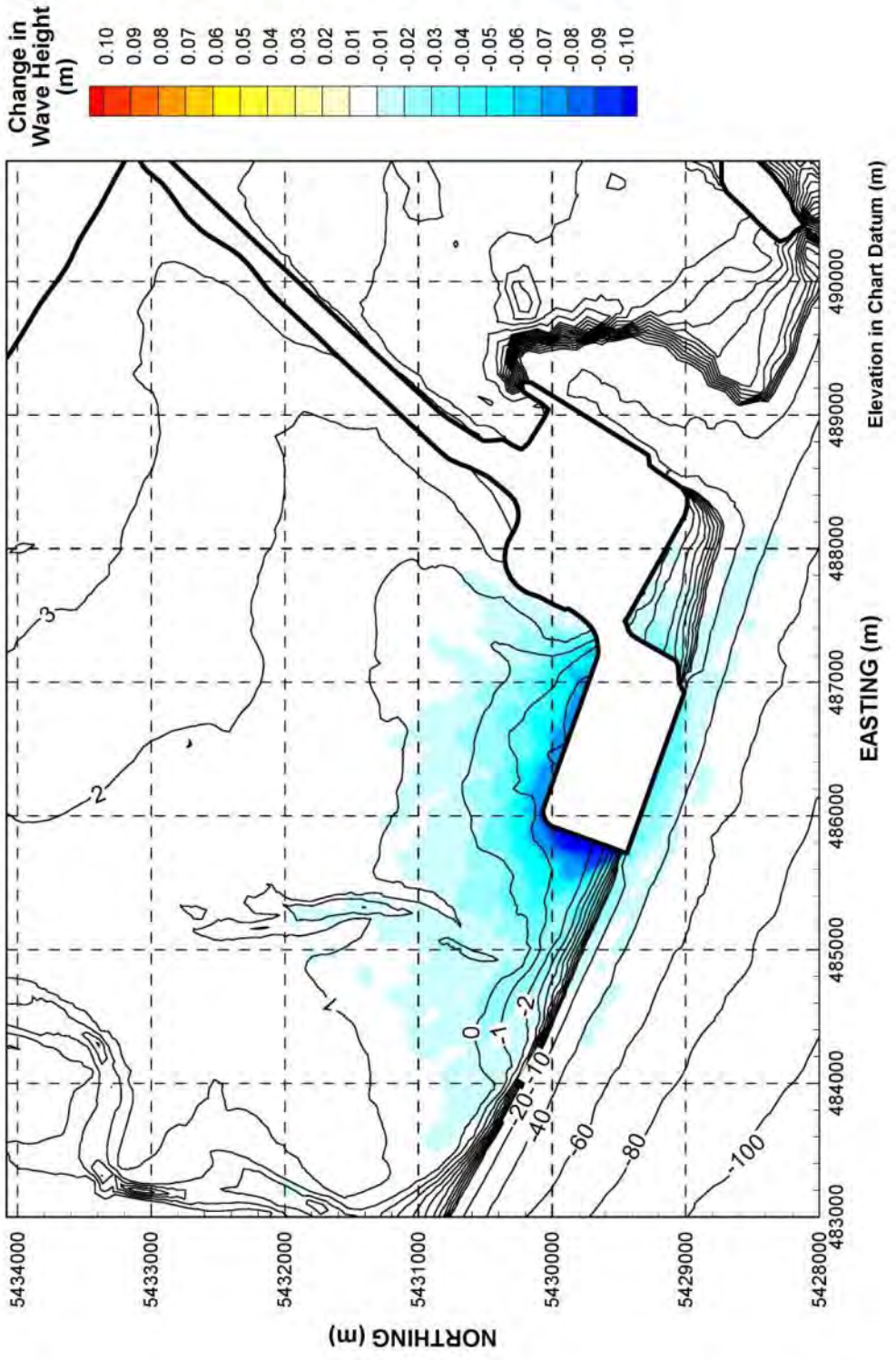

Figure 94: **Predicted change in 50th percentile wave height associated with the Project footprint (future conditions with the Project compared to existing conditions) – winter season (October to December).**

The main difference in the existing conditions scenario shown on the 50th percentile wave height maps between the summer season (May to July) and the winter season (October to December) is that the summer season (**Figure 89**) has slightly smaller incident waves in the deep water offshore of the tidal flats. This is mainly reflective of the lower overall wind speeds in the summer. The dominance of the southeast storms during the winter season (**Figure 91**) is visible in the pattern of variable offshore wave heights and the slightly larger wave shadow effect of the existing terminal and causeway. The change from the Project on the 50th percentile wave height is greater in the summer season (**Figure 90**) for the area immediately shoreward of the proposed terminal because of the predominance of winds from the northwest during this period, while the wave shadow effect extends further across the tidal flats to the west of the Project during the winter season (**Figure 92**) because of the dominant southeast storm direction in winter.

The difference plots show that the reduction in the 50th percentile wave height due to the proposed terminal is typically less than 10 cm (**Figure 93** and **Figure 94**) but this represents a reduction of 50% to 100% in the zone immediately adjacent to the terminal. The extent of the net wave height reduction with the Project in place is similar in the summer and the winter seasons, although the effect extends further west inshore of the delta foreslope in the winter months. The area that would experience a reduction in wave height of 5 cm or more extends about 750 m from the western edge of the proposed terminal. With the modest calmer wave climate, there will be less frequent sediment mobilization and suspension by wave action than under existing conditions.

The proposed terminal would have a negligible influence on wave regime in the upper intertidal, since no change is predicted shoreward of the +2.0 m CD elevation contour.

The short east face of the terminal pad is directly exposed to waves from the southeast and south directions. Complex wave reflection and short-crested standing waves may occur in between the proposed terminal face and the southern face of the Westshore Terminals, and some local scour may occur as a result.

6.5 CHANGES FROM CLIMATE CHANGE ON NEARSHORE WAVE CLIMATE

The state of knowledge of the potential effect of future climate change on the driving forces that influence the coastal geomorphology of Roberts Bank is discussed in **Section 4.5**. The assumption that sea levels will increase by 0.5 m over the next 50 years has been adopted for hydrodynamic model analysis. For the reasons outlined in **Section 4.5**, the intensity and duration of winds and the discharge of sediment and water from Fraser River are assumed to remain the same.

A sea level rise (SLR) of 0.5 m will result in greater average depths of water over the tidal flats, complete immersion of the portion of the tidal flats that are below 0.5 m CD, and longer immersion times for those areas above 0.5 m CD. A series of model runs were made to assess the effect of future SLR on the nearshore wave climate on the tidal flats. A number of simplifications are inherent in this approach that should be considered in the context of the presented results, namely:

1. Present-day Roberts Bank bathymetry (based on 2011 surveys) is used in the model with a 0.5 m rise is sea level. In reality, SLR would occur gradually over time and the tidal flat morphology would, to some extent, evolve over this 50-year time frame. Modelling of the tidal flat longitudinal profiles included in the Hill *et al*. (2013) study of the effects of SLR on Roberts Bank are useful in providing a possible future scenario; however, these predictions are independent of time and so cannot be directly applied to the present analysis.

2. Increasing the water levels in the model also results in changes to the predicted magnitude and direction of ocean currents. Since it is not reasonably possible to predict the future bathymetry of the tidal flats under the influence of SLR, it is similarly unreasonable to make predictions of changes to the ocean currents independent of future bathymetry. Waves and currents are coupled in the model, and waves are affected to some extent by the currents. As it is not possible to model the waves independently of the rising and falling tide, it is necessary to accept the nearshore wave climate presented here as an imprecise approximation of future conditions.

In light of these unavoidable simplifications, the effect of SLR on the nearshore wave climate is potentially most useful to understanding the effect that SLR will have on the upper tidal flats.

6.5.1 EXPECTED CONDITIONS SCENARIO

The potential effect of SLR on wave climate is illustrated by plotting the 50th percentile wave heights in the vicinity of the Project area. The expected conditions scenario for the winter southeasterly wind-dominant period (October to December) under future sea levels is shown in **Figure 95** and can be visually compared to the existing conditions 50th percentile wave results for the same period under current sea levels (**Figure 91**). The difference between the 50th percentile wave height under the SLR scenario and under the existing sea level conditions is presented in **Figure 96**. In both of the following figures, the results map uses a neutral colour (white) to indicate wave heights that are approaching zero as well as areas that are outside the model domain, namely dry land, the existing terminal and the causeway.

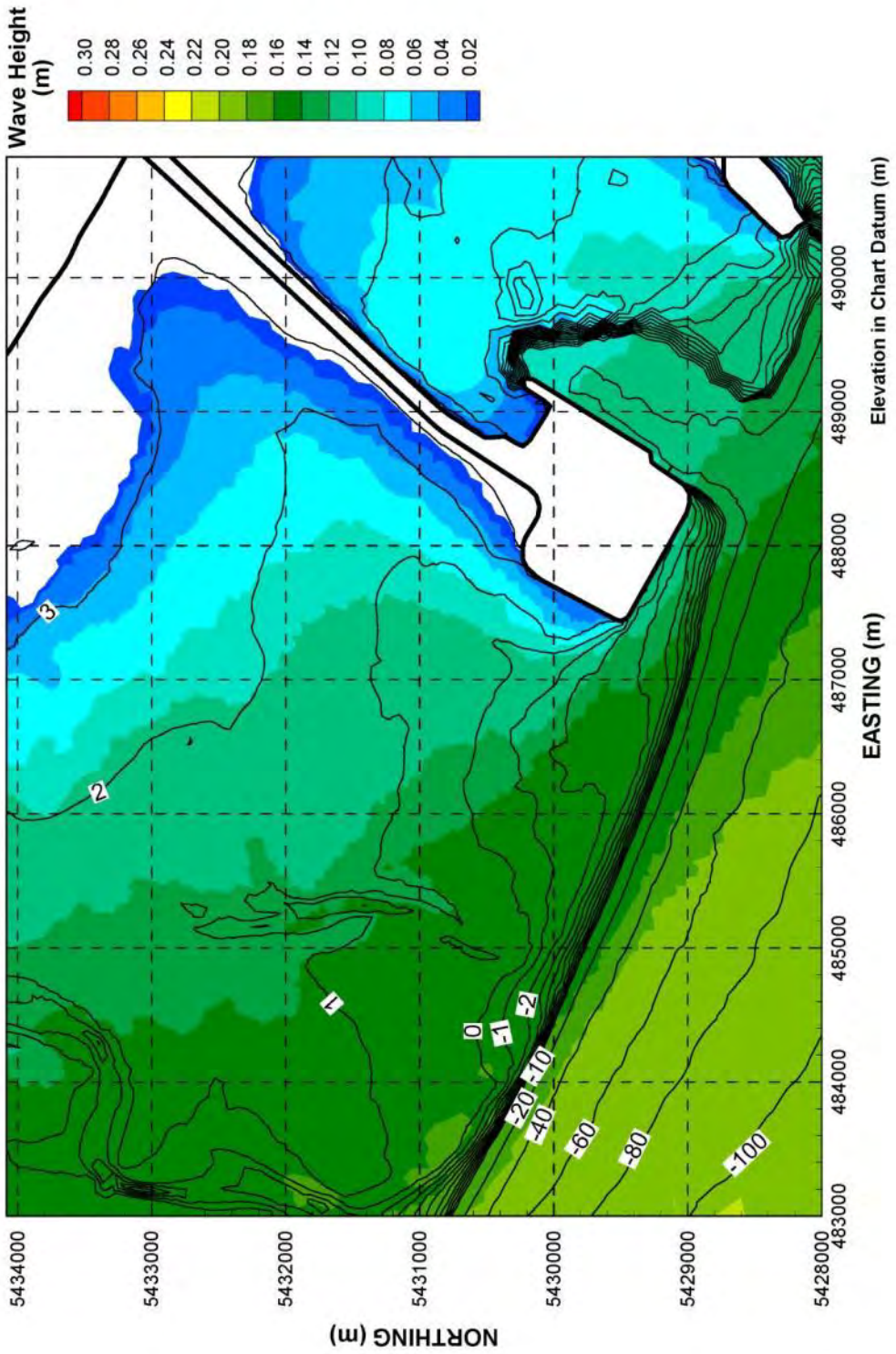

Figure 95: **50th percentile wave heights associated with the winter season (October to December) under expected conditions, with an assumed sea level rise of 0.5 m.**

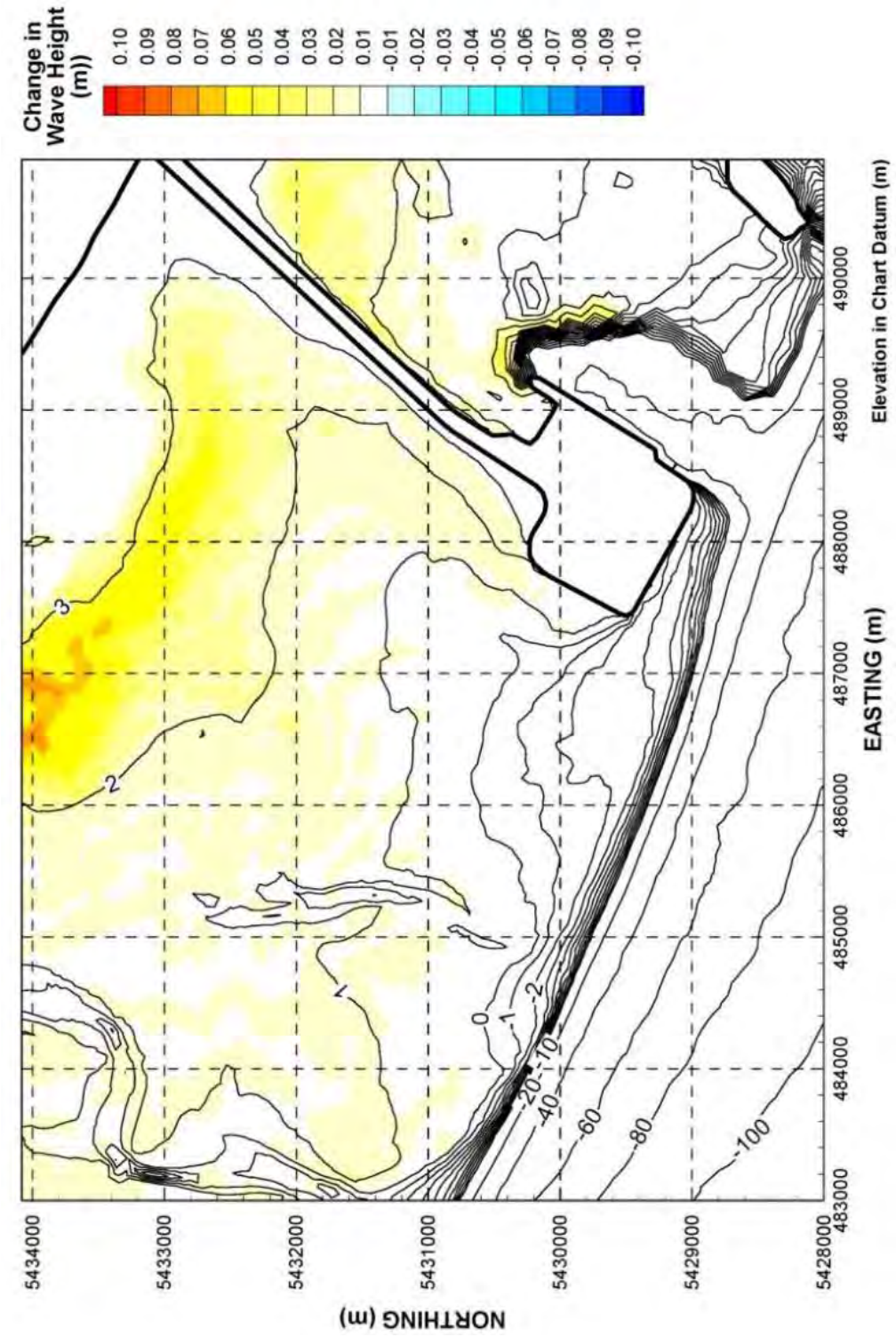

Figure 96: Predicted effects of sea level rise on 50th percentile wave heights (expected conditions compared to existing conditions) – winter season (October to December).

The model results indicate that an increase in sea level of 0.5 m projected on the existing conditions bathymetry results in slightly larger waves over the tidal flats. Comparing **Figure 91** to **Figure 95** shows that the general trend is for a shoreward shift of each wave height class by approximately 500 m. The difference plot shown in **Figure 98** quantifies the expected wave height increase. The predicted increase in wave height at most locations is about 0.02 m to 0.05 m, but the increase is greater in the upper foreshore region between elevations +2 m CD and +3 m CD where the 50th percentile wave height is shown to increase by 0.05 m to 0.07 m. At elevations above +3 m CD, where 50th percentile wave heights are less than 0.02 m under the present water level conditions, there is no predicted increase to wave heights under the SLR scenario.

Given that onshore wave height decay is largely a function of water depth and bottom friction, the general results are not surprising. However, the absence of an increase in the 50th percentile wave height at the highest tidal flat elevations is counterintuitive, except that the biomat zone that exists between +3.5 m and 4 m CD (described in **Section 3.4.5** and **Section 5.3.3**) creates a rise in the topography of the upper tidal flats that effectively excludes wave incursion inshore during most tide heights. These 50th percentile wave results in the area of biofilm are insensitive to SLR but there may be an effect at the upper end of the wave height spectrum during large storms.

6.5.2 FUTURE CONDITIONS WITH PROJECT SCENARIO

The potential change from SLR on wave climate for the existing conditions bathymetry is outlined above. The additional change from the Project is illustrated by plotting the 50th percentile wave heights in the vicinity of the Project area. The future conditions with Project scenario for the winter southeasterly wind-dominant period (October to December) under future sea levels is shown in **Figure 97** and can be visually compared to the future conditions with Project 50th percentile wave results for the same period under current sea levels (**Figure 92**). The difference between the 50th percentile wave height under the SLR scenario and under the existing sea level conditions with the Project in place is presented in **Figure 98**. In both of the following figures, the results map uses a neutral colour (white) to indicate wave heights that are approaching zero as well as areas that are outside the model domain, namely dry land, the terminal and the causeway.

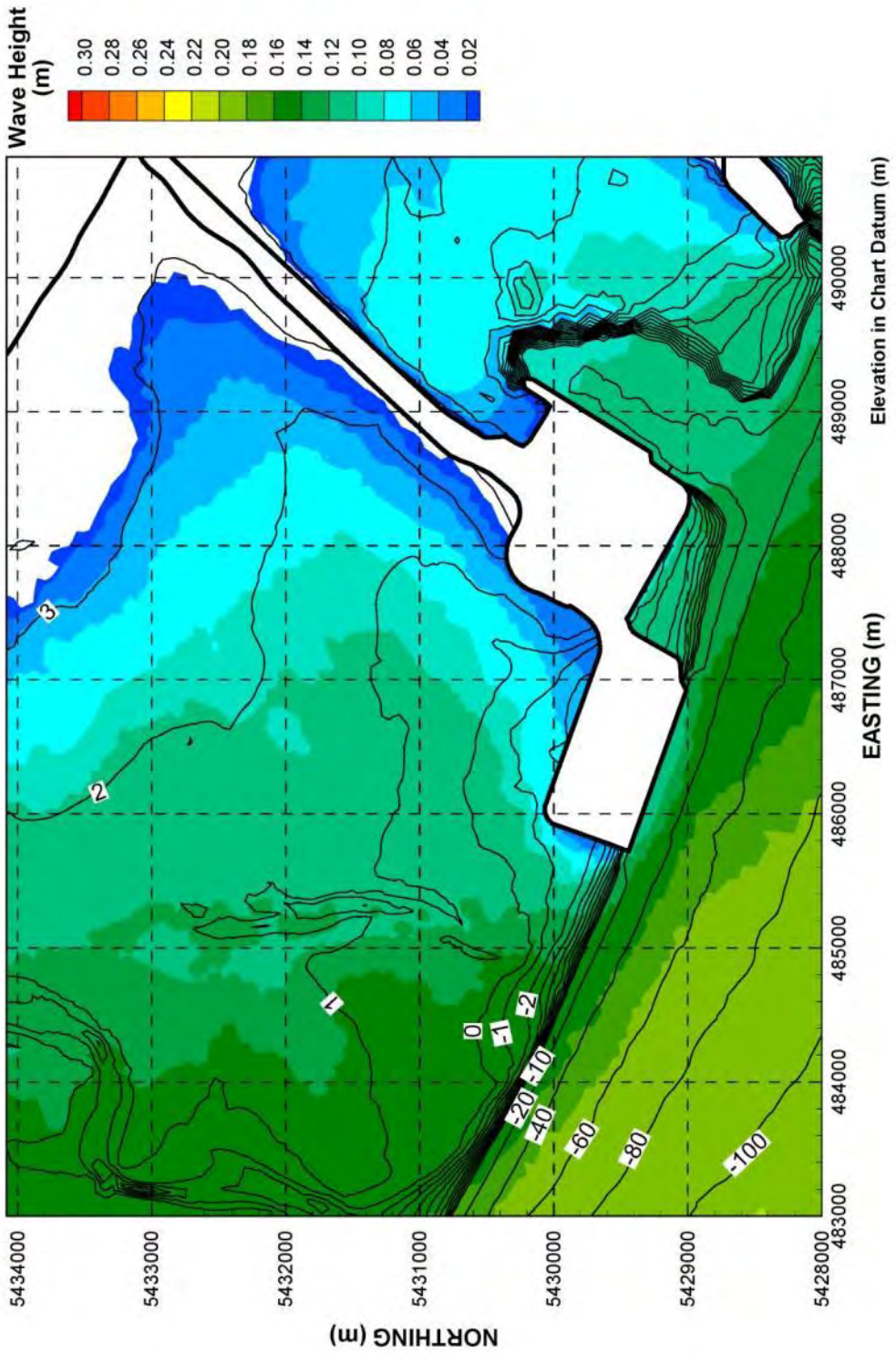

Figure 97: **50th percentile wave heights associated with the winter season (October to December) under future conditions with Project and with an assumed sea level rise of 0.5 m.**

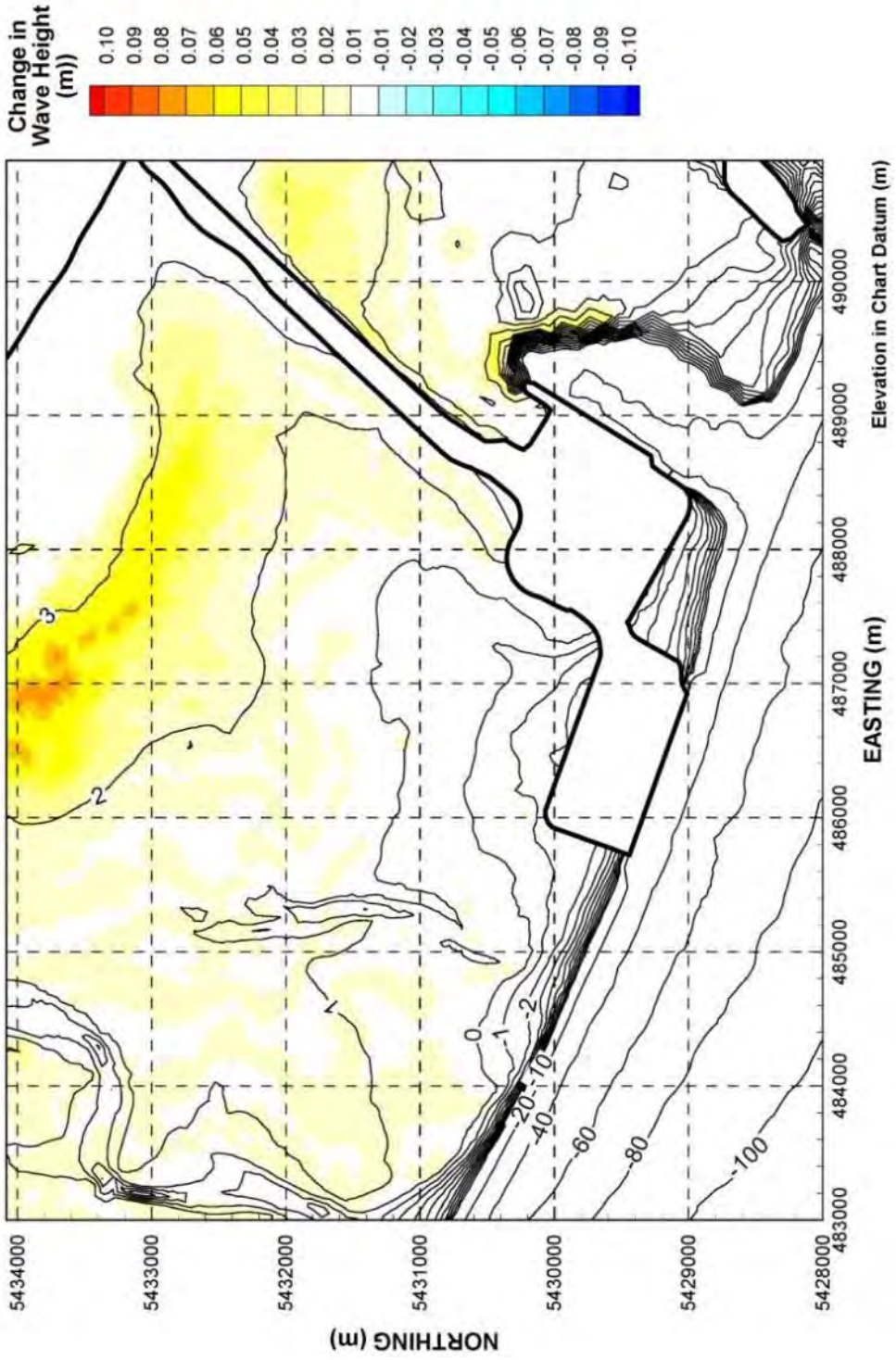

Figure 98: Predicted changes on wave heights from sea level rise under future conditions with Project: 50th percentile wave height difference map – with Project winter season (October to December).

The general pattern of increased wave heights over the tidal flats, including incursion of larger waves further inshore that was discussed above in **Section 6.5.1** is similarly evident in the future conditions with Project results presented in **Figure 97**. Similar to previous discussion of the wave shadow effect that the Project will have on the tidal flats for storms from the southeast, a similar wave shadow effect occurs under SLR conditions.

The difference map presented in **Figure 98** is nearly identical to the difference map for scenarios without the Project in place (**Figure 96**). This is not surprising given that the SLR effects occur in the upper tidal flat zone, which is well outside the Project effect area for waves. SLR and the Project are essentially independent of each other with respect to the effect on wave climate.

6.5.3 ASSESSMENT OF RESULTS

The results show that changes to wave height due to sea level rise have a greater impact in shallow water where waves are affected by the ocean bottom than in the deep water region. The increase in wave height on the tidal flat due to SLR is predicted to be similar under the expected conditions and future conditions with Project scenarios. Localized slope profile adjustments will take place across the tidal flats (see Hill *et al*. 2013), but this anticipated response has not been considered in this analysis.

7 SEDIMENT DYNAMICS

7.1 MORPHODYNAMIC MODELLING APPROACH

Sediment transport and sedimentation patterns on the tidal flats near the Project site are governed by ocean currents and waves as well as the sediment inputs from the Fraser River distributaries, primarily Canoe Passage. Local bed changes (scour and deposition) around the Project were computed by coupling the sediment transport and morphodynamic model SISYPHE to TELEMAC-3D and TOMAWAC. SISYPHE uses the tide and wave information from the other two models to compute scour and deposition of the seabed. The new bed elevation computed by SISYPHE is fed back into TELEMAC-3D to re-compute the flow hydrodynamics. The Bijker formula is used to compute bedload and suspended transport induced by current and wave action. The sediment incorporated in the simulation that characterises the bed materials on the tidal flats is assigned a constant grains size of 175 μm, which is consistent with the D_{50}, or median sediment size that is known to be present. Sediment in the Canoe Passage channel are coarser (D_{50} = 350 μm), so the bed in the model was ascribed this coarser sediment, effectively armouring it in this region to prevent excess sediment movement.

The wave-current sediment transport modelling is extremely computationally intensive, making multi-year morphodynamic simulations impractical. In order to reduce computation time, an efficient modelling approach that adequately captures the dominant processes was needed. The wave climate assessment (**Section 6.3.4**) results show that the Project will have a greater effect on waves approaching from the southeast (which dominate in the winter season) than waves approaching from the northwest (which dominate in the summer season). Tidal currents are strongest during periods when the daily variation in tide height is greatest, which are of similar magnitude in summer (May to July) as in winter (October to January) (see **Section 4.1**).

The relative effect of the wave component on changes to the seabed in the vicinity of the Project was tested for both without and with Project scenarios. **Figure 99** and **Figure 100** show the change in bed elevation under existing conditions after three winter months with and without waves respectively. The wave climate during the winter months is dominated by southeast storms but not to the exclusion of northeast winds. The comparison shows that the intensity of bed level changes is slightly greater when the waves are included in the analysis but that the pattern is similar. A three month model run was also made for the same period with and without waves with the Project in place (**Figure 101** and **Figure 102** respectively). The comparison shows a similar pattern in erosion and deposition regardless of waves, confirming that the Project does not induce greater changes to the bed when waves are present.

Based on this comparison, a model run of 1,440 model days was made prescribing ocean currents but not waves, to estimate the equilibrium bed condition that would develop near the corner of the proposed terminal. The rate of change over time in the area near the northwest corner in the model runs that extended longer than 1,440 model days was found to be very low. The model used a recurring winter period (October to December) in order to maximise model efficiency, thus avoiding computation time during periods of low tidal amplitude.

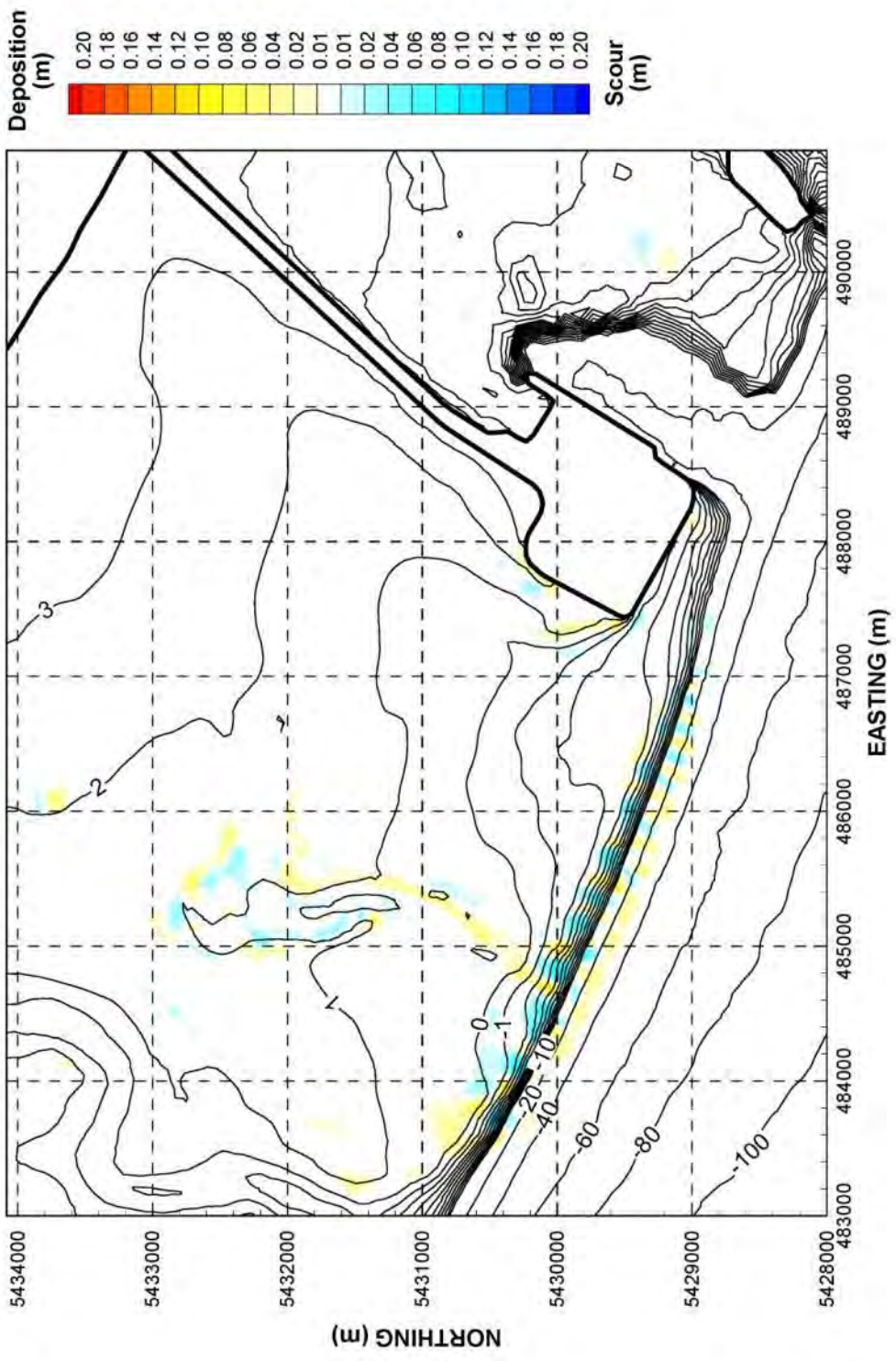

Figure 99: Morphodynamic evolution from tidal currents and waves after three winter months – expected conditions scenario.

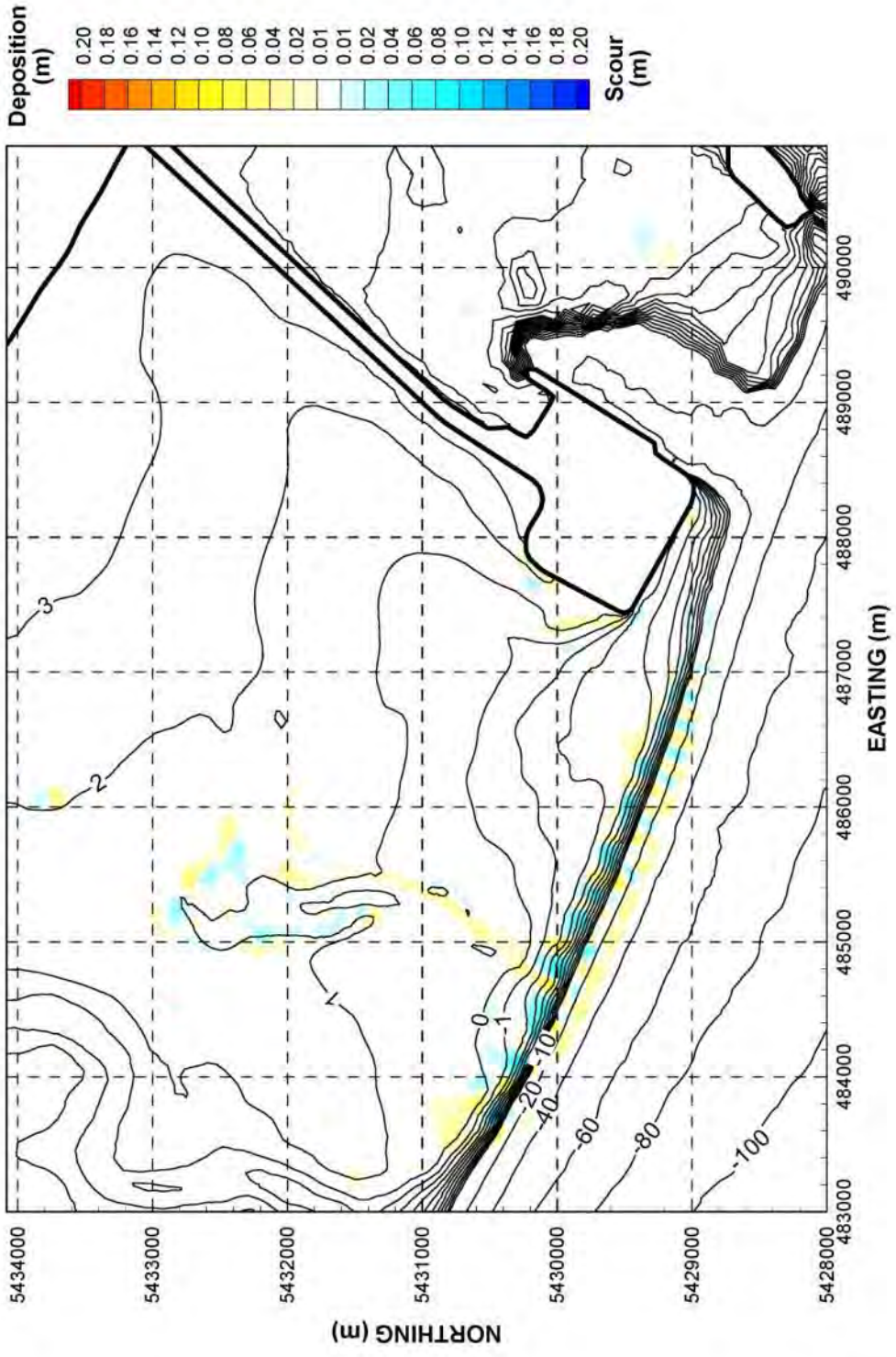

Figure 100: Morphodynamic evolution from tidal currents (not waves) after three winter months – expected conditions scenario.

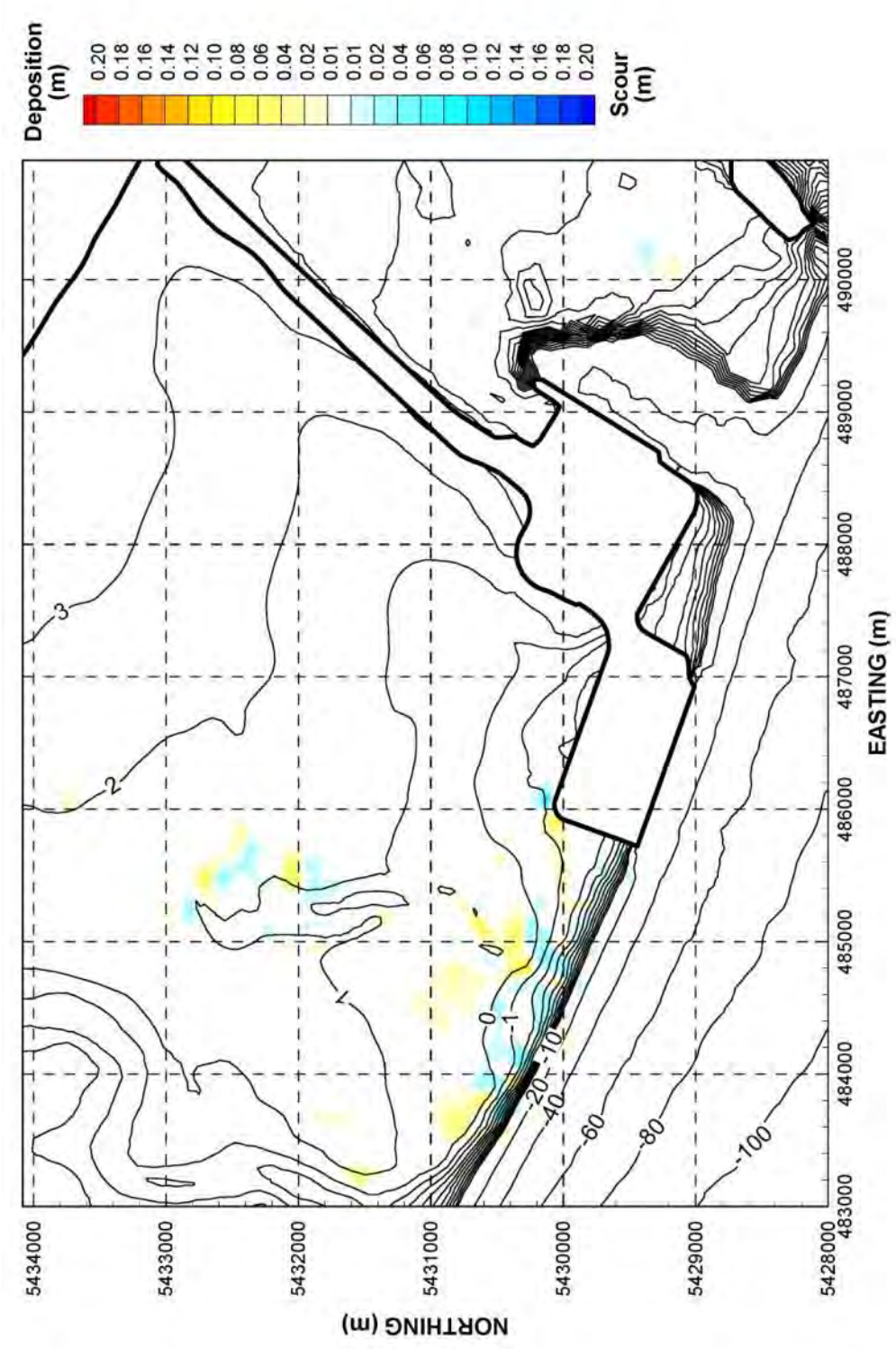

Figure 101: Morphodynamic evolution from tidal currents and waves after three winter months – future conditions with Project scenario.

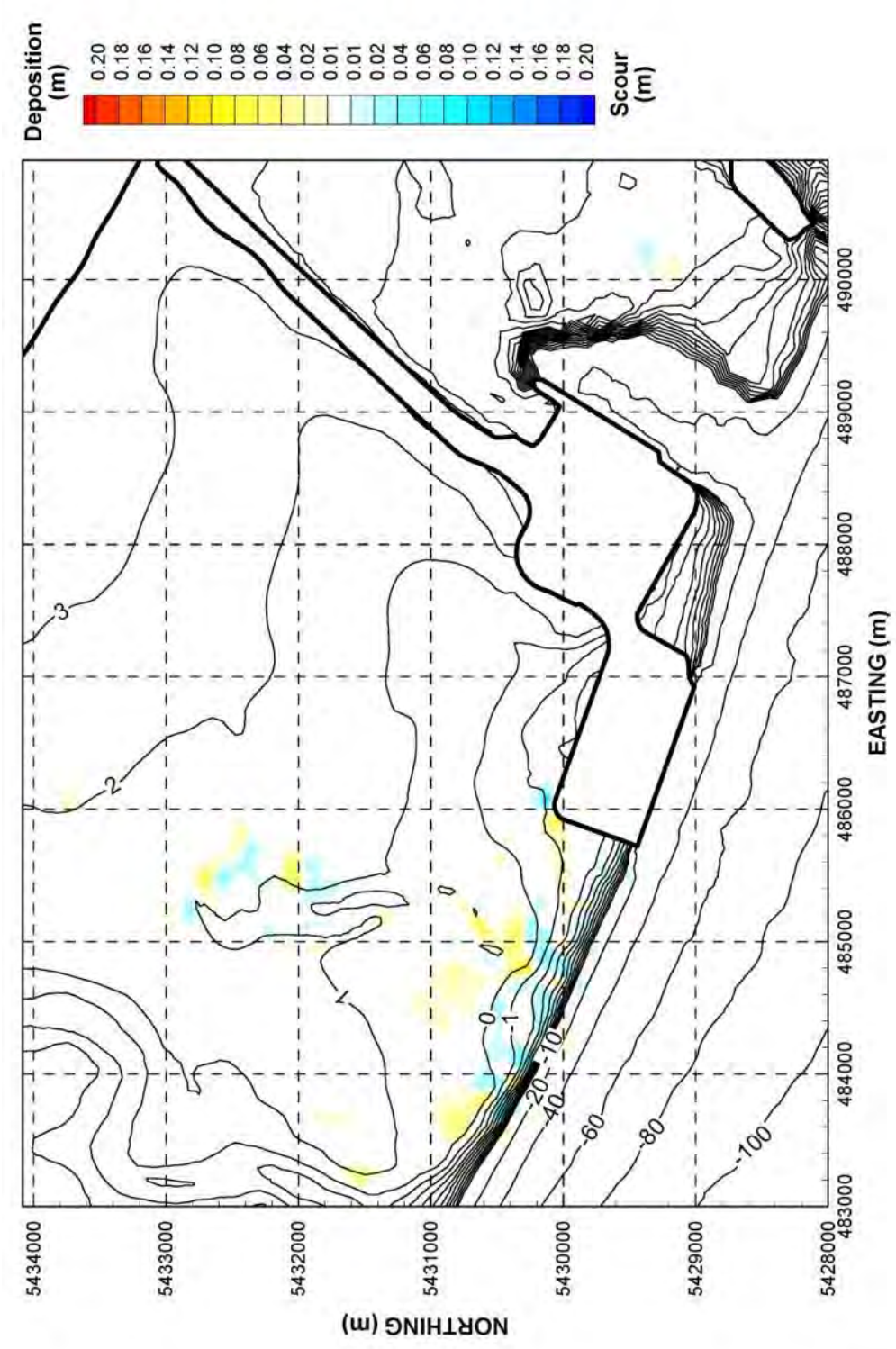

Figure 102: Morphodynamic evolution from tidal currents (not waves) after three winter months – future conditions with Project scenario.

7.2 MORPHODYNAMIC MODEL RESULTS

The predicted scour and deposition patterns presented in the morphodynamic model test runs in **Section 7.1** are consistent with the results from the hydrodynamic-wave model (**Section 6.4**). **Figure 101** shows that a scour zone is predicted to develop near the northwest corner of the proposed terminal. Scouring in this area occurs at ebb tide, as can be expected based on the current map shown in **Figure 66**. The hydrodynamic modelling of tidal currents (**Figure 65** and **Figure 66**) and waves (**Figure 93** and **Figure 94**) indicates that the wave climate shoreward of the proposed terminal and along the causeway will be calmer and will experience slower tidal currents with the Project in place. The morphodynamic model also shows reduced sediment transport in this region with the Project in place.

The evaluation of potential changes from the Project on tidal currents (**Figure 66**) indicates that current velocities in the region north of the proposed terminal will decrease in the upper foreshore region (between +1 m CD and +3 m CD elevation contours) and will increase in the lower foreshore region (between +1 m CD and -5 m CD). The morphodynamic model results show a corresponding reduction in sediment transport in the upper foreshore region and an increase in sediment transport in the lower foreshore region.

Tidal currents appear to play a more dominant role in producing changes in the vicinity of the proposed terminal. To evaluate the morphodynamic changes due to tidal currents only, simulations were conducted over the same period (2012 winter season) without including the wave effects for the expected conditions and future conditions with Project scenarios. The bed evolution results are shown in **Figure 100** and **Figure 102**. The without-wave morphodynamic results show that the magnitude of scour and deposition is reduced slightly on the tidal flats north of the Project when the wave effect is excluded from the simulation. The predicted amount of bed movement along the causeway does not change noticeably when waves are discounted. The general sedimentation pattern does not change significantly.

Based on the above review of the short-term results and the general observations included in **Section 7.1**, it is reasonable to exclude waves from the long-term morphodynamic modelling. The model was run for a period of 1,440 days without the wave effects, and replicating the 2012 winter tide conditions. The bed evolution at the end of the simulation is shown in **Figure 103**. These results show that there will likely be an adjustment along the delta foreslope as well as sedimentation on the tidal flats to the north and west of the proposed terminal between elevations -1 m CD and +1 m CD. The erosion of the foreslope is one of the sources of this sedimentation while shoreward extension of the existing relict tidal channel also contributes sediment. The extent to which these changes are influenced by the Project versus ongoing processes is explored below.

The primary change from the Project is focused on the northwest corner. **Figure 104** shows the same model results as **Figure 103** but in greater detail for this zone. The scour level at the northwest corner of the proposed terminal reached approximately elevation of -2.2 m CD after 1,440 days of model simulation. The temporal evolution of the scour zone is recorded at the scour hole close to the corner and summarised in **Figure 105**. The scour rate decreases over time and although the final equilibrium state has not been reached after 1,440 days, the trend of the plot indicates that the ultimate scour will

be near elevation -2.6 m CD or 1.6 m below the surrounding general bed level, and the extent of scour is approximately 1 km^2. The areal extent of scour is predicted to be approximately 5.5 ha, with an average scour depth of 0.2 m below the adjacent seabed elevation. This includes a smaller area of approximately 0.5 m scour below the surrounding seabed level around which there is a larger area of scour to 0.1 m. The area of scour is expected to be confined to the sub-tidal portion of the seabed and is not expected to trigger headcutting.

Localized deposition of up to an elevation of -0.3 m CD is predicted on the west side of the proposed terminal immediately next to the scour zone. In addition, a far-field deposition region with an average deposition 0.5 m extending approximately 1 km from the west side of the terminal is predicted. The material that is deposited in this region originates from the scouring of the bed in the zone at the northwest corner of the proposed terminal during ebb tide. In addition, this region now experiences flood-dominant tidal currents that promote net onshore sediment transport, which will continue after Project completion.

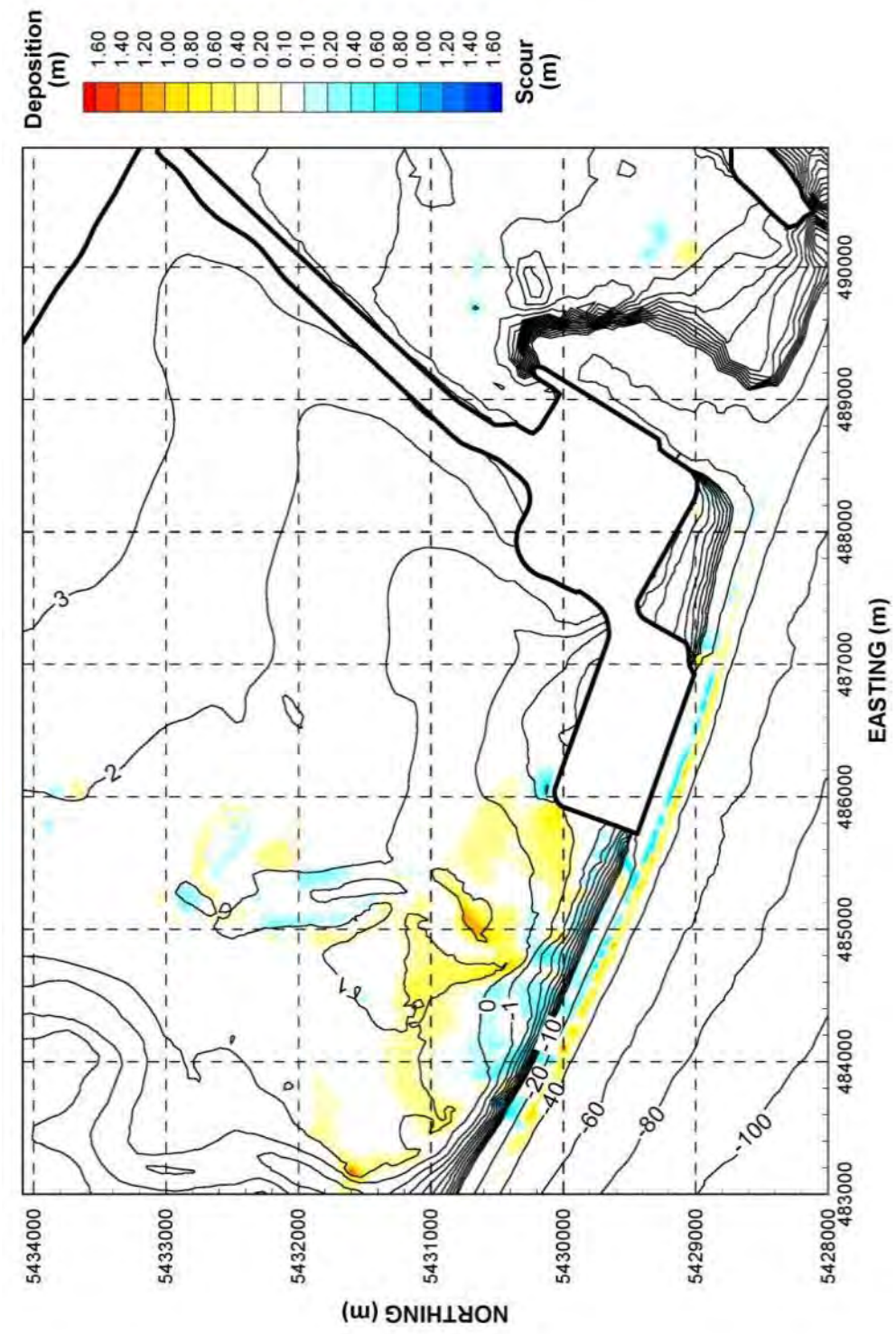

Figure 103: Morphodynamic evolution from tidal currents after 1,440 simulated days – future conditions with Project scenario.

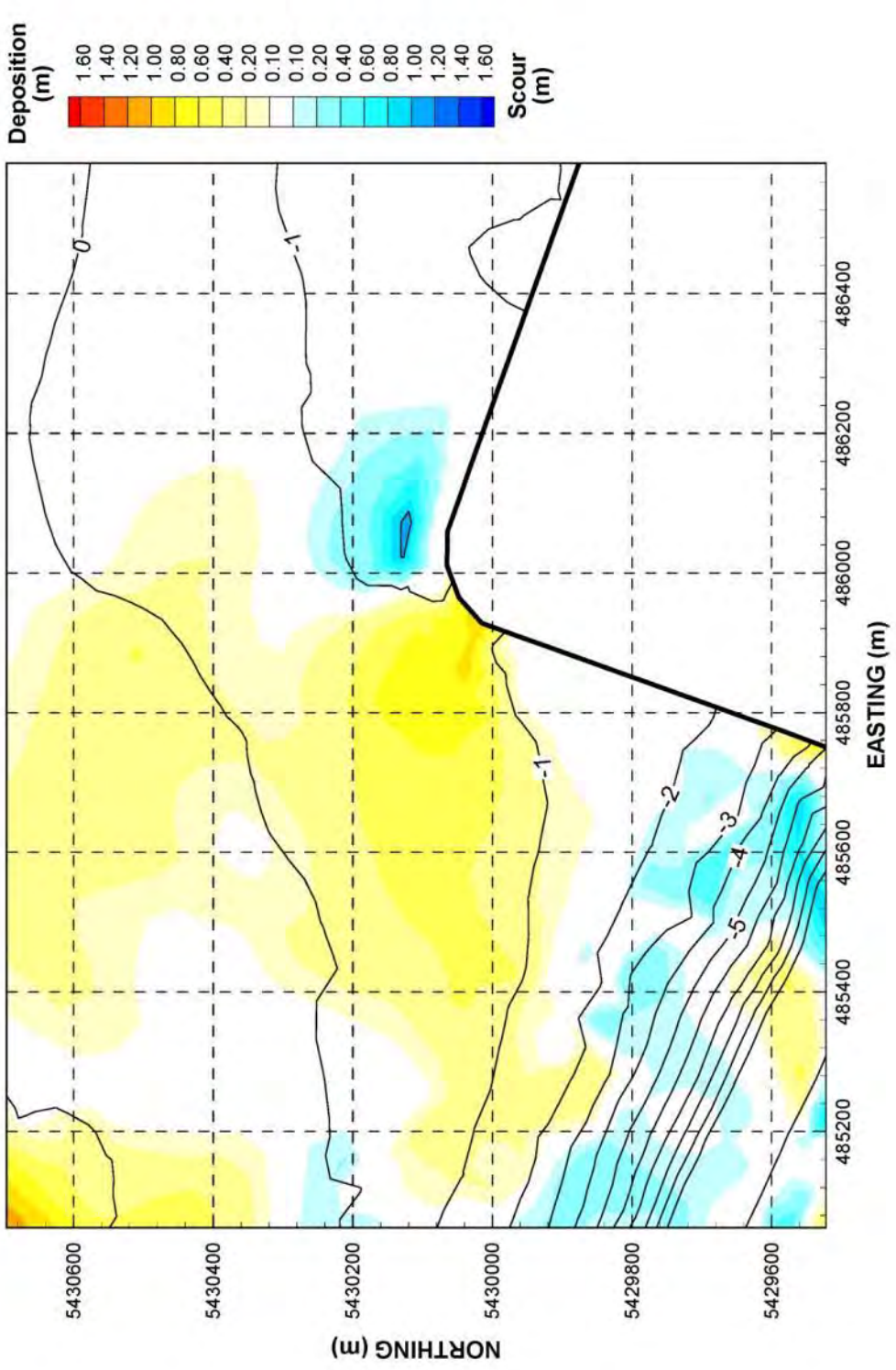

Figure 104: Morphodynamic evolution from tidal currents after 1,440 simulated days – future conditions with Project scenario – detail view.

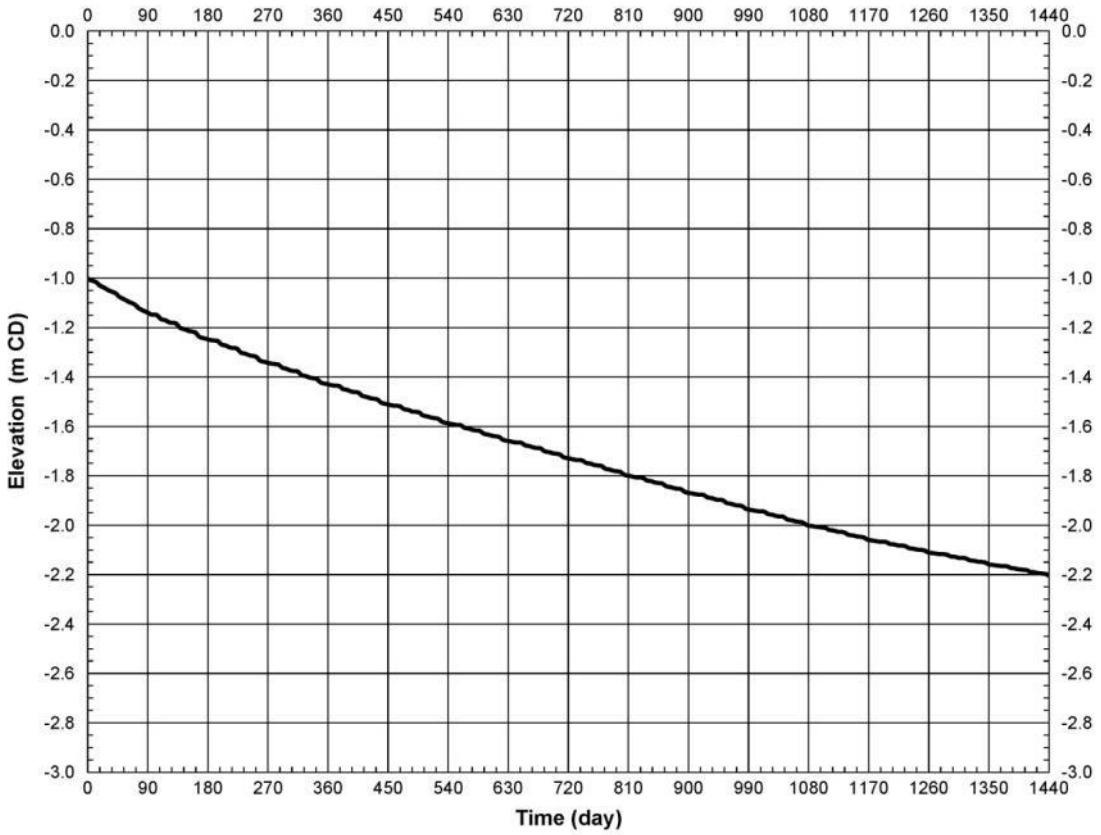

Figure 105: Evolution of the bottom elevation in the scour hole at the northwest Project corner.

Although the scour and deposition at the northwest corner of the proposed terminal can be ascribed directly to the changes that the Project will have on local tidal currents, the more far-field evolution of the tidal flats is anticipated to be only partially caused by the Project. The tidal flats and delta foreslope exist in a dynamic environment where ongoing change is expected and the magnitude and spatial pattern of future change that would occur in the absence of the Project should also be considered. **Figure 107** shows the difference in elevation between expected conditions and future conditions with Project cases after 1,440 days of model simulation. There is a similar pattern of erosion and deposition along the delta foreslope as compared to the results for the with Project scenario (**Figure 103**). The expected conditions morphodynamic evolution is noticeably different from the with Project scenario in two key aspects: i) the pattern and magnitude of erosion and deposition in the area immediately adjacent to the existing terminal, and ii) the evolution of the tidal flats in the area around the existing relict tidal channel. The differences in these two areas are discussed below.

i) The expected morphodynamic evolution (assuming no Project) (**Figure 106**) predicts erosion and deposition on the order of ±0.3 m in the portions of the outer tidal flats in close proximity to the existing Roberts Bank terminal structure. However, the area of deposition immediately to the west of the existing terminal would be covered by the Project footprint, while the tidal currents that result in the zone of erosion along the seaward face of the existing terminal will be substantially altered by the Project. The difference shown in **Figure 107** is positive (deposition)

because this zone would not be expected to erode with the Project in place, in effect reflecting the absence of future erosion at this location.

ii) The evolution of the tidal flats in the vicinity of the existing relict Canoe Passage tidal channel for the expected conditions scenario is fairly localised around the channel itself. With the Project in place, a relatively broad zone across the outer tidal flats is expected to experience deposition on the order of 0.5 m to 0.6 m, extending up to 2 km west of the Project shoreward of the 0 m CD elevation contour, while in the immediate vicinity of the tidal channel outlet, deposition would exceed 1 m above expected conditions. The result is an acceleration of the processes currently modifying the channel but not a large change in the channel processes that would likely lead to further channel formation. **Figure 107** shows that the majority of this zone of deposition is related to the Project.

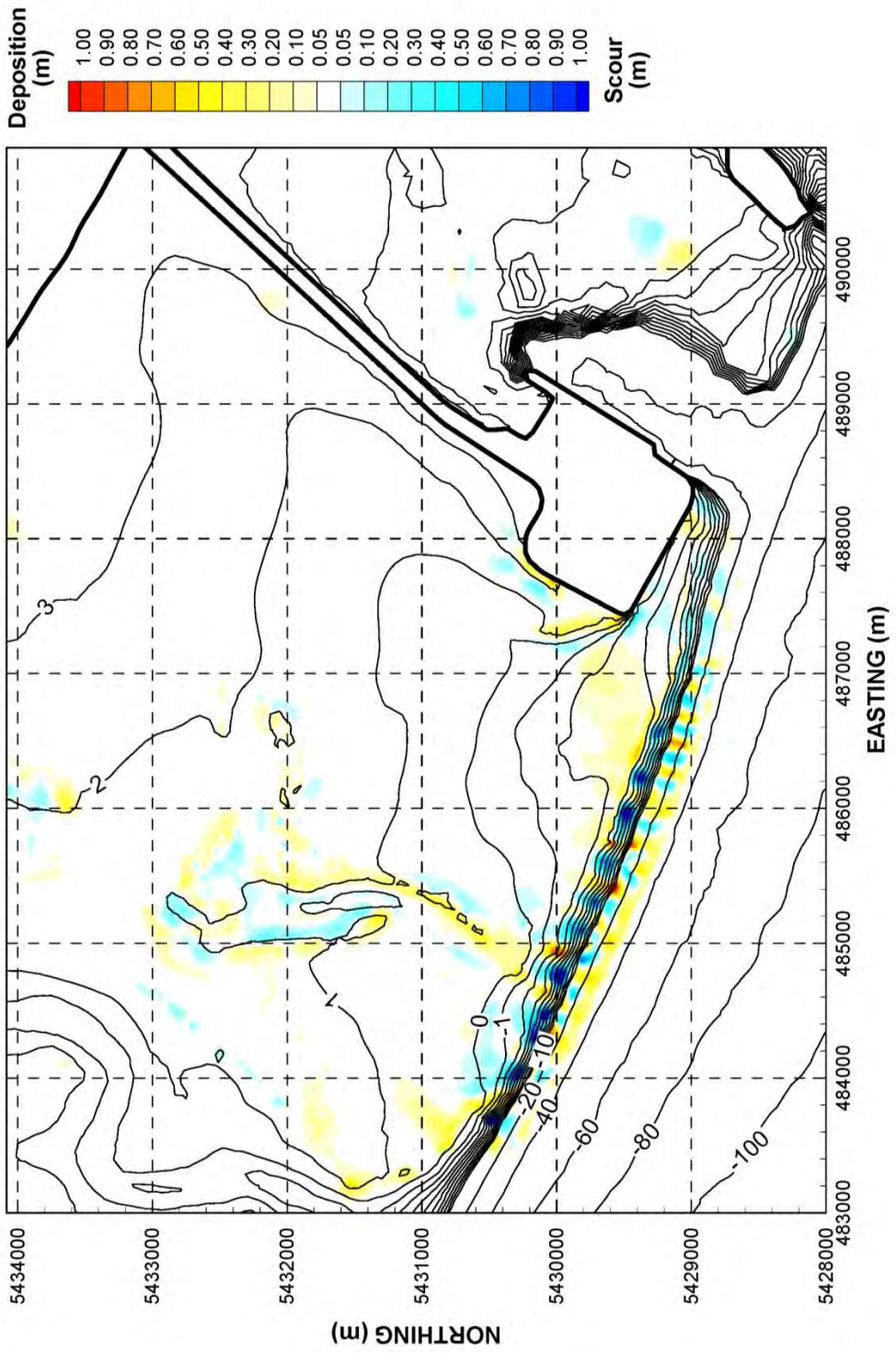

Figure 106: Morphodynamic evolution of the tidal flats in the LSA based on numerical modelling after 1,440 simulated days under expected conditions scenario.

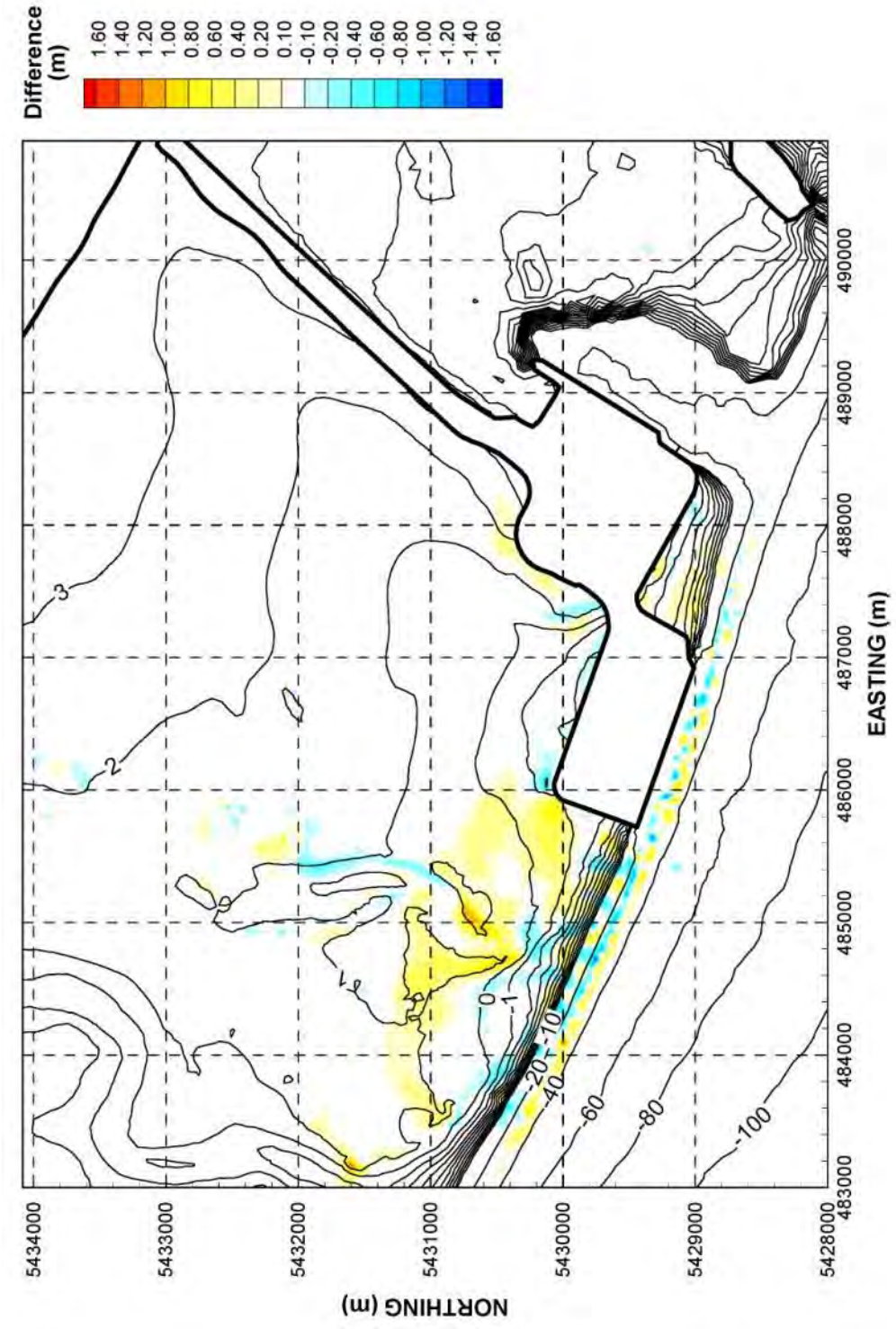

Figure 107: Morphodynamic evolution from tidal currents after 1,440 simulated days – difference between expected conditions and future conditions with Project scenarios.

8 EVALUATION OF PROJECT-RELATED CHANGES

8.1 GENERAL CONSIDERATIONS

This chapter describes the anticipated changes following construction of the Project on the coastal landforms, as well as potential changes during construction. The final evaluation is based on a synthesis of the geomorphic studies, field observations, hydrodynamic modelling and morphodynamic model results. No single approach was relied on without cross-validation with the other approaches. In some cases, predicted changes observed in the model have been used to infer additional changes in other parameters and processes. For example, salinity was used as an indirect and inverse indicator of turbidity, which relates to suspended sediment load. This, in turn, is based on the understanding that temporal and spatial changes in salinity reflect the relative influence of turbid Fraser River outflows and lower turbidity, more saline, seawater that enters the Strait of Georgia from the Pacific Ocean.

8.1.1 PREDICTIVE UNCERTAINTY

There is inherent uncertainty in the predictive capacity of the various approaches (interpretive geomorphic studies, analytical methods, and numerical modelling) that have been adopted as part of this coastal geomorphology study. Uncertainty has been mitigated by combining these three approaches outlined in **Section 1.3**, but some residual uncertainty remains, which can be described qualitatively.

Uncertainty was minimised in the quantification of the existing conditions by employing the most accurate data collection methods that were available, or by relying on data that were reliably collected by others (e.g. LiDAR data). Interpretation of existing conditions and processes using more subjective methods, such as interpretation of airphotos, carries inherent uncertainty because these methods rely in part on professional judgement.

The greatest uncertainty lies in predicting future conditions. Numerical modelling is at a relatively advanced level of development for application to coastal processes, but all models are a simplification or generalisation of complex processes. There is relatively low uncertainty with regard to predictions of waves and tidal currents, but predictions based on the morphodynamic (sediment transport) modelling are greater. While interim morphodynamic modelling results were reviewed periodically to ensure that they were in keeping with the observed general processes, results presented on projected bed level evolution should be interpreted as one of the reasonably possible outcomes, rather than as having a high degree of certainty. With respect to changes in wave conditions associated with SLR, it should be noted that while there is relatively low uncertainty with regard to modelling of waves, there is considerable uncertainty with respect to predictions of the magnitude and rate of future sea level rise.

8.2 POTENTIAL CONSTRUCTION PHASE CHANGES

There are four main components to the Project:

1. Berth Pocket
2. Marine Terminal
3. Tug Basin Expansion

4. Causeway Widening

Short-term construction activities for each of the component, particularly those that have the potential to affect morphology, are discussed below.

8.2.1 BERTH POCKET

In situ sediments will be dredged for the berth pocket. Dredged material will be pumped into the containment dykes described in **Section 8.2.2** for use as terminal fill. Suspended fines and excess water will be disposed of at sea. Densification of *in situ* sediments below the base of the dredged berth pocket will then occur. Finally, mattress rock will be installed to prevent scour from marine traffic and for stability of the toe of the adjacent caisson structure.

8.2.2 MARINE TERMINAL

Perimeter and interior dykes for the terminal area will be constructed using rock, gravel and riprap. An underwater transfer pit, used as a temporary holding area for the annual Fraser River dredgeate, will be dredged in the subtidal area of the inter-causeway to accommodate the terminal and causeway fill and preload. Densification of dykes and the preloading of the interior cells will follow.

For the three-berth wharf, *in situ* sediments will be dredged for the caisson trench. The dredged material will be pumped for use as fill within the containment dykes, and suspended fines and excess water out of the containment area will be disposed of at sea. Densification of the dredged caisson trench will follow, and then the caissons transported to the site will be installed by sinking them into place. Finally, the area between the caisson structure and the terminal containment dyke will be filled, along with installation of riprap at the toe of the caissons.

8.2.3 TUG BASIN EXPANSION

The existing tug basin will be dredged to expand it longitudinally (in a north-south direction) and deepen it by 0.5 m. The existing tug basin crest protection structure will be removed and replaced with a new tug basin crest protection structure. Riprap will be placed around the exposed perimeter of the expanded tug basin, to a crest elevation of approximately 1.3 m CD, to protect the adjacent mudflats from landward erosion of the knickpoint and thus mitigate the formation of tidal channels. Finally, two pivot gangways each with a single-span trestle structure will be installed for pedestrian access to shore and pontoon floats arranged along the dyke shoreline for mooring.

8.2.4 CAUSEWAY WIDENING

Perimeter and interior dykes will be established for the widened causeway. The subgrade will be brought to the level of the existing tidal flat sediments. Dredged material will be pumped or placed within the containment dykes, and suspended fines and excess water from the dredgeate will be disposed of at sea. Fill will be graded towards shore along the widened causeway. Densification of the soils under the widened causeway will be accomplished once the causeway fill is in place.

Construction of the Project is expected to last approximately six years, with partial operations starting after approximately four years. Key construction activities and their associated schedule are shown in Table **1**.

Table 5: Anticipated Project construction schedule including key activities. From PMV (2013).

Activity	Years of Construction					
	Year 1	Year 2	Year 3	Year 4	Year 5	Year 6
Terminal Dyking						
Fill Material Stockpiling						
Dredging of Berth Pocket and Caisson Trench						
Caisson Foundation & Wharf Construction						
Terminal Fill and Preloading						
Terminal Infrastructure						
Causeway Dyking						
Causeway Fill, Ground Improvement and Preloading						
Causeway Infrastructure						
Tug Basin Expansion						

8.2.5 POTENTIAL CHANGES TO MORPHOLOGY

Potential construction-phase changes were identified based on experience with changes observed as a result of previously completed projects in the Roberts Bank area and assessed using input from the results of the localised River2D model results (**Appendix D**). It is expected that many of the possible changes to morphology from construction will be avoided by siting the marine terminal component of the Project almost entirely within the subtidal zone of Roberts Bank. Only a small section of the northeast corner of the terminal intersects the intertidal zone.

The construction of the containment dyke along the causeway is predicted to result in localised changes to coastal geomorphology. All of the causeway widening will occur in the intertidal zone. A phased construction approach is anticipated with the western and eastern portions of the containment dyke and the placement of sand fill within it. The containment dyke will be semi-pervious, and the area between the dyke and the existing causeway will fill with ocean water during a rising tide and drain on a falling tide. The rate of flow through the dyke is expected to be insufficient to equalise the water levels on each side during the rising and falling limbs of the tide cycle, leading to temporary storage of water inside the dyke during falling tide conditions, which will discharge through the structure and onto the adjacent tidal flats.

Drainage channels are expected to extend out from the containment dyke and terminate where tide height would typically inundate the tidal flats during the critical period of through-dyke discharge as delineated in **Figure 107**. The size, form and density of channels can be assumed to be similar to the channels that formed adjacent to the DP3 structure during the construction phase of that project (Hemmera et al. 2008) as the tidal flat substrate and slope, and dyke construction methods and materials are similar. The western section of dyke (CD1) will be constructed and the widened causeway

filled before the eastern section (CD2) is constructed. Therefore, channels will form and then cease to be active in the western section before they begin to form in the eastern section.

Based on experience with the DP3 Project, it can be assumed that approximately 20% of the area between the erosion extent and the causeway dyke (**Figure 108)** will be occupied by temporary channels, and the area between the channels will be undisturbed. The channels adjacent to the DP3 structure have persisted as relict features since their formation in 2007, despite the fact that there is no ongoing discharge of water, because waves and currents in that area are too small to redistribute sediments. Conditions on the north side of the Roberts Bank causeway are much more energetic, and it is expected that the channels would eventually infill once the area between the dyke and the causeway is filled and water no longer drains through the dyke.

It is expected that the temporary channel formation could be partially mitigated through Project design to divert some of the flow laterally along the toe of the dyke. This would potentially reduce the distance from the dyke over which channel formation would occur.

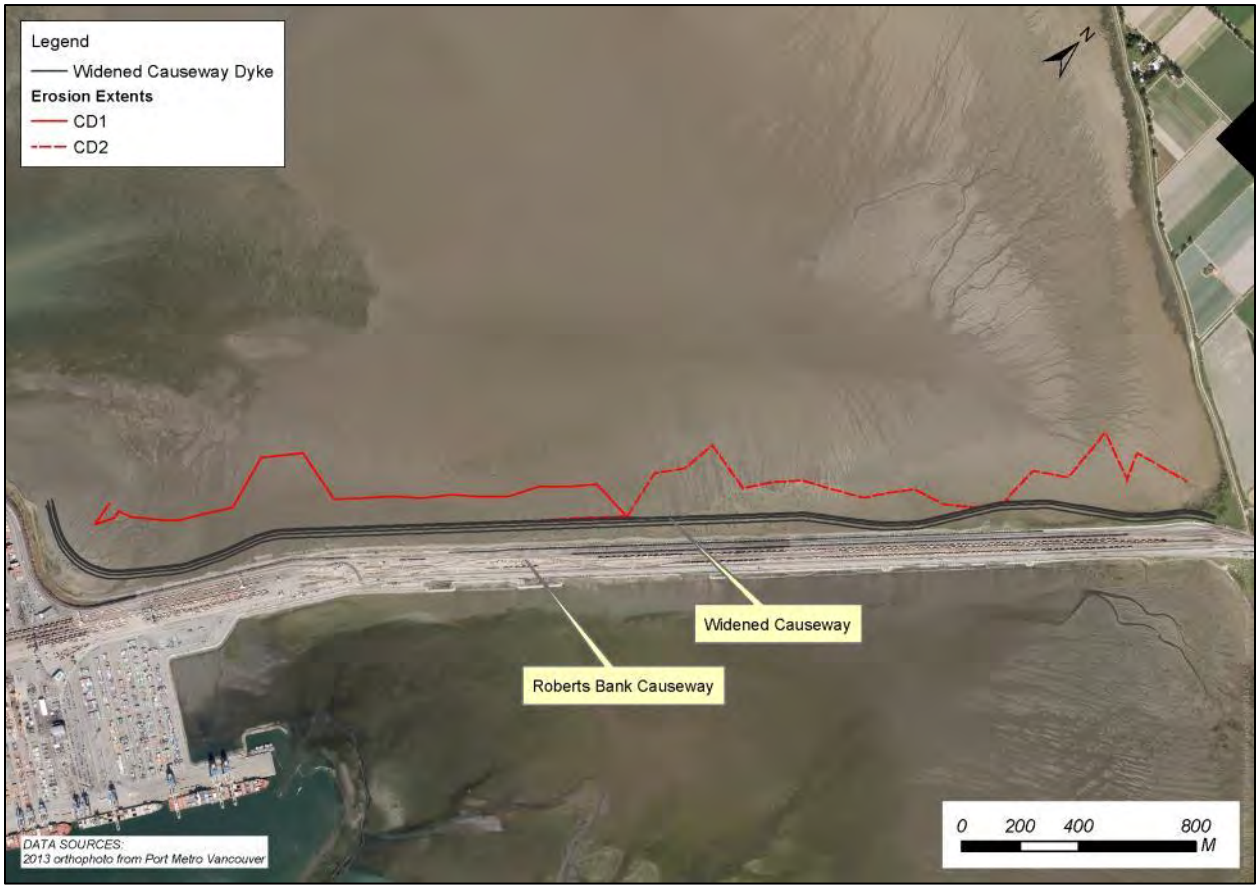

Figure 108: Extents of drainage channel development during the construction phase associated with the causeway dyke.

8.3 OPERATION PHASE CHANGES

The Project will change coastal geomorphology by creating physical structures that interact with the driving coastal processes, including tidal currents and wind-generated waves. Changes to the coastal processes will in turn result in changes to sediment transport, erosion and deposition, the elevation of the seabed, and the distribution of freshwater from the Fraser River. The changes associated with the terminal and widened causeway were assessed separately from the changes associated with the expanded tug basin due to their physical isolation from each other and the different approaches taken to studying the Project components.

8.3.1 MARINE TERMINAL AND WIDENED CAUSEWAY OPERATION-PHASE CHANGES

Changes caused by the widened causeway were too small to be resolved by the TELEMAC model, and a separate study was conducted to address this Project component (**Appendix D**). The following subsections summarise the results of the model study with respect to changes to tidal currents, salinity, waves, and morphodynamics caused by the proposed marine terminal.

Current Velocity

Tidal currents in the Strait of Georgia flood to the northwest and ebb to the southeast in deep water. The tidal flow direction is altered over shallower waters so that at Roberts Bank, the flow is dominantly onshore-offshore on the tidal flats. The proposed terminal will be positioned in the path of this dominant flow direction and will divert both flooding and ebbing water to the west around the end of the structure.

Changes to tidal currents are quite similar for the freshet and non-freshet period, although the area over which the 50th percentile velocity is altered is slightly larger during the freshet. Flow acceleration around the western end of the proposed terminal would result in an increase in 50th percentile current velocities by about 0.1 m/s over a 2 km by 2 km area. This area will likely experience increased sediment mobilisation. There will be a velocity reduction in the elbow formed where the proposed terminal connects to the existing Westshore Terminals of about 0.3 m/s. As well, the 50th percentile velocity in the foreshore along the eastern side of the proposed terminal is predicted to be approximately 0.05 m/s slower.

Wave Climate

As described previously, winds most frequently blow from the northwest and southeast and are the dominant driving force for wave generation in the southern Strait of Georgia. The proposed terminal will partially block incoming waves from the open waters of the Strait of Georgia from propagating onto the tidal flats, creating a wave shadow. The wave shadow effect will be strongest for waves coming from the southeast because of the orientation of the long axis of the terminal and its position relative to the existing Roberts Bank terminals.

The Project is predicted to reduce the 50th percentile wave height to be generally less than 10 cm, but this represents a reduction of 50% to 100% in the zone immediately adjacent to and inshore from the

terminal. The predicted spatial extent of the net wave height reduction with the Project in place is similar in the summer and winter seasons, although the predicted change extends farther west inshore of the delta foreslope in the winter months. Regardless of season, the area experiencing a reduction in wave height of 5 cm or more extends about 750 m from the western edge of the terminal. With a moderately calmer wave climate, there will be less frequent sediment mobilisation and suspension by wave action compared to under existing conditions.

No change is predicted in wave heights shoreward of approximately 1.5 m CD elevation, which includes the upper intertidal zone. Wave heights over non-inundated areas of the tidal flats are zero and are therefore insensitive to the Project. Changes to wave height caused by the Project, therefore, are limited to the near-field zone around the proposed terminal.

The east face of the proposed terminal will be directly exposed to waves from the southeast and south directions and potentially result in some local bed scour between this face and the southern face of the existing Westshore Terminals.

Sea level rise of 0.5 m will result in greater average depths of water over the tidal flats, complete immersion of that portion of the tidal flats below 0.5 m CD, and longer immersion times for those areas above 0.5 m CD. Modelled results to assess the effect of future SLR on the nearshore wave climate on the tidal flats show little difference in the predicted areal extent and magnitude of change in wave height between future conditions with the Project and future conditions with the Project and SLR. Similar to the predicted wave shadow effect that the proposed terminal will have on the tidal flats for storms from the southeast, a comparable wave shadow also occurs under SLR conditions. Changes in wave climate due to SLR occur in the upper tidal flat zone, which is well outside the Project influence area for waves. SLR and the Project are essentially independent of each other with respect to the change on wave climate.

Sediment Dynamics

The bed condition at the end of the morphodynamic model simulation (the model was considered to have achieved a quasi-equilibrium bed condition in 1,440 days) predicts an adjustment along the delta foreslope as well as sedimentation of the tidal flats to the north and west of the terminal between elevation contours of -1 m CD and +1 m CD.

The primary direct change from the Project is focused on the area of seabed near the northwest corner of the proposed terminal. The scour near the northwest corner of the proposed terminal was predicted through modelling and subsequent forecasting to reach a maximum elevation of approximately -2.6 m CD, or 1.6 m below the surrounding seabed. The areal extent of scour is predicted to be approximately 5.5 ha, with an average scour depth of 0.2 m below the adjacent seabed elevation. This includes a smaller area of approximately 0.5 m scour below the surrounding seabed level around which there is a larger area of scour to 0.1 m. The area of scour is expected to be confined to the sub-tidal portion of the seabed and is not expected to trigger headcutting.

Localised deposition up to an elevation of -0.3 m CD is predicted on the west side of the proposed terminal immediately next to the scour zone. In addition, a far-field deposition region with an average deposition of 0.5 m is predicted to extend about 1 km from the west side of the terminal. Deposition material will originate from bed scouring at the northwest corner of the proposed terminal during ebb tide.

The more far-field evolution of the tidal flats is anticipated to be only partially attributable to the Project. An exception is a broad zone of deposition across the outer tidal flats and in the vicinity of the relict tidal channel outlet that would result in an acceleration of the processes currently modifying the channel; however, this change in the channel processes is not anticipated to be large enough to lead to further channel formation.

Salinity and Turbidity

With the Project in place, there is a greater retention of freshwater across the tidal flats, particularly along the causeway. The result is a decrease in the average salinity along the north side of the Roberts Bank causeway extending 2 to 3 km and an increase in salinity in the area of the outer tidal flats between the Canoe Passage outlet and the Project. The maximum change in 50th percentile value is -8 and +4 PSU during the freshet and -7 and +4 during the non-freshet period.

The zone of reduced salinity in the area parallel to the causeway is expected to receive additional inputs of fine sediment, which is carried by the freshwater emanating from the Fraser River. It is not possible to accurately predict rates of deposition of the fine sediment fraction that is carried in suspension, but the zone is expected to experience a slight increase in sedimentation rates above the existing low rates of accumulation.

8.3.2 TUG BASIN OPERATION-PHASE CHANGES

The expanded tug basin, which consists of a dredged area, slope protection, and new crest protection structure, will change coastal geomorphology within the localised area immediately surrounding the tug basin. The assessment was made using an interpretive geomorphology approach (detailed numerical modelling of the tug basin expansion was not conducted) as the tug basin is physically isolated from the Project's marine terminal and widened causeway. Changes to tidal currents and waves associated with the proposed terminal are considered to be independent of changes at the tug basin, as was demonstrated previously by NHC and Triton (2004). The tug basin location is largely protected from wind-generated waves from the Strait of Georgia such that locally-generated waves are typically less than 0.3 m.

Existing features of the tug basin include the basin, original crest protection structure, and the pour-over channels, located based on an orthophoto taken in 2013 at a very low tide. **Figure 109** shows these existing features and proposed elements.

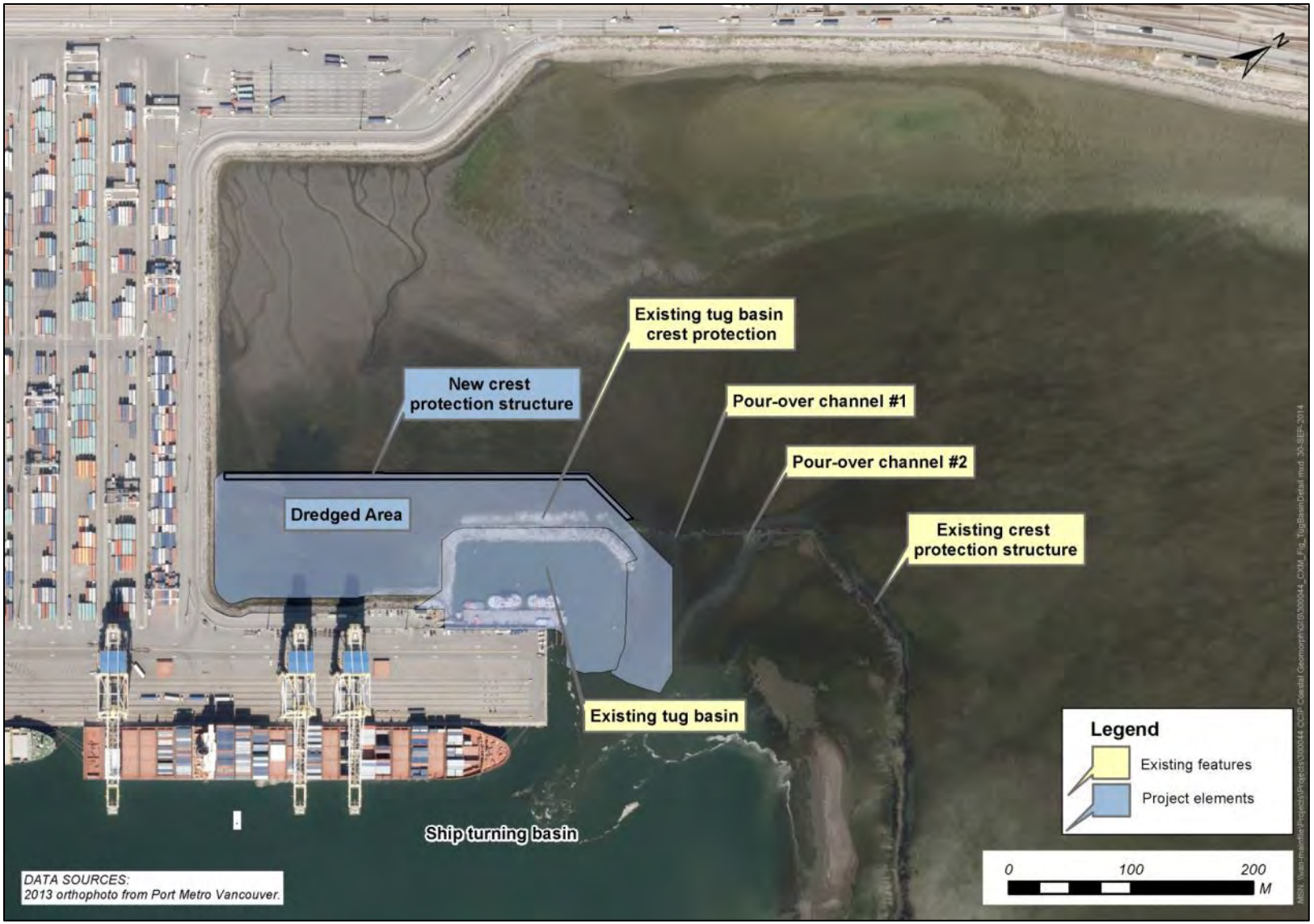

Figure 109: Schematic layout of Project's expanded tug basin and existing tug basin features.

Under existing conditions, the exposed areas of tidal flat visible in **Figure 109** are regularly inundated by tidal water, which floods from the tug basin inland. During the falling tide, water drains from the tidal flats towards the tug basin and interacts with the crest protection structure, which has a crest elevation that is typically up to 0.5 m higher than the surrounding tidal flats. At an ebb tide level below approximately 1.0 m CD, water is preferentially diverted laterally along the shoreward side of the crest protection structure until it reaches distinct locations that are slightly lower than the surrounding crest through which it drains seaward. This has led to the formation of the pour-over channels noted in **Figure 109**.

The expanded tug basin will convert additional areas of tidal flats from intertidal to sub-tidal, including the seaward portion of pour-over channel #1. The new tug basin crest protection structure will be located further shoreward than the existing tug basin crest protection structure and will have a crest elevation of approximately 1.3 m CD, approximately 0.3 m above the present elevation of the tidal flats. Water draining from the tidal flats during an ebb tide will interact with the crest protection structure and at elevations below 1.3 m CD will be diverted laterally toward pour-over channel #1. There may be a moderate increase in channel width of 1 to 2 m along the residual length of channel following the tug basin expansion (estimated at 40 m) to accommodate the increased flow. There is a very low potential for the expanded tug basin to result in the formation of additional tidal channels or to accelerate growth of existing tidal channels.

8.4 SUMMARY OF ASSESSMENT

Construction-phase changes to coastal geomorphology associated with the Project are related to drainage of tidal waters through the causeway dyke, which will result in drainage channels forming on the tidal flats adjacent to the causeway. The channels will be temporary, as the seepage flow will not occur once the area between the dyke and the existing causeway is filled with sediment, and coastal processes will eventually fill the channels through redistribution of existing sediments.

Potential operation phase changes associated with the Project are summarised in

Table 6, and their anticipated spatial extents are illustrated in **Figure 110**. The spatial boundaries are drawn to the outer edge of the potential zone of changes to be conservative, but actual changes are likely to be more limited spatially and concentrated towards the central portion of the polygons.

A scour zone (Zone 1) is expected to develop near the northwest edge of the proposed terminal structure due to flow acceleration around the west side of the terminal pad. General lowering in bed elevation in the primary scour zone is predicted to be approximately 0.5 m and the maximum scour elevation is expected to be to a depth of approximately -2.6 m CD, or 1.6 m below the surrounding seabed level. Eroded sediment from the scour zone will be deposited on the west side of the structure (Zone 2). The general rise in bed level in this zone was estimated to be about 1.0 m.

The flow acceleration and bed scour at the northwest corner is expected to increase flow exchange in a relict tidal channel (formerly draining a portion of Canoe Passage) west of the terminal (Zone 3). Modelling of tidal currents predicted an increase in current velocity at the seaward end of the channel with the Project in place, and the morphodynamic model results indicate general bed accretion in this zone adjacent to the higher velocity channel. Based on the observation of similar channels elsewhere in the Fraser River estuary, the channel response to the accretion is expected to migrate laterally near the mouth and downcut through the accumulating sediments in order to meet base level. This channel is expected to become more active, experiencing higher flood tide velocities, channel widening, and lateral shifting. It is unlikely that severe headcutting will be induced at the head of the channel.

The proposed terminal is predicted to locally reduce tidal currents (Zone 4) and create a local wave shadow (Zone 5) on its north side, particularly where it meets the existing terminal. These areas are expected to experience increased deposition of fine sediment that is currently carried in suspension (mainly silt). Nonetheless, sedimentation rates are expected to be low given that there is a limited annual supply as discussed in **Section 4.2**.

The Project is predicted to affect the wave energy and salinity environment on Roberts Bank north of the causeway (Zone 7). The proposed terminal will interrupt the landward movement of seawater during rising tides, causing the saline flow to be deflected further to the northwest. This will increase the residence time of lower salinity Fraser River water in the area shoreward of the proposed terminal and north of the causeway. In addition, the proposed terminal configuration will modify the movement of the Fraser River plume across the tidal flats, directing more turbid water along the western end of the widened causeway. This will promote fine sediment (silt) deposition on the tidal flats and a corresponding increase in bed elevation over time near the western end of the causeway.

The ridge and runnel complex located further from the Project is expected to be minimally affected by the terminal structure. While the wind and current environment are unlikely to be affected, salinity may be lower while turbidity may be higher. This could result in an increased sedimentation rate within the ridge and runnel complex over and above the ongoing sedimentation (see **Section 5.3.3**).

The change from the expanded tug basin component of the Project (Zone 8) includes a lateral expansion to the existing pour-over channel. Formation of additional tidal channels or acceleration in growth of existing channels is not anticipated. The expansion area will encompass an area to the immediate northwest that presently only partially drains during the higher magnitude ebb tide events.

Table 6: Predicted morphological changes from the proposed Project footprint.

Zones in Figure 9.5-34	Hydrodynamic Processes Affected by the Project	Gross Area	Local Changes	Potential to Trigger Wider-area Morphological Changes
1	Scour around NW corner of terminal pad	5.8 ha	Local scour (localised decrease in tidal flat elevation, up to 1.6 m below current seabed elevation or to 2.6 m CD)	Moderate
2	Deposition along west side of terminal pad	20 ha	Deposition adjacent to scour hole (raising of seabed by ~1.0 m).	Low
3	Accelerated tidal channel	50 ha	Possible acceleration of tidal channel to the west of NW corner scour and associated deposition in adjacent areas.	Moderate
4	Deposition off NE corner of terminal pad	40 ha	Local deposition from combination of back-eddy, wave shadow, and increased turbidity.	Low
5	Wave shadow	70 ha	Reduction for waves in the lee of the structure.	Low
6	Wave scour	1 ha	Limited wave scour at east face of terminal.	Nil
7	Increased turbidity, reduced salinity	Not quantified	Decline in salinity, associated increase in turbidity, and increase in sedimentation.	Nil
8	Tug basin	80 m^2	Lateral adjustment of the pour-over channel	Low

Figure 110: Approximate spatial extent of potential changes associated with the Project footprint.

9 CONCLUSIONS

Roberts Bank Terminal 2 Project will induce local changes to the hydrodynamic and sediment transport patterns on the Roberts Bank tidal flats. Key locations where Project-induced morphologic changes are predicted during the operations phase include:

- Local scour near the northwest corner of the proposed terminal;
- Local deposition seaward of the scour hole;
- Increased flow and sediment transport in the relict drainage channel west of the Project, leading to widening and increased channel shifting; further headcutting at the upper end of the channel is not anticipated;
- Fine sediment deposition on the north side of the proposed terminal in the zone of wave shadowing and reduced tidal current velocities; and,
- Fine sediment deposition along the lower portion of the sand flats near the south end of the causeway due to increased residence time of turbid water.

In addition to the operations phase changes to coastal geomorphology, temporary erosion and channel formation is expected to occur in a zone of the tidal flats parallel to the causeway during the construction phase. The channels are expected to be active only during the period before the expansion area between the dyke and the existing causeway is filled with sediment to form the widened causeway. Coastal processes such as wave action and currents will eventually re-distribute sediments and fill the channels. It is expected that the temporary channel formation could be partially mitigated through Project design to divert some of the flow laterally along the toe of the dyke. This would potentially reduce the distance from the dyke over which channel formation would occur.

Wave modelling indicated that a 0.5 m rise in sea level will not amplify or significantly alter the predicted changes from the Project.

The sediment supply to the southern Roberts Bank tidal flats is limited mainly to fine suspended load (silt and clay) sediments from the Fraser River plume. The amount of sand-sized sediment supplied to the flats from Canoe Passage is small. The intertidal sand flats undergo periodic scour and fill but show no obvious trend of lowering or infilling over time.

The upper section of the tidal flats in the ridge and runnel complexes is accreting. In the absence of sea-level rise and land subsidence, the ridges associated with the ridge and runnel complexes may attain accretion rates on the order of 1 cm/year as vegetation continues to become established. The low-lying zones adjacent to the ridge and runnel complexes that have a high density of biofilm, especially those that are located inland, are also anticipated to increase in relative elevation and be colonized by vegetation communities. These trends are not expected to be affected by the Project.

Modelling of Fraser River freshwater mixing with ambient saline water in the Strait of Georgia indicates that the Project will change the distribution of freshwater within the portion of the local assessment area between the causeway and Canoe Passage. The area adjacent to the causeway will experience an average decrease in salinity and the area of the outer tidal flats between the new terminal and Canoe Passage will experience and average increase in salinity. This effect will be greatest during the freshet period, and less pronounced during the winter low-flow period. The change in salinity is not directly related to changes in coastal geomorphology but the correlation between freshwater and higher turbidity has informed the overall assessment.

10 REFERENCES

Anibal, J., C. Rocha, and M. Sprung. 2007. Mudflat surface morphology as a structuring agent of algae and associated macroepifauna communities: A case study in the Ria Formosa. Journal of Sea Research 57:36–46.

Attard, M. E., J. G. Venditti, and M. Church. 2014. Suspended sediment transport in Fraser River at Mission, British Columbia: New observations and comparison to historical records. Canadian Water Resources Journal 39:356–371.

Ausenco-Sandwell. 2011. Climate Change Adaptation Guidelines for Sea Dikes and Coastal Flood Hazard Land Use: Guidelines for Management of Coastal Flood Hazard Land Use. Report prepared by Ausenco-Sandwell for BC Ministry of Environment.

Bell Dawson, W. 1923. Tide Levels and Datum Planes on the Pacific Coast of Canada. Department of Marine and Fisheries, Ottawa.

Blanchard, G. F., D. M. Paterson, L. J. Stal, P. Richard, R. Galois, V. Huet, J. Kelly, C. Honeywill, J. de Brouwer, K. Dyer, M. Christie, and M. Seguignes. 2000. The effect of geomorphological structures on potential biostabilisation by microphytobenthos on intertidal mudflats. Continental Shelf Research 20:1243–1256.

Christian, H. A., D. C. Mosher, J. V. Barrie, J. A. Hunter, and J. L. Luternauer. 1998. Seabed slope instability on the Fraser River delta. Pages 217–230 *in*. Geology and Natural Hazards of the Fraser River Delta, British Columbia,. (ed.) J.J. Clague, J.L. Luternauer, and D.C. Mosher. Geologic Survey of Canada, Bulletin 525.

Church, M., and W. Hales. 2007. The tidal marshes of Fraser River: 75 years of growth and change. Discovery 36:28–33.

City of Delta. 2013. City of Delta Flood Hazards. Municipal. <http://www.corp.delta.bc.ca/EN/main/residents/public_safety/26737/26719/flood_hazards.html>. Accessed 12 Nov 2013.

Clague, J. J., and B. Turner. 2006. Vancouver, city on the edge. Tricouni Press Ltd, Vancouver, BC.

Coleman, J. M., and L. D. Wright. 1975. Modern river deltas: variability of processes and sand bodies. Pages 99–149 *in*. Deltas, Models for Exploration. Houston Geological Society, Houston, TX.

Compass Resource Management Ltd. 2013*a*. Proposed Roberts Bank Terminal 2 Project - Coastal Geomorphology Technical Advisory Group Summary Report. Report prepared on behalf of TAG Participants for Port Metro Vancouver, Vancouver, BC.

Compass Resource Management Ltd. 2013*b*. Proposed Roberts Bank Terminal 2 Project - Coastal Geomorphology Technical Advisory Group Summary Report. for Port Metro Vancouver, Vancouver BC.

Delcan. 2012. Cost of Adaptation - Sea Dikes & Alternative Strategies (Final Report). Report prepared by Delcan Corporation for BC Ministry of Forests, Lands and Natural Resource Operations.

Department of Fisheries and Oceans. 2005. WebTide Tidal Prediction Model (v0.7.1). Bedford Institute of Oceanography. <http://www.mar.dfo-mpo.gc.ca/science/ocean/coastal_hydrodynamics/WebTide/webtide.html>.

Einstein, H. A. 1950. The Bed-Load Function for Sediment Transportation in Open Channel flows. United States Department of Agriculture, Washington, D.C.

Foreman, M. G. G., W. R. Crawford, J. . Cherniawsky, R. F. Henry, and M. R. Tarbottom. 2000. A high-resolution assimilating tidal model for the northeast Pacific Ocean. Journal of Geophysical Research 105:629–652.

Fraser Basin Management Board. 1994. Review of the Fraser River Flood Control Program.

Friedrichs, C. 2011. Tidal Flat Morphodynamics: A Synthesis. Elsevier.

FSM Management Group Inc., and Hatch Ltd. 2012. Fraser River Delta Biofilm: Sensitivity to Jet A Fuel Spills Summary Report. Vancouver Airport Facilities Corporation.

GL Williams & Associates Ltd., and NHC. 2009. Roberts Bank and Sturgeon Bank Reach Overview Backgrounder. Prepared by GL Williams & Associates Ltd. and Northwest Hydraulic Consultants for Fraser River Estuary Management Program.

Hales, W. 2000. The impact of human activity on deltaic sedimentation, Marshes of the Fraser River delta, British Columbia. PhD, University of British Columbia, Vancouver BC, Vancouver, BC.

Hansen, J. C. R., and M. A. Reidenbach. 2013. Seasonal Growth and Senescence of a Zostera marina Seagrass Meadow Alters Wave-Dominated Flow and Sediment Suspensn Wtihin a Coastal Bay. Estuaries and Coasts 36:1099–1114.

Hay and Company. 1996. Erosion at Roberts Bank geophysical evaluation. Report prepared for Vancouver Port Corporation and BC Ferry Corporation.

Hemmera. 2014. Roberts Bank Terminal 2 Technical Data Report: Sediment and Water Quality Characterisation Studies. Prepared for Port Metro Vancouver, Vancouver, B.C. In Port Metro Vancouver (PMV). 2015. Roberts Bank Terminal 2 Environmental Impact Statement: Volume 2. Environmental Assessment by Review Panel. Submitted to Canadian Environmental Assessment Agency.

Hemmera, NHC, and Precision. 2008. Deltaport Third Berth Adaptive Management Strategy 2007 Annual Report. Report prepared by Hemmera Envirochem Inc., Northwest Hydraulics Consultants and Precision Identification for Port Metro Vancouver, Vancouver, BC.

Hemmera, NHC, and Precision. 2012. Deltaport Third Berth Adaptive Management Strategy 2010 Annual Report. Report prepared by Hemmera Envirochem Inc., Northwest Hydraulics Consultants and Precision Identification for Port Metro Vancouver, Vancouver, BC.

Hill, P. R. 2013. RE: Luternauer 1976 sediment dataset.

Hill, P. R., R. W. Butler, R. W. Elner, C. Houser, M. L. Kirwan, A. Lambert, D. G. Lintern, S. Mazzotti, A. Shaw, T. Sutherland, S. Morrison, S. Petersen, and S. Solomon. 2013. Impacts of sea level rise on Roberts Bank (Fraser Delta, British Columbia). Geological Survey of Canada.

Hill, P. R., K. Conway, G. Lintern, S. Meule, K. Picard, and J. V. Barrie. 2008. Sedimentary processes and sediment dispersal in the southern Strait of Georgia, BC, Canada. Marine Environmental Research 66:539–548.

Holland, S. 1964. Landforms of British Columbia - A Physiographic Outline. Bulletin No. 48, British Columbia Department of Mines and Petroleum Resources, Victoria, B.C.

Hunter, J. A., and H. A. Christian. 2001. Use of shear waves velocities to estimate thick soil amplification effects in the Fraser River delta, British Columbia. Proceedings Application of Ecophysics to Evironmental Engineering Problems, Denver, CO.

IPCC. 2013. Climate Change 2013: The Physical Science Basis - Summary for Policymakers. Working Group I contribution to the Fifth Assessment Report of the Intergovernmental Panel on Climate Change.

Johannessen, S. C., R. W. Macdonald, C. A. Wright, B. Burd, D. P. Shaw, and A. van Roodselaar. 2008*a*. Distribution and cycling of suspended particles from transmissivity in the Strait of Georgia, Haro Strait and Juan de Fuca Strait. Marine Environmental Research 66:12–20.

Johannessen, S. C., R. W. Macdonald, C. A. Wright, D. P. Shaw, and A. van Roodselaar. 2008*b*. Joined by geochemistry, divided by history: PCBs and PBDEs in Strait of Georgia sediments. Marine Environmental Research 66:S112–S120.

Keane, J. C. B. 1957. Report on the Hydrometric Surveys and Discharge Computations for the Fraser River Estuary for May, June and August, 1954. A Technical Monograph, Open File Report, Fraser River Board, Victoria BC.

Kellerhals, P., and J. W. Murray. 1969. Tidal flats at Boundary Bay, Fraser River Delta, British Columbia. Bulletin of Canadian Petroleum Geology 17:67–91.

Ladakis, M., M. Dassanakis, and A. Pantazidou. 2006. Nitrogen and phosphorus in coastal sediments covered by cyanobacteria mats. Journal of Soils and Sediments 6:46–54.

Lavelle, J. W., G. J. Massoth, and E. A. Crecelius. 1986. Accumulation rates of recent sediments in Puget Sound, Washington. Marine Geology 72:59–70.

Luternauer, J. L. 1976. Fraser Delta Sedimentation, Vancouver, British Columbia. Report of Activities, Part A, Geological Survey of Canada. <ftp://ftp2.cits.rncan.gc.ca/pub/geott/ess_pubs/119/119844/pa_76_1a.pdf>.

Luternauer, J. L., D. C. Mosher, and J. J. Clague. 1998. Sedimentary environments of the Fraser River delta. Pages 27–39 *in*. Geology and Natural Hazards of the Fraser River Delta, British Columbia,. (ed.) J.J. Clague, J.L. Luternauer, and D.C. Mosher. Geologic Survey of Canada, Bulletin 525.

Luternauer, J. L., and J. W. Murray. 1973. Sedimentation on the western delta-front of the Fraser River, British Columbia. Canadian Journal of Earth Sciences 10:1642–1663.

Mathews, W. H., and F. P. Shepard. 1962. Sedimentation of the Fraser River Delta, British Columbia. Bulletin of the American Association of Petroleum Geologists 46:1416–1438.

McKinnell, S. M., and W. R. Crawford. 2007. The 18.6-year lunar nodal cycle and surface temperature variability in the northeast Pacific. Journal of Geophysical Research: Oceans 112.

McLaren, P., and P. Ren. 1995. Sediment Transport and Its Environmental Implications in the Lower Fraser River and Fraser Delta. Environment Canada.

McLean, D. G., M. A. Church, and B. Tassone. 1999. Sediment transport along lower Fraser River 1: Measurements and hydraulic computations. Water Resources Research 35:2533–2548.

McLean, D. G., and B. Tassone. 1988. Budget of the Lower Fraser River. Page 16 *in*. Federal Inter-Agency Committee on Sedimentation, 5th International Conference. Las Vegas, Nevada.

Morton, K. W. 1949. Fraser River System, Province of British Columbia, History of Improvements 1876 to Date. Dominion Public Works Department, New Westminster, BC.

Nelson, A. D., and M. Church. 2012. Placer mining along the Fraser River, British Columbia: The geomorphic impact. Geological Society of America Bulletin 124:1212–1228.

NHC. 2006. Lower Fraser River Hydraulic Model Final Report. Prepared by Northwest Hydraulic Consultants and Triton Consultants or Fraser Basin Council.

NHC. 2008. Fraser River Hydraulic Model Update. Report prepared by Northwest Hydraulic Consultants for the BC Ministry of Environment.

NHC, and Triton. 2004. Roberts Bank Container Expansion Coastal Geomorphology Study. Prepared by Northwest Hydraulic Consultants Ltd. and Triton Consultants Ltd. for Vancouver Port Authority.

PMV. 2013. Roberts Bank Terminal 2 Project Description. Prepared by Port Metro Vancouver for The Canadian Environmental Assessment Agency and The BC Environmental Assessment Office.

Precision Identification. 2008. VFPA T2 Baseline Monitoring Report. Eelgrass Habitat Assessment. Vancouver Fraser Port Authority, Vancouver BC.

Sinclair, F. N. 1961. A History of the Sumas Drainage, Dyking and Development District. Chilliwack Historical Society, Chilliwack, BC.

Stevens, A. W., and J. R. Lacy. 2011. The influence of wave energy and sediment transport on seagrass distribution. Estuaries and Coasts 35:92–108.

Stewart, I., and B. Tassone. 1989. The Fraser River Delta: A Review of Historic Sounding Charts. Environment Canada Conservation & Protection.

Swinbanks, D. D. 1979. Environmental Factors Controlling Floral Zonation and the Distribution of Burrowing and Tube-Dwelling Organisms on Fraser Delta Tidal Flats, British Columbia. PhD Thesis, University of British Columbia, Vancouver BC.

Tarbotton, M., and P. G. Harrison. 1996. A Review of the Recent Physical and Biological development of the Southern Roberts Bank Seagrass System 1950-1994. Report prepared by Triton Consultants Ltd. and Paul Harrison for Roberts Bank Environmental Review Committee, Vancouver, B.C.

Teeter, A. M., B. H. Johnson, C. Berger, G. Stelling, N. W. Scheffner, M. H. Garcia, and T. M. Parchure. 2001. Hydrodynamic and sediment transport modeling with emphasis on shallow-water, vegetated areas (lakes, reservoirs, estuaries and lagoons). Hydrobiologia 444:1–23.

Thomson, R. E. 1981. Oceanography of the Britsh Columbia Coast. Canadian special publication of Fisheries and Aquatic Sciences 56:25–41.

Thomson, R. E., B. D. Bornhold, and S. Mazzotti. 2008. An examination of the factors affecting relative and absolute sea level in Coastal British Columbia. Canadian Technical Report of Hydrography and Ocean Sciences.

TRE Canada. 2014. Erosion Study over Sturgeon Bank, West of Lulu Island using Historical Geo-referenced Spacebourne Radar imagery, Amplitude Image Analysis. Report prepared by TRE Canada Inc. for Port Metro Vancouver. Doc Ref.:JO14-3021-Rep1.1. Report authored by Vicky Chun-yi Hsiao and Jean Pascal Iannacone, approved by Giacomo Falorni., Vancouver BC.

USACE. 2002. Coastal morphodynamics. Engineering Manual, EM1110-2-1100 Part IV, US Army Corps of Engineers.

Warburg. 1922. Tides and Tidal Streams. Pages 45–69 *in*. Volume Part II - General Physical Oceanography. Department of Fisheries and Oceans. <http://www.dfo-mpo.gc.ca/Library/487-06.pdf>.

Water Survey of Canada. 1970. Hydrometric and Sediment Survey, Lower Fraser River, Progress Report, 1965-68. Inland Waters Branch, Department of Energy, Mines and Resources, Ottawa.

Williams, H. F. L., and T. S. Hamilton. 1995. Sedimentary Dynamics of an Eroding Tidal Marsh Derived from Stratigraphic Records of 137Cs Fallout, Fraser Delta, British Columbia, Canada. Journal of Coastal Research 11:1145–1156.

WorleyParsons. 2012. Biofilm Desktop Study. Worley Parsons, North Vancouver.

WorleyParsons. 2013. Basis of Design, Roberts Bank Terminal 2 (RBT2) - Environmental Impact Statement (EIS) Phase. Worley Parsons, Burnaby, BC.

WorleyParsons. 2015. Roberts Bank Terminal 2 Technical Data Report: Biofilm Community at Roberts Bank - Analyses to Support Hyperspectral Mapping. Prepared for Port Metro Vancouver. Available at: http://www.robertsbankterminal2.com/, Burnaby, BC.

APPENDIX A

DATA SOURCES

TABLE OF CONTENTS

LIST OF TABLES

1 AVAILABLE DATA

1.1 PROJECT BACKGROUND

The Roberts Bank Terminal 2 Project (RBT2) is a proposed new multi-berth container terminal which would provide 2.4 million TEUs (twenty-foot equivalent unit containers) of additional container shipping capacity. The project is part of the Container Capacity Improvement Program (CCIP), Port Metro Vancouver's long-term strategy to deliver projects to meet anticipated growth and demand for container capacity until 2030.

Port Metro Vancouver retained Hemmera to undertake environmental studies related to the Project. This appendix forms part of a technical report that describes the results of the Coastal Geomorphology Study effects assessment undertaken by Northwest Hydraulic Consultants Ltd. (NHC).

Data describing the historical and contemporary conditions are available from a variety of sources, which are described in this appendix. The purpose of including this description is to provide the reader with a) a comprehensive catalogue of available data, and b) an appreciation of the scope of effort that was undertaken to include as much information as possible in this study. NHC also conducted extensive field data collection as part of this study, which is described in **Appendix C** of this report.

1.2 DATA SOURCES

Existing data was collected from a variety of sources including:

- Recent and historic bathymetric surveys, including charts;
- Recent LiDAR surveys;
- Recent and historic airphotos and orthophotos;
- Physical data collected by government agencies;
- Published academic papers and reports; and
- Published and unpublished consultants reports and scientific studies.

In addition, data on several physical parameters were collected by NHC during field visits in 2012 and 2013. The field data collection program is described in detail in **Appendix C**.

1.3 BATHYMETRY

Bathymetric charts are available from as early as 1860 from sources that include the Admiralty of the United Kingdom. However, these cannot be relied upon for specific evidence about depths and planform at the time because the survey methods used were subject to inaccuracies and the level of artistic representation varied. In 1932, the Canadian Hydrographic Service (CHS) conducted the first reliable survey at Roberts Bank. They followed-up with another more reliable survey in 1967 (published in 1968) and the Vancouver Port Authority continued with two more surveys in 1982 and 2002 (**Table** 1). These datasets vary in their extent of coverage, with the 1967 and 2002 being most comprehensive. Bathymetric charts have historically been developed for navigation purposes so regions of the tidal flats, which lie outside the normal shipping channels, are not surveyed at the same level of detail.

The 2002 bathymetric chart was prepared by McElhanney Consulting Services and was reduced to Tide Datum, defined as 6.465 m below DBM81 (CHS). The area of coverage included portions of both the north and south sides of the Roberts Bank causeway. This data was compiled in digital format by Triton Consultants Ltd. and was combined with other published CHS charts to extend the coverage to the BC Ferries Terminal.

The 1982 dataset has very good coverage, although it is limited to the region adjacent to the dredge pit and dendritic channels. The 1967 dataset's coverage is much greater, extending across the tidal flats from the Canada-U.S. border to the mouth of the Fraser River main channel, and seaward beyond the delta front to the deep ocean. The 1968 dataset was compiled by the Canadian Hydrographic Service and the Marine Sciences Branch of the Department of Energy Mines and Resources and represents several surveys by the lead agency. The 1967 data was received in low quality paper format and contains discrepancies on the units used to express elevation. The dataset needed significantly more interpretation, and contained more uncertainty than the newer datasets. Elevations on the tidal flats were considered to be accurate to within ±0.25 metres.

More recently, bathymetric surveys of the Fraser River were conducted in 2004/2005 by Public Works and Government Services of Canada (PWGSC) for a hydraulic model study of the river. Soundings collected near the mouth of the Fraser River were of value to the Roberts Bank investigations. Terra Remote Sensing Inc. (TRSI) carried out a bathymetric survey in 2011 to coincide with a LiDAR survey. The inter-causeway area was surveyed by NHC (bathymetric and ground-based RTK survey) in 2007, 2010, and 2013, with particular detail at the dendritic channels and crest protection structure (Hemmera et al. 2008, 2012).

Table 1: Historical bathymetric surveys in the Roberts Bank and lower Fraser River area.

Date of Survey	Source	Published Chart Scale	Comments
1932	Canadian Hydrographic Service	Expressed as 40" latitude and longitude – converted to UTM NAD83 using GIS software	Clarke 1866 projection NAD27. Referenced to Sand Heads datum (8.5 ft below Geodetic)
1967	Canadian Hydrographic Service	1:30,000	Active Pass to Burrard Inlet. Sounding reduced to 5.857 m below "MN 19 1959".
1982	Vancouver Port Authority	1:1,000	Bathymetric Survey – Intertidal Channels near Crest Protection. Sounding reduced to sounding datum.
2002	Vancouver Port Authority	1:1,000	Sounding in metres, reduced to sounding datum.
2004	PWGSC	Digital dataset	Coverage from mouth of the Fraser River to New Westminster
2010	NHC	Digital dataset	Inter-causeway channels and crest protection structure
2011	TRSI	Digital dataset	Bathymetry and LiDAR of Roberts Bank

LiDAR (Light Detection and Ranging) refers to a remote sensing technology that is used to capture high resolution imagery. The first known LiDAR survey in the area was collected in 2001 and covers the intertidal portion of Roberts Bank from Point Roberts north to the Fraser River main arm (Hill et al. 2013); however, this dataset appears to suffer from post-processing issues between flight passes and shows elevation banding. Other surveys were conducted by TRSI for Fraser Basin Council in 2005 but these were limited to upland areas adjacent to the Fraser River. As noted, TRSI completed another LiDAR survey for WorleyParsons in 2011. The coverage extended from the tidal flats of Roberts Bank between Steveston Arm of the Fraser River and the Canada/USA border, and from the high water level (HWL) in the east to an approximate water depth of 20 m in the west, with a one-metre point spacing.

Triton Consultants previously built a numerical model for Roberts Bank based on data in Puget Sound, Strait of Georgia and Juan de Fuca Strait. The original sources of the data that form the model geometry are not well documented but trace to the year 2000 or earlier. Portions of the data correspond to the CHS Chart 3492 for Roberts Bank.

The 2011 LiDAR and bathymetric survey dataset was combined with data from Triton, the 2004/2005 Fraser data (PWGSC survey plus 2005 LiDAR), and the 2010 NHC survey to create a single

DEM with a variable grid. Point spacing is smaller (approximately 10 m) near the mouth of the Fraser River and on the tidal flats, and is greater in the Strait of Georgia and more distal areas.

1.4 FIELD PHOTOS

1.4.1 AIRPHOTOS

One of the most important sources of information for analysis of long-term changes at Roberts Bank is the record of historical airphotos. **Table 2** lists the airphotos that were available for use in this study. All of the photos listed, except for the June 5, 1948 photos (BC576 flight line), are overhead vertical photos with the majority at a scale of 1:20,000 or greater.

The earliest available photos date back to 1932 and the most recent to 2013; however, there is some variation in the quality of the photos, both in terms of photo clarity, and tidal emergence of the flats. Image quality is generally quite good, and it is excellent in the photos since 1959. Many of the photos were taken at a very low tide level, giving maximum exposure of the tidal flats. Unfortunately, in some of the years in the coverage history, the tide is above the 1 m contour, obscuring detail in the lower flats. These higher tide photo years include 1990 and 2004.

Photos were collected by NHC on the ground and from aircraft over the course of various Roberts Bank field investigations using a hand-held camera and are discussed in **Appendix C**.

Table 2: Airphotos available for the coastal geomorphology investigations.

Year	Date	Roll & Photo Number	Format	Scale or Resolution (m)	Agency	Coverage
1932	07-Sep-1932	A4527 22-25	BW	1:15,000	Fed	Intercauseway marsh to ferry causeway
	07-Sep-1932	A4527 26-30	BW	1:15,000	Fed	Canoe Passage to intercauseway marsh
1938	18-May-1938	A5936 36-41, 45-50, 65-69, 70-83	BW	1:10,000	Fed	Canoe Passage, Roberts Bank
	18-May-1938	A5938 9-11	BW	1:10,000	Fed	Canoe Passage, Roberts Bank
	06-Jun-1938	A5984 9-16	BW	1:12,000	Fed	Canoe Passage and westward
1948	27-Jun-1948	BC483 38-43	BW	1:10,000	BC	Fraser Valley Flood
	05-Jun-1948	BC575 49-54	BW	1:10,000	BC	Fraser Valley Flood
	05-Jun-1948	BC576 31-32	BW	1:10,000	BC	Roberts Bank - Oblique
	?	? 26-30	BW	1:10,000		Fraser Valley Flood
1949		BC725 112-119	BW		BC	Canoe Passage and westward
		BC726 5-10, 84-86, 97-98	BW		BC	Brunswick Point to Port causeway, Intercauseway marsh
		BC727 60-65	BW		BC	Intercauseway marsh
	06-Jun-1949	BC819 27-33, 63-70	BW	1:18,800	BC	Causeways to Canoe Passage
1950	01-Jun-1950	BC 1056 2-5	BW		BC	Westham Island, Fraser River, Delta facing SE
1954		BC1673 24-28, 34-36, 91-95	BW		BC	Canoe Passage (not the mouth) to Port causeway
		BC1674 2-6, 54	BW		BC	Westham Island, Canoe Passage, Brunwick Point
1959	18-Jun-1959	W624B 35913-35920	BW	1:20,000	PSC	Roberts Bank to Canoe Passage
	18-Jun-1959	W624A 35721-35725	BW	1:20,000	PSC	North Arm, Sturgeon Bank
		A16831 7-10, 14-17, 26-28	BW		Fed	Westham Island, Canoe Passage; Canoe Passage and westwards; Brunswick Point to ferry causeway; Intercauseway marsh to border
1960	28-Apr-1960	BC5011 63	BW	1:9,800	BC	BC Ferries Causeway
1961		PSC 61055-59			PSC	Mouth of Canoe Passage
1962	24-Jun-1962	W825 65732-65805	BW	1:12,500	PSC	Roberts Bank
1963	04-May-1963	BC5066 48-54	BW		BC	North bank of Canoe Passage to mouth and westwards; Westham Island marsh
	18-May-1963	BC5072 1-5, 169-173, 174-177	BW		BC	Brunswick Point, mouth of Canoe Passage and westwards, port causeway, intercauseway marsh, ferry causeway
	18-May-1963	BC5073 36-40	BW		BC	Ferry causeway to US border
1967	27-Apr-1967	W1157 15350-15362	BW	1:24,000	PSC	Roberts Bank
1969	01-Jul-1969	W1295 38513	BW	1:24,500	PSC	Both causeways
	01-Jul-1969	W1295 38515-38517	BW	1:24,500	PSC	Both causeways
		BC5317 3-5, 135, 137-139	BW		BC	Both causeways
1970		BC5371 106-110	BW		BC	Both causeways
1971		BC5431				Canoe Passage to Port causeway
1972					PSC	Westham Island tidal flats
1975	11-Jun-1975	A37170 39-40	Colour	1:20,000	Fed	Both causeways, Canoe Passage
1978	19-Jul-1978	PSC 1613 6, photos 99-102	BW	1:24,000		Canoe Passage
1979	08-Aug-1979	BCC227 62-70, 142-150	Colour	1:12,000	BC	Canoe Passage to south of ferry terminal; both causeways
1980				1:40,000		Mouth of Canoe Passage and westwards
1982			Colour IR			Roberts Bank; Strait of Georgia
1983		BR83076 L1-22-L1-28	Colour	1:5,000		Coal port and intercauseway
		BR83076 L2-57-L2-64	Colour	1:5,000		Coal port and intercauseway
1984		A26527 4-7, 50-55	BW		Fed	Roberts Bank
1989		A27396 256-260, 270-272	BW		Fed	Roberts Bank
1990	24-May-1990	SRS4317 1-23	BW	1:5,000	SRS	Intercauseway
1990	09-Jul-1990	SRS4352 1-19	Colour	1:20,000	SRS	Causeways to Canoe Passage
1991	27-Jun-1991	Line 1-5, Photos 1-61	Colour	1:5,000	G&A Ltd	Causeways, very low level
1992	03-Jul-1992	Line 1-6, Photos 1-71	Colour	1:5,000	G&A Ltd	Causeways, very low level
1994	08-Jul-1994	Line 1-3, Photos 4-71	Colour	1:5,000	G&A Ltd	Causeways, very low level
	05-Aug-1994	DAS94091 1-19	Colour	1:5,000	DAS/SRS	Causeways, very low level
1995	14-May-1995	SRS5458 17-25	Colour	1:30,000	SRS, TMC	Roberts Bank
2002	29-Apr-2002	SRS6558 127-141	Colour	1:20,000; 25 cm	SRS, FREMP	Roberts Bank
2004	21-Mar-2004	SRS6912 1-6	Colour	1:20,000	SRS	Causeways
	02-Apr-2004	SRS6912 103-111, 219-225, 233-235	Colour	1:20,000	SRS	Causeways to Canoe Passage; Main arm near mouth
2006	13-May-2006	Orthophoto	Colour	10 cm		Roberts Bank, south of Brunswick Point
2007	16-Jul-2007	Orthophoto	Colour	10 cm		Roberts Bank, south of Brunswick Point
2008	Jul-2008	Orthophoto	Colour	10 cm		Roberts Bank, south of Brunswick Point
2009	24-Jul-2009	Orthophoto	Colour	10 cm; 50 cm		Roberts Bank, south of Brunswick Point
2010	09-Jul-2010	Orthophoto	Colour	10 cm; 50 cm		Roberts Bank, south of Brunswick Point
2011	17-May to 19-May-2011	Orthophoto	Colour	15 cm		Tidal flats from just north of Cannery Channel (Fraser River) to US border
2011	29-Jul-2011	Orthophoto	Colour	10 cm; 50 cm		Roberts Bank, south of Brunswick Point
2012	2012	Orthophoto	Colour	10 cm; 50 cm		Roberts Bank, south of Brunswick Point
2013	2013	Orthophoto	Colour	10 cm; 50 cm		Tidal flats from just north of Cannery Channel (Fraser River) to US border

1.5 HYDRODYNAMIC DATA

1.5.1 WIND

For model input and validation purposes, batch data from several weather stations located in the Strait of Georgia and Juan de Fuca Strait were provided by Environment Canada upon request. Stations included Discovery Island, Nanaimo Airport, Pam Rocks, Point Atkinson, Race Rocks, Sand Heads, Vancouver International, Victoria Gonzales, and White Rock. Wind speed and wind direction collected on an hourly basis since station installation was made available. Environment Canada's wave buoy at Halibut Bank also provided hourly wind data at that location since 1992.

Wind data from in and around Puget Sound was also acquired. National Oceanic and Atmospheric Administration (NOAA) stations in this area include Cherry Point, New Dungeness, Port Angeles, Port Townsend, Sequim, Smith Island, and West Point. Hourly records of wind speed and wind direction were obtained for the period from January 2011 and December 2012.

A non-standard meteorological station is installed at the BC Ferries Tsawwassen terminal. Wind data from this station was made available to the study for the period 2010 to 2012 but analysis conducted by others indicated that there was bias and inaccuracy in the data caused by the location of the anemometer.

1.5.2 WATER LEVEL

Fisheries and Oceans Canada has several stations in the Strait of Georgia including at Point Atkinson, New Westminster, and Victoria. Hourly observed data was acquired for the period between January 2011 and December 2012. NOAA also operates a station at Neah Bay, at the entrance of Juan de Fuca Strait, from which water level data was obtained over the same time period.

Water level data at Hornby Island, Port Renfrew and Irvines Landing were also obtained from the Canadian Hydrographic Service (CHS) website for the period between September 2011 and July 2012.

1.5.3 TIDAL CURRENTS AND WAVES

Worley Parsons collected current and wave data at several locations within the study area in 2011, which is summarized in **Table 3**.

Table 3: Available current and wave data in the study area.

Data Type	Provider	Location	Instrument	Date Acquired
Currents	WorleyParsons	Tidal flat, NW of terminal	ADV	06-Jul-2011 to 14-Jul-2011
Currents and waves	WorleyParsons	Shelf slope near terminal	AWAC (16 m depth)	18-Jan-2011 to 07-Mar-2011
Currents and waves	WorleyParsons	Shelf slope near terminal	AWAC (16 m depth)	07-Jul-2011 to 04-Aug-2011
Waves	WorleyParsons	PMV #15474	TWR-2050	06-Mar-2011 to 25-May-2011
Currents	WorleyParsons	Close to Canoe passage	ADCP (5 m depth)	08-Jul-2011 to 22-Jul-2011
Discharge (flow transects)	WorleyParsons	George Massey Tunnel, Westham Island Bridge	ADCP (from boat)	07-Jul-2011 to 09-Jul-2011
Currents and waves	ASL Environmental	Shelf slope near terminal	AWAC & ADCP	08-Aug-2012 to 09-Sep-2012
Currents and waves	ASL Environmental	Shelf slope near terminal	AWAC & ADCP	17-Dec-2012 to 20-Feb-2013
Currents	VENUS	Westshore coal terminal	CODAR	01-Jan-2012 to 01-Jan-2013
Waves	Environment Canada	Halibut Bank, Strait of Georgia	Wave buoy	13-Mar-1992 to 30-Apr-2013
Currents	NOAA	New Dungeness, Strait of Juan de Fuca	3 m discus data buoy	Jan-2011 to Dec-2012

Current and wave data was also collected by ASL Environmental Sciences in 2012-2013 during two deployments of the Acoustic Wave and Current Profiler (AWAC) and Acoustic Doppler Current Profiler (ADCP) instruments (**Table** 3) as detailed in **Appendix C**. As the instruments measure similar parameters and were sited relatively close together (approximately 1200 m apart), in the area northwest of the Westshore terminals, only the AWAC dataset was selected for use in validating the model.

The University of Victoria's VENUS program (Victoria Experimental Network Under the Sea) monitored currents at a network of stations in the Strait of Georgia starting in 2010. Whereas many of these stations measured currents at depth, CODAR (Coastal RADAR) technology provided measurements of surface ocean current velocities at a distance using the Doppler shift of reflected radio waves. As one of two VENUS CODAR stations, the station located at the Westshore Coal Terminal in Tsawwassen measured radial velocities of ocean currents in the Strait of Georgia in the study area. NHC obtained hourly data for the period between January 2012 and December 2012.

NHC also obtained wave data from Environment Canada's wave buoy at Halibut Bank in the Strait of Georgia. Farther afield in the Strait of Juan de Fuca, a NOAA station at New Dungeness provided current data.

1.5.4 SALINITY

As part of the wave and current monitoring using the AWAC and the ADCP, ASL Environmental also measured salinity at depth over time. Measurements were collected every three seconds during the summer and winter deployments in 2012-2013.

NHC collected salinity profiles on the tidal flats over selected tidal cycles as well as measurements at a fixed point in Canoe Passage every 15 minutes from May 2012 to September 2013. A more detailed discussion of this data collection program is provided in **Appendix C**.

Environment Canada operates a water quality buoy in the Fraser River upstream of Deas Island. Whereas a range of physical parameters are measured there, including water velocity, current direction and turbidity, specific conductivity was used to provide a record of the salinity fluctuations further up the Fraser River. Hourly data was available from April 2012 onwards.

1.5.5 TURBIDITY

WorleyParsons carried out short-term turbidity monitoring for the study in 2011. An OBS sensor (in conjunction with water level and temperature sensors) was deployed on the lower Fraser River, just upstream of the Massey Tunnel from July 6th to August 11th. The data, collected at 10-minute intervals in NTU (Nephelometric Turbidity Unit), was provided to NHC. For a shorter period between July 6th and July 14th, an OBS turbidity sensor was deployed on the Roberts Bank tidal flats (49^{o} 02.244' N, 123^{o} 11.299' W). The sensor was calibrated with bed sediment collected at Roberts Bank, and the readings converted from units of NTU to mg/L.

NHC collected turbidity profiles on the tidal flats over selected tidal cycles as well as measurements at a fixed point in Canoe Passage every 15 minutes from May 2012 to September 2013. A more detailed discussion of this data collection program is provided in **Appendix C**.

1.6 SEDIMENT PROPERTIES

Information on grain size was derived mainly from two published sources: Luternauer (1976) and McLaren and Ren (1995). More recently, four field programs provided additional data.

The dataset from Luternauer consisted of over 600 samples collected in 1975 during the pre-freshet winter season and the post-freshet summer season. Unfortunately, the complete dataset has been lost (Hill 2013), and only a subset of the data is accessible via the published manuscripts. The data from McLaren and Ren consisted of 1,484 surface samples collected between February 9th and April 7th, 1993 across the delta and in the distributaries of the Fraser River.

More recently, Hemmera collected 442 samples between April 19th and September 25th, 2012. They were collected around the proposed Project footprint and across Roberts Bank and Sturgeon Bank. Archipelago also collected 37 samples in the summer of 2012 at or near the delta foreslope as part of beach spawn and trawl surveys. In 2013, Hemmera collected an additional 344 samples near the project area (McPhie 2013). An ROV survey collected an additional 30 samples from the subtidal environment in the summer of that year. Between April and August 2013, NHC collected samples from nine (9) sediment cores and two (2) soil pits in the upper tidal flats – north of the causeway and in the inter-causeway area – and made qualitative and quantitative assessments of the sediment composition. Dating analysis was also carried out on the NHC samples, and further information on the data collection program can be found in **Appendix C**.

WorleyParsons collected two sets of sediment samples on the tidal flats in 2011: samples were collected at six (6) locations north of the Project site in March and at 14 locations in July and August. Grain size analysis (hydrometer) results were provided to NHC.

1.7 HABITAT DATA

Hemmera provided habitat mapping in August 2011 based on FREMP 2005/6 Habitat Inventory and Precision Identification eelgrass mapping.

In April 2013, WorleyParsons provided classification maps of various species' habitat interpreted from hyperspectral imagery, including biofilm habitat shapefiles. Habitat extents of sea pens (shapefile format) and supplementary reports were made available by Hemmera in the same month.

2 REFERENCES

Hemmera, NHC, and Precision. 2008. Deltaport Third Berth Adaptive Management Strategy 2007 Annual Report. Report prepared by Hemmera Envirochem Inc., Northwest Hydraulics Consultants and Precision Identification for Port Metro Vancouver, Vancouver, BC.

Hemmera, NHC, and Precision. 2012. Deltaport Third Berth Adaptive Management Strategy 2010 Annual Report. Report prepared by Hemmera Envirochem Inc., Northwest Hydraulics Consultants and Precision Identification for Port Metro Vancouver, Vancouver, BC.

Hill, P. R., R. W. Butler, R. W. Elner, C. Houser, M. L. Kirwan, A. Lambert, D. G. Lintern, S. Mazzotti, A. Shaw, T. Sutherland, S. Morrison, S. Petersen, and S. Solomon. 2013. Impacts of sea level rise on Roberts Bank (Fraser Delta, British Columbia). Geological Survey of Canada.

Hill, P. R. 2013. RE: Luternauer 1976 sediment dataset.

Luternauer, J. L. 1976. Fraser Delta Sedimentation, Vancouver, British Columbia. Report of Activities, Part A, Geological Survey of Canada. <ftp://ftp2.cits.rncan.gc.ca/pub/geott/ess_pubs/119/119844/pa_76_1a.pdf>.

McLaren, P., and P. Ren. 1995. Sediment Transport and Its Environmental Implications in the Lower Fraser River and Fraser Delta. Environment Canada.

McPhie, R. 2013. Re: D50 (and D16, D84) request.

APPENDIX B

MODEL DEVELOPMENT

TABLE OF CONTENTS

LIST OF TABLES

LIST OF FIGURES

1 INTRODUCTION

The Roberts Bank Terminal 2 Project (the Project) is a proposed new multi-berth container terminal which would provide additional container shipping capacity. The project is part of the Container Capacity Improvement Program (CCIP), Port Metro Vancouver's long-term strategy to deliver projects to meet anticipated growth and demand for container capacity until 2030.

Port Metro Vancouver retained Hemmera to undertake environmental studies related to the Project. This appendix forms part of a technical report that describes the results of the Coastal Geomorphology Study effects assessment undertaken by Northwest Hydraulic Consultants Ltd. (NHC).

Three methods were used to assess the physical response of Roberts Bank to the proposed development:

1 Interpretive geomorphic studies using historical data, site observations and measurements;

2 Analytical methods; and

3 Numerical modelling of tidal currents, waves and sediment transport.

This report describes the development of the numerical models utilized for the effects assessment that is part of the Coastal Geomorphology Study.

2 NUMERICAL MODELS: THE TELEMAC-MASCARET SYSTEM

The potential effects of the Project on tidal currents (hydrodynamics), wave climate and local seabed scour and deposition (morphodynamics) were investigated using the TELEMAC-MASCARET modelling system (TELEMAC SYSTEM). TELEMAC SYSTEM is an integrated suite of finite element (FE) computer programs initially developed by the Laboratoire National d'Hydraulique et Environnement (LNHE), which is part of the research and development (R&D) group of Électricité de France. TELEMAC SYSTEM is a modelling tool recognized throughout the world, with over 4,000 users including HR Wallingford, BC Hydro, Hydro-Quebec and the Canadian Coast Guard. In the case of the Canadian Coast Guard, TELEMAC-2D is used to predict water levels and current speeds and patterns in the lower Fraser River. The model output is published online on a weekly basis and available to river pilots, Port Metro Vancouver, and shipping companies to assist them in determining maximum draft and the best sailing times[1]. Due to its origin, the TELEMAC SYSTEM is used by most French design offices as well as French state organizations. In addition, it is used by a

[1] TELEMAC is used by the Canadian Coast Guard to forecast available water depths for vessels navigating the Fraser River South Arm Channel (see http://www2.pac.dfo-mpo.gc.ca/ for more details).

large number of universities, engineering schools and research centres including Federal Waterways Engineering and Research Institute in Germany.

The various TELEMAC SYSTEM modules use high-capacity algorithms based on the FE method. Space is discretized in the form of an unstructured grid of triangular elements, which means that it can be refined in areas of special interest. This approach avoids the need for systematic use of embedded models, as is the case with the finite-difference method. All TELEMAC SYSTEM modules were developed in accordance with the quality assurance procedures followed in Electricité de France's Studies and Research Division.

Three TELEMAC models were applied to compute the physical processes of tidal currents (TELEMAC-3D), wind-generated waves (TOMAWAC), and sediment transport (SISYPHE). Brief descriptions of these modules are provided below.

2.1 TELEMAC-3D – HYDRODYNAMIC MODEL

TELEMAC-3D is a three-dimensional (3D) model that solves the Reynolds-Averaged Navier-Stokes (RANS) equations in unstructured meshes obtained by superimposition of two-dimensional (2D) meshes of triangles. Its main outputs, obtained at each point in the resolution mesh in 3D, are velocity in all three directions and the concentrations of transported quantities. TELEMAC-3D's prominent applications can be found in free surface flow, in both seas and rivers, and can take the following processes into account:

- Influence of temperature and/or salinity on density;
- Bottom friction;
- Influence of the Coriolis force;
- Influence of weather elements: air pressure and wind;
- Consideration of the thermal exchanges with the atmosphere;
- Sources and sinks for fluid moment within the flow domain;
- Dry areas in the computational domain: tidal flats; and
- Current drift and diffusion of a tracer, with generation or disappearance terms.

When drying occurs, the water depth falls to zero and the planes collapse to a zero inter-layer spacing. Finite-volume style numerical techniques are used to ensure that both water and a tracer can be well-conserved in the presence of drying and subsequent re-wetting.

TELEMAC-3D was written primarily to solve the shallow water equations in 3D format, but an option is also available to solve the governing equations including dynamic pressure thereby allowing shorter waves than those in a shallow water context (where wavelengths are required to be at least twenty times the water depth).

2.2 TOMAWAC – SPECTRAL WAVE MODEL

TOMAWAC is a third generation spectral wave model that simulates wave propagation in the coastal zone based on solving the wave action density balance equation. By means of a FE type method, TOMAWAC solves a simplified equation for the spectro-angular density of wave action. The model can take into account the following physical phenomena:

- Wind-generated waves;
- Refraction on the bottom;
- Refraction by currents;
- Dissipation through bathymetric wave breaking; and
- Dissipation through counter-current wave breaking.

At each point of the computational mesh, TOMAWAC calculates the following information:

- Significant wave height;
- Mean wave frequency;
- Mean wave direction;
- Peak wave frequency;
- Wave-induced currents; and
- Radiation stresses.

2.3 SISYPHE – Sediment Transport Model

SISYPHE is the sediment transport and bed evolution module of the TELEMAC SYSTEM. SISYPHE can be used to model complex morphodynamic processes in diverse environments, such as coastal, rivers, lakes and estuaries, for different flow rates, sediment size classes and sediment transport modes. In SISYPHE, sediment transport processes are grouped as bed load, suspended load or total load, with an extensive library of bed load transport relations. SISYPHE is applicable to non-cohesive sediments that can be uniform (single-sized) or non-uniform (multiple-sized), cohesive sediments (multi-layer consolidation models), as well as sand-mud mixtures.

A number of physically-based processes are incorporated into SISYPHE, such as the influence of secondary currents to precisely capture the complex flow field induced by channel curvature, the effect of bed slope associated with the influence of gravity, bed roughness predictors, and areas of non-erodible bed, among others.

For currents only, SISYPHE can be tightly coupled to the depth-averaged shallow water module, TELEMAC-2D, or to the three-dimensional Reynolds-averaged Navier-Stokes module, TELEMAC-3D. In order to account for the effect of waves or combined waves and currents, SISYPHE can be internally coupled to the wave module TOMAWAC.

2.4 Model Framework

For this study, TELEMAC-3D, TOMAWAC and SISYPHE are internally coupled to simulate tidal currents, wave climate and local bed scour and deposition. The current field is first simulated by the hydrodynamic model TELEMAC-3D. TELEMAC-3D then transfers the values of current velocities and water depths to the wave model, TOMAWAC, to solve the wave action density conservation equation and returns the updated values of the wave driving forces acting on the current to TELEMAC-3D. The wave field from TOMAWAC and modified current field from TELEMAC-3D are then transferred to the morphodynamic model, SISYPHE, to compute scour and deposition of the seabed. The new bed elevation computed by SISYPHE is fed back into TELEMAC-3D to re-compute the flow hydrodynamics. The model coupling flow diagram is shown in **Figure 1**.

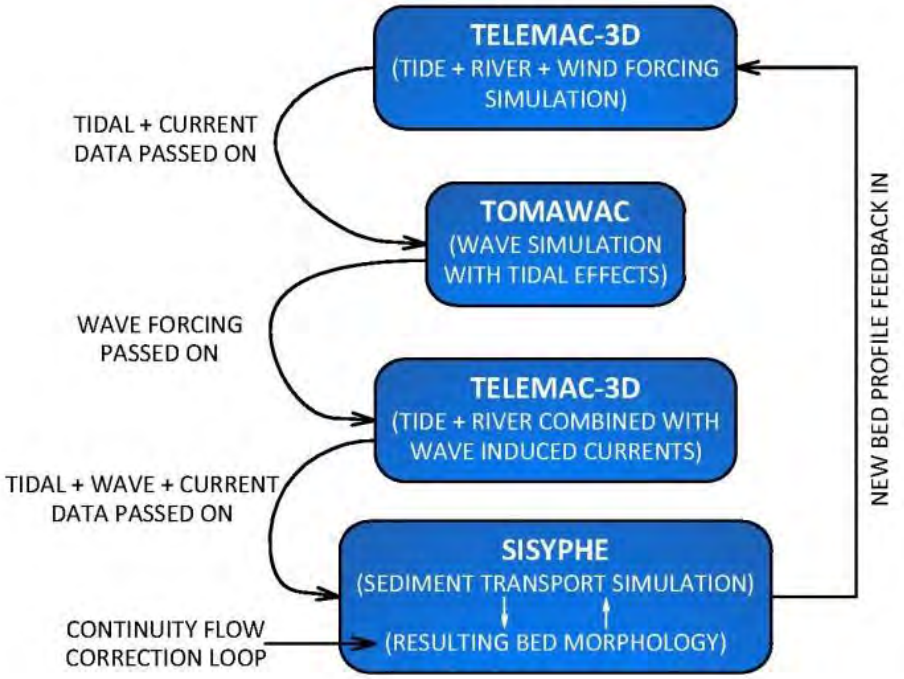

Figure 1. TELEMAC model coupling flow diagram.

3 STRAIT OF GEORGIA HYDRODYNAMIC-WAVE SEDIMENT TRANSPORT MODEL

3.1 MODEL GRID

TELEMAC-3D uses a computational mesh, as a mathematical representation of the physical environment under study. A mesh typically includes information on the shoreline geometry, the bathymetric features, and the bottom-type characteristics of the area involved. The TELEMAC-3D Strait of Georgia (SOG) Model FE mesh (**Figure 2**) extends from Ballenas Island (just south of Hornby Island) to Port Renfrew (west entrance of Juan de Fuca Strait) and south into Puget Sound. The model also includes the Fraser River up to km 36, upstream of New Westminster and downstream of the Skytrain Bridge. These extents were developed with due consideration given to the need to balance the size of the model, and hence computation time, with the need to provide accurate tide and wave conditions at the Project site.

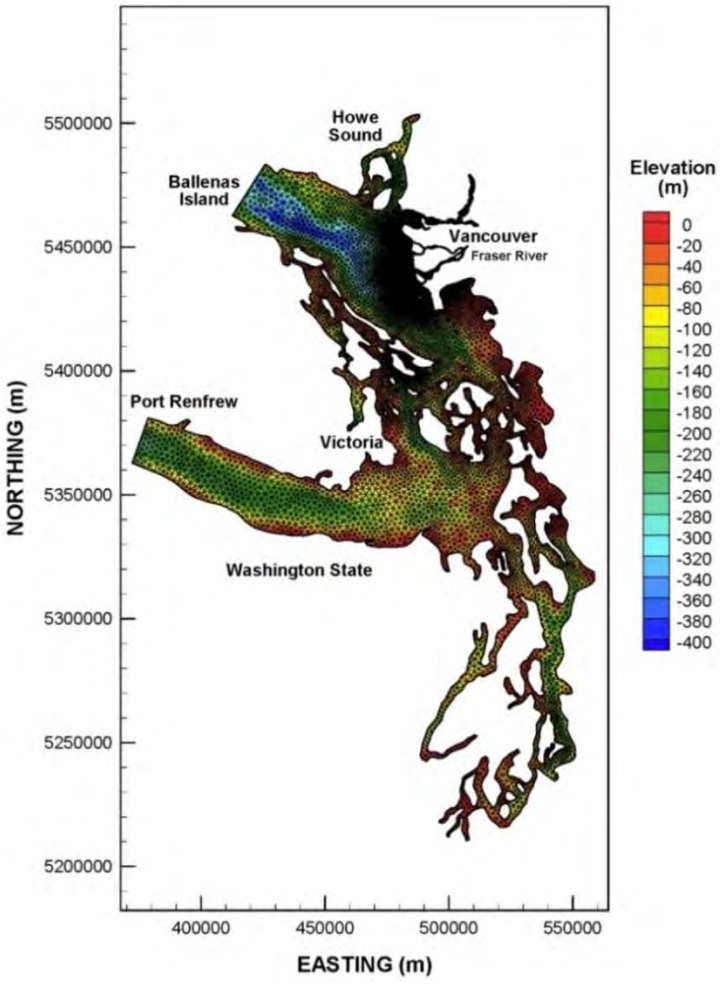

Figure 2: TELEMAC Strait of Georgia model mesh.

The model grid has on the order of 28,000 nodes, 51,000 elements and 11 vertical levels. The element lengths vary from approximately 3,000 m in the Strait of Georgia to about 25 m in the vicinity of the Project. The model bathymetry was derived using the following distinct datasets:

1. In the Port and surrounding areas, 2011 bathymetric surveys and LiDAR were used;

2. In the Fraser River, 2004 Public Works and Government Service Canada (PWGSC) bathymetric surveys and 2005 Fraser Basin Council LiDAR were used; and

3. In Puget Sound, the Strait of Georgia and Juan de Fuca Strait, the coarse dataset comprised of Canadian Hydrographic Service (CHS) bathymetry data used in the Deltaport Third Berth (DP3) project was used.

3.2 BOUNDARY CONDITIONS

The principle driving force for the TELEMAC-3D SOG model is water level fluctuations, primarily tidal, derived from water level variations at the open boundaries. The TELEMAC-3D SOG model consists of two open boundaries:

- Ballenas Island, just south of Hornby Island; and

- Port Renfrew, just west entrance of Juan de Fuca Strait.

Since no measured elevation data are available for specifying boundary conditions in this model domain, tidal levels at the open boundaries (Ballenas Island and Port Renfrew) were obtained using the WebTide Tidal Prediction model (Fisheries and Oceans 2005) based on Foreman (2000). The program uses eight tidal constituents including M2, S2, N2, K2, K1, O1, P1 and Q1[2].

Inflows to the Fraser River at New Westminster were computed using a hydraulic model of the Fraser River that uses the MIKE11 one-dimensional hydrodynamic software developed by the Danish Hydraulic Institute. NHC developed the Fraser River MIKE11 model for the Fraser Basin Council in 2006 (NHC 2006) and updated it for the BC Ministry of Environment two years later (NHC 2008).

The initial salinity field and salinity profiles along the open boundaries were estimated based on April, June and September 2012 water properties data collected by Department of Fisheries and Oceans Canada[3]. A salinity value of zero is prescribed for the Fraser River inflow.

[2] M2=principal lunar, S2=principal solar, N2=larger lunar elliptic, K2=luni-solar, K1=luni-solar diurnal, O1=principal lunar diurnal, P1=principal solar diurnal, Q1=larger lunar elliptic.
[3] http://www.pac.dfo-mpo.gc.ca/science/oceans/

3.3 WIND FORCING

Consideration of wind forcing is important as it causes both current and water level differences. To account for wind stress acting at the water surface, hourly wind data were obtained from five Meteorological Service of Canada (MSC) stations (Nanaimo Airport, Pam Rocks, Race Rocks, Sand Heads, and Victoria), Environment Canada's Halibut Bank wave buoy and four National Oceanic and Atmospheric Administration (NOAA) stations (Cherry Point, Port Townsend, Smith Island and West Point) and prescribed to the TELEMAC-3D SOG model. Corrections were applied to convert all wind measurements to 10 m above ground. The locations of these stations are shown in **Figure 3**.

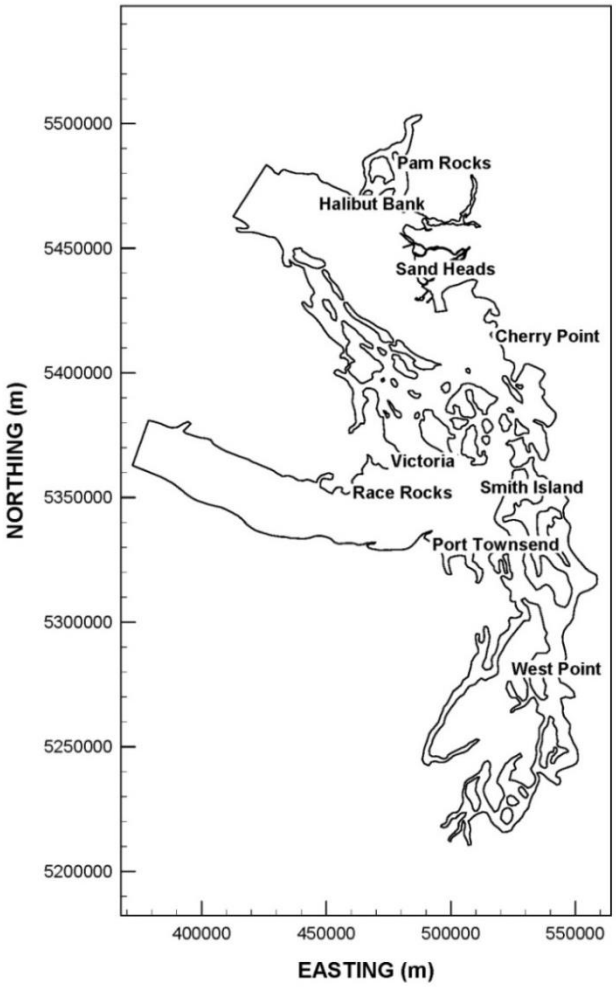

Figure 3: Location of wind stations in the model area.

3.4 WAVE FORCING

The TOMAWAC model is used to predict the input wave field for the study. The TOMAWAC SOG model is run with 25 exponentially-spaced frequencies ranging from 0.125 Hz to 1 Hz, in 12 evenly-spaced directions. TOMAWAC is implemented as a non-stationary model to replicate the growth and decay of storm waves. The same wind data used to provide wind forcing for the hydrodynamic model were used in TOMAWAC to generate waves based on the method described by Yan (1987). The whitecapping-induced dissipation is based on van der Westhuysen, et al. (2007).

3.5 SEDIMENT TRANSPORT

The prediction of the total load transport (bedload and suspended load) is calculated by means of the Bijker formula (Bijker 1968). The formula is an extension of a steady flow formula to account for the effect of wave-enhanced shear stress. The sediment incorporated in the simulation consists of a median grain size (D_{50}) of 175 μm, which characterizes the bed sediment on the tidal flats. It should be noted that sediment in the Canoe Passage channel are coarser (D_{50} = 350 μm), and so the bed in this region of the model was armoured to prevent excess sediment movement.

The time step of the SISYPHE model is the same as the time step of the TELEMAC-3D SOG model. This allows the hydrodynamic variables to be transferred to SISYPHE at each time step, which in turn, sends the updated bed elevation back to the hydrodynamic model.

3.6 OTHER PHYSICAL PARAMETERS

Other significant features of the TELEMAC-3D SOG model are as follows:

- Horizontal eddy viscosity is implemented using the Smagorinsky (1963) formulation, with coefficient of 1.0 m^2/s;
- Vertical eddy viscosity and diffusivity are implemented using standard Prandtl's (1925) model. The background vertical diffusion and viscosity were set to 1 x 10^{-6} m^2/s; and
- Spatially varying Nikuradse bottom friction coefficients ranging between 0.001 m, representing the open ocean floor, and 0.005 m, representing the vegetation, were used.

4 MODEL VALIDATION

The hydrodynamic-wave model results are compared against observed datasets, including:

- Water levels at Point Atkinson (Canadian Hydrographic Service 7795);
- Water levels and salinity at Canoe Passage (NHC Station UTM 489470 5435216);
- Currents and wave heights at Roberts Bank (AWAC Station (UTM 485729 5429608);
- Wave heights at Halibut Bank (Environment Canada Wave Buoy 46146); and
- Salinity profiles at Roberts Bank (NHC field program).

The locations of these stations are shown in **Figure 4**.

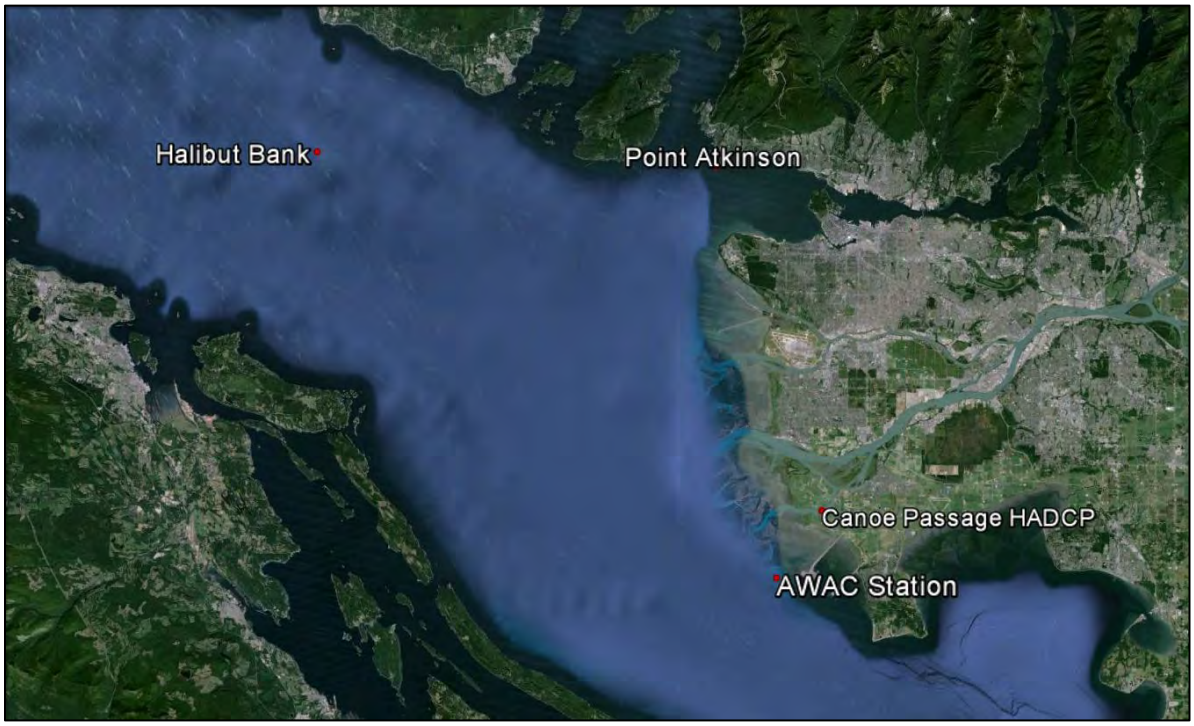

Figure 4: Map showing Point Atkinson, Canoe Passage HADCP, AWAC and Halibut Bank station locations.

Data from August 2012 were used to validate the model. This period was selected because data for all four physical parameters (water levels, waves, currents and salinities) were collected in this month.

4.1 WATER LEVELS AT POINT ATKINSON AND CANOE PASSAGE

Figure 5 and **Figure 6** show the modelled water level (blue line) and the observed water level (red circle) at the CHS Point Atkinson station and at NHC's Canoe Passage station respectively for August 2012. Elevations in the numerical model are referenced to Geodetic Datum (GD) because the model extends across numerous Chart Datum (CD) boundaries.

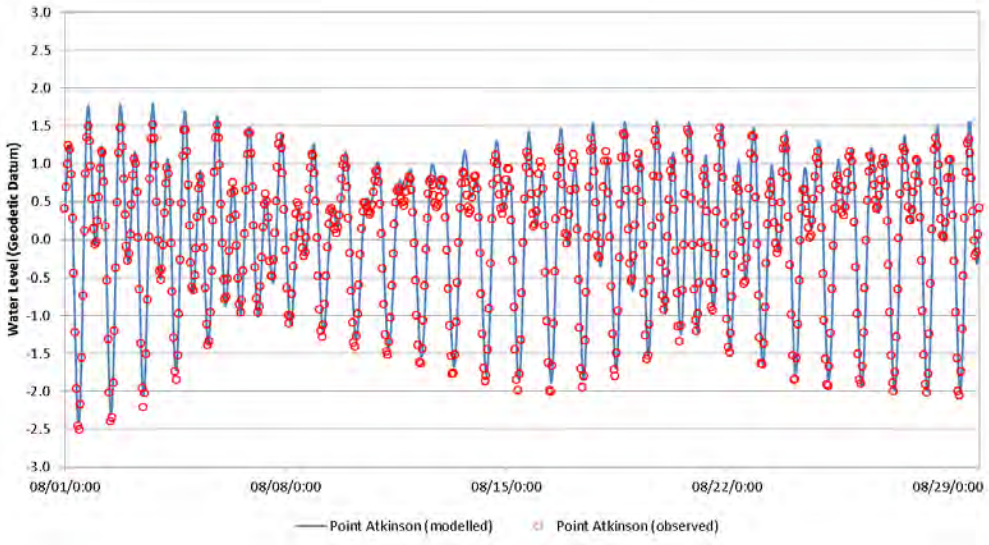

Figure 5: Modelled and observed water levels at Point Atkinson – August 2012.

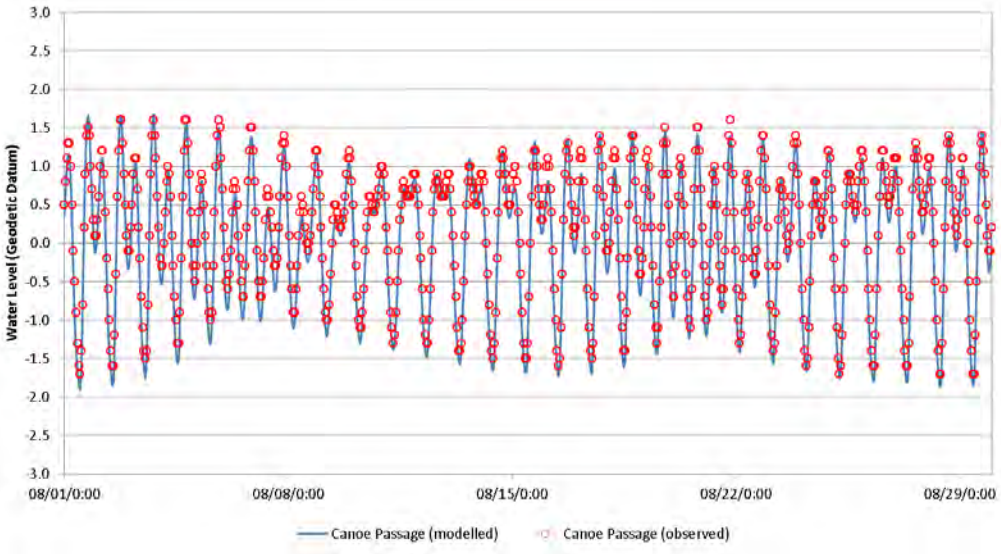

Figure 6: Modelled and observed water levels at Canoe Passage – August 2012.

The results show that the model replicates the observed tidal characteristics well. The model reproduces the tidal ranges between the spring and neap tidal cycle, and times of high and low waters. The RMSD (Root Mean Square Deviation) between hourly modelled and observed data are 0.30 m and 0.23 m for Point Atkinson and Canoe Passage respectively. These are within reasonable agreement given the large observed ranges of 4.0 m at Point Atkinson and 3.3 m at Canoe Passage over this period. The reason for the difference in elevations could be attributed to the approximations made in the formulation of the elevation boundary condition. The predicted tide elevation is solely a function of the moon and sun while the actual tide elevation includes the influence of the moon and sun as well as local atmospheric conditions, which can play a role at a given location and time.

4.2 FLOW AT CANOE PASSAGE STATION

To quantify the flow through Canoe Passage, a stage-discharge curve was developed based on ADCP and HADCP (horizontal ADCP) measurements collected at the Canoe Passage cross-section during various tidal stages and during a wide range of Fraser River flows. The location of the HADCP is shown in **Figure 7**.

Figure 7: Map showing the site of NHC's HADCP station in Canoe Passage.

Detailed information on NHC field data measurements can be found in **Appendix C** of the technical report. The flow derived from this stage-discharge curve is denoted as 'observed flow' and compared with the computed flow across Canoe Passage.

The modelled flow (blue line) and the 'observed flow' (red circle) across Canoe Passage are shown in **Figure 8**. Positive discharge values represents downstream outflow associated with an ebbing tide and negative discharges represents upstream flow associated with a rising tide.

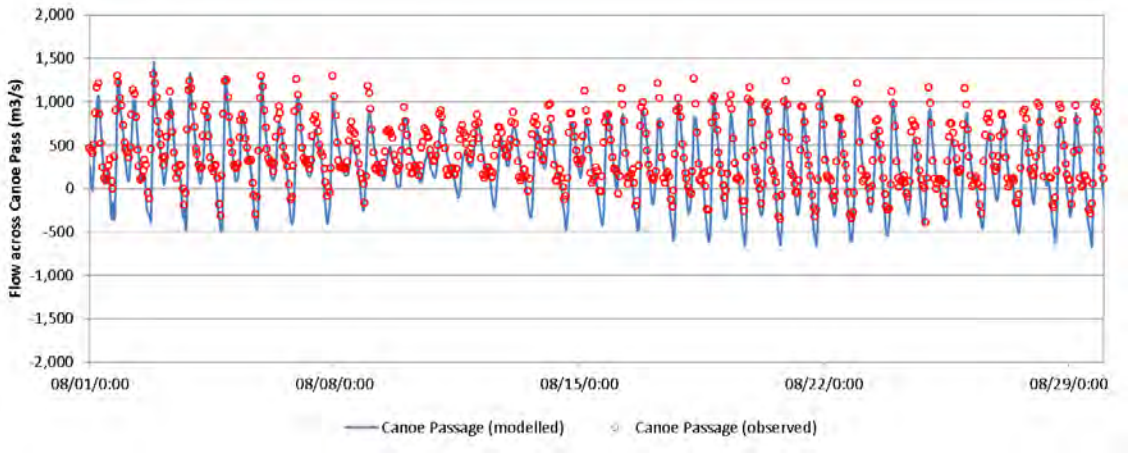

Figure 8: Modelled and observed flow at NHC's Canoe Passage station – August 2012.

The results show that the timing of the flow reversal and the flow range between maximum outflow and maximum inflow from the model were consistent with the observed data. The model generally overestimated the outflow and underestimated the inflow at Canoe Passage. The RMSD value between hourly modelled and observed flow over this period is 232 m^3/s. This difference is within the natural variability[4] of the system and uncertainties associated with the observed flow values that were interpolated from the stage-discharge curve. The stage-discharge curve was developed based on ADCP flow measurements. The mouth of the Canoe Passage is strongly influenced by ocean conditions and the water levels and flows vary rapidly as the tide rises and falls. Thus, ADCP flow measurements are sensitive to the time they were taken. Additional description on the development of the stage-discharge curve can be found in **Appendix C** of this report.

Other reasons that could contribute to the difference in flow rates include:

- The use of the flow predictions from the MIKE11 model as input to the TELEMAC model at the upstream boundary (New Westminster).

  The Fraser River MIKE11 model was developed for predicting flood levels on the Fraser River. Hence, the model was calibrated using peak flow conditions on the Fraser River. In August 2012, the freshwater Fraser River discharge at Hope ranged from 2,550 to 5,600 m^3/s, whereas flood conditions can result in discharges in excess of 10,000 m^3/s. Thus, the

[4] Natural variability – refers to the randomness observed in nature.

MIKE11 model may not perform as well for lower river discharges as observed in August 2012.

- Model bathymetry in Ladner Reach, Sea Reach and Canoe Passage.

  The bathymetry used in these secondary channels (**Figure 9**) was obtained from the PWGSC 2004 bathymetric survey. These secondary channels are considered areas of net deposition, and limited maintenance dredging activities have been conducted since the federal dredging program terminated in 1999. The infilling of these channels over the years, in particular where Ladner Reach, Sea Reach and Canoe Passage connect, could have an impact on the local channel hydraulics. The model results could be further improved by acquiring more recent bathymetry data in these secondary channels, assuming that conditions have not changed greatly since 2012.

Figure 9: Map showing Ladner Reach, Sea Reach and Canoe Passage reaches of the Fraser River.

4.3 CURRENTS

Current and wave data were measured using a 1,000 kHz Nortek AWAC profiler approximately 1.7 km west of the Roberts Bank terminals between August 8th and September 9th, 2012 by ASL Environmental Sciences (Birch and Mudge 2012). The location of the profiler is shown in **Figure 10**.

The instrument was deployed on bottom frame moorings situated at approximately -6.3 m Geodetic Datum (GD).

Figure 10: Location of the AWAC station at Roberts Bank.

Figure 11 and **Figure 12** show the hourly modelled current velocity (blue line) and measured velocity (red circle) at elevations 4.4 m and 2.4 m off the seabed respectively for August 2012. Overall there is a good agreement between the modelled and observed current magnitudes as well as the timing of flood and ebb tides.

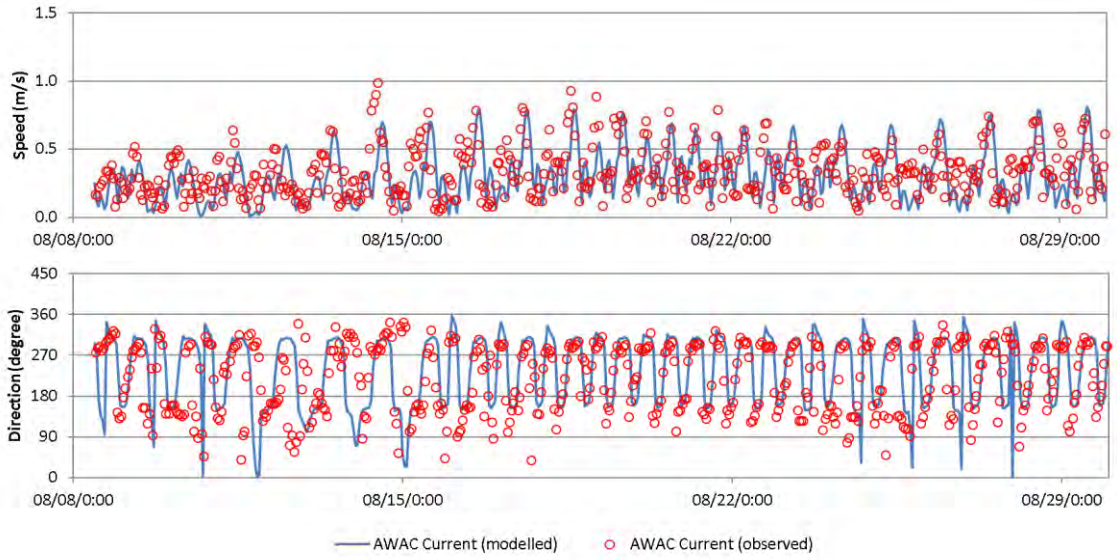

Figure 11: Modelled and observed current speed and direction at the AWAC station, 4.4 m off bottom.

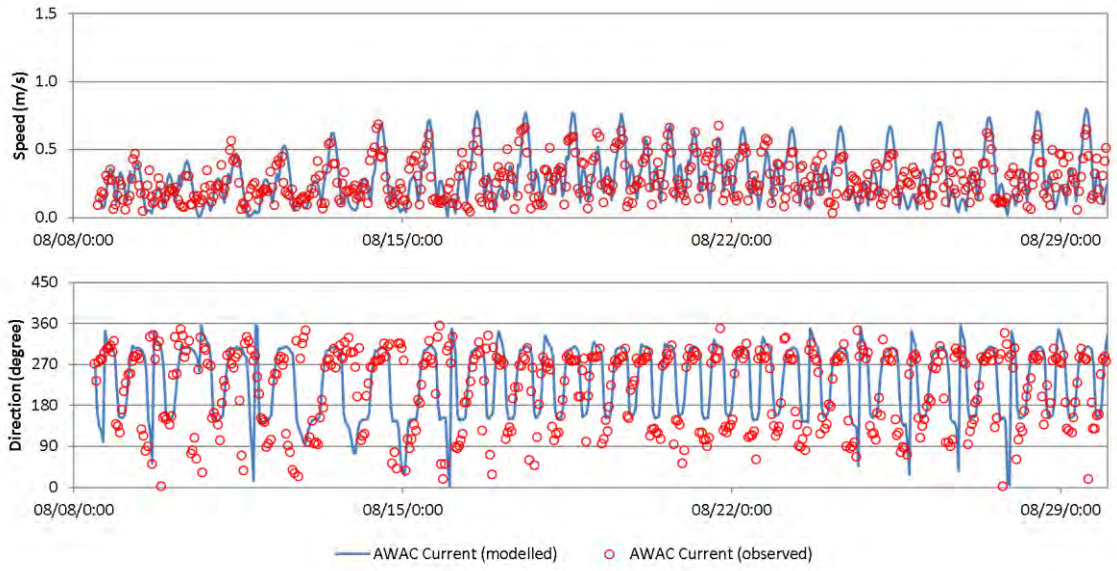

Figure 12: Modelled and observed current speed and direction at the AWAC station, 2.4 m off bottom.

4.4 WAVES

Figure 13 and **Figure 14** show the computed wave height (blue line) and measured wave height (red circle) at the AWAC station and at the Halibut Bank wave buoy respectively for August 2012.

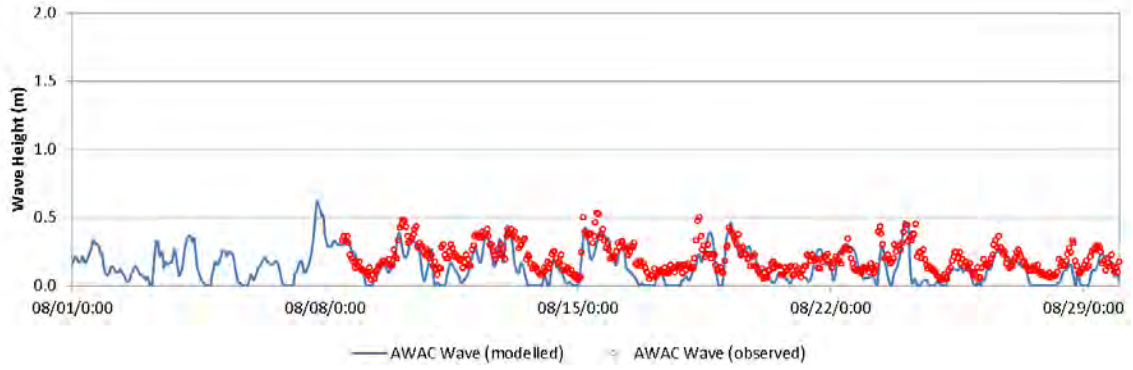

Figure 13: Modelled and observed wave height at the AWAC station.

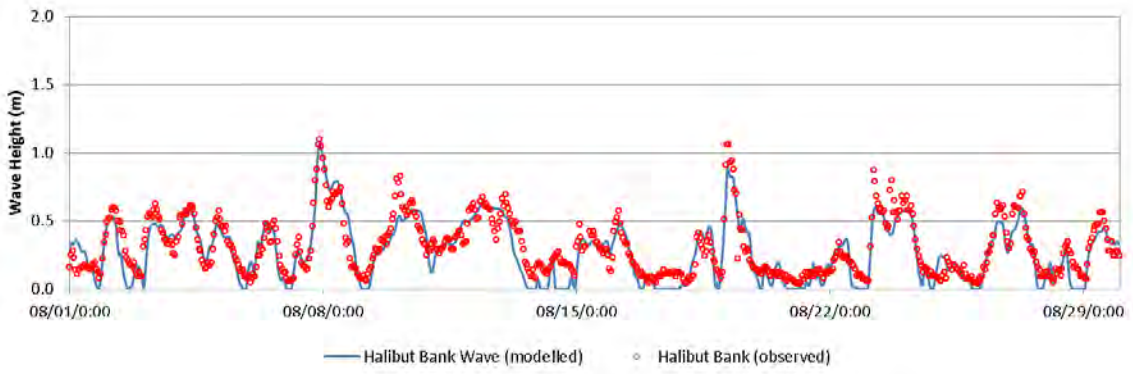

Figure 14: Modelled and observed wave height at the Halibut Bank station.

The results show that the numerical model reproduces the wave climate at both the AWAC station and at Halibut Bank well. The model has the tendency to underestimate waves during calmer weather conditions. Under these conditions, waves are typically less than 0.20 m and are not expected to have significant impacts to the coastal geomorphological process at Roberts Bank.

4.5 SALINITY

Figure 15 shows hourly modelled salinity (blue line) and the measured salinity (red circle) at NHC's Canoe Passage station for August 2012.

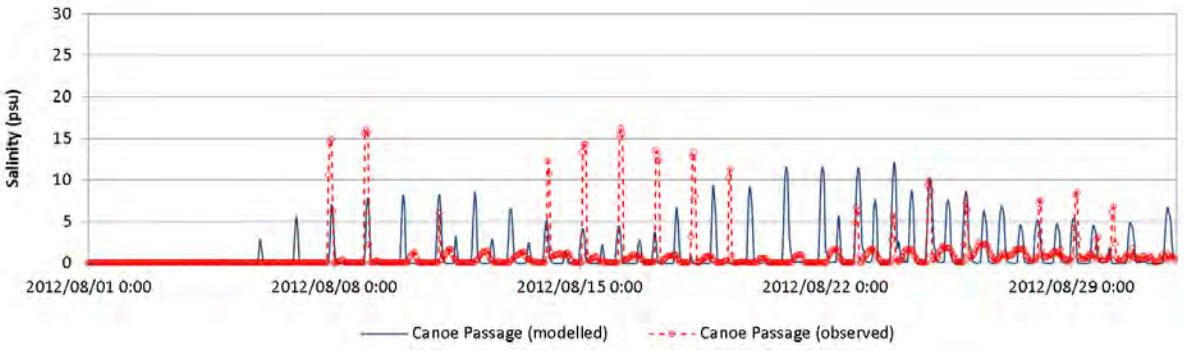

Figure 15: Modelled and observed salinity at NHC's Canoe Passage station – August 2012.

The results indicate that the model reproduces the timing of the salt intrusion well during spring tides with the large tidal currents. The model does not reproduce the salinity intrusion as well during the neap tides with relatively weak tidal currents. This is likely because of the use of the flow output from the MIKE11 model as input at the upstream end, and bathymetry data in the secondary channel as discussed in **Section 4.2**.

In addition to the salinity data collected at the Canoe Passage station, turbidity and salinity profile measurements were collected at selected locations (**Figure 16**) to capture the Fraser River plume distribution over the study area at various times between June and August, 2012. The timing of profile collection in August is summarised in **Table 1**.

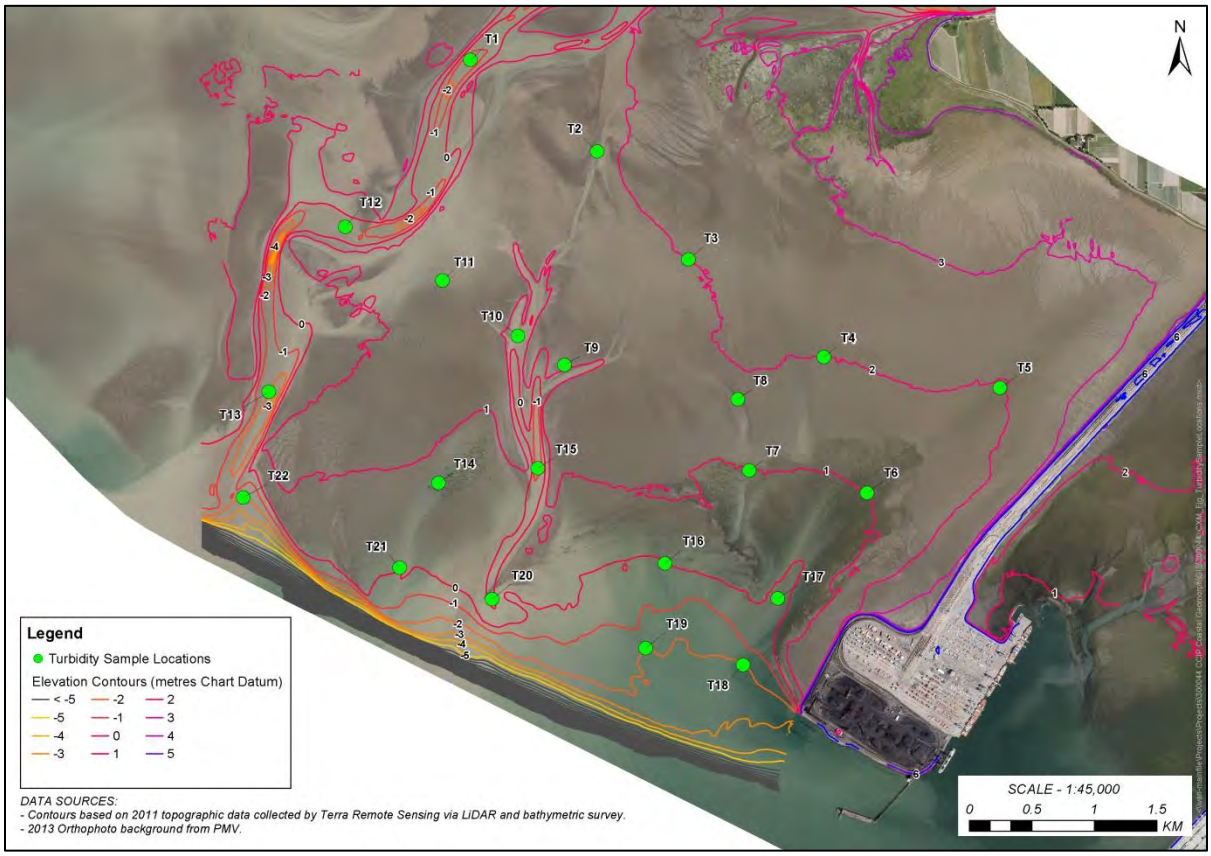

Figure 16: Turbidity and salinity sampling locations on Roberts Bank.

Table 1: Summary of turbidity and salinity profiles collected on the Roberts Bank tidal flats.

Date	Station Name	Measurement Start Time	Measurement End Time	Tide condition over measurement	Corresponding Fraser River Discharge at Hope
8/2/2012	T1, T5, T10, T16	4:39	6:06	High-slack, falling	5,460
8/29/2012	T1, T10, T16	5:42	6:25	Falling	2,778

Figure 17 and **Figure 18** show measured and observed salinity profiles at T1, T10 and T16 respectively for August 2nd. **Figure 19** shows the depth-averaged salinity distribution map from the numerical model for the corresponding time period. The black contour lines shown in the figure represents elevation in metres CD.

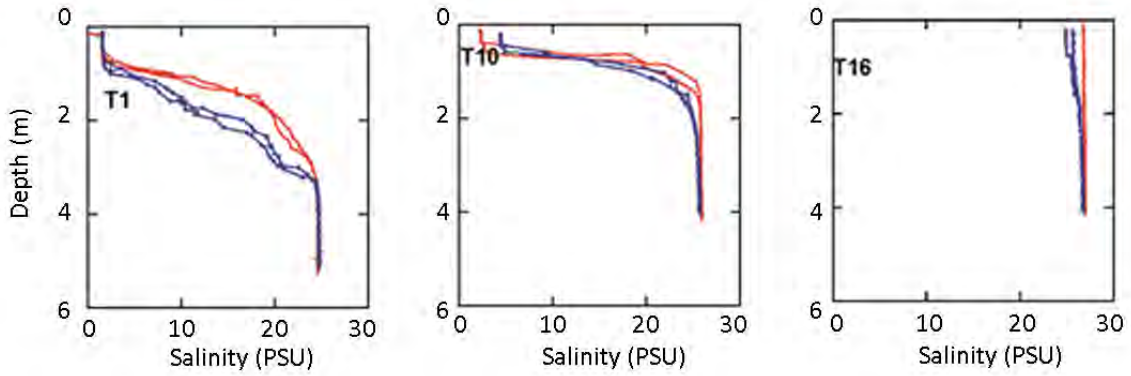

Figure 17: Observed salinity profiles at locations T1, T10, and T16 – August 2nd, 2012 5:00 am.

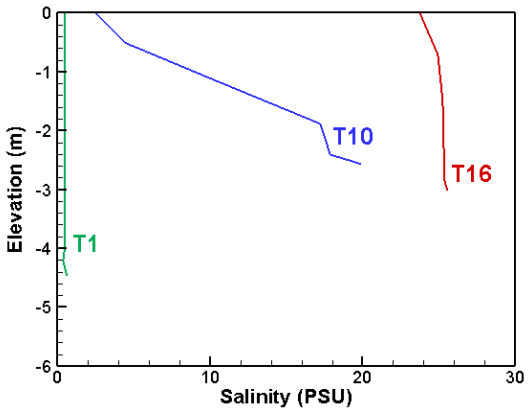

Figure 18: Modelled salinity profiles at locations T1, T10, and T16 – August 2nd, 2012 5:00 am.

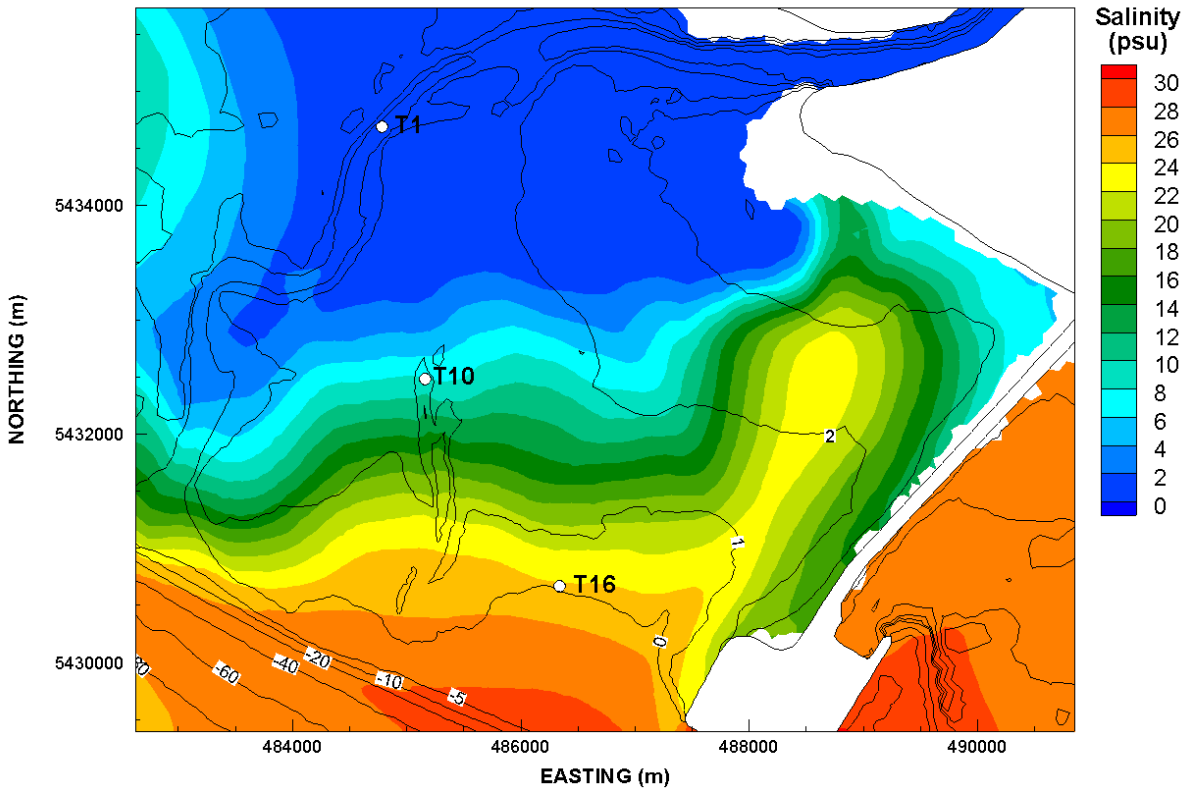

Figure 19: Modelled salinity map – August 2nd, 2012 5:00 am.

Figure 20 and **Figure 21** show measured and observed salinity profiles respectively at T1, T10 and T16 for August 29th. **Figure 22** shows the corresponding depth-averaged salinity distribution map for this time. The black contour lines shown in the figure represent elevation in metres CD.

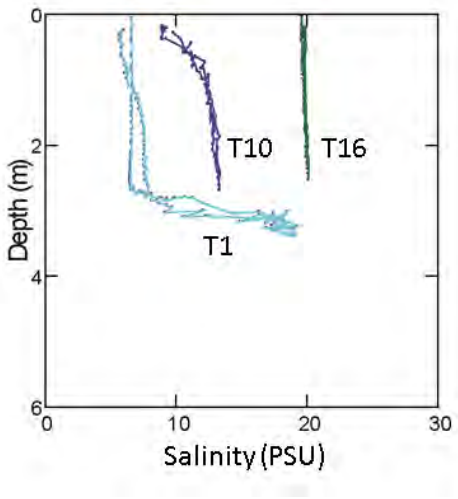

Figure 20: Observed salinity profiles – August 29th, 2012 6:00 am.

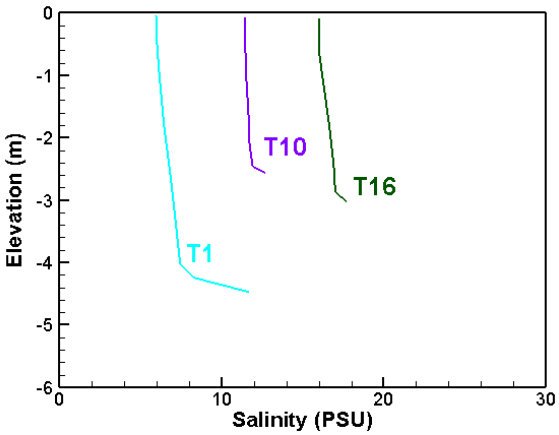

Figure 21: Modelled salinity profiles – August 29th, 2012 6:00 am.

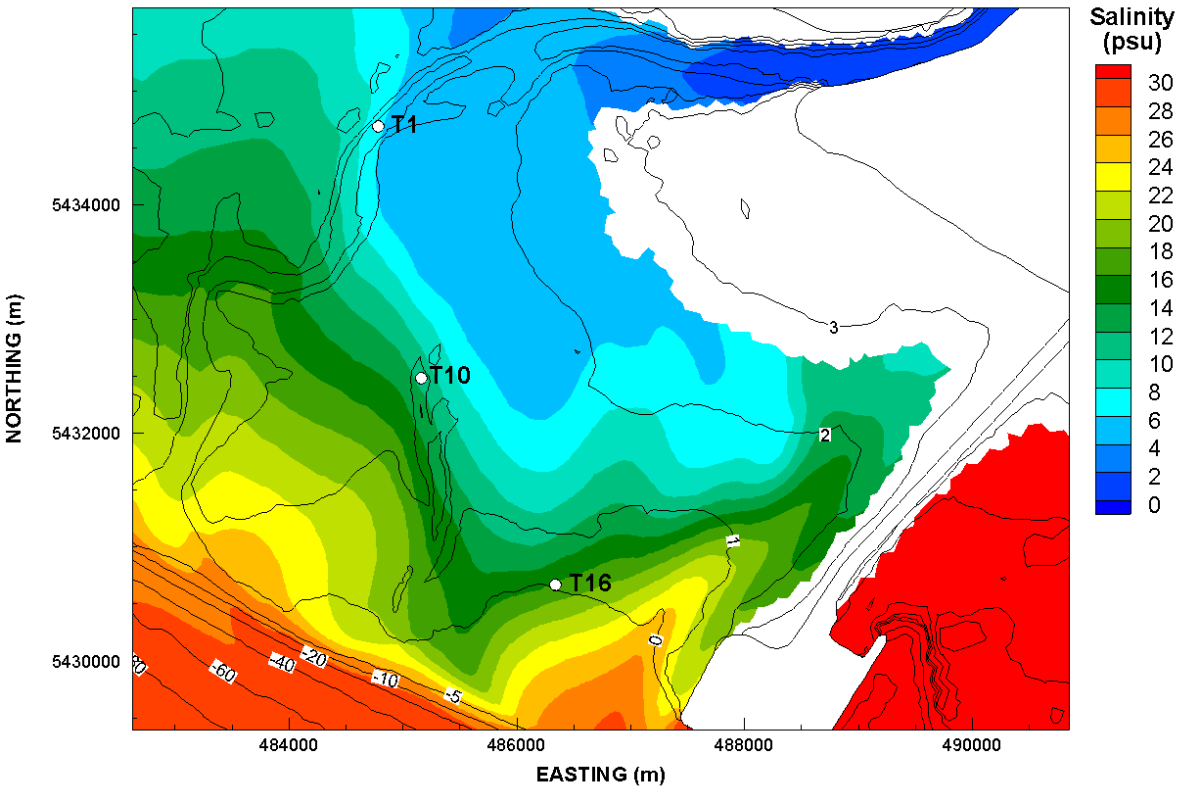

Figure 22: Modelled salinity map – August 29th, 2012 6:00 am.

The results show that the model predicted more fresh water input from the Fraser River during the high-slack tide condition. However, the model is able to capture the spatial distribution of the Fraser River plume well during both the high-slack tide and falling tide conditions. Thus, the model can be used to assess the relative changes on the salinity distribution expected from the Project.

A notable source of uncertainty is the limited availability of salinity data at the model's open boundaries (Port Renfrew and Hornby Island). The initial salinity field and salinity profiles along the open boundaries were estimated based on April, June and September 2012 water properties data collected by Department of Fisheries and Oceans Canada. The model results can be improved if additional field salinity profiles at Port Renfrew and Hornby Island were available as inputs; however, to the best of our knowledge, data were only collected during the months stated above.

4.6 MORPHODYNAMICS

Hydrodynamic-wave and sediment transport simulation were conducted using the 2012 winter season (October to December) as a reference period that was repeated to create a longer-term simulation. **Figure 23** shows the predicted deposition and erosion in the area within the expected

zone of influence from the Project after 1,440 simulated model days. The blue shading indicates regions of scour and yellow to red shadings represent regions of deposition.

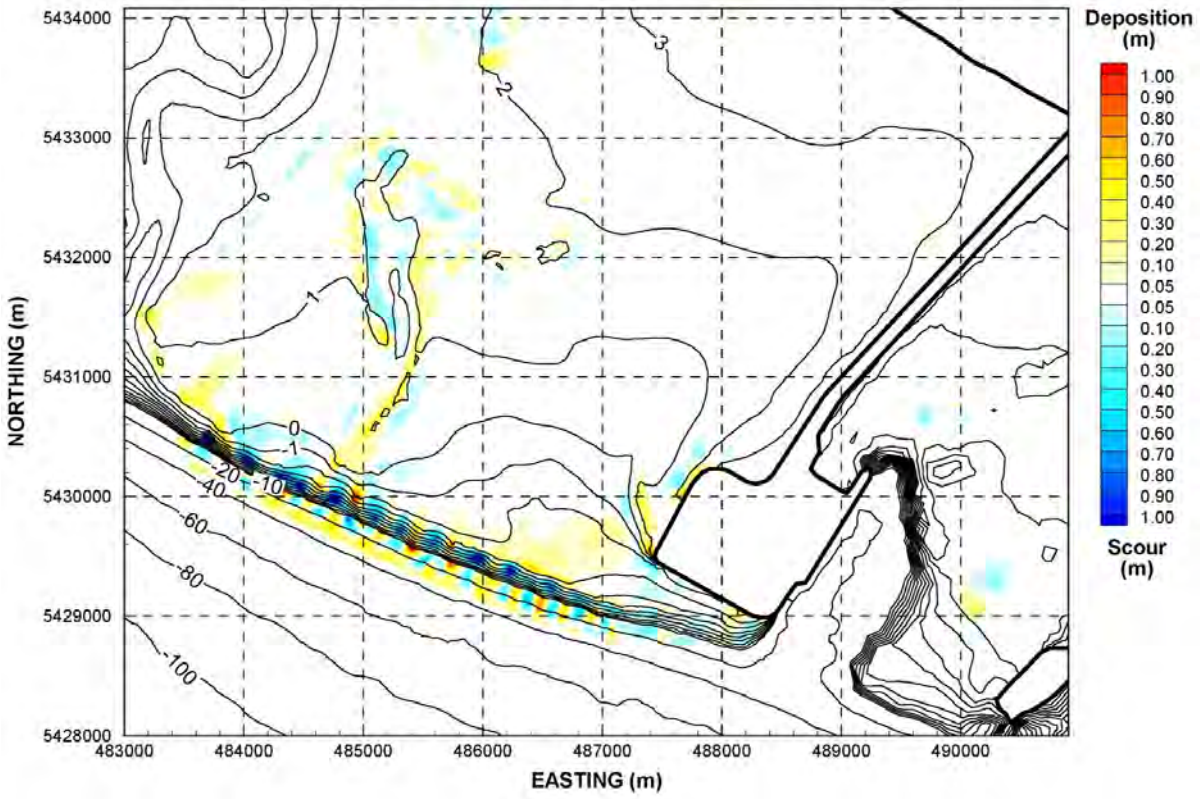

Figure 23: Modelled bed changes after 1,440 model days of simulation.

The model predicted limited vertical changes on much of the tidal flats north of the causeway and in the inter-causeway area. Regions of deposition were predicted in the vicinity of the northwest and southwest corners of the terminal. The relict channel south of the outlet of Canoe Passage and north of the Roberts Bank terminals experienced greater change.

A comparison of bathymetric and LiDAR-derived surfaces over a nine-year period from 2002 to 2011 is shown in **Figure 24**. Note that in this figure, the blue, yellow and red shading indicates regions of scour and pink and blue shading represents areas of deposition. Similar to the model results, the observed results show limited vertical changes of both accretion and erosion of less than 0.25 m over much of the tidal flats and in the inter-causeway area. As well, deposition occurred in the vicinity of the northwest and southwest corners of the existing terminal. The relict channel south of the outlet of Canoe Passage was shown to experience a greater change, on the order of 1 m. The alternating spatial pattern of erosion and deposition suggests that the channel has undergone some lateral shifting in the intervening period. While sedimentation patterns over different time periods

were compared, the results show that the computed sedimentation pattern generally matched well with the observed sedimentation pattern.

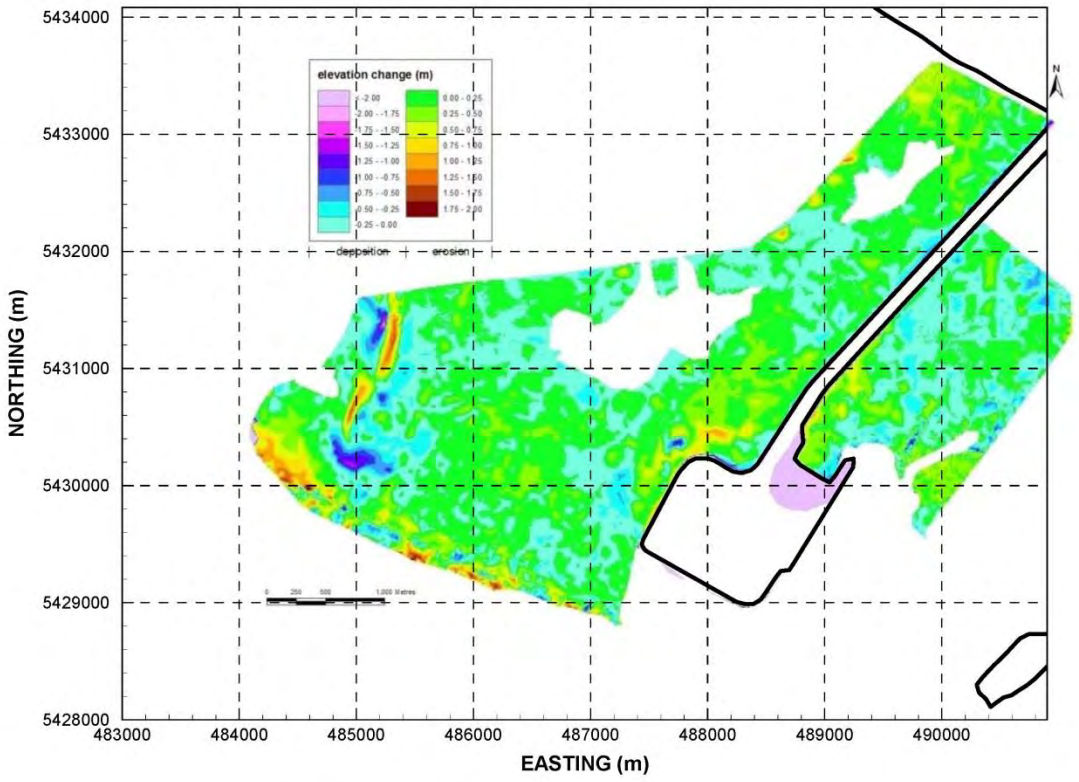

Figure 24: Topographic changes on the tidal flats from 2002 to 2011 based on bathymetric and LiDAR data.

5 SUMMARY

A hydrodynamic-wave sediment transport model was developed to provide current, salinity, wave and local bed scour and deposition information for Roberts Bank. The validation results have demonstrated that the model is capable of reproducing the characteristics of the tides, currents, salt intrusion, wave climate and sedimentation pattern reasonably well. Major discrepancies between modelled and observed results are the result of approximations made in the formulation of the elevation boundary condition. The predicted tide elevation used for the boundary condition is solely a function of the moon and sun whereas the actual tide elevation includes the influence of the moon and sun as well as the local atmospheric conditions, which can have a large influence at a given location and time. The model results can be further enhanced by obtaining actual water levels and salinity near the model's open boundaries and bathymetry data in Ladner Reach, Sea Reach and Canoe Passage.

6 REFERENCES

Bijker. 1968. Littoral drift as function of waves and current. Pages 415–435 *in*. Proceedings of the 11th International Coastal Engineering Conferences.

Birch, R., and T. Mudge. 2012. Sea Pen Study, Roberts Bank, Summer 2012 - QA-QC of ADCP, AWAC and CTD Data Collected by ASL. Report prepared by ASL Environmental Sciences, Victoria, BC.

Fisheries and Oceans. 2005. WebTide Tidal Prediction Model. <http: //www.mar.dfo-mpo.gc.ca/science/ocean/coastal_hydrodynamics/WebTide/webtide.html>.

Foreman, M. G. G., W. R. Crawford, J. . Cherniawsky, R. F. Henry, and M. R. Tarbottom. 2000. A high-resolution assimilating tidal model for the northeast Pacific Ocean. Journal of Geophysical Research 105:629–652.

NHC. 2006. Lower Fraser River Hydraulic Model Final Report. Prepared by Northwest Hydraulic Consultants and Triton Consultants or Fraser Basin Council.

NHC. 2008. Fraser River Hydraulic Model Update. Report prepared by Northwest Hydraulic Consultants for the BC Ministry of Environment.

Prandtl, L. 1925. Über die ausgebidete turbulenz. Zeitschrift für augewandte Mathematik und Mechanik 5:136–139.

Smagorinsky, J. 1963. General circulation experiments with the primitive equations. Monthly Weather Review 91:99–164.

Van der Westhuysen, A. J., M. Zijlema, and J. A. Battjes. 2007. Nonlinear saturation-based whitecapping dissipation in SWAN for deep and shallow water. Coastal Engineering 54:151–170.

Yan. 1987. An improved wind input source term for third generation ocean wave modelling. Technical Report, Royal Dutch Meteor. Inst.

APPENDIX C

FIELD DATA COLLECTION PROGRAM

TABLE OF CONTENTS

LIST OF TABLES

LIST OF FIGURES

1 INTRODUCTION

1.1 PROJECT BACKGROUND

The Roberts Bank Terminal 2 Project (RBT2) is a proposed new multi-berth container terminal which would provide 2.4 million TEUs (twenty-foot equivalent unit containers) of additional container shipping capacity. The project is part of the Container Capacity Improvement Program (CCIP), Port Metro Vancouver's long-term strategy to deliver projects to meet anticipated growth and demand for container capacity until 2030.

Port Metro Vancouver retained Hemmera to undertake environmental studies related to the Project. This appendix forms part of a technical report that describes the results of the Coastal Geomorphology Study effects assessment undertaken by Northwest Hydraulic Consultants Ltd. (NHC).

NHC conducted an extensive field data collection program as part of this study, which is described in this appendix. The purpose of including this description is to provide the reader with a) a comprehensive description of the methods used and the data that was collected, and b) an appreciation of the scope of effort that was undertaken to collect data describing the physical environment and processes that was not available in the existing body of knowledge. Data describing the historical and contemporary conditions are available from a variety of existing sources, which are described in **Appendix A** of this report.

1.2 FIELD STUDY PROGRAM OVERVIEW

Various field studies were conducted by NHC between April 2012 and August 2013 to supplement the body of existing information about the Roberts Bank area and to improve the understanding of key processes. These studies focused on:

- Measuring channel discharge, sediment concentration, temperature and salinity, and collecting repeated bathymetric surveys, in Canoe Passage;
- Measuring salinity and turbidity within the water column at various locations across Roberts Bank during freshet conditions;
- Measuring flows in select tidal channels on Roberts Bank;
- Measuring short-term erosion and deposition in the upper, middle and lower tidal flats;
- Collecting sediment cores and detailed sediment profiles from the upper tidal flats;
- Measuring wave height and period at three locations on a transect across the tidal flats; and
- Measuring waves and current velocities offshore from the Roberts Bank tidal flats.

Figure 1 presents a summary of the field investigations and the duration of data collection. The field studies were supplemented by reconnaissance-level site visits and overflight inspections in a small fixed-wing aircraft to observe conditions at various tide stages and seasons.

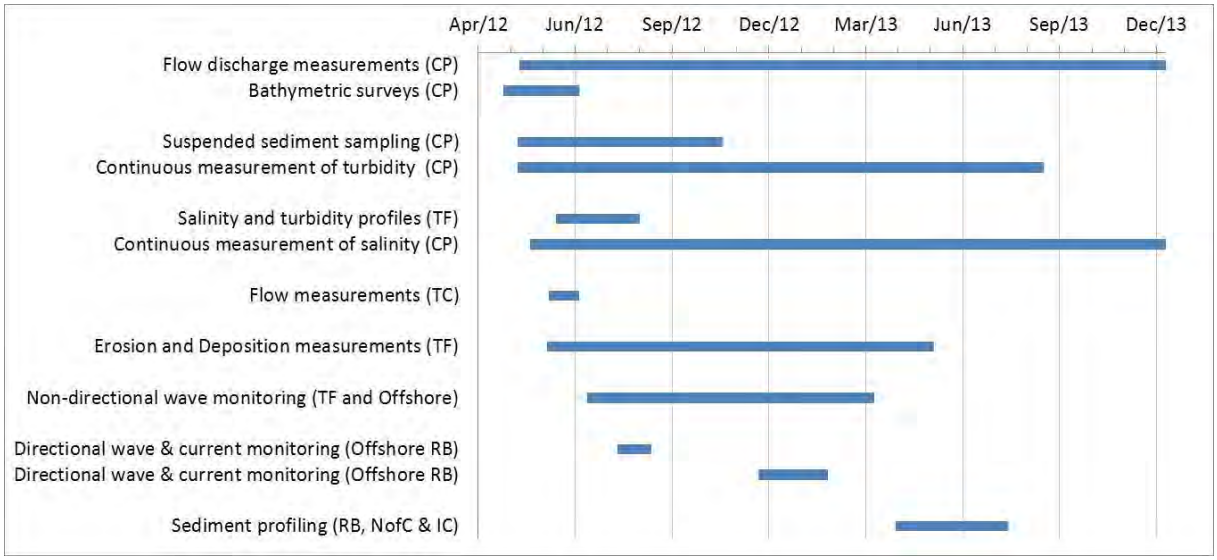

Figure 1: Summary timeline of the field investigations and data collection. CP = Canoe Passage; TF = Tidal Flats; TC = Tidal Channels; RB = Roberts Bank; NofC = North of Causeway; IC = Inter-causeway.

2 FIELD STUDIES

2.1 CANOE PASSAGE CURRENT AND FLOW MEASUREMENTS

The purpose of the Canoe Passage flow study was to provide accurate numerical model boundary conditions and to understand the amount, character and timing of water delivery to Roberts Bank. These measurements are important because Canoe Passage discharges directly to the area of the proposed port expansion. Prior to this study, few measurements of discharge were made in Canoe Passage. To quantify discharge in Canoe Passage, measurements were collected during various tidal stages and during a wide range of Fraser River flows.

The standard instrument for measuring discharge and water velocity is the Acoustic Doppler Current Profiler (ADCP), which detects the phase shift returned from particles in the water column to measure the three-dimensional velocity vector at various depths in the water column. A velocity sensor (Teledyne RD instruments horizontal ADCP) was installed on May 8, 2012 on the outside corner of a mild bend characterized by reasonably uniform velocities across the Canoe Passage channel. The horizontal ADCP (HADCP) was mounted on an aluminum frame anchored on the left bank (at elevation -4.05 m geodetic) that enables periodic removal and cleaning during low and medium-low water levels. The instrument was programmed to sample at 15 minute intervals and provided summary data to the connected Campbell CR200 datalogger that was monitored remotely once per week. The complete data record was downloaded every seven weeks on average during the study period.

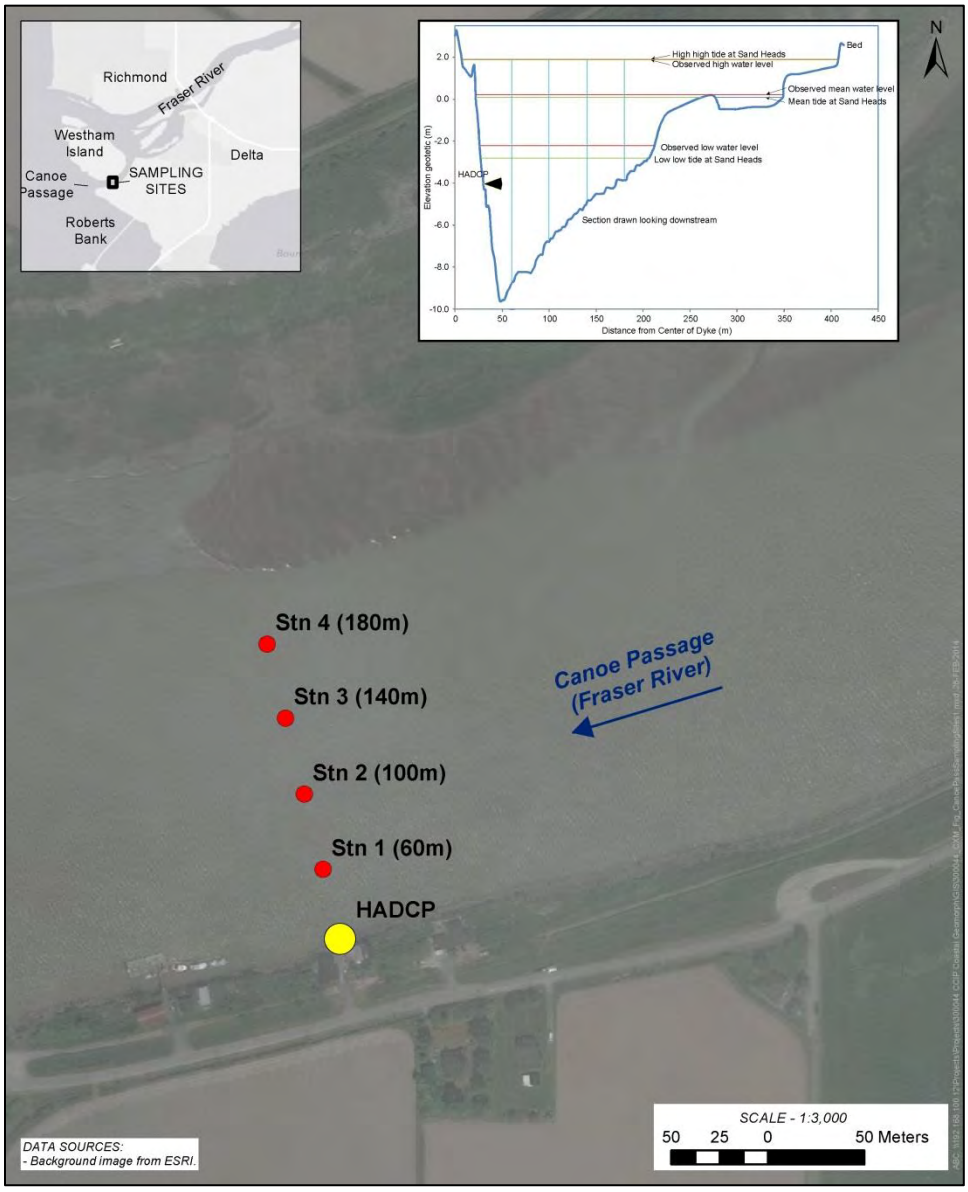

Figure 2: Location and general arrangement of the Canoe Passage station, including the location of the HADCP and suspended sediment sampling sites.

Direct measurements of discharge were collected with a boat-mounted ADCP using bottom tracking or GPS positioning depending on bed mobility[1]. The discharge through the channel was measured on various dates in 2012 – April 24, May 8-9, June 5-6, August 29, and November 14 – and each gauging consisted of at least three measurements along the section (**Figure 2**). The May, August and

[1] Mobile bed conditions require that a GPS be used to provide instrument velocity.

November measurements were completed using a RiverRay ADCP, while additional measurements made in June were made with a 600 kHz Workhorse ADCP or Sontec ADP. Averaging of discharge values, which is the standard approach when dealing with river discharge measurements, was not practical in this case because the tidal cycle causes unsteady (constantly changing) discharge in Canoe Passage. Instead, the individual discharge measurements were used to develop the correlation between index-velocity and mean velocity.

A total of 189 discharge measurements were made at the HADCP cross-section. One hundred and fifty-five (155) of these could be paired with an HADCP velocity measurement. A relation between index velocity measured using the ADCP and the mean velocity determined during the discharge measurements is shown in **Figure 3**. The measured discharge varies between -390 m^3/s and 1,280 m^3/s (negative discharges and velocities represent upstream flow associated with a rising tide). A preliminary relation between index velocity measured using the ADCP and the mean velocity determined during the discharge measurements is shown in **Figure 3**. Four outliers are clearly visible on the graph and were investigated in some detail.

The four points date to the morning of November 14th, 2012 when the flow was ebbing from a 1.613 m CD high tide that followed a -2.11 m CD low tide (see salinity profile data from November 14th, 2012 that includes the tidal cycle in **Figure 8**). Based on the index velocity, the flow declined from 0.18 m/s to 0.87 m/s over a 40-minute period (**Figure 4**). The flow measurements were collected in close succession with each other, and the last of the four measurements was carried out at 8:44 am, with the next measurement occurring at 8:54 am. The 8:54 am measurement plots along the established index velocity relations (**Figure 3**). **Figure 4** shows flow direction at the transect during the four outlying measurements, and the first subsequent measurement that adheres to the main index velocity relation. The top portion of the flow is clearly westbound (outflow) while the bottom portion of the flow is mixed. The elevation of the boundary between the outgoing freshwater flow and the near-bed saline water is visibly reduced over the 40-minute period. For reference, in these plots, the HADCP is located at a depth of about 5 m. These plots suggest a salt wedge was in place in the lower portion of the channel and that the salt wedge was progressively pushed downwards and downstream. Salinity profiles collected later on the same day confirm that a salt wedge is established during this time of year (**Figure 5**). Plots of velocity show a similar trend (**Figure 6**) and illustrate that fast down-channel flow was occurring in the top portion of the channel, while the flow was slow from about mid-depth to the bottom of the channel. The observed data are interpreted to be caused by the salt wedge, and the low HADCP velocities are attributed to the HADCP's location in the low velocity zone during the first four measurements. Once the flow becomes fully established, the HADCP index velocity is representative of the mean velocity and the calibration points return to lying along the index velocity relationship established when the salt wedge was not present (**Figure 7**).

Based on the analysis of the data from November 14th, 2012, the entire data record from the HADCP was inspected to see if a pattern of depressed index velocities during falling tides could be observed.

A portion of the record is illustrated in **Figure 8**, and a section with depressed velocities is highlighted with a circle. Examining the data from other days reveals that a similar pattern is visible when there is a small falling tide that coincides with a high initial tidal stage. In particular, the index velocity falls off the main trend and is depressed for a short period of time before increasing rapidly. This period usually lasts for about an hour.

Rather than adding another instrument, or developing a correction for the suppressed index velocity, the velocity data are taken as provided, recognizing that the velocities may be underestimated for about one hour on some days. For the main purposes of the coastal geomorphology study, the potential error that this introduces is considered to be insignificant as it only occurs when the flows are low and sediment concentrations are also low – a condition that is of lesser interest to the study.

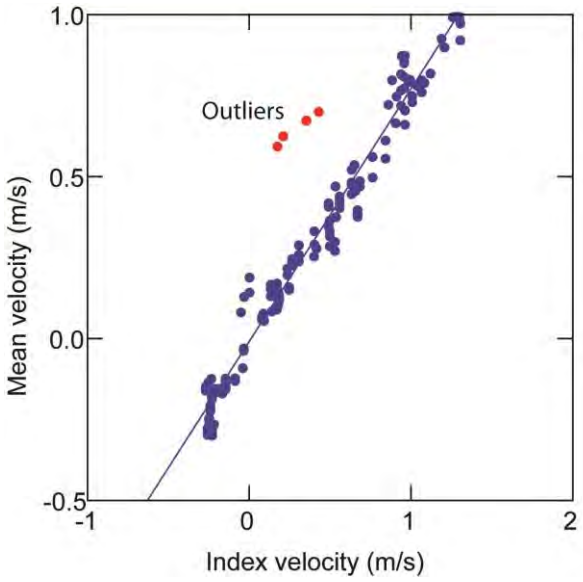

Figure 3: **Relationship between mean velocity measured with the ADCP and index velocity measured with the HADCP for the Canoe Passage site. The index velocity is measured using bins located 14-17 m from the sensor.**

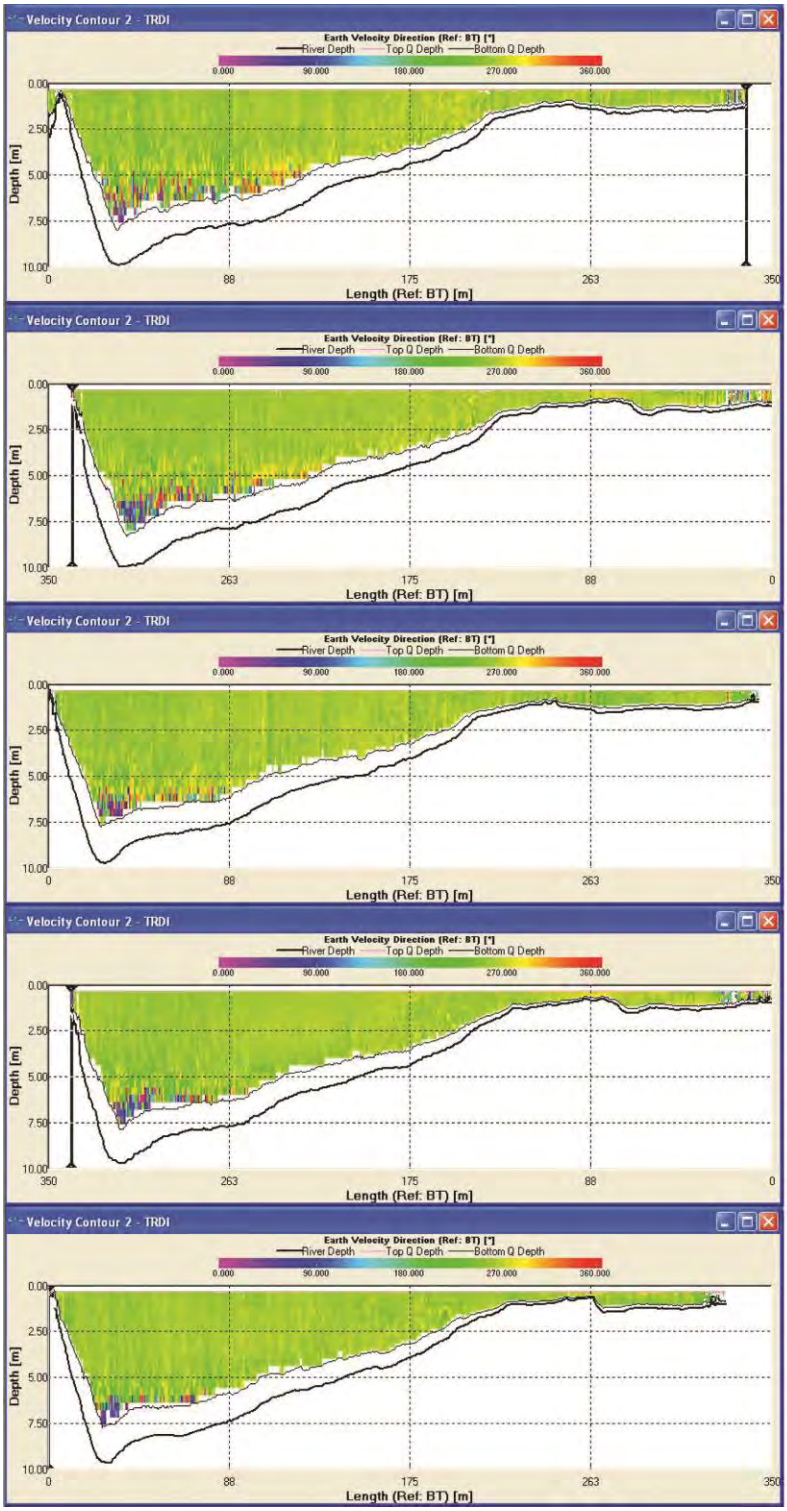

Figure 4: Plots showing the direction of flow at the sampling cross-section in Canoe Passage on the morning of November 14th, 2012.

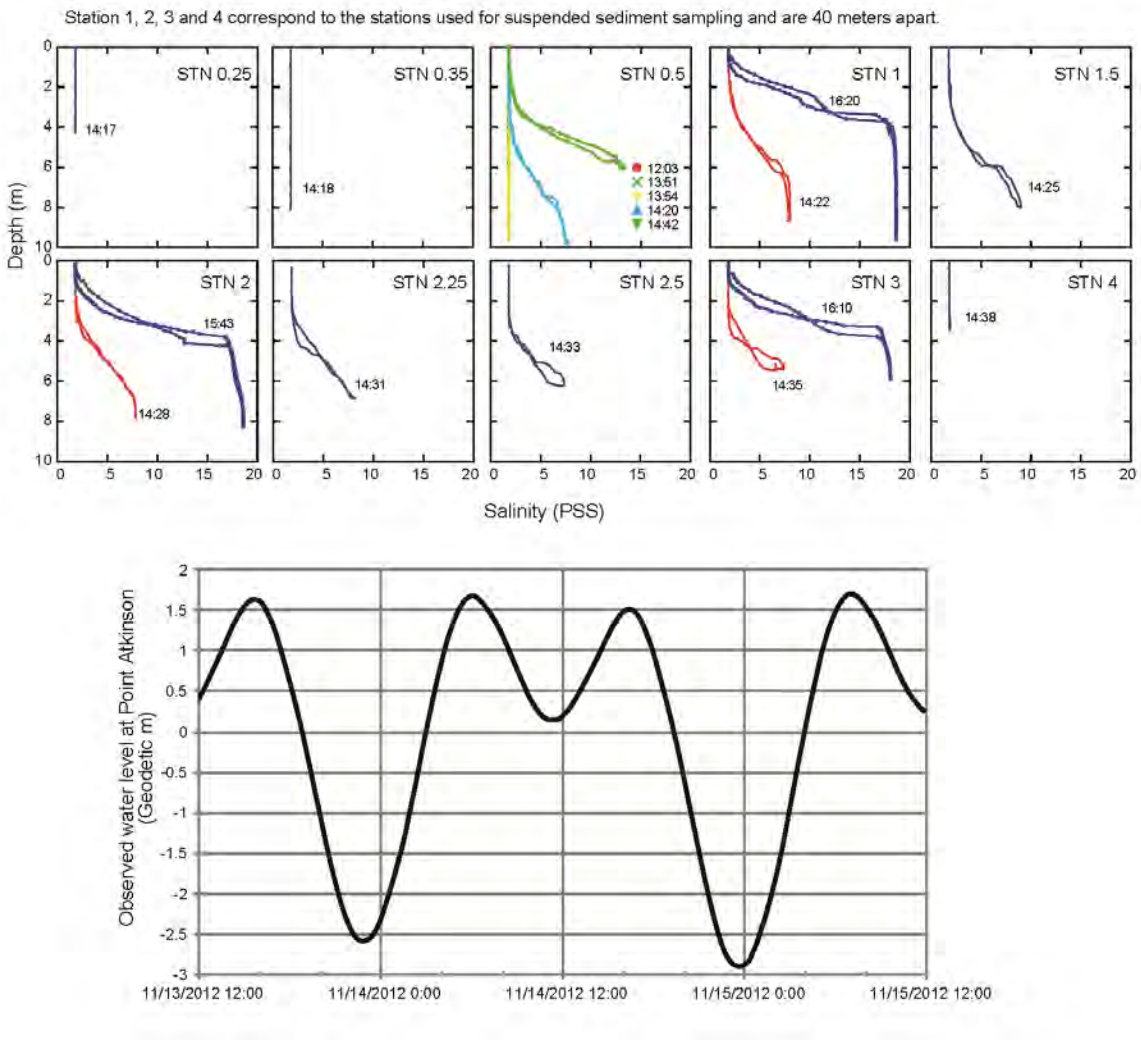

Figure 5: **Turbidity and salinity profiles collected on November 14th, 2012 at the Canoe Passage cross-section. The tide curve during the period of measurement is also shown.**

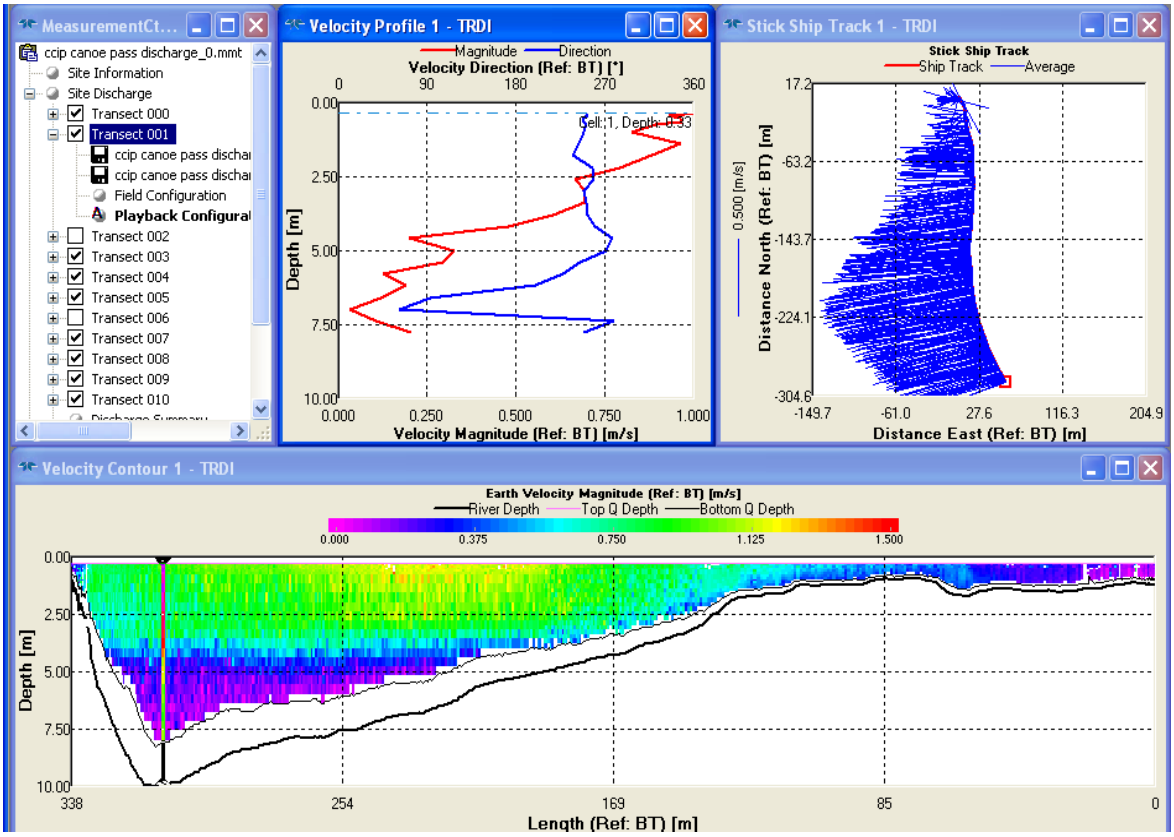

Figure 6: **Velocity pattern at Canoe Passage cross-section on November 14th, 2012 at 8:22 am.**

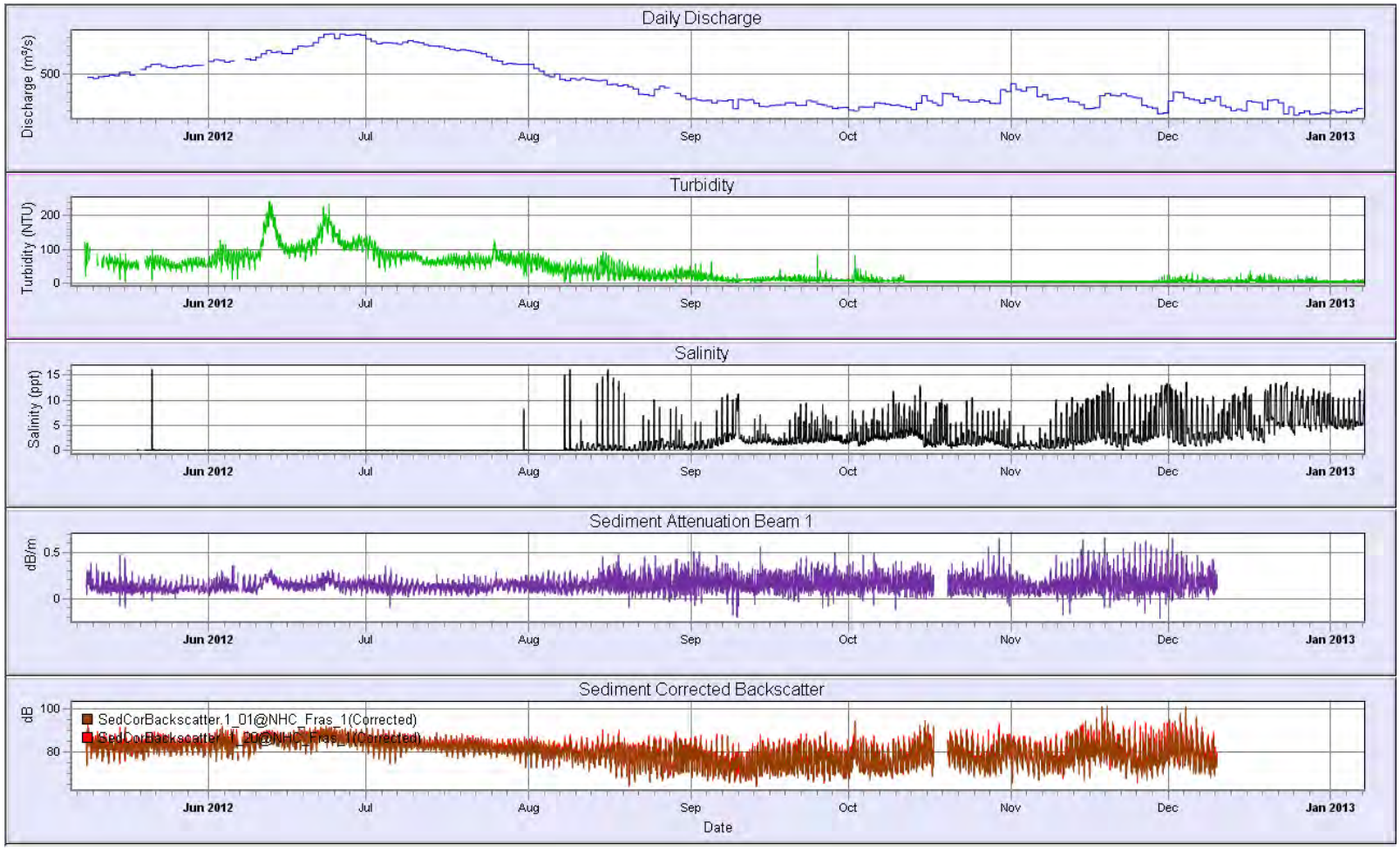

Figure 7: **Daily Discharge, Turbidity, Salinity, Sediment Attenuation Beam 1 and Sediment Corrected Backscatter record for May through December 2012 in Canoe Passage.**

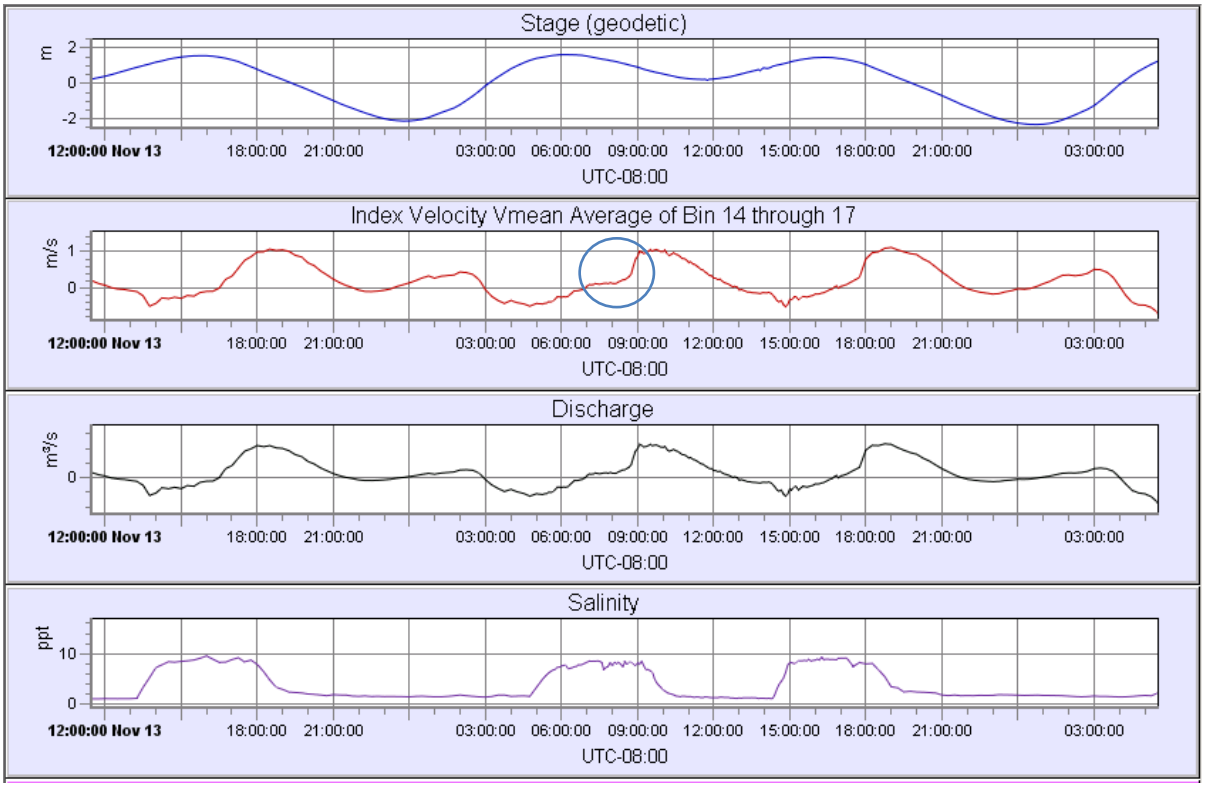

Figure 8: Time series illustrating stage, index velocity, discharge and salinity in Canoe Passage for November 14th, 2012 when flow measurements were made. A blue circle highlights the period when the index velocity was suppressed due to the salt wedge.

During November lower-low water tides, it was observed that the velocity signal was erroneous in bins 18, 19 and 20. This is attributed to the HADCP beam hitting the water surface. It was also noticed that there was a small y-velocity component. Thus, the magnitude of the velocity was calculated (V_{mean}), and the sign based on the x component. Based on the observation that the bins closest to the center of the channel produce the best index relations, a forward stepwise regression was performed with V_{mean} from bins 14 through 20. The data from bin 20 entered the relation first, but all of the V_{mean} values had very similar correlation coefficients (**Table 1**). Only data from bins 17 and lower were considered in the final analysis to avoid the potential for errors associated with the beam making contact with the water surface. The analysis shows that an average of bins 14-17 gives a strong correlation and is likely to be less susceptible to errors than any single bin.

Table 1: Correlation coefficients between potential index velocities and mean velocity.

Parameter	Correlation Coefficient	Parameter	Correlation Coefficient
V_{mean14}	0.9881	V_{X14}	0.9880
V_{mean15}	0.9879	V_{X15}	0.9879
V_{mean16}	0.9874	V_{X16}	0.9874
V_{mean17}	0.9871	V_{X17}	0.9871
V_{mean18}	0.9869	V_{X18}	0.9869
V_{mean19}	0.9870	V_{X19}	0.9871
V_{mean20}	0.9876	V_{X20}	0.9876
V_{AVG14_17}	0.9878	$V_{X\_17\_20}$	0.9874

The final index velocity relation is:

$$V_{avg} = 0.8069V_{index}+0.0167Stage - 0.0196 \quad [1]$$

Mean velocity is uniformly lower than index velocity because the former applies to the entire cross-section of Canoe Passage while the latter includes current velocities within and near the thalweg, which is the fastest flowing portion of the river channel. Note that the least-squares best-fit line passes through a point of zero velocity for both index and mean velocities as would be expected.

To predict discharge, a relationship between wetted area and stage is also needed. **Figure 9** shows the relation between wetted area and stage based on the individual flow measurements and cross-section survey data. The ADCP data agree reasonably well with the bathymetry survey, although on average the ADCP over-predicts the wetted area. Some variability is expected as the ADCP data have not been adjusted for small errors that can occur at the ends of the transect when starting and completing the cross-sections in the field. The stage-wetted area relation for the site is:

$$\text{Wetted area} = 28.06Stage^2 + 283.87Stage + 1138 \quad [2]$$

Figure 10 shows data from 155 discharge measurements (including the outliers) plotted against the predicted discharge using the index velocity relation. The linear best fit has an intercept that is not significantly different from zero ($p< 0.05$; i.e., the line passes through the origin), the slope is not significantly different from one (1.0), and the predictive relationship explains 98% of the variability in the actual discharge measurement data ($r^2 = 0.98$), when the four outliers from November 4th, 2012 are excluded ($r^2 = 0.93$ if included). Based on the quality of the fit, the index velocity relation is considered complete.

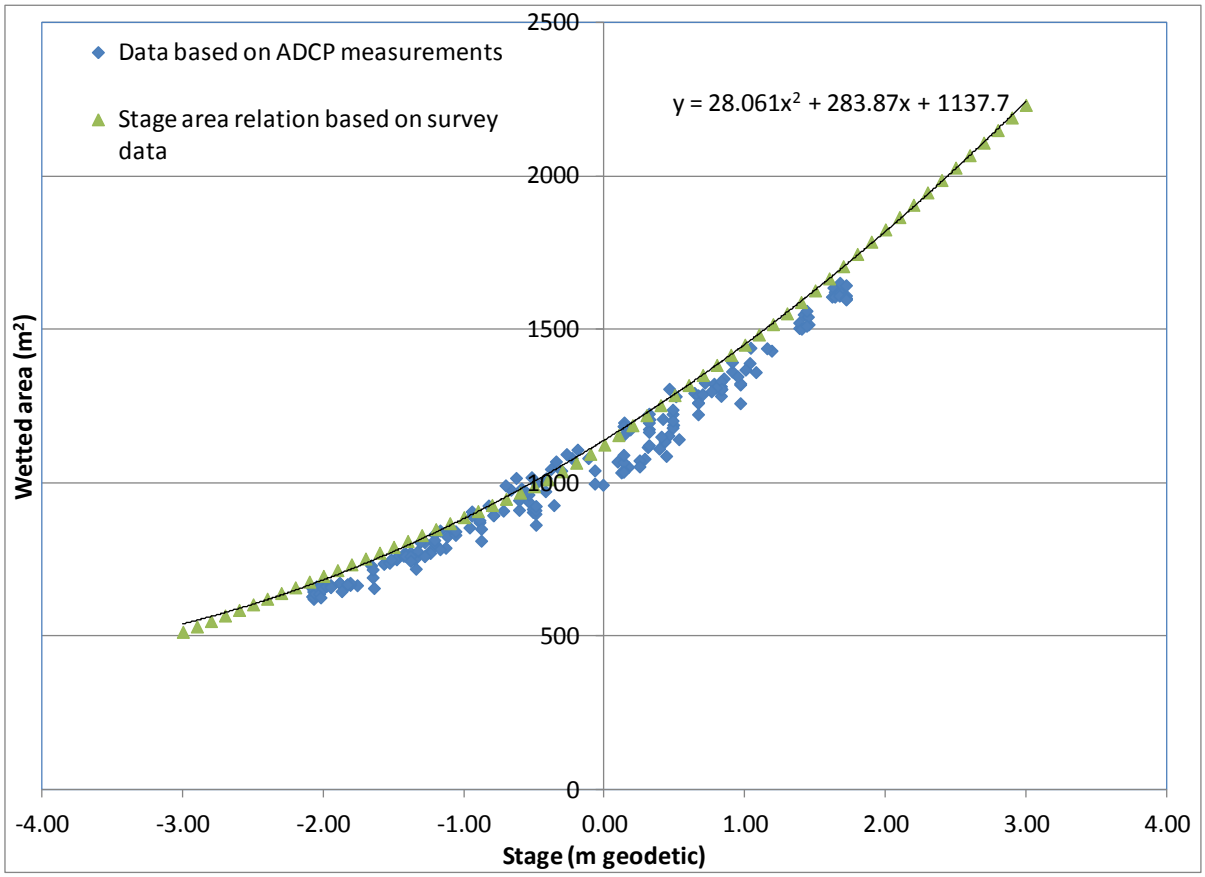

Figure 9: **Relationship between wetted area and water surface elevation at the Canoe Passage monitoring site.**

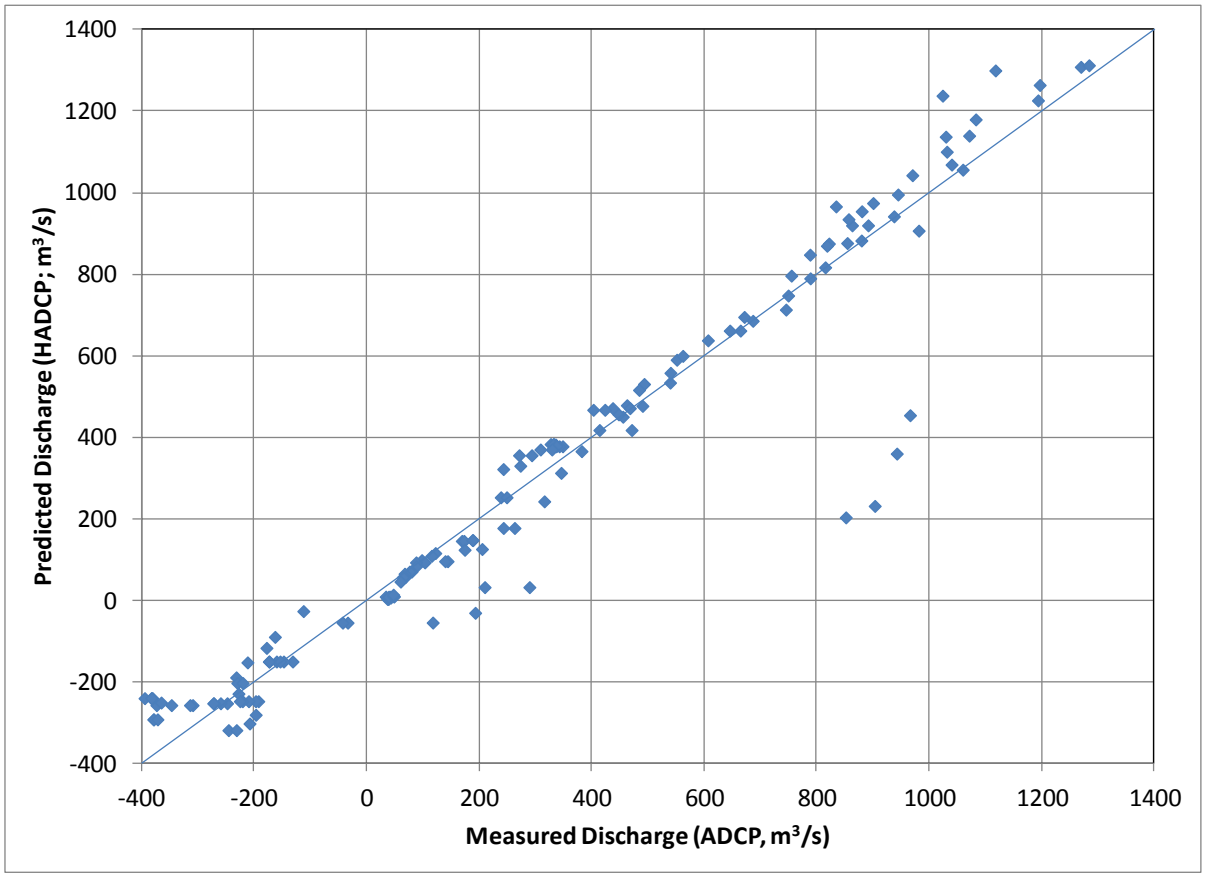

Figure 10: **Plot comparing measured and predicted flows at Canoe Passage.**

The long-term discharge hydrograph for Canoe Passage, obtained using the above relation, is shown in **Figure 11**. Continued operation of the station through to the end of December, 2013 provided a valuable prolonged record[2].

[2] The Canoe Passage station continues to collect data at the time of writing this report but the data are not reported here.

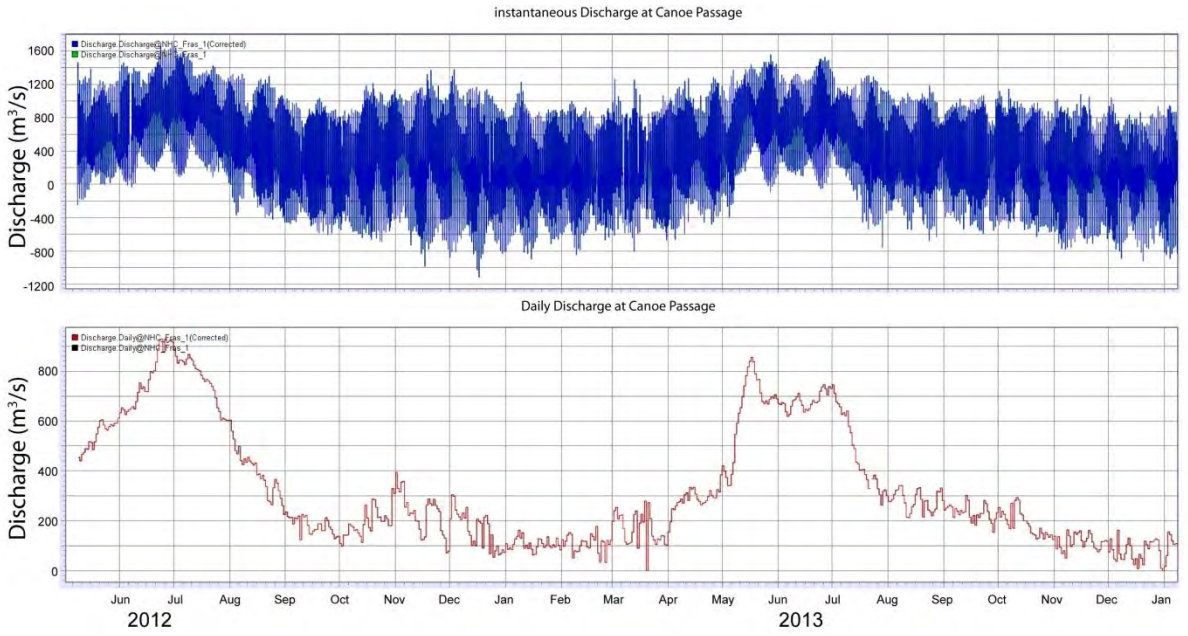

Figure 11: Instantaneous and daily discharge data from Canoe Passage.

The continuous monitoring of discharge in Canoe Passage provides an opportunity to conduct a more detailed analysis of the proportion of the Fraser River that exits via Canoe Passage. Previous measurements have been limited to individual flows measurements in different channels that are closely spaced in time.

To determine the flow split, the total flow of the Fraser River into the Strait of Georgia needs to be established. This could be resolved using data from the Fraser River at Mission, where a horizontal ADCP has been installed; however, the index velocity relationship remains preliminary and has not been developed for low flows which are also of interest. Instead, the existing Fraser River MIKE11 model (NHC 2008) for the period spanning January 1, 2012 to May 31, 2013 was used to predict flows at New Westminster. Subsequently, the monthly ratio between the flow at New Westminster and the Fraser River at Hope gauge was averaged for each month to determine typical inflow scaling coefficients. These where used to extend the flow record at New Westminster until the end of August 2013. The monthly scaling coefficients are not applicable for the fall and winter of 2013-2014 on account of the unusually dry weather that occurred during this period. The results from the flow split analysis are shown in **Figure 12**. The results indicate that Canoe Passage conveys 8% of the Fraser River discharge, which is a relatively small amount compared to other distributaries.

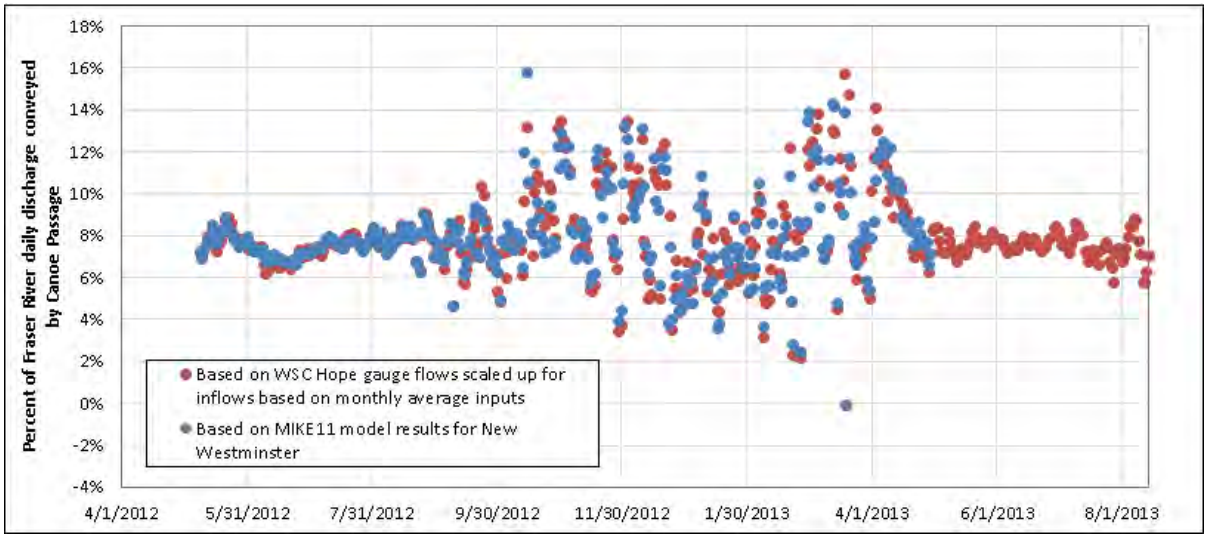

Figure 12: Percent of daily discharge in the Fraser River that is conveyed by Canoe Passage.

2.2 SUSPENDED SEDIMENT MEASUREMENTS

Turbidity measurements were collected to understand the spatial and temporal distribution of the freshwater lens within Canoe Passage and the Fraser River plume over the Roberts Bank tidal flats. A turbidity sensor was installed in the Canoe Passage channel on May 8th, 2012 to acquire a continuous record of sediment concentration. The Analite 395 turbidity probe was mounted about 2 m below the low tide water elevation on the same platform that holds the HADCP (**Figure 2**). This probe was connected to a datalogger (CR200) which records the turbidity and water temperature every 15 minutes. Remote download was set up to allow weekly review to limit the potential loss of data. The turbidity probe was equipped with a wiper that cleaned the lens prior to collecting each measurement. Near-monthly maintenance visits were carried out until the instrument was fouled irreparably around September 8th, 2013. The complete turbidity record is shown in **Figure 13**.

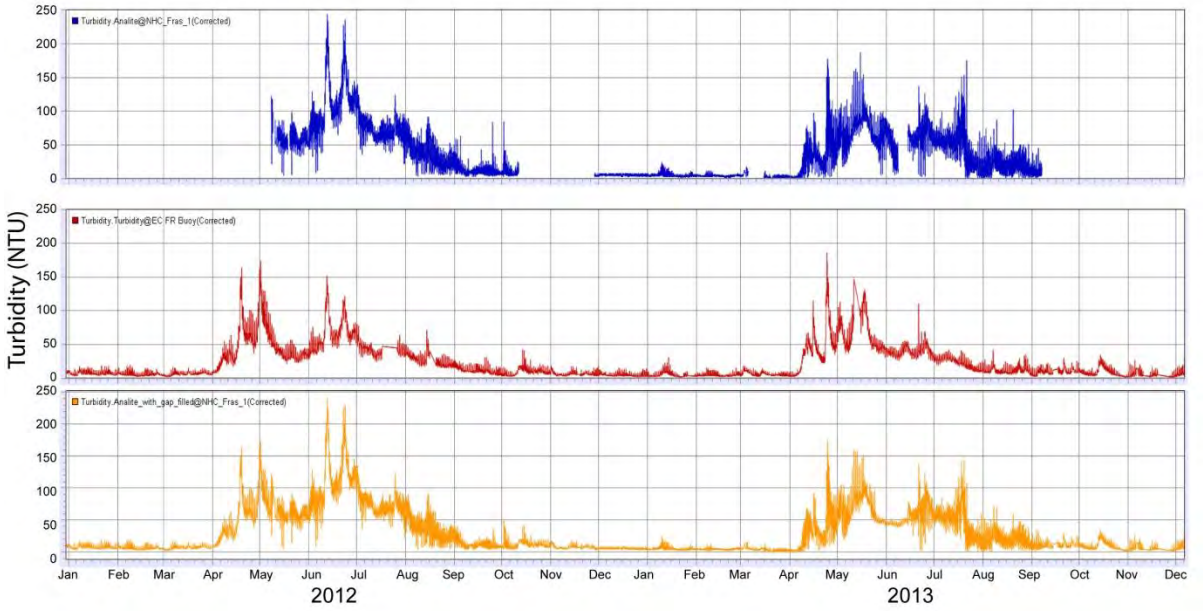

Figure 13: Turbidity data from Canoe Passage (top) and Fraser River Water Quality Buoy (middle) located 12 km upstream on the main arm of the Fraser (Environment Canada 2013). Bottom plot shows composite series corrected for sensor fouling.

The sensor is limited to making measurements in an area that is a few cubic centimetres in volume; it does not directly measure the sediment concentration of the entire river. A correlation between the turbidity sensor reading and the mean concentration across the river could be used instead.

In order to develop this correlation, direct measurements of suspended sediment concentration were made at four stations across the channel cross-section adjacent to the installed turbidity sensor (**Figure 2**). A number of water samples were collected on various dates and are summarized in **Table 2**. Depending on flow depths and velocities, a United States Geological Survey (USGS) P-61 or P-63 (point-integrated) sampler was used. These cast-bronze 'fish' have electrically-operated nozzles that allow the sample to be collected within discrete portions of the vertical profile into a glass bottle stored in the housing. The sampler was lowered into the flow to the specified depth on a mechanical reel from a boat or bridge.

In addition to the P-61/P-63 sampling, a LISST-SL was used to measure sediment concentrations and grain size during a number of the field visits (**Table 2**). This instrument uses a pitot tube to detect the water velocity and then pumps a sample of the river water through a test chamber at a flow rate such that the intake velocity matches the stream velocity. A laser beam in the test chamber is sent through the water sample and the refraction of the laser beam is used to determine the particle size and concentration.

Table 2: Summary of water samples collected during sampling trips from August to November, 2012.

Sampler	5/8/2012	5/9/2012	6/6/2012	6/13/2012	7/5/2012	11/14/2012
LISST-SL				51		
P61/LISST-100		15				
P61/LISST-SL/LISST-100			11		20	
P63/LISST-100	16					
P63/LISST-SL/LISST-100					24	
P63/LISST-SL						13
Total	16	15	11	51	44	13

Table 3: Summary of complete sets of water samples collected at Canoe Passage.

Date	Samples
5/8/2012	4
5/9/2012	4
6/6/2012	3
6/13/2012	12
7/5/2012	7
11/14/2012	3

Each measurement consisted of vertical profiles spaced every 40 metres across the channel (**Figure 2**). **Table 3** summarizes the number of complete sets of water samples collected at the three or four stations (at low tide, the fourth station was not sampled). Samples collected at different locations across the width of the channel needed to be collected within a one-hour period for the individual samples to be grouped together. This criterion was based on the observation that turbidity (and thus, suspended sediment concentration) can change relatively quickly during the tidal cycle.

The individual samples collected across the width of the channel were combined based on wetted area weighting and the average sediment concentration and grain size of the sediment was determined in the lab. A sediment concentration-turbidity relationship was developed to convert the instantaneous turbidity measurements (sampled every 15 minutes in NTU) at Canoe Passage to the mean suspended sediment concentration (red data points in **Figure 14**). The power function [$SS = 0.156(\text{turbidity})^{1.51}$] was found to describe the relationship between the two variables, which was then used to predict the mean suspended sediment concentration. The relationship between turbidity and suspended sediment developed based on samples from Roberts Bank is plotted as well in **Figure 14** and is discussed in more detail below.

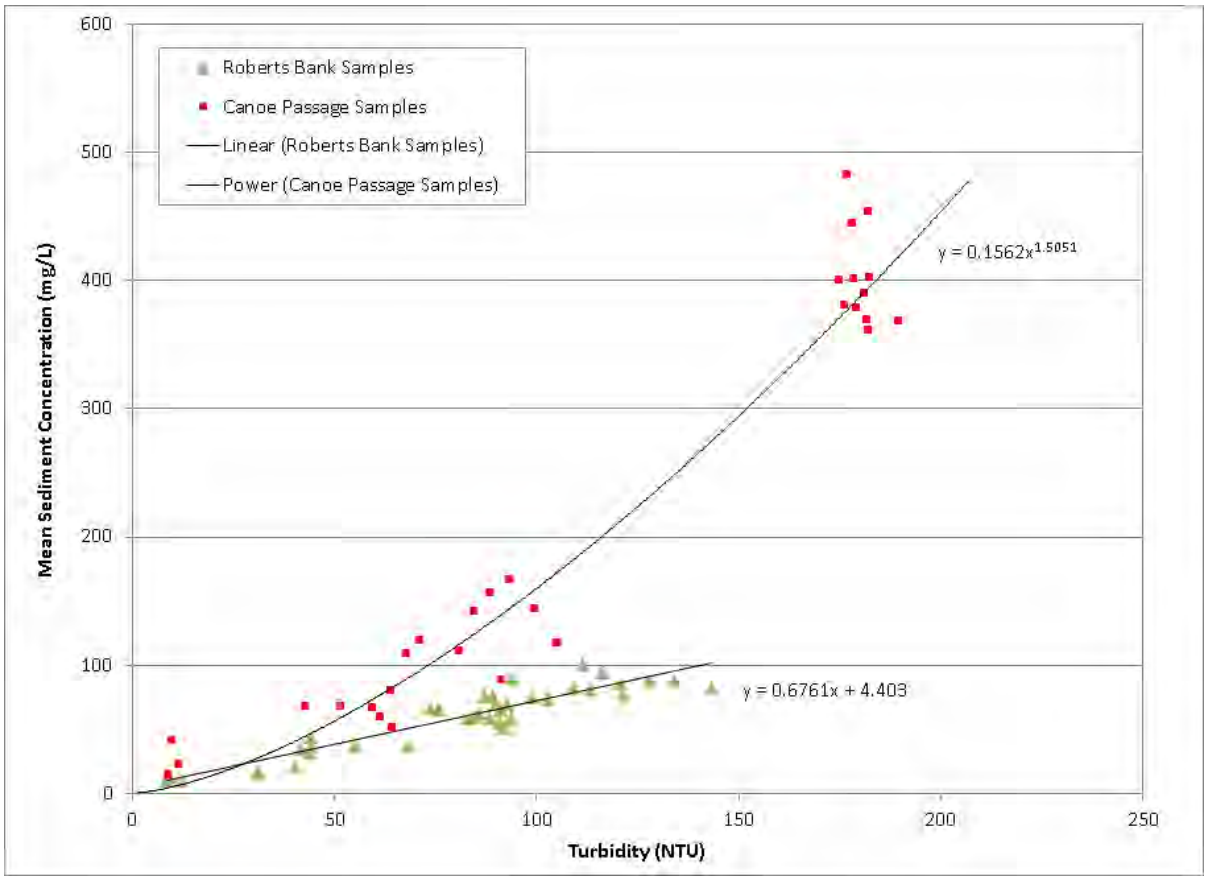

Figure 14: Relation between sediment concentration and turbidity at Canoe Passage.

The power function developed for Canoe Passage in combination with the discharge record, enabled the calculation of a suspended sediment load time-series in Canoe Passage. Continued operation of the station through the 2012 and 2013 freshet periods and beyond provided a valuable long-term record and is shown in **Figure 15**. The suspended sediment load series was derived from: turbidity and discharge data from Canoe Passage; Fraser River Buoy turbidity data and Canoe Passage discharge data; and Fraser River Buoy turbidity data and modelled Fraser River flows at New Westminster scaled to Canoe Passage. The latter two time series were used to fill in the data gaps in the period of record.

The samples from each profile were weighted based on the wetted cross-sectional area and used to determine the mean grain size distribution of the sediment in transport and the proportion of the sediment composed of sand (>0.064 mm). The sand composition varied between zero and 20%, and averaged 7%. The average is used to provide a first-order estimate of the sand load through Canoe Passage.

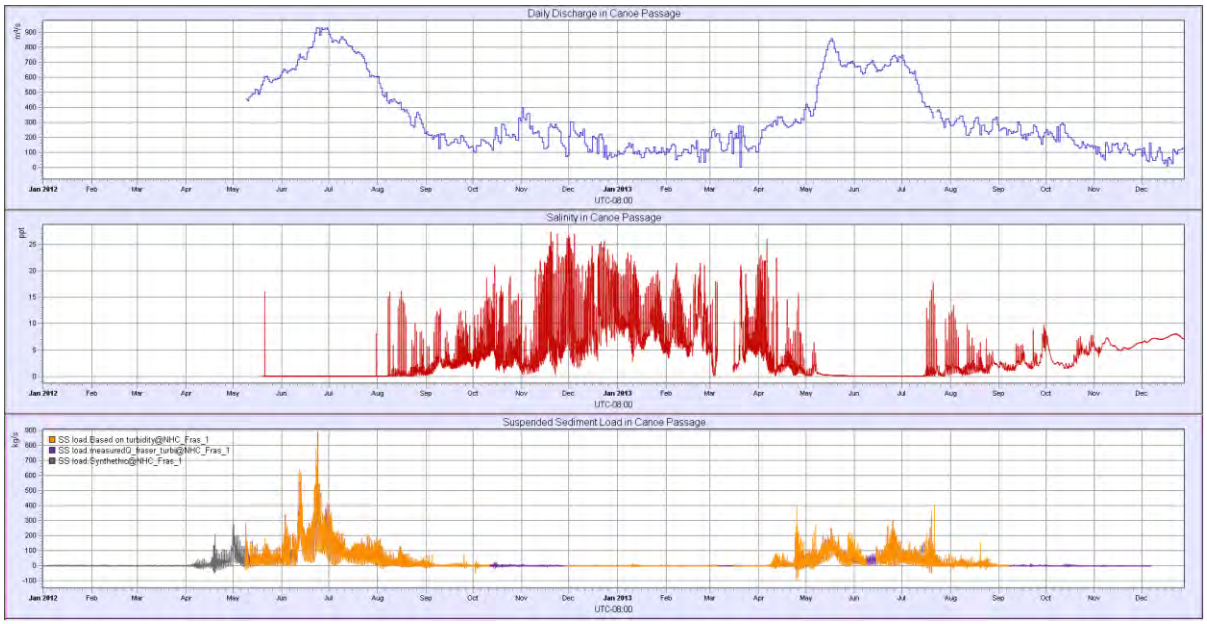

Figure 15: **Daily discharge and instantaneous salinity, and sediment load for Canoe Passage during 2012 and 2013. The suspended sediment load series is derived from Canoe Passage turbidity and discharge data (yellow), Fraser River Buoy turbidity and Canoe Passage discharge data (purple), and Fraser River Buoy turbidity and modelled Fraser River flows at New Westminster scaled to Canoe Passage (grey).**

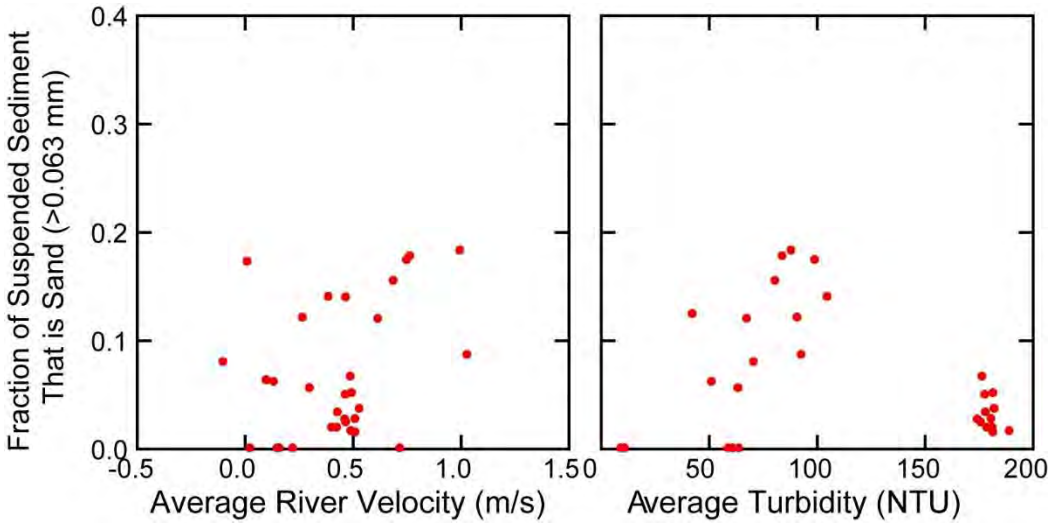

Figure 16: **Fraction of suspended sediment composed of sand based on composite samples across the channel and through the flow depth.**

In order to obtain two years of sediment data and include the Fraser River sediment pulse in early April before the station was established (see **Figure 13**), turbidity data from the Fraser River water

quality buoy was used to fill in the turbidity record for the period from January 1st to May 8th, 2012. Likewise, a gap in the month of August 2013, and another in the fall of 2013 were filled with turbidity data from the Fraser River buoy. The last 26 days in December of sediment load were estimated using the average of the previous month. The synthetic portions of the record generally have a low turbidity and low river flow, so any biases that may be introduced are unlikely to affect the overall load estimates. The synthetic portion of the records contributes 16% of the estimated sediment yield in 2012 and 6% in 2013. The annual suspended sediment yield data are summarized in **Table 4** for 2012 and 2013. Based on preliminary Water Survey of Canada (WSC) data from the Fraser River at Hope gauge, the peak daily discharge for 2012 and 2013 was about a 1:20 and 1:5 year recurrence event, respectively. As such, it is expected that the sediment loads measured for these years would be somewhat higher than the average load. The observed sediment load is less than the average load predicted based on historic measurements in the Fraser River scaled to Canoe passage using a flow split of 8%.

Table 4: Summary of suspended sediment load at Canoe Passage.

Year	Total Load (Tonnes/yr)	Sand Load (>0.064 mm; Tonnes/yr)	Bed Material Load (>0.18 mm; Tonnes/yr)	Fraction of total load based directly on Canoe Passage data
2012	935,000	65,000	NA	84%
2013	465,000	32,000	NA	94%
Estimated based on previous Fraser River estimates[3] and 8% flow split	1,380,000		220,000	N/A

2.3 SALINITY AND TURBIDITY PROFILES

Once the plume exits the Fraser River distributary channels, its distribution over the Roberts Bank study area is also important to understand for a variety of physical and biological processes. At each location on the tidal flats (**Figure 17**), the Manta2 sonde (which also collected salinity, conductivity and depth data down-profile) was lowered towards the seabed from a boat and used to make turbidity measurements at one-second intervals within the water column (**Figure 18** to **Figure 26**). The timing of profile collection is summarized in **Table 5**.

[3] Sediment loads on the lower Fraser River were measured by Water Survey of Canada at Hope, Agassiz and Mission during the period 1965 to 1986. Based on that data, the total suspended load of the Fraser River averaged 17.3 million tonnes/year (range 12.3 million to 31.0 million), with the load consisting of 35% sand, 50% silt and 15% clay (McLean and Tassone 1988, McLean *et al*. 1999).

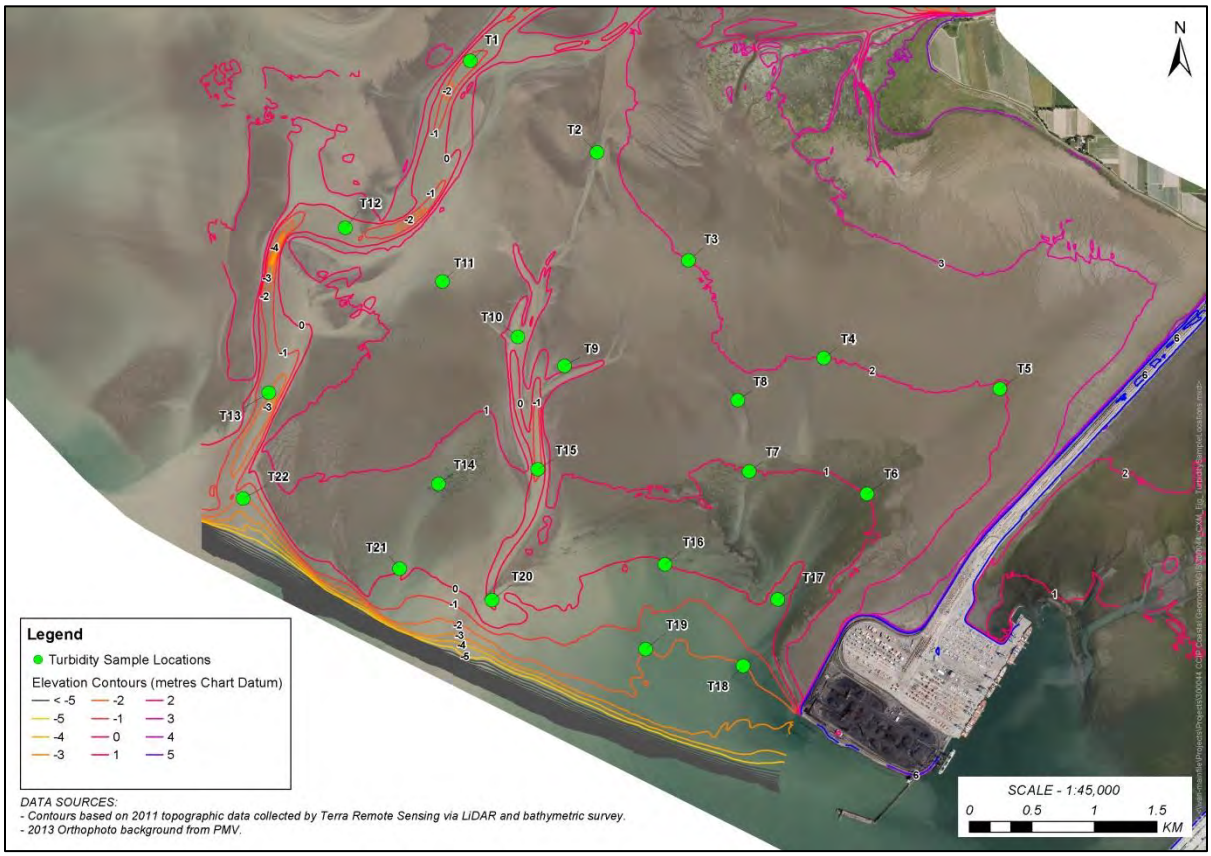

Figure 17: **Turbidity and salinity sampling locations on Roberts Bank.**

Table 5: **Summary of turbidity and salinity profiles collected on the Roberts Bank tidal flats.**

Date	Station Name	Measurement Start Time	Measurement End Time	Tide condition over measurement	Corresponding Fraser River Discharge at Hope
6/12/2012	T2-T22	11:24	17:03	Low-slack to high-slack, and falling	9219
6/14/2012	T1, T10, T16, T5	15:20	19:44	High-slack to low-slack	8846
6/20/2012	T1, T10, T16, T5	4:54	9:04	High-slack, falling	10713
6/23/2012	T1, T10, T16, T5	7:04	14:22	High-slack to low-slack,	11622
7/4/2012	T1, T10, T16, T5	5:07	9:15	High-slack, falling	9154
7/11/2012	T6, T7, T15, T16, T17, T18, T20	12:27	16:25	High-slack to low-slack	8356
8/2/2012	T1, T5, T10, T16	4:39	6:06	High-slack, falling	5460
8/29/2012	T1, T10, T16	5:42	6:25	Falling	2778

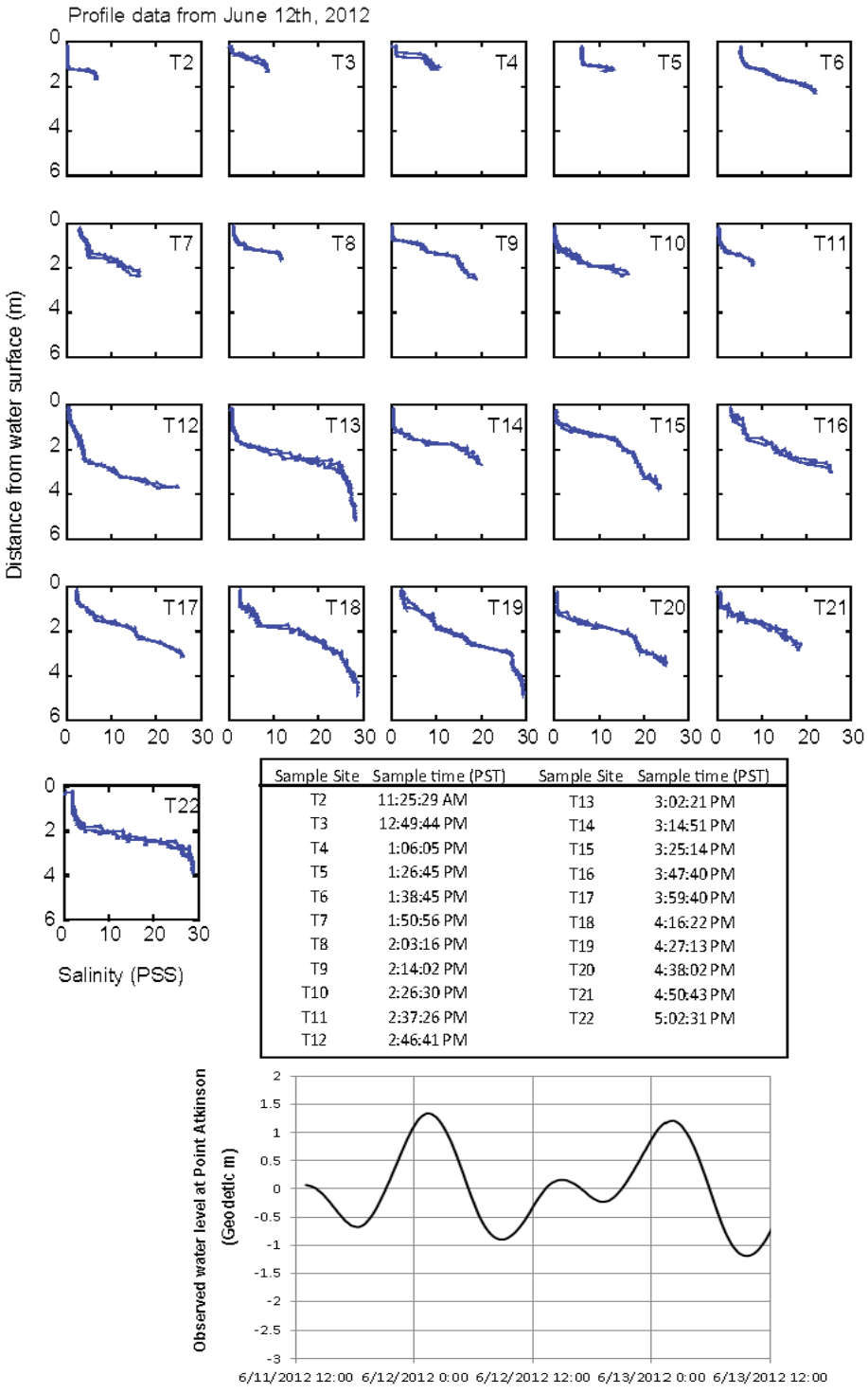

Sample Site	Sample time (PST)	Sample Site	Sample time (PST)
T2	11:25:29 AM	T13	3:02:21 PM
T3	12:49:44 PM	T14	3:14:51 PM
T4	1:06:05 PM	T15	3:25:14 PM
T5	1:26:45 PM	T16	3:47:40 PM
T6	1:38:45 PM	T17	3:59:40 PM
T7	1:50:56 PM	T18	4:16:22 PM
T8	2:03:16 PM	T19	4:27:13 PM
T9	2:14:02 PM	T20	4:38:02 PM
T10	2:26:30 PM	T21	4:50:43 PM
T11	2:37:26 PM	T22	5:02:31 PM
T12	2:46:41 PM		

Figure 18: **Turbidity profiles collected on June 12th, 2012 at select locations across the Roberts Bank tidal flats. The tide curve during the period of measurement is also shown.**

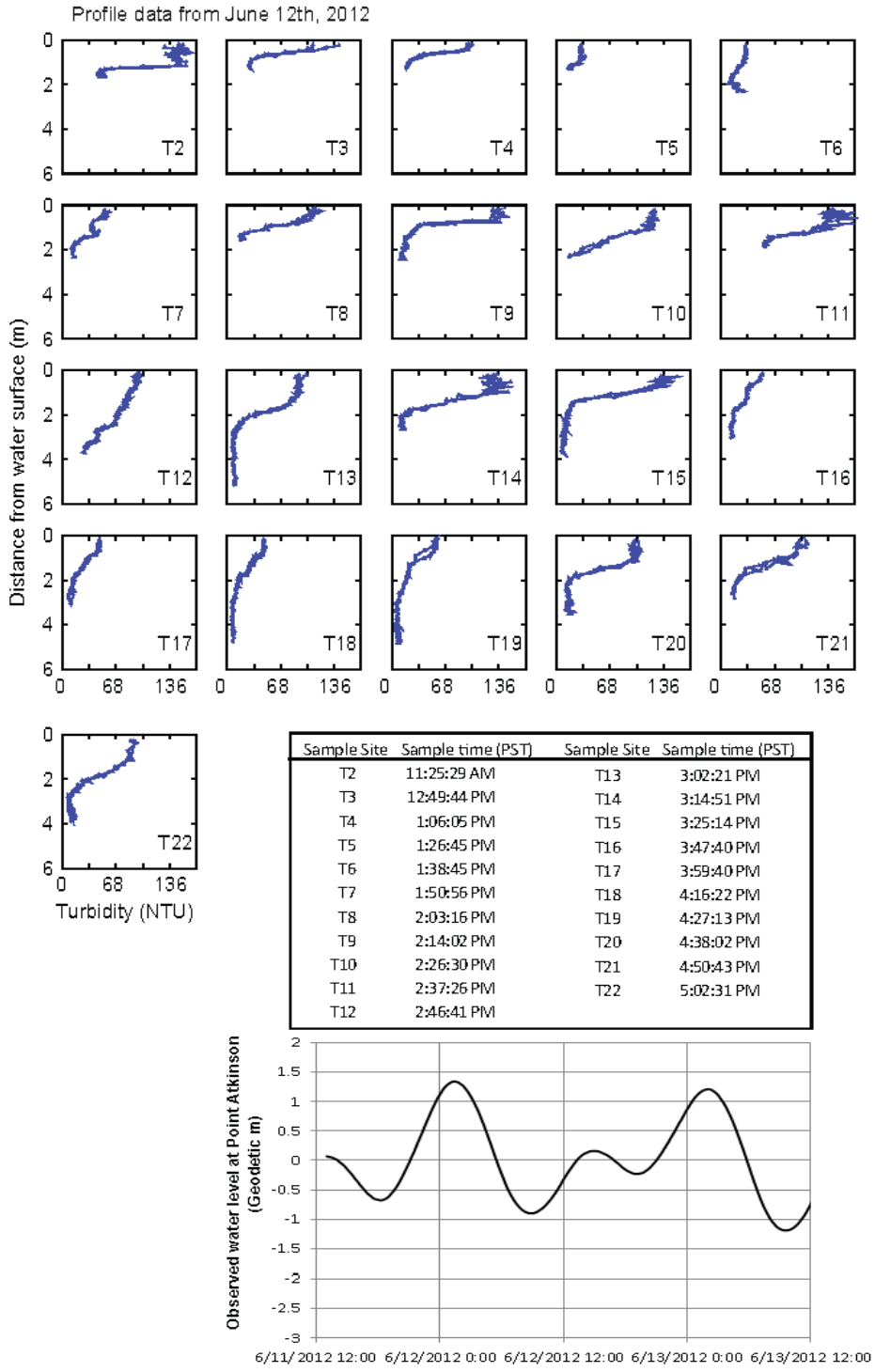

Sample Site	Sample time (PST)	Sample Site	Sample time (PST)
T2	11:25:29 AM	T13	3:02:21 PM
T3	12:49:44 PM	T14	3:14:51 PM
T4	1:06:05 PM	T15	3:25:14 PM
T5	1:26:45 PM	T16	3:47:40 PM
T6	1:38:45 PM	T17	3:59:40 PM
T7	1:50:56 PM	T18	4:16:22 PM
T8	2:03:16 PM	T19	4:27:13 PM
T9	2:14:02 PM	T20	4:38:02 PM
T10	2:26:30 PM	T21	4:50:43 PM
T11	2:37:26 PM	T22	5:02:31 PM
T12	2:46:41 PM		

Figure 19: **Salinity profiles collected on June 12th, 2012 at select locations across the Roberts Bank tidal flats. The tide curve during the period of measurement is also shown.**

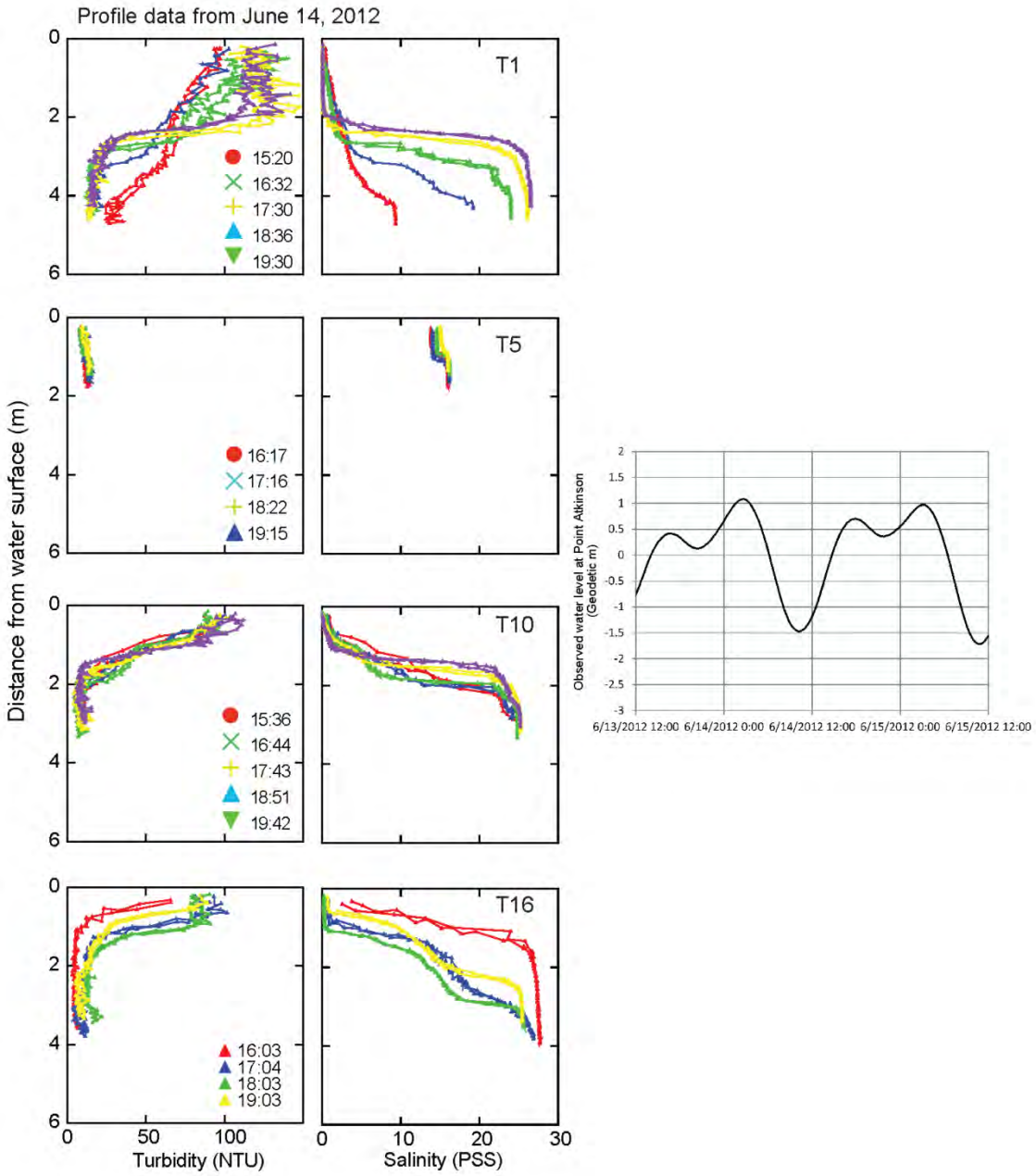

Figure 20: **Turbidity and salinity profiles collected on June 14th, 2012 at select locations across the Roberts Bank tidal flats. The tide curve during the period of measurement is also shown.**

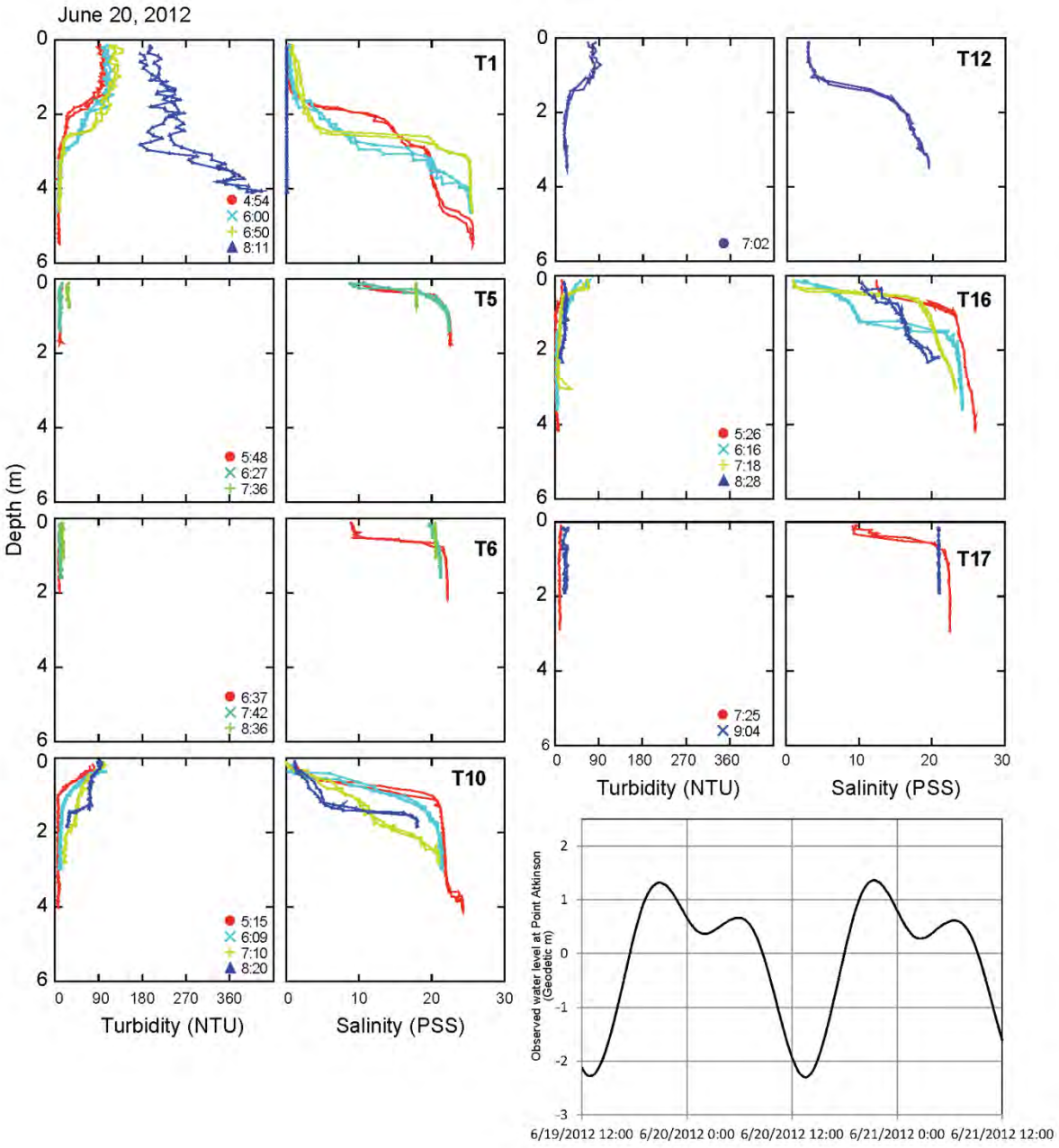

Figure 21: **Turbidity and salinity profiles collected on June 20th, 2012 at select locations across the Roberts Bank tidal flats. The tide curve during the period of measurement is also shown.**

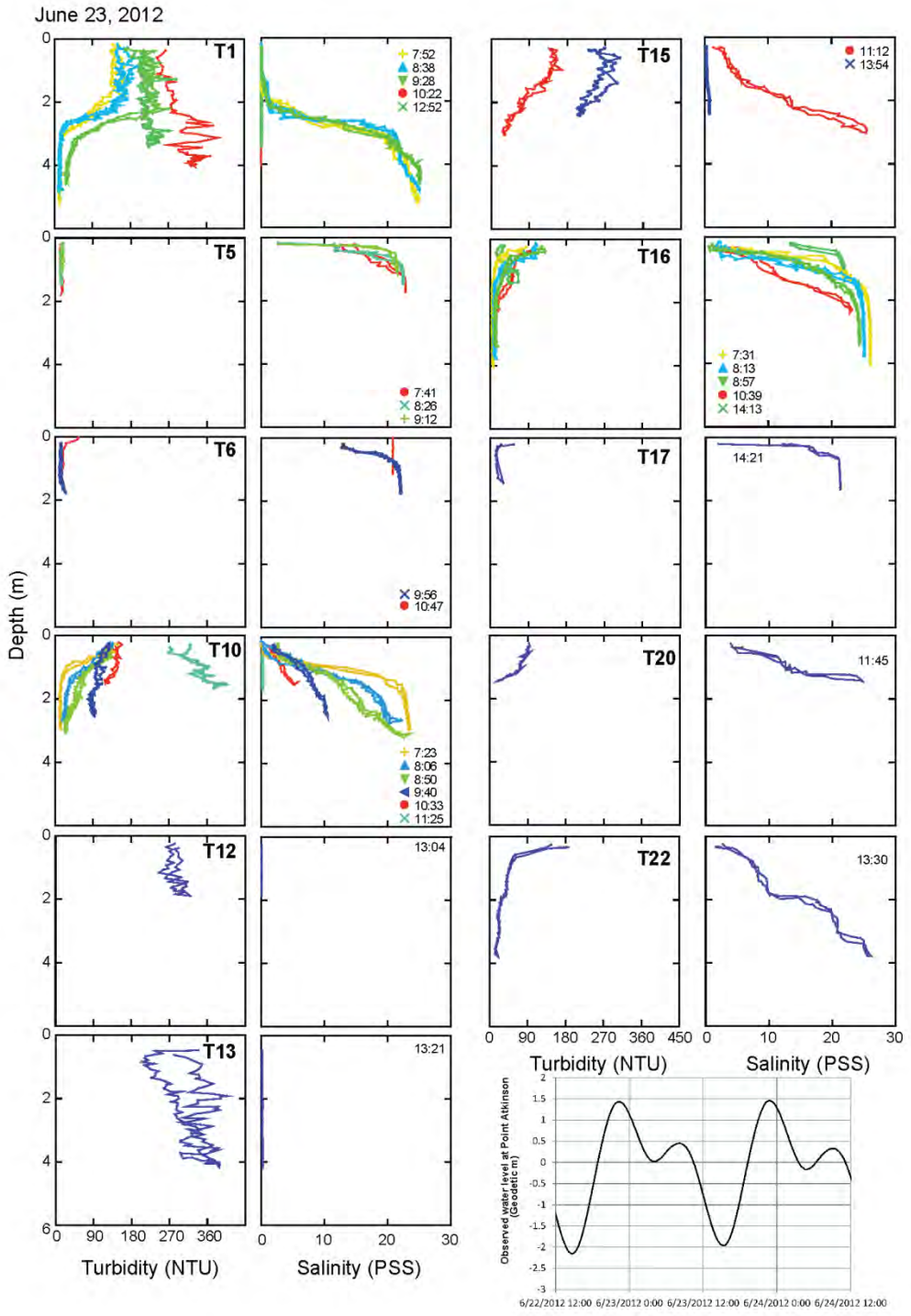

Figure 22: **Turbidity and salinity profiles collected on June 23rd, 2012 at select locations across the Roberts Bank tidal flats. The tide curve during the period of measurement is also shown.**

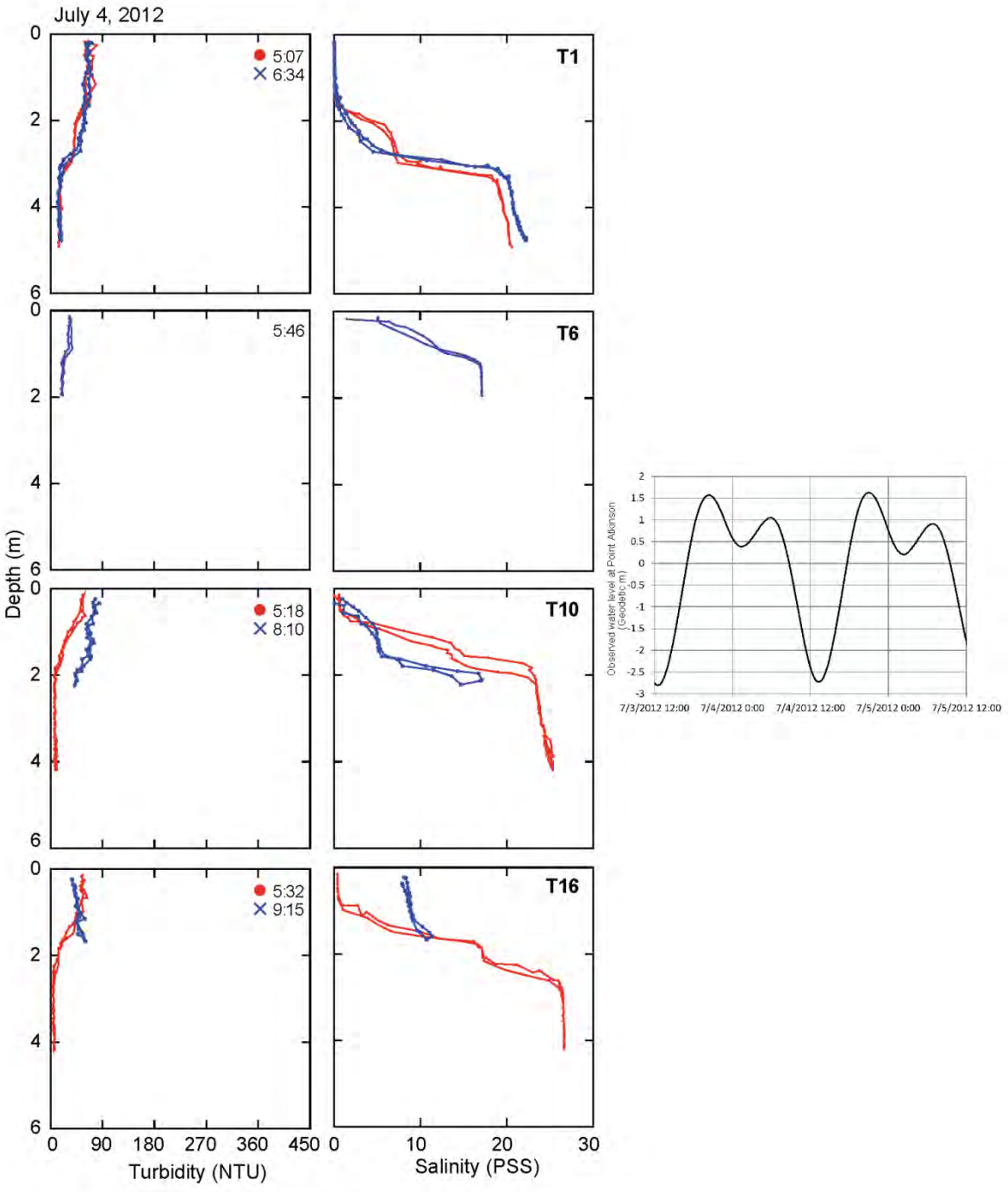

Figure 23: **Turbidity and salinity profiles collected on July 4th, 2012 at select locations across the Roberts Bank tidal flats. The tide curve during the period of measurement is also shown.**

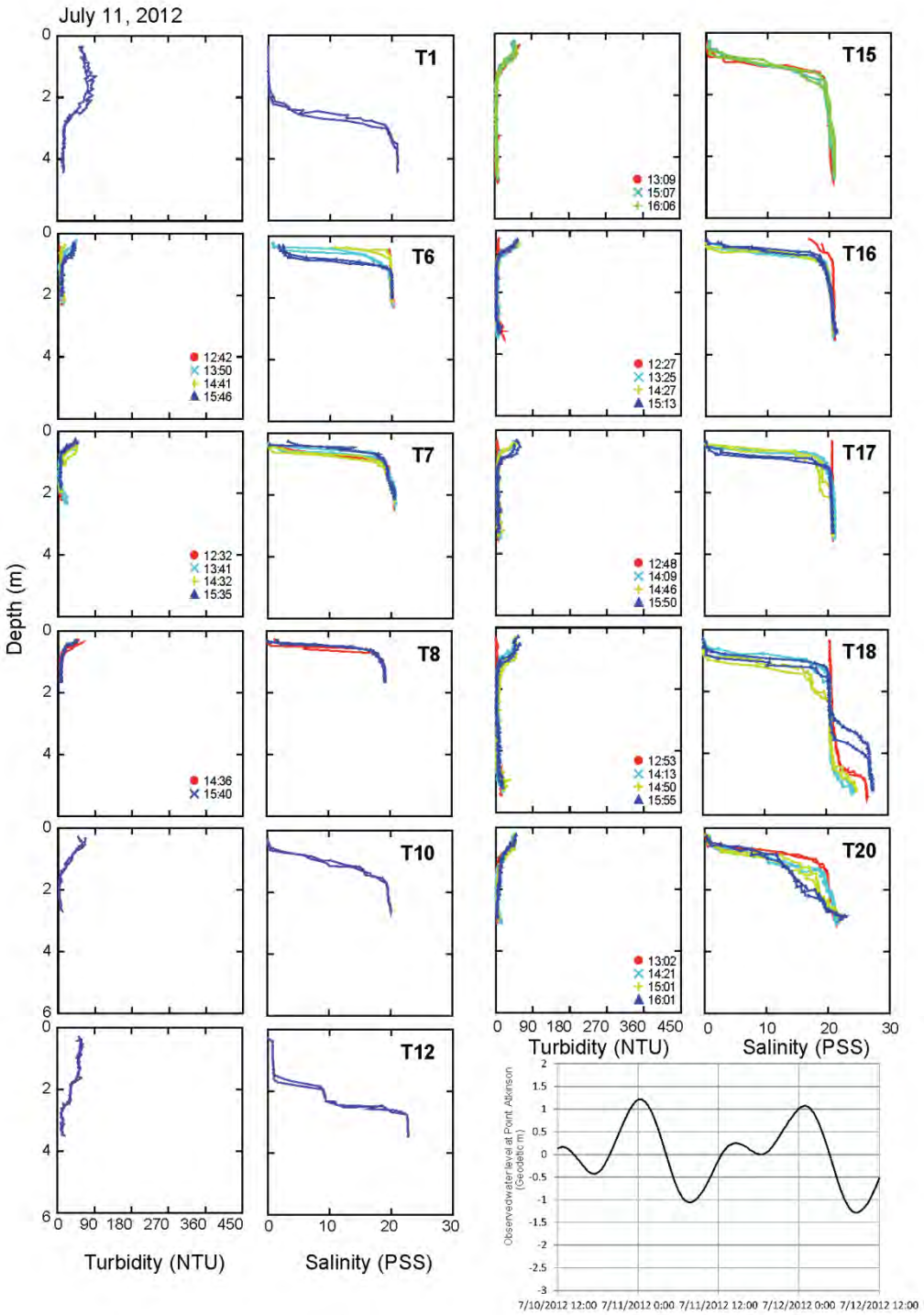

Figure 24: **Turbidity and salinity profiles collected on July 11th, 2012 at select locations across the Roberts Bank tidal flats. The tide curve during the period of measurement is also shown.**

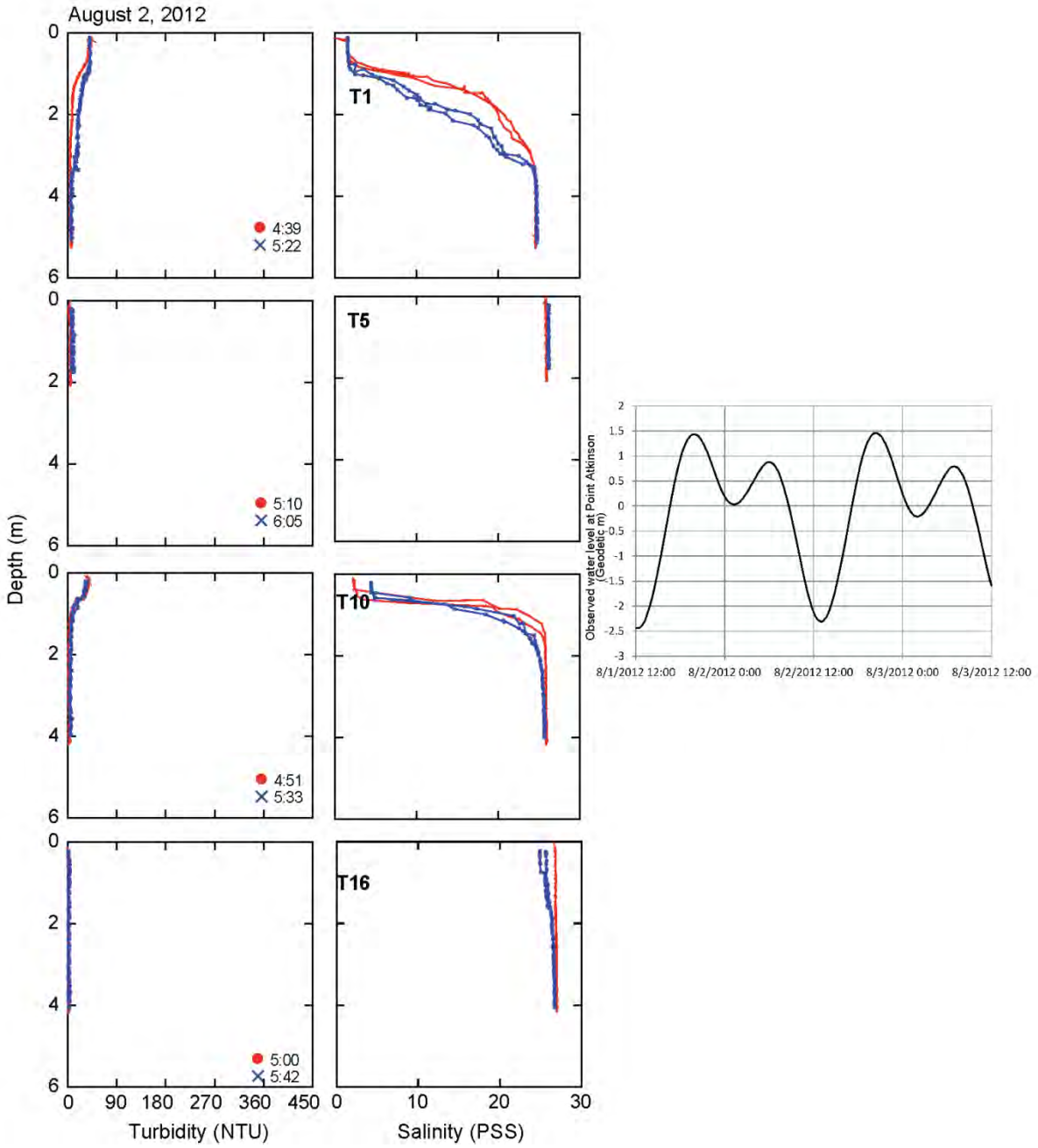

Figure 25: **Turbidity and salinity profiles collected on August 2nd, 2012 at select locations across the Roberts Bank tidal flats. The tide curve during the period of measurement is also shown.**

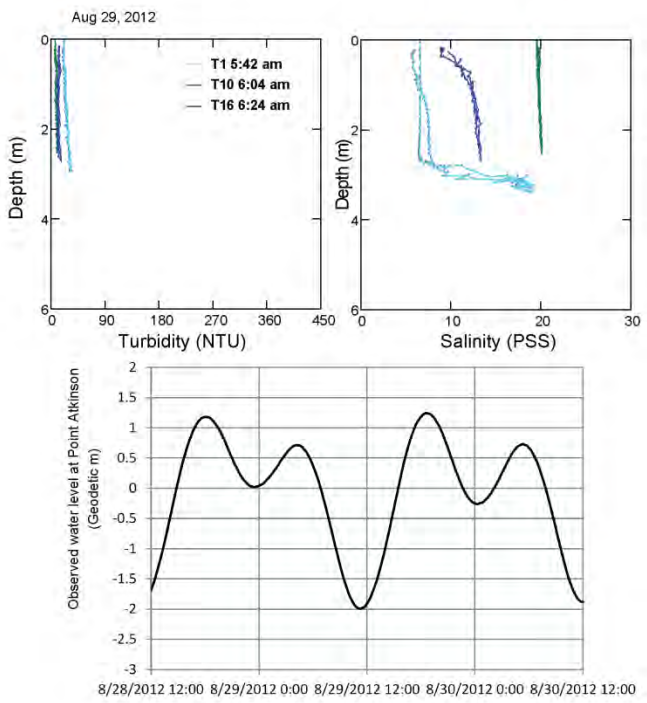

Figure 26: Turbidity and salinity profiles collected on August 29th, 2012 at select locations across the Roberts Bank tidal flats. The tide curve during the period of measurement is also shown.

Water samples at a subset of the sites were collected during the profiling work using a DH-48 hand-held sampler that was held near the surface until the sample bottle was nearly full. Concurrently, the Manta2 turbidity sensor collected data at the same water depth. Average turbidity values were calculated for each water sample, and the total suspended solids (TSS) and grain size distribution were then measured by NHC in the lab. These results were used to develop a turbidity-TSS relation for this portion of the Roberts Bank tidal flats (**Figure 14**). Turbidity-TSS relationships tend to vary depending on the specific characteristics of the suspended particulates (for example, based on the relative proportions of biogenic versus geogenic particulates), and as such, differ between Canoe Passage and Roberts Bank. The main reason the curves differ is likely due to the additional sand that is mobilized in Canoe Passage where water velocities were considerably higher, especially at higher turbidity conditions associated with higher river flows.

2.4 SALINITY AND CONDUCTIVITY MEASUREMENTS

As with the turbidity measurements, the objective of collecting salinity measurements was to examine the existence of a salt wedge within Canoe Passage and to document the salinity pattern across Roberts Bank and how it changes with time during freshet conditions. The salinity sensor at the Canoe Passage site provided continuous data along the river bank, while profile measurements

across Roberts Bank provided spatially variable data. Both data series were used to calibrate and validate numerical models.

The locations of the measurements across the tidal flats targeted specific tidal features while also providing a suitable spatial distribution of sampling locations (**Figure 17**). The Manta2 sonde was also used to collect salinity measurements down-profile at one-second intervals within the water column (**Figure 18** to **Figure 26**). These salinity profiles were collected on various dates between April and August 2012 (June 12, June 14, June 20, June 23, July 4, July 11, August 2, and August 29).

A set of salinity profiles was also collected at the HADCP cross-section (**Figure 2**) to measure variation with depth on November 14th, 2012. This was done using a C4E-15 Digisens conductivity probe; the attached Campbell datalogger and a level-logger recorded corresponding water depths.

Salinity data was also collected at a fixed location along the river bank of Canoe Passage with the C4E-15 Digisens conductivity probe. It was installed beside the HADCP on May 8th, 2012 and continuously recorded salinity data until September 8th, 2013, after this date it was not maintained and the probe has likely become partially fouled by sediment. **Figure 15** shows the extended time-series of salinity in Canoe Passage.

2.5 EROSION AND DEPOSITION MEASUREMENTS

Contemporary rates of erosion and deposition in the area of Roberts Bank that critical to an understanding of the stability of the tidal flats but were not established in detail from existing studies prior to commencing the coastal geomorphology study. Thirty Depth of Disturbance (DoD) rods were installed in the tidal flats on the north side of the Roberts Bank causeway on June 4th, 2012. DoD rods were installed in groups of 10 to monitor erosion and deposition in three separate regions of the tidal flats (**Figure 27**): (i) the lower flats, which are only exposed during tides lower than approximately 1 m CD; (ii) the middle flats seaward of the biomat region, which include soft muddy sediments and outlet channels from the ‘mumblies’ in the upper tidal flats; and (iii) the upper tidal flats, which include biofilm and biomat regions near the shoreward dyke where water often ponds following a high tide above 4 m CD. Rods were installed in pairs in the biomat area to measure both the top surface and the deeper channels. DoD rods were assigned a letter designating relative location (L-Lower, M-Middle, U-Upper) and a sequential number.

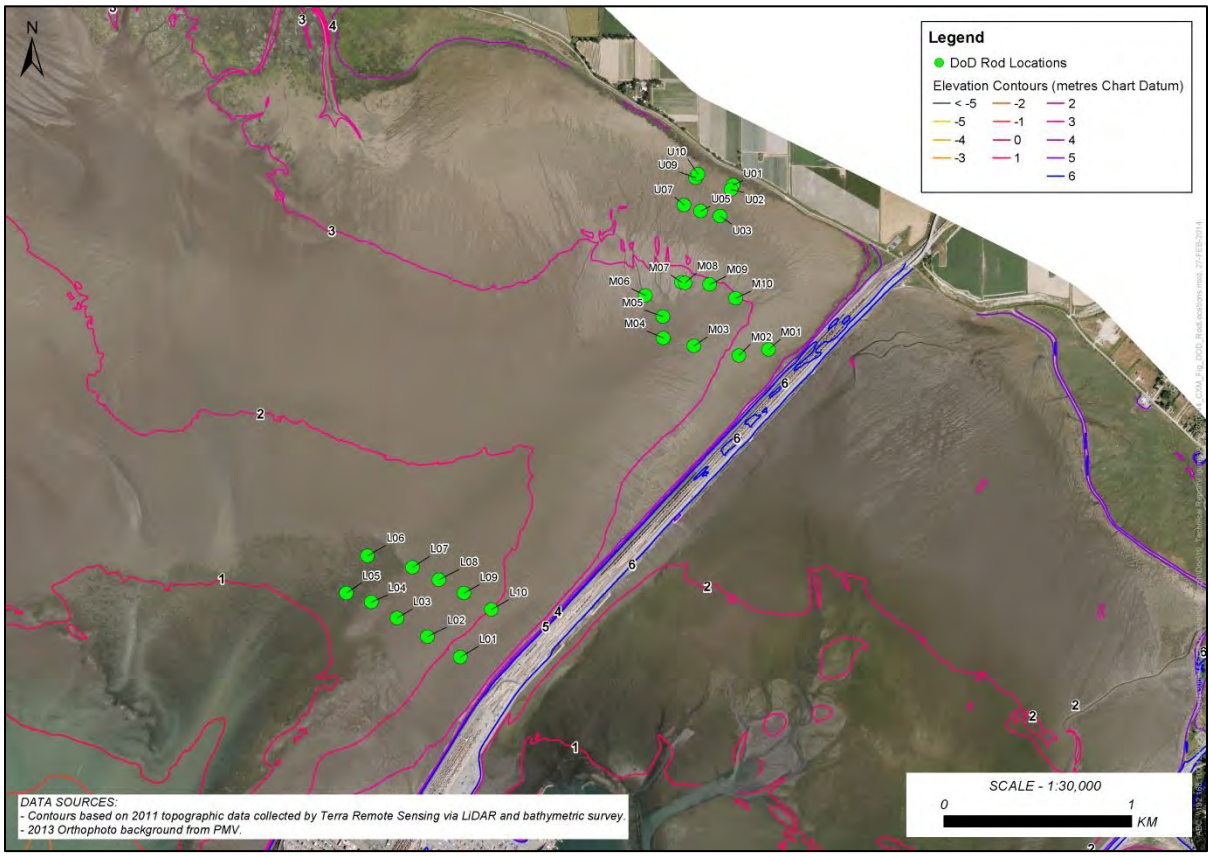

Figure 27: Location of Depth of Disturbance (DoD) Rods on Roberts Bank.

Conventional depth of disturbance rods consist of a length of metal conduit that is embedded into the tidal flats and a large flat disk with a central hole (essentially a washer) is placed over it, flush with the ground. The initial distance from the top of the rod to the disk is recorded at the time of installation. If the ground is lowered as a result of scour, the distance from the top of the rod to the disk will increase over time. If deposition occurs, the sediment buries the disk (**Figure 28**).

The DoD rods were monitored, initially at approximately one-month intervals but at increasing time intervals, from deployment in early June to determine the magnitude of erosion and deposition. DoD rods were initially installed on June 4th, 2012 and then monitored on July 3, July 31, August 30, October 17, December 12, 2012 and January 9 and May 30, 2013, providing seven dates for comparison. The initial one-month monitoring interval was increased after the end of the Fraser River freshet season because the magnitude of change at most DoD rod locations was found to be quite small.

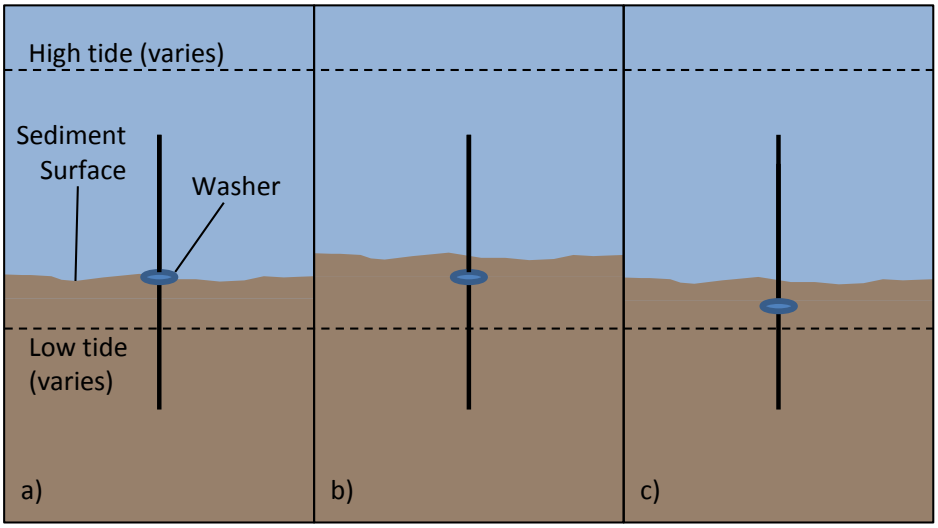

Figure 28: Schematic illustrating DoD rod monitoring; a) shows initial installation, b) shows subsequent deposition, and c) shows erosion with subsequent deposition.

Vegetation was observed to have accumulated around the DoD rods on a seasonal basis related to growth and die off of the various plant species found at Roberts Bank. The presence of vegetation was photo-documented, and the height of the accumulation was recorded. The plant matter was then carefully removed by hand to expose the bare sediment underneath and allow measurement of the washer height.

During the July and August field visits, a majority of the DoD rods had accumulated large mats of marine vegetation that included filamentous weed and eelgrass (*Z. marina*) fronds. These mats generally measured between approximately 1 and 4 square meters and were on average approximately 15 cm thick at the base of the rod. It is likely that the significant accumulations of marine vegetation have an effect on the measurements; for instance, there were observations of local scour of the tidal flat sediment seemingly in response to some of the large accumulations of weed on certain rods in the lower grouping (L-series). Another expected effect is that, in some instances, the vegetation protected the rods from waves, currents, and sediment deposition, masking the natural processes.

Although this technique of assessing short-term changes in erosion and deposition on the tidal flats worked well in the inter-causeway area of Roberts Bank (e.g. (Hemmera et al. 2012), the greater exposure and higher prevalence of marine vegetation in the RBT2 study area have introduced unexpected challenges. The results of the DoD rod monitoring, therefore, can only provide supplementary evidence for drawing conclusions about the stability of the tidal flats.

Table 6 summarizes the changes on the tidal flats during the monitoring program. Statistics on the range of the elevation change over the complete period are shown, in addition to the differences between summer and winter. Positive values denote deposition while negative values represent erosion or scour. As expected, there is more deposition over the summer period related to the

growth of biomat and ensuing trapping of fine sediment. In winter, erosion is a more dominant process associated with the storm season.

Changes in elevation also vary depending on the position of the DoD rod groups relative to shore. The lower tidal flats are more affected by waves and characterized by ripple bedforms, which results in larger elevation changes, in both a positive and negative direction. The upper flats have been separated in **Table 6** into ridge, runnel and biofilm as their unique biophysical character impacts ground elevation differently. For instance, sediment and vegetation moving into the runnels with the incoming tide can wrap around the rods and promote deposition at these sites. As well, the quiescent nature of the biofilm-dominant area seaward of the 'mumblies' makes it suited to deposition. Overall, however, based on the average values, there is little positive or negative change in the tidal flat surface over the 12-month monitoring period. Caution should be exercised in extending these results to the broader region of the tidal flats as there are potentially localised effects caused by the rod itself. For instance, localised scour around the rod can occur in certain circumstances that is not reflective of the general conditions.

Table 6: Statistics associated with change in DoD Rod elevations measured on different parts of the tidal flats between June 2012 and May 2013.

	ELEVATION CHANGE (cm)				
	LOWER FLATS	MIDDLE FLATS	UPPER FLATS		
			Ridge	Runnel	Biofilm
Maximum	4.7	3.0	0.8	8.4	2.5
Minimum	-5.0	-2.7	-0.4	-0.9	-1.1
Average	-0.4	0.0	0.1	2.0	0.2
Summer average	0.0	0.2	0.2	2.5	
Winter average	-1.3	-0.3	0.1	1.3	

2.6 BED SEDIMENT SAMPLING

To assess whether the ridge and runnel complex is accreting or eroding, sediment cores were collected on April 24th, 2013 and May 27th, 2013, and profiles collected on August 6th, 2013.

2.6.1.1 APRIL 24TH, 2013 SEDIMENT CORING

A short hand-corer with an inside diameter of 1 ¾" was used to collect three cores from Roberts Bank and two cores from the inter-causeway area (**Figure 29**). The corer, equipped with a Plexiglas liner, was pushed vertically into the soft sediments (**Figure 30**) at select locations on the top of ridges and at the bottom of runnels. The distance along the outside of the corer tube, from the sediment surface to the top of the corer was measured. In addition, the equivalent distance was measured within the corer tube to provide the basis for calculations of the amount of sediment

compaction. A small volume of water, sourced from nearby standing water, was poured into the top of the corer tube to assist with extraction of the sediment core from the tube. Once the tube was pulled out from the ground, the liner containing the core was capped at its bottom. Before capping the cores, the water was poured out from the top of the tube while ensuring no loss of silt. The cores were placed in a freezer and remain there as the compaction observed in the field was substantial and not suitable for further analysis.

A schematic of the cores and their relative location is shown in **Figure 31**. The cores originate from two types of morphologies. Three were collected from the ridges, which are raised areas dominated by silt/clay and some fine sand. They are typically about 0.6 m higher than the runnels. At a depth equivalent to the elevation of the runnels (0.6 m), medium sand was typically encountered, a strata that continues with depth. The remaining two cores were collected in the runnels (small channels) and are almost entirely composed of medium or fine sand.

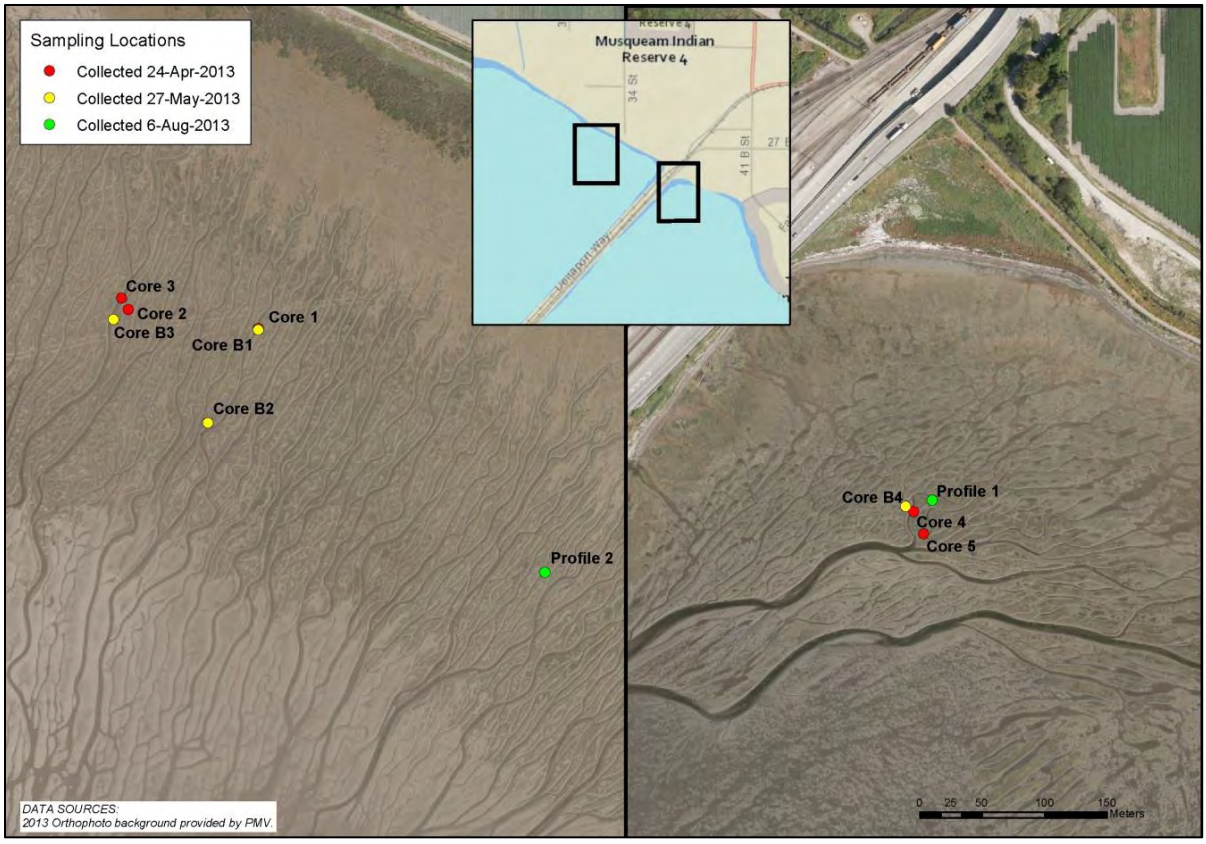

Figure 29: **Overview map showing the sites at which sediment cores and profiles were collected within the ridge and runnel complex at Roberts Bank.**

Figure 30: **Sediment core being collected from the top of one ridge in the ridge and runnel complex (Core 2) using a short hand-corer.**

Core 1: Likely entirely fine sediment, hit hard surface at bottom, and didn't push deeper. 0.54 m of sediment compacted to 0.26 . Compaction factor 2.1:1

Core2: pushed through sand. Assuming sand compress same as core 3, Mud compaction factor is 3.1:1

Core 3: mostly sand, some softer portions, but still much harder than mumblie portion

Core 4: Fairly soft, sand layer felt. Assuming sand compaction is same as core 5, mud compaction factor is 4.7:1. When pouring water out of core surface sediments were not disturbed (indicating no mobile silt present; unlike area north of causeway). Sediment appears to be eroding.

Core 5: In channel, mostly sand. Compaction factor 1.5:1.

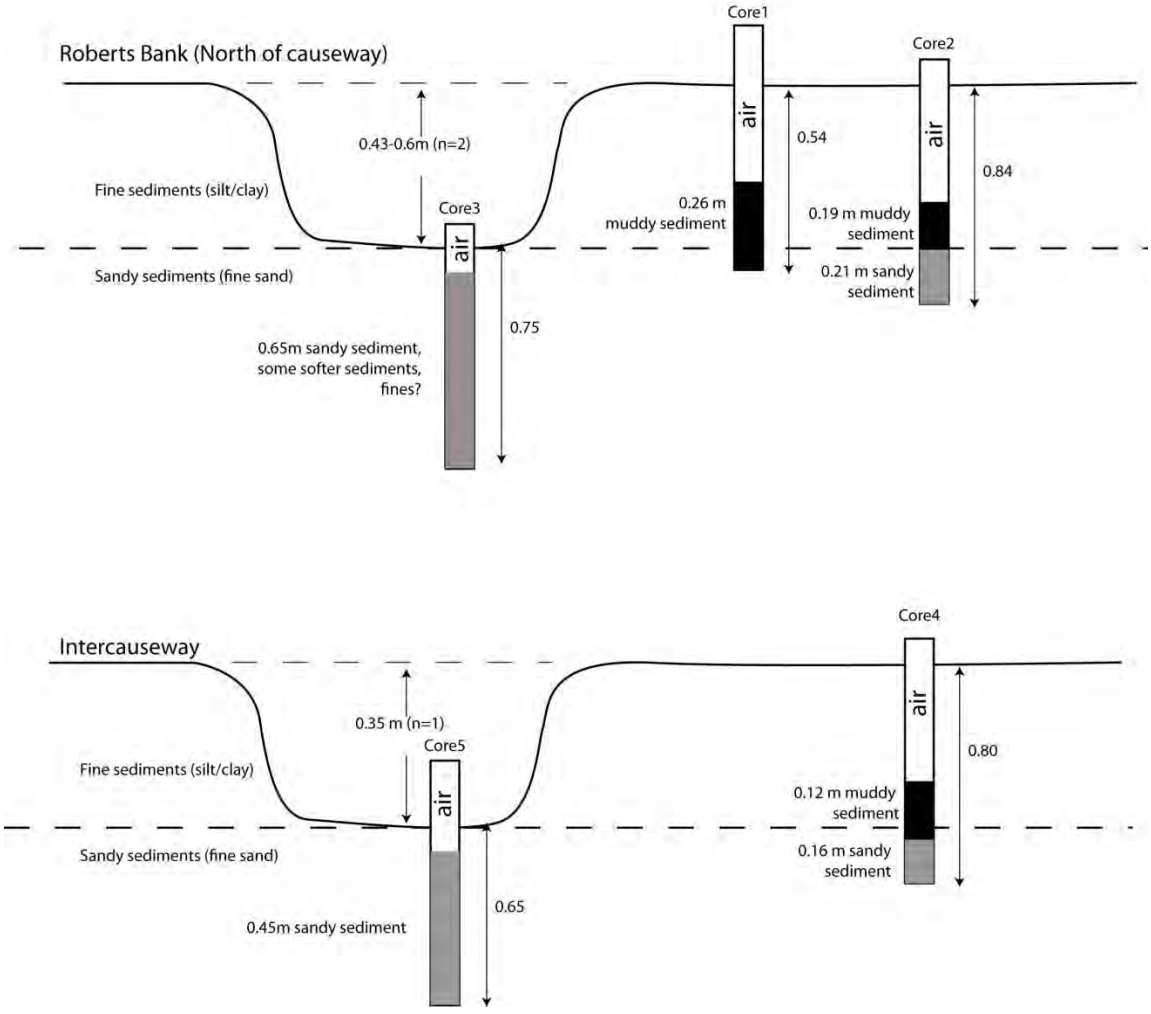

Figure 31: Schematic showing the cores collected at Roberts Bank and their relative locations.

2.6.1.2 MAY 27TH, 2013 SEDIMENT CORING

On May 27th, 2013, a second set of cores were extracted from the ridge and runnel complex with a three-inch diameter corer to reduce the amount of compaction observed. At the same time, soil pits were excavated into the mud flats to better examine the substrate. These observations are summarized in **Figure 32**. The sampling was carried out in a similar area as on the previous date. Soil pits were also excavated into the sediment to assess the substrate, and sand was clearly evident in the bottom of the pits, at elevations similar to that of the adjacent runnels.

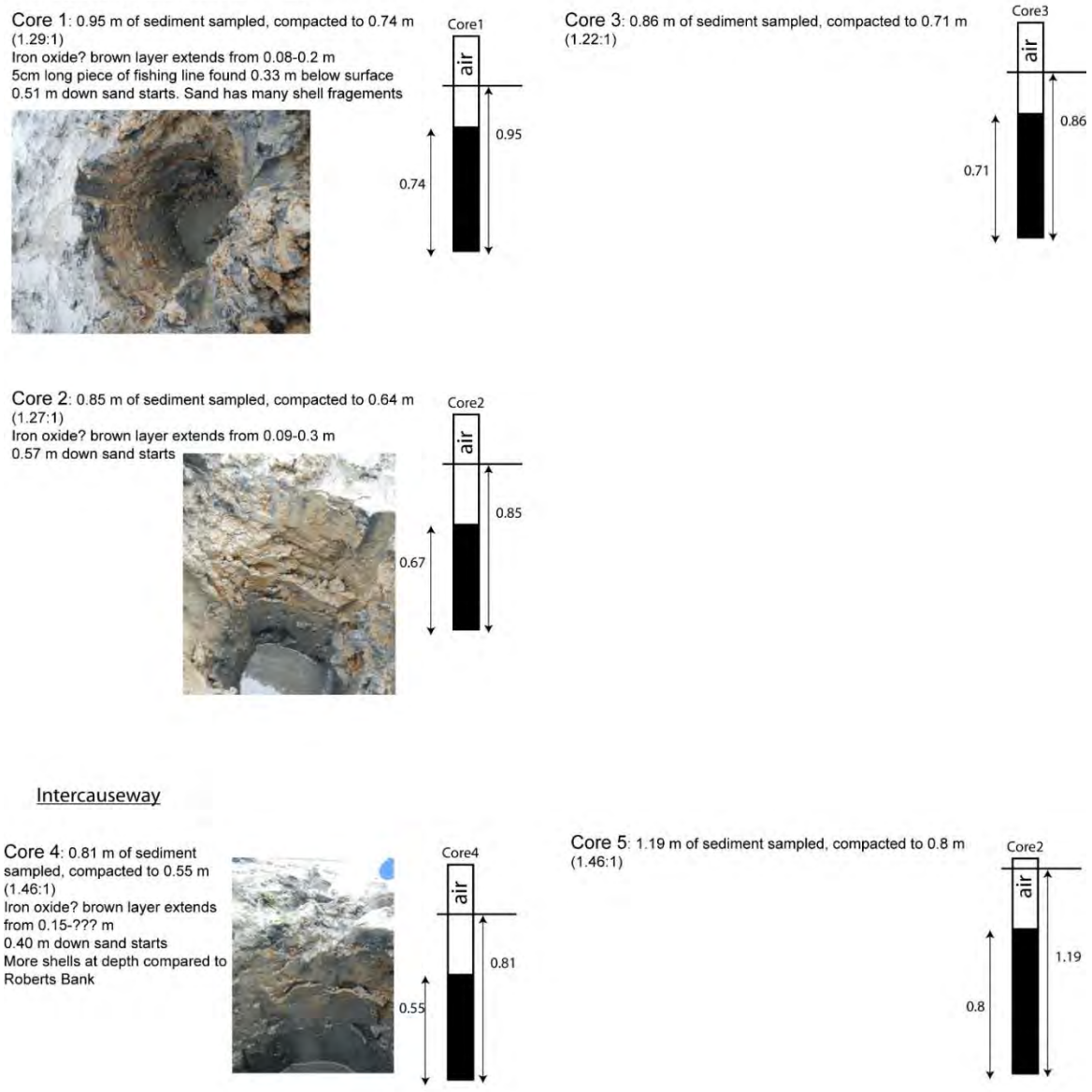

Figure 32: Observations of sediment cores and profiles collected from the ridge and runnel complex on May 27th, 2013.

2.6.1.3 AUGUST 6TH, 2013 SEDIMENT PROFILING

To provide a better estimate of sedimentation rates, a new set of samples was collected on August 6th, 2013 by excavating soil pits and sediment sampling down-profile. This sampling method was chosen so as to avoid the issue of compression of sediment associated with core collection. The sampling procedure consisted of using half-cylinder to retain the rest of the soil while removing 2 cm slabs of sediment with a spatula. Each slab of sediment was sub-sampled using three rings of known diameter and thickness (11 mm) (**Figure 33**). This approach ensured that there was no cross-contamination or compaction and that the initial volume of sediment associated with each sample was known (39 cm^3). Plots of bulk dry density for the two profiles are shown in **Figure 34** and illustrate a similar pattern of increasing density with depth.

To determine sedimentation rates, both ^{137}Cs and ^{210}Pb dating techniques were applied as these are commonly used for marine sediments in the region (Lavelle et al. 1986, Williams and Hamilton 1995, e.g. Johannessen et al. 2008), and they provide two independent means of assessing sedimentation. The ^{137}Cs approach was made possible by the atmospheric fallout of the radioactive isotope, which was first produced in 1954 and peaked in 1963 due to nuclear testing. Since then, its concentration has diminished but it continues to be produced. The benefit of this approach is that a certain layer of sediment is assigned a date, thereby providing an average sedimentation rate since 1964 to the overlying sediment. As such, a constant rate of sediment accretion is not required. The main disadvantage of the approach is that biomixing can result in an overestimate of the sedimentation rate from ^{137}Cs being mixed down-core (Johannessen and Macdonald 2012).

The ^{210}Pb approach is based on the continuous fallout of this isotope from the atmosphere. Once produced, ^{210}Pb decays at a constant rate, and as a result, its concentration in depositional environments decreases with depth. The rate at which the amount of ^{210}Pb decreases with depth, along with the half-life of ^{210}Pb, can be used to determine the sedimentation rate. This approach is commonly applied assuming a constant sedimentation rate (which may not be the case here because of the installation of causeways), and the amount of ^{210}Pb in the sediment can depend on grain size as this isotope tends to be preferentially retained in finer grained deposits. The initial sampling showed a distinct grain size shift at depth, and as a result, the validity of the ^{210}Pb results was initially uncertain. For this reason, both ^{137}Cs and ^{210}Pb approaches were used.

Figure 35 shows the concentrations of ^{137}Cs in the sediment from the two sites, and there is a distinct ^{137}Cs peak present in both profiles. In Profile 1, a negative value occurs below the peak, suggesting that this sediment layer dates to before 1954. At both sites, the grain size changes from a mud to sand just below the spike in ^{137}Cs, and this shift likely represent a discontinuity associated with the completion of the Deltaport and BC Ferries causeways in 1967 and 1960 respectively.

Figure 33: **Half-cylinder being used to retain the sides of the excavated pit while removing 2 cm slabs of sediment with a spatula. Each slab of sediment was sub-sampled using rings of known diameter and thickness.**

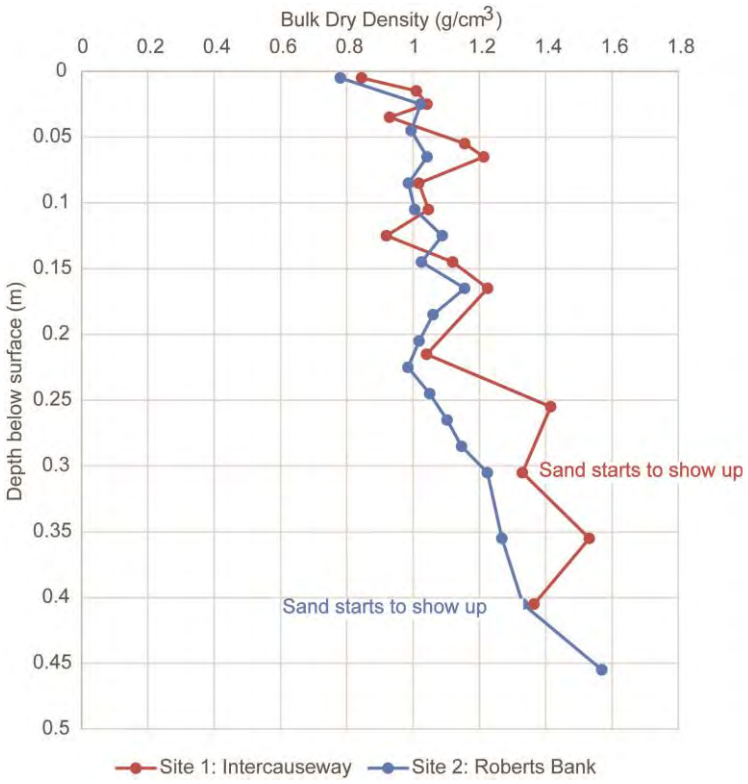

Figure 34: **Bulk density observed for sediment profiles from the inter-causeway and north of the causeway ("Roberts Bank") sites.**

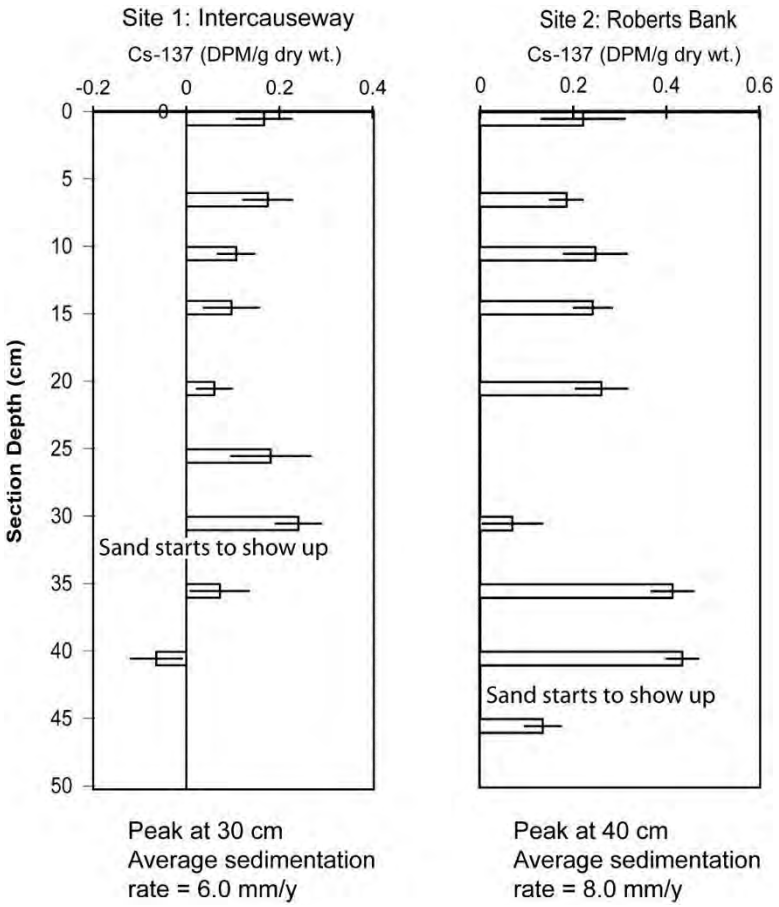

Figure 35: **^{137}Cs analysis results from two cores collected north of the causeway ("Roberts Bank") and in the inter-causeway area. Error bars represent one standard deviation of uncertainty.**

To calculate excess ^{210}Pb, two samples of ^{226}Ra were collected from each profile: one sample from near the surface, and the other, near the bottom. The data from these samples and total ^{210}Pb (**Figure 36**) shows that the ^{226}Ra activity is similar at the surface and near the bottom of the profile At the inter-causeway site, the ^{210}Pb concentration reached background levels at the bottom of the profile (41 cm), whereas at the site north of the causeway, the ^{210}Pb concentrations were very close to background at a depth of 46 cm. The average ^{226}Ra for each core was used to determine the excess ^{210}Pb activity, which is plotted in **Figure 37**.

In the profile for Site 1, located in the inter-causeway area, there is no evidence of surficial biomixing layer in the ^{210}Pb data; however, at 30 cm below the surface, there is a significant discontinuity in the ^{210}Pb profile. This occurs at the same location where the sand appears in the profile. At Site 2, located north of the causeway, the top 10-15 cm suggests that a biomixing layer may exist. Alternatively, a change in sedimentation rate may be the cause of the break in the profile observed at about 15 cm. For the purposes of this analysis, two different biomixing interface depths

were considered (10 cm and 15 cm), and for each, a different sedimentation rate was calculated using the approach provided by Lavelle et al. (1986). The resulting profiles and sedimentation rates are shown in **Figure 37**. Similar to the inter-causeway results, a break in the profile is observed at the depth where sand begins to appear (40 cm).

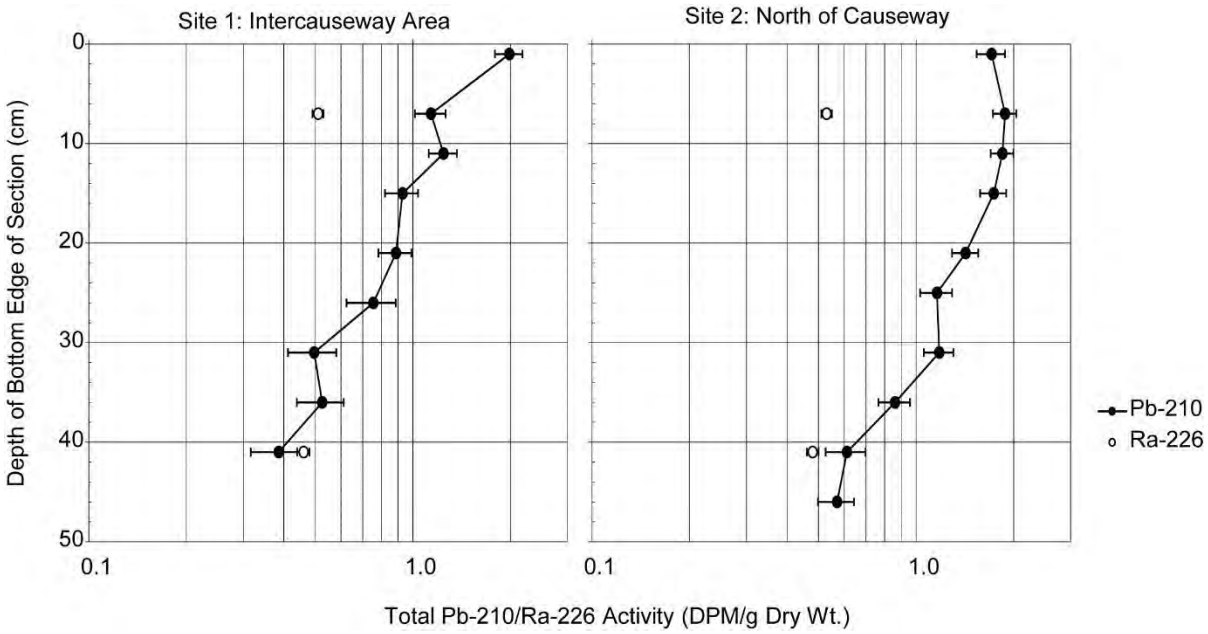

Figure 36: Total ^{210}Pb and ^{226}Ra activity from two cores collected at Roberts Bank in 2013.

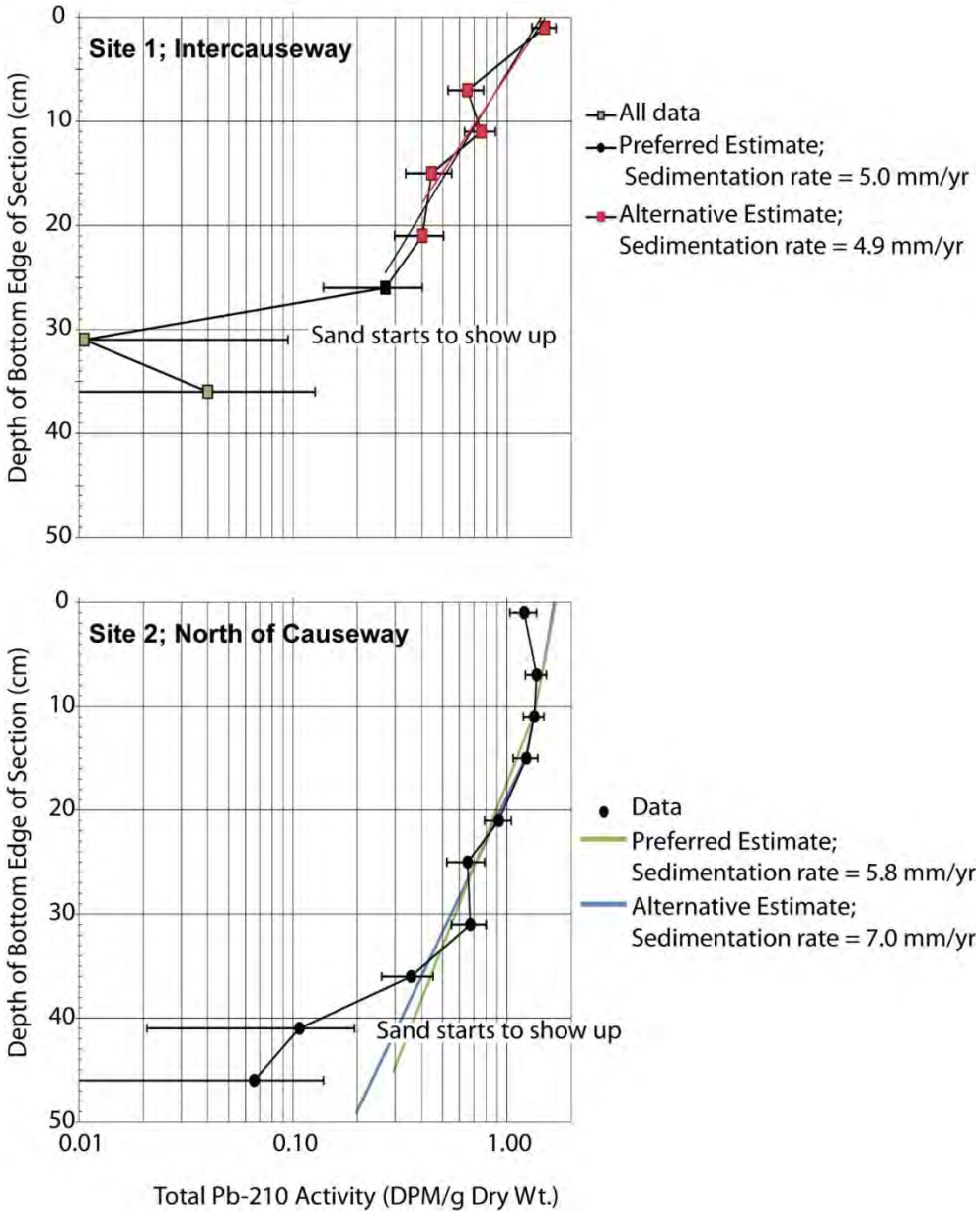

Figure 37: ^{210}Pb data from two cores collected at Roberts Bank in 2013.

2.7 WAVE AND CURRENT MEASUREMENTS

Wind-generated waves are one of the main geomorphic mechanisms that form and maintain the tidal flats as well as control sediment grain size. The collection of data describing the wave environment at Roberts Bank is important to understanding the mobilization and transport of sediment along the foreshore.

2.7.1 NON-DIRECTIONAL WAVE MEASUREMENTS

Three RBR Virtuoso wave recorders were installed on July 4th, 2012, at locations chosen to sample the wave environment on the north side of the Roberts Bank causeway (**Figure 38**). Waves were measured along a transect running from deeper (W1) to shallower (W3) water (**Figure 39** and

Table 7). This transect allows for characterization of the changing wave environment through the transition from the delta front to the mid-intertidal environment.

Figure 38: Location of non-directional wave recorders at Roberts Bank.

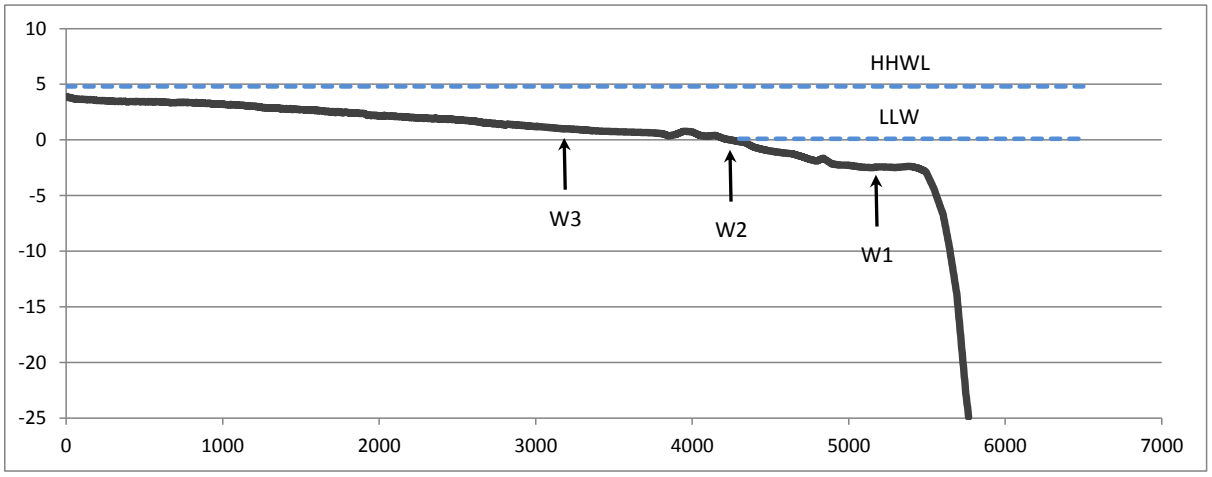

Figure 39: **Elevation profile across tidal flats showing the relative location and depth of the three wave recorders. HHWL and LLW denote Higher High Water Level and Lower Low Water.**

Table 7: **The location and depth of the three wave recorders.**

Wave Recorder	Location (UTM)	Depth (mean tide)
W1	10 U 485297 5429850	5.6 m
W2	10 U 486234 5430726	3.1 m
W2b	10 U 486319 5430340	3.1 m
W3	10 U 486901 5431445	2.1 m

The wave recorders were rated to a maximum depth of 20 m and provided an accuracy of ±0.01 m. They were programmed to collect tidal measurements every 15 minutes, as well as take burst samples of waves. The bursts consist of 4096 samples taken at 6Hz, which is long enough for detection of low-frequency waves while the high sampling rate will catch high frequency waves. With a 6 Hz sampling frequency, the Nyquist frequency is 3 Hz, indicating that waves with a period as short as 0.3 s could theoretically be sampled. Wave direction was not measured by these instruments but was measured periodically using the AWAC and ADCP instruments (see below).

Initially, each of the three recorders was installed in a protective PVC housing and lodged within a concrete weight with a float attached to allow for retrieval from a boat (**Figure 40**). The weights had aluminum spreader feet to increase their stability and prevent the instrument from being overturned or moved during large wave events. During subsequent site visits to download the wave data, W1 and later, W2, could not be located. W1 was not found even after commercial divers were tasked with retrieving the instrument. W2 was located a distance away from the installation site on a subsequent site visit, and may have moved during high tide event in September 2012. The

replacement sensors that were installed on November 14th, 2012 were fitted with a timed-release buoy and tether system (**Figure 41**), which reduced the likelihood of future tampering by limiting the amount of time that the retrieval buoy is at the surface. **Table 8** provides a summary of wave sensor downloads, and **Figure 42** provides a summary timeline of recorded wave data, including data collected with the AWAC and ADCP instruments.

Figure 40: **A wave recorder housed in a black PVC tube and lodged in a concrete weight and ready for deployment. The aluminum feet increase the stability of the concrete weight to prevent rolling of the recorder.**

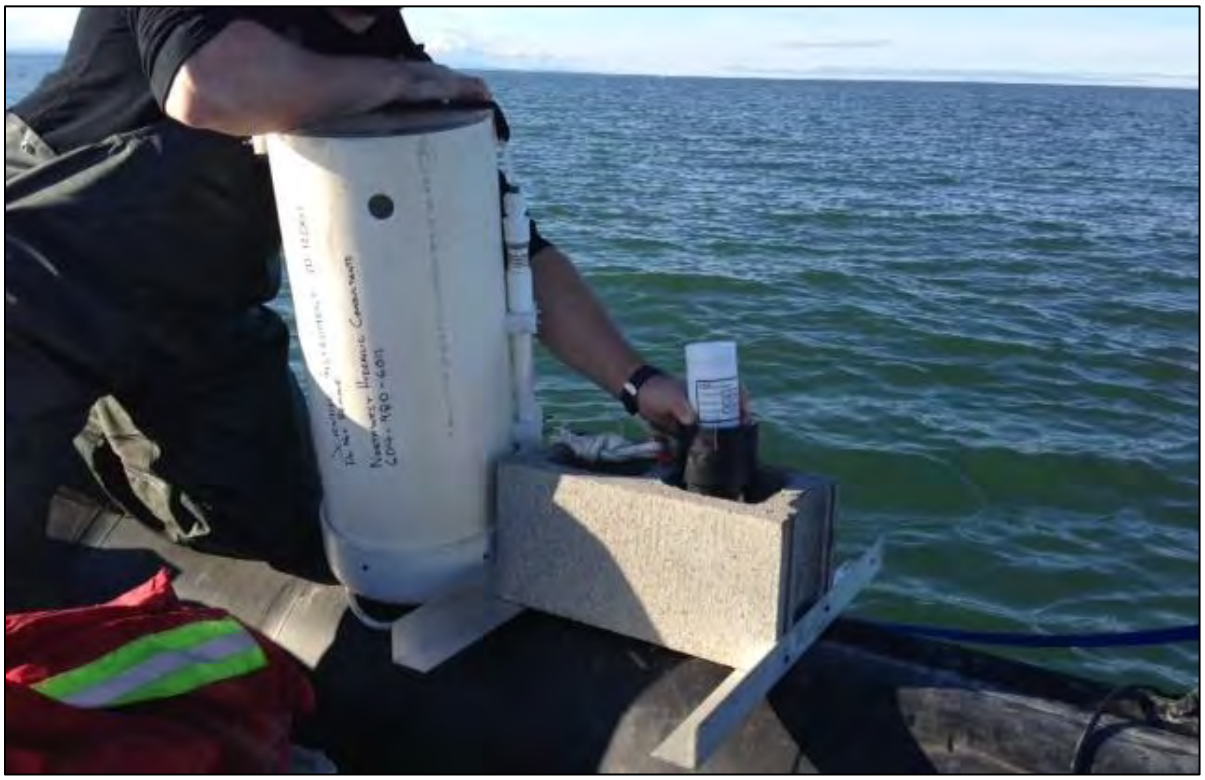

Figure 41: **Wave recorder mount fitted with a timed-release buoy (inside the white housing) and tether.**

Table 8: **Summary of RBR wave recorder downloads.**

Date	Field Visit Notes
July 4, 2012	Initial sensor deployment
July 11, 2012	Interim sensor download
August 2, 2012	Sensor download
August 29, 2012	Sensor download – W1 missing
October 10, 2012	Sensor download – W2 missing
November 14, 2012	Sensor download (W2 located off-target) and all re-deployed
December 10, 2012	Sensor download – W1 missing
December 12, 2012	Sensor re-deployment – W1
January 8, 2013	Sensor download – W2 missing
February 7, 2013	Sensor download
March 7, 2013	Sensor download (W1 recovered prior and re-deployed)
April 4, 2013	Sensor download and retrieval

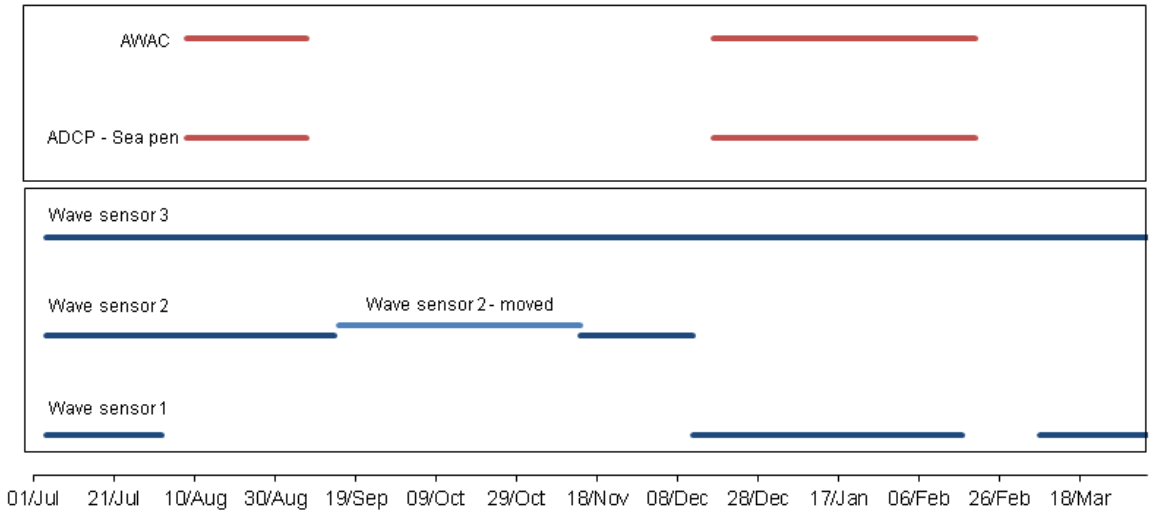

Figure 42: Summary timeline of recorded wave data.

Currents and waves were also measured using a 600 kHz Teledyne RDI Acoustic Wave and Current Profiler (ADCP) and a 1,000 kHz Nortek Acoustic Wave and Current profiler (AWAC). The instruments were deployed between August 8th and September 9th, 2012 on bottom frame moorings by ASL Environmental Sciences (ASL) and detailed in Birch and Mudge (2012). A second monitoring program was carried out in the winter period to measure the effect of storms on waves and currents. This deployment spanned from December 17th, 2012 to February 20th, 2013. NHC was tasked with the analysis of the data that was collected by these instruments. **Figure 43** shows the significant wave heights recorded at the three locations on the tidal flats in the winter 2013-2013 period.

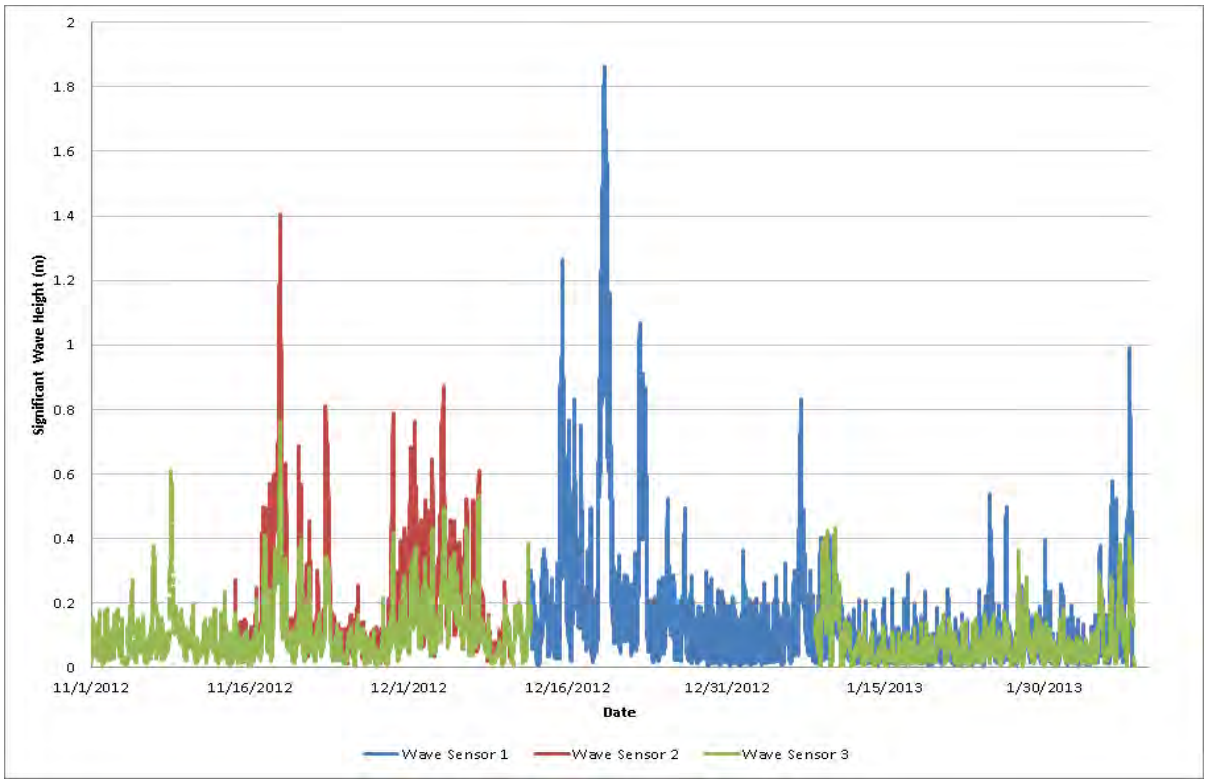

Figure 43: Significant wave heights recorded at Wave Sensor 1, Wave Sensor 2 and Wave Sensor 3 locations on the tidal flats from November 2012 to February 2013.

2.7.2 AWAC AND ADCP MEASUREMENTS

The location of the AWAC and ADCP is shown in **Figure 44**. **Figure 45** shows their positions relative to the wave sensors. As can be seen in the figure, W1 and the AWAC and ADCP are exposed to waves coming from similar directions. W2, and more so, W3 are protected from certain waves by the tidal flats of Roberts Bank to the north and Deltaport terminal to the south. As such, the wave energy at these sites is reduced due to both physical shadowing and the effects of shoaling.

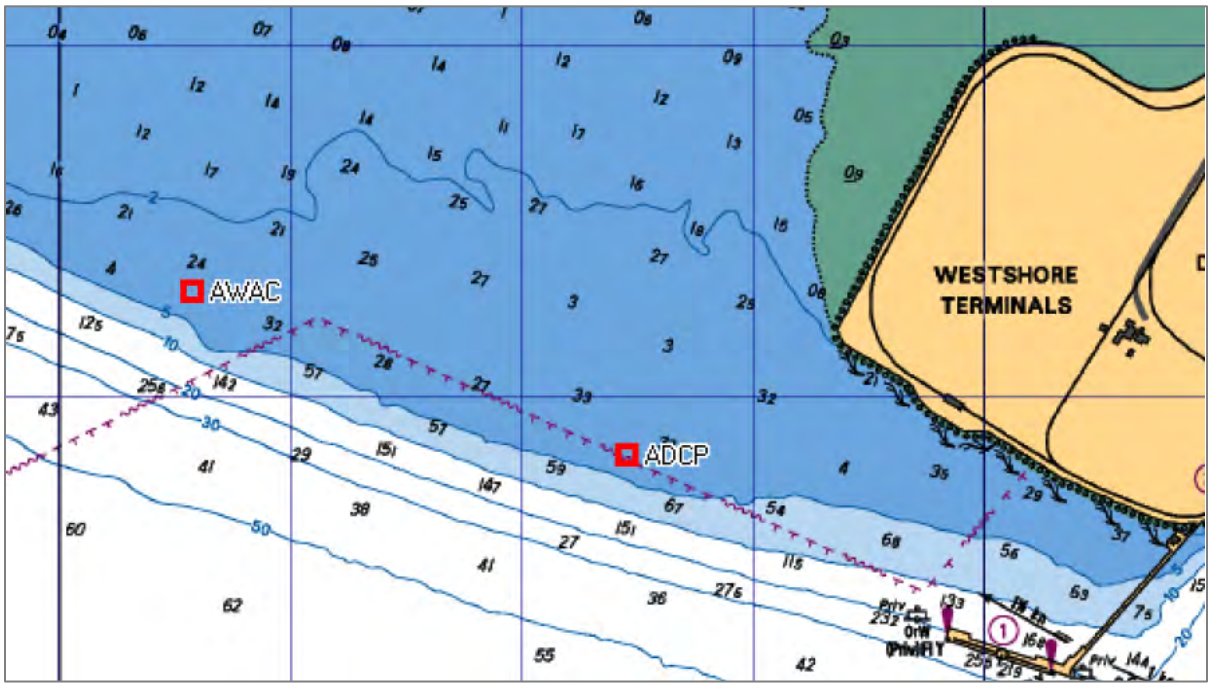

Figure 44: **Location of AWAC and ADCP (from Birch and Mudge 2012).**

Figure 45: **Location of ADCP and AWAC wave and current sensors in the study area. The approach angles of waves that arrive at the sensor without significant shoaling are illustrated.**

Both the AWAC and the ADCP measure waves and currents using similar technology. Sound energy is transmitted into the water column and the Doppler shift is measured from the energy returned to the instrument that is reflected by particles at various locations in the water column. This is then resolved into a three-dimensional velocity vector that describes the motion of each 'bin' – or section of the water column. The water column is divided into bins (or cells) having a vertical height that is dependent on the resolution of the instrument and the total depth of water. Bins are grouped into an ensemble with a blanking distance immediately above the instrument and immediately below the water surface where no measurements are collected (**Figure 46**). A vertical beam measures the location of the water surface directly.

Current profiles were recorded every 10 minutes. In order to collect these, the ADCP was set up with a bottom blanking distance of 1.61 m and a bin size of 0.5 m. A 3D measurement of the velocity was recorded for each bin, the first one being centered at 1.86 m above the bed. The AWAC was set up with a blanking distance of 0.9 m and a bin size of 1 m; the first bin was therefore centered at 1.4 m above the bed. The current magnitude and direction were extracted from each 3D measurement.

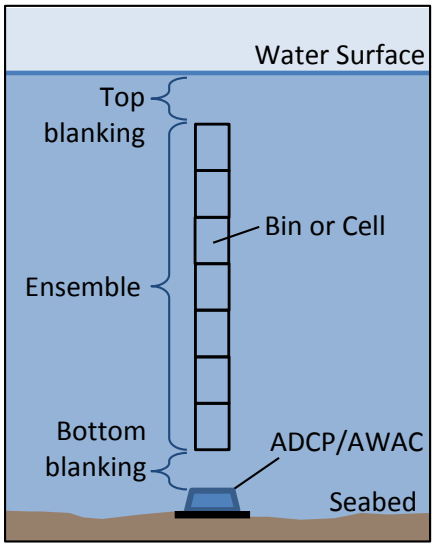

Figure 46: Schematic diagram illustrating the collection of data using an ADCP or AWAC.

For the wave measurements, a set of 2,400 samples were collected with a frequency of 2 Hz every hour with the ADCP. Analysis of each dataset (of length about 20 min) provided the significant wave height and peak wave period. The minimum wave period that could be resolved was 1.05 s. The peak wave direction was then computed by combining the vertical beam data to the other beam velocities. For the AWAC, 1,024 samples (and 2,048 samples in the second deployment) of the water surface location were collected at a frequency of 1 Hz (2 Hz in the second deployment) for each wave measurement. Significant wave height, peak wave period and direction were computed in a similar way as the ADCP measurements. The minimum wave period that could be resolved was 2 s.

2.8 PHOTO COLLECTION

2.8.1 OVERFLIGHT PHOTOS

Oblique airphotos of the study area were collected from a fixed-wing aircraft on July 13, 2011. Low tide level on that date at the Tsawwassen station (#7590) was 0.6 m CD. Approximately 250 photos were collected from three separate vantage points on the airplane.

On July 22, 2013, another overflight was carried out to coincide with the summer low tides. The low tide on this date was 0.4 m CD at Tsawwassen. Two sets of photos taken from different directions out of the aircraft provided a total of about 2,300 photos, with one set at higher-resolution (6.5 MB photos).

Coastal geomorphologists and numerical modellers on the study team participated in both flights to view features of interest to their respective sub-areas of study.

2.8.2 GROUND PHOTOS

Ground photos were also taken during various field data collection activities, such as DoD rod monitoring and sediment coring.

3 REFERENCES

Birch, R., and T. Mudge. 2012. Sea Pen Study, Roberts Bank, Summer 2012 - QA-QC of ADCP, AWAC and CTD Data Collected by ASL. Report prepared by ASL Environmental Sciences, Victoria, BC.

Environment Canada. 2013. Environment Canada - Water - Fresh Water Quality Monitoring. <http://aquatic.pyr.ec.gc.ca/fraserriverbuoy/default.aspx>. Accessed 8 Jan 2014.

Hemmera, NHC, and Precision. 2012. Draft – Adaptive Management Strategy 2011 Annual Report, Deltaport Third Berth, Delta, BC. Report prepared by Hemmera Envirochem Inc., Northwest Hydraulics Consultants and Precision Identification for Port Metro Vancouver, Vancouver, BC.

Johannessen, S. C., and R. W. Macdonald. 2012. There is no 1954 in that core! Interpreting sedimentation rates and contaminant trends in marine sediment cores. Marine Pollution Bulletin 64:675–678.

Johannessen, S. C., R. W. Macdonald, C. A. Wright, D. P. Shaw, and A. van Roodselaar. 2008. Joined by geochemistry, divided by history: PCBs and PBDEs in Strait of Georgia sediments. Marine Environmental Research 66:S112–S120.

Lavelle, J. W., G. J. Massoth, and E. A. Crecelius. 1986. Accumulation rates of recent sediments in Puget Sound, Washington. Marine Geology 72:59–70.

McLean, D. G., M. A. Church, and B. Tassone. 1999. Sediment transport along lower Fraser River 1: Measurements and hydraulic computations. Water Resources Research 35:2533–2548.

McLean, D. G., and B. Tassone. 1988. Budget of the Lower Fraser River. Page 16 *in*. Federal Inter-Agency Committee on Sedimentation, 5th International Conference. Las Vegas, Nevada.

NHC. 2008. Fraser River Hydraulic Model Update. Report prepared by Northwest Hydraulic Consultants for the BC Ministry of Environment.

Williams, H. F. L., and T. S. Hamilton. 1995. Sedimentary Dynamics of an Eroding Tidal Marsh Derived from Stratigraphic Records of 137Cs Fallout, Fraser Delta, British Columbia, Canada. Journal of Coastal Research 11:1145–1156.

APPENDIX D

CAUSEWAY CONTAINMENT DYKE SEEPAGE STUDY

TABLE OF CONTENTS

LIST OF EQUATIONS

LIST OF TABLES

LIST OF FIGURES

1 INTRODUCTION

The Roberts Bank Terminal 2 Project (the Project) is a proposed new multi-berth container terminal that would provide additional container shipping capacity. The Project is part of the Container Capacity Improvement Program (CCIP), Port Metro Vancouver's long-term strategy to deliver projects to meet anticipated growth and demand for container capacity until 2030.

Port Metro Vancouver retained Hemmera to undertake environmental studies related to the Project. This appendix forms part of a technical report that describes the results of the Coastal Geomorphology Study effects assessment undertaken by Northwest Hydraulic Consultants Ltd. (NHC).

Three methods were used to assess the physical response of Roberts Bank to the proposed development:

1. Interpretive geomorphic studies using historical data, site observations, and measurements;
2. Analytical methods; and
3. Numerical modelling of tidal currents, waves, and sediment transport.

The Coastal Geomorphology Study that was undertaken by NHC identified a potential issue with respect to seepage of tidal water through the causeway containment dyke that would be constructed during the construction phase as part of the causeway widening. The report contained within this appendix describes a detailed study that was undertaken to quantify seepage flow through the containment dyke during ebbing tide conditions and determine potential changes to coastal geomorphology that might result, as well as investigate options to mitigate those changes. The results of this study contribute to the effects assessment that is part of the Coastal Geomorphology Study.

1.1 STATEMENT OF THE ISSUE

According to the Modified Preliminary Design included in Section 4.0 (Project Description) of the Environmental Impact Statement (EIS), the causeway expansion requires the construction of a 5.2-km long pervious rock-filled containment dyke to be built in two stages (**Figure 1**). Dyke CD1 will be built in the lower tidal flat (seaward of station 22+000 m) and, once completed, dyke CD2 will be built in the upper (shoreward) 2 km (between stations 20+000 and 22+000 m).

The dyke will be pervious and so seawater is expected to temporarily fill the area between the dyke and the existing causeway in response to tidal fluctuations – both because of flow through the dyke as well as flow around the end of the dyke during construction. Furthermore, water levels on the shoreward side of the dyke are expected to be out of phase with those on the seaward side, leading

to residual seepage flows draining to the exposed tidal flats during an ebbing tide. The effect is expected to continue only until the storage area is filled with sediment to construct the widened causeway.

Figure 1. Plan view showing location of containment dykes and stationing.

Water draining through the terminal containment dyke to the exposed tidal flats during the construction phase of the Deltaport Third Berth Terminal (DP3) resulted in erosion of the sediments and formation of channels (Hemmera et al. 2008). **Figure 2** shows that discharge along the toe of the dyke was not uniform and that the flow was captured by small channels that quickly joined to form fewer but larger channels immediately offshore of the dyke toe. The channels ceased to be active once the terminal area was filled with sediment. Based on this prior occurrence, the potential for erosion of the tidal flats and formation of channels associated with the causeway expansion for the RBT2 Project was investigated in detail.

Figure 2. Seepage flow through containment dyke at DP3 and induced tidal flat erosion (18 April 2007).

1.2 SCOPE OF WORK

The purpose of this detailed investigation is two-fold:

1. To determine the amount and timing of seepage flows through the containment dyke, focusing primarily on the period when seepage flows may discharge on to the adjacent tidal flats when they are exposed during an ebbing tide; and
2. To determine change to coastal geomorphology (e.g. erosion and channel formation) that would result from the seepage flows.

The detailed study area for this investigation lies completely within the local study area (LSA) of the Coastal Geomorphology Study (see **Section 1.2 Scope of Work** of the Coastal Geomorphology Technical Report). **Figure 3** shows the extent of the 2-dimensional model domain, which defines the detailed study area.

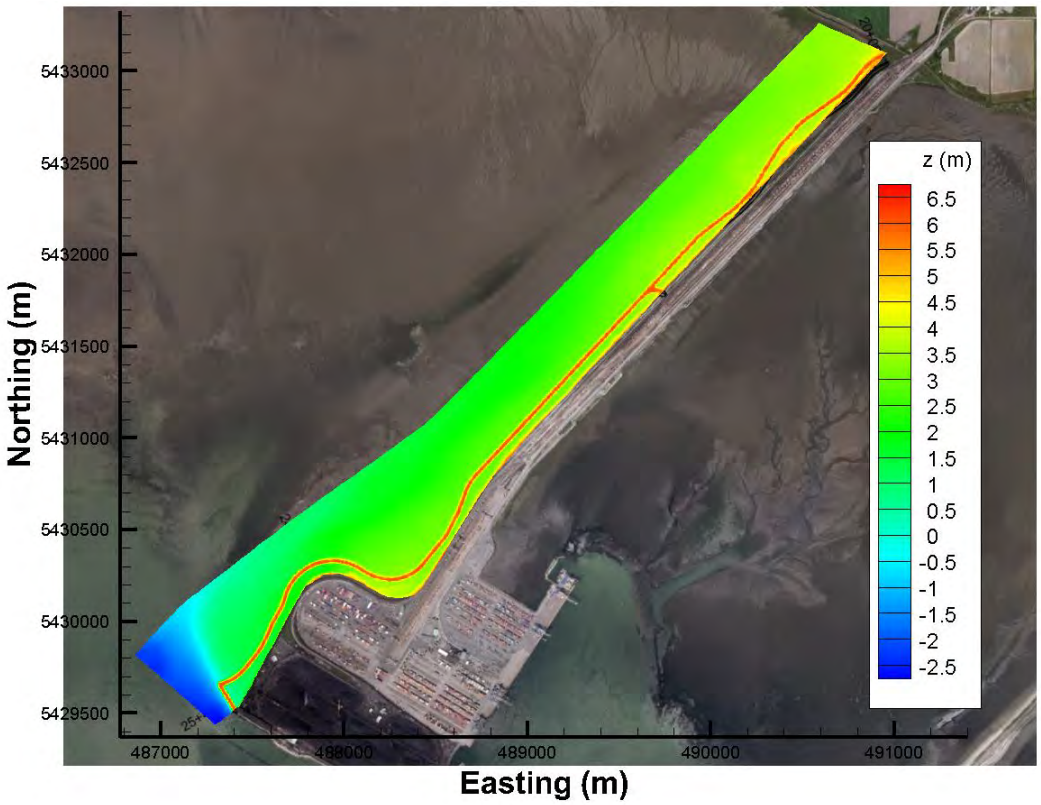

Figure 3. River2D model domain of causeway expansion showing containment dyke.

1.3 METHOD OF APPROACH

The technical issues associated with this investigation are complex. Tidal fluctuations in the Strait of Georgia govern water levels and extent of inundation on Roberts Bank, which in turn determine the timing of when seepage flows onto the exposed tidal flats occur. Seepage through the dyke is determined, in part, by the physical properties of the dyke core material, as well as the difference in height of water on either side of the dyke.

Based on a review of dyke and dam seepage problems, the technical problem of calculating seepage flow through the proposed causeway perimeter dyke is unique and there is no published example of a similar study. Existing methodology exists for calculating seepage flow through dams, but the assumption of static water surface is not applicable. Further complicating the calculations, is the fact that the elevation of the toe of the containment dyke varies along the causeway so that some sections of the dyke toe may be under water while other sections are exposed above the tide level.

The following methods were used as part of this investigation:

1. Numerical modelling of tides, seepage flow, and channel flow;
2. Analytical methods, such as solving the mathematical functions that describe groundwater flow;
3. Physical laboratory flume experiments; and
4. Interpretive geomorphology.

1.3.1 NUMERICAL MODELLING

River2D is a two-dimensional (2D) model that was used to calculate tidal exchange within the detailed study area, including flow through the permeable containment dyke (Steffler and Blackburn 2002). Although River2D is a surface flow model, it has the unique capability of switching to a depth-averaged groundwater model in areas where the water levels fall below the ground elevation (i.e. become dry). Since the crest of the dyke is always dry above the water level, River2D treats the dyke as porous media while surrounding wet areas (tidal flat and expansion area) are treated using the conventional surface flow equations.

1.3.2 PHYSICAL LABORATORY FLUME EXPERIMENTS

The permeability of gravel, the material specified for the dyke core, is known to vary by several orders of magnitude, with reported values between 10^{-3} and 10^{1} m/s (Fetter 2001). Preliminary calculations demonstrated that the calculation of seepage flow is quite sensitive to the permeability value so it was necessary to measure the permeability of the gravel mixture specified in the preliminary design. Flume experiments were conducted at NHC's physical hydraulics laboratory in North Vancouver.

2 MEASUREMENT OF DYKE CORE PERMEABILITY

Physical model flume experiments were undertaken to measure the permeability of the 4" minus crushed stone that is specified for the perimeter dyke core.

2.1 PHYSICAL MODEL DESCRIPTION

The model was constructed within an existing flume at the NHC hydraulic laboratory in North Vancouver, BC. The flume was approximately 0.9 m in width and height. The trapezoidal dyke was built 2.8 m long at the base and 0.6 m high with an upstream slope of 1:1.5 and a downstream slope of 1:1.75. These dimensions and slopes were established by attaching wooden strips to the sides of the flume, which also reduced the edge effects of the rock material being placed against a smooth wall.

Both upstream and downstream of the dyke there was a 60 degree V-notch weir installed in the flume to measure inflow and outflow discharges (**Figure 4**). Seven pressure taps were installed in the flume, with two of these pressure taps used to record the water levels of the V-notches using a point gauge.

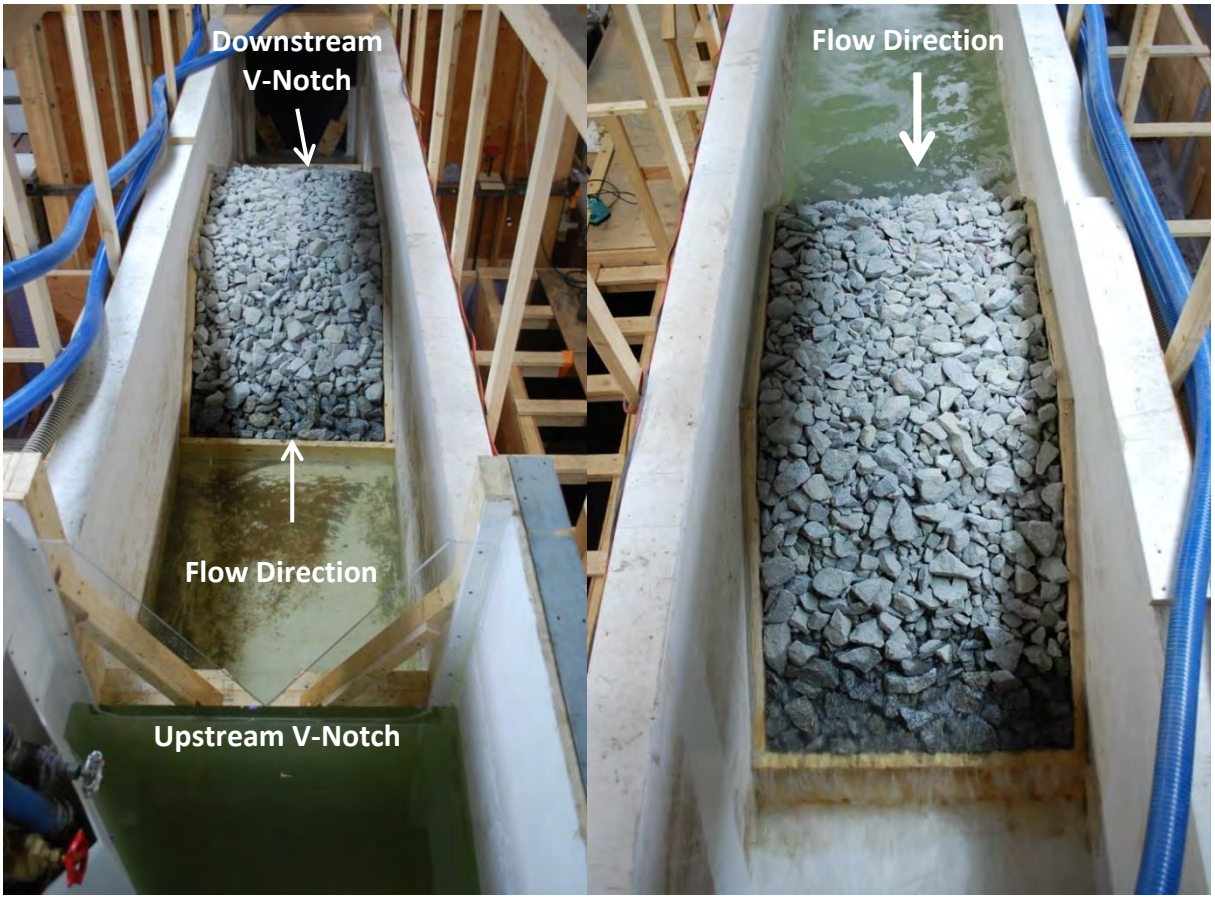

a) View of model from headbox looking downstream, showing general layout and V-notches.

b) View of model from tailbox looking upstream showing the model running with at 0.013 $m^3/s/m$.

Figure 4. Photographs of physical model arrangement used to determine permeability of containment dyke.

2.2 ROCK GRADATION

The Technical Specifications document prepared by AECOM and Klohn Crippen Berger (KCB) as part of the RBT2 preliminary design specifies that the rock core material shall be less than 100 mm with less than 3% fines. The exact rock gradation of the dyke's core material will be determined at the time of construction; but it is expected that rock sizes up to 4" (100 mm) will be present. As a reference, during the construction of the mattress rock for Deltaport Third Berth (DP3), Deltaport

Constructors Ltd. used the rock gradation bounded by the two dashed curves in **Figure 5**, which had grain sizes up to 100 mm and this can be considered as representative of conditions at RBT2[1]. The rock gradation used for DP3 is not a readily available rock mixture that can be purchased directly from a supplier. It was necessary for NHC to match the proposed gradation with the selection of two commercially-available rock gradations. One rock gradation sourced from Mainland Sand and Gravel consisted of a 75 mm Minus with the fines (>5 mm) removed, while the other gradation sourced from LaFarge was a 25 mm - 75 mm Clear Crush. The two rock gradations were mixed 1 to 1 by weight, and a sieve analysis was conducted on the resulting mix used in the physical model and presented in **Figure 5**. The resultant mix of material is slightly coarser than the range used at DP3, but lies within the general range of the preliminary specifications.

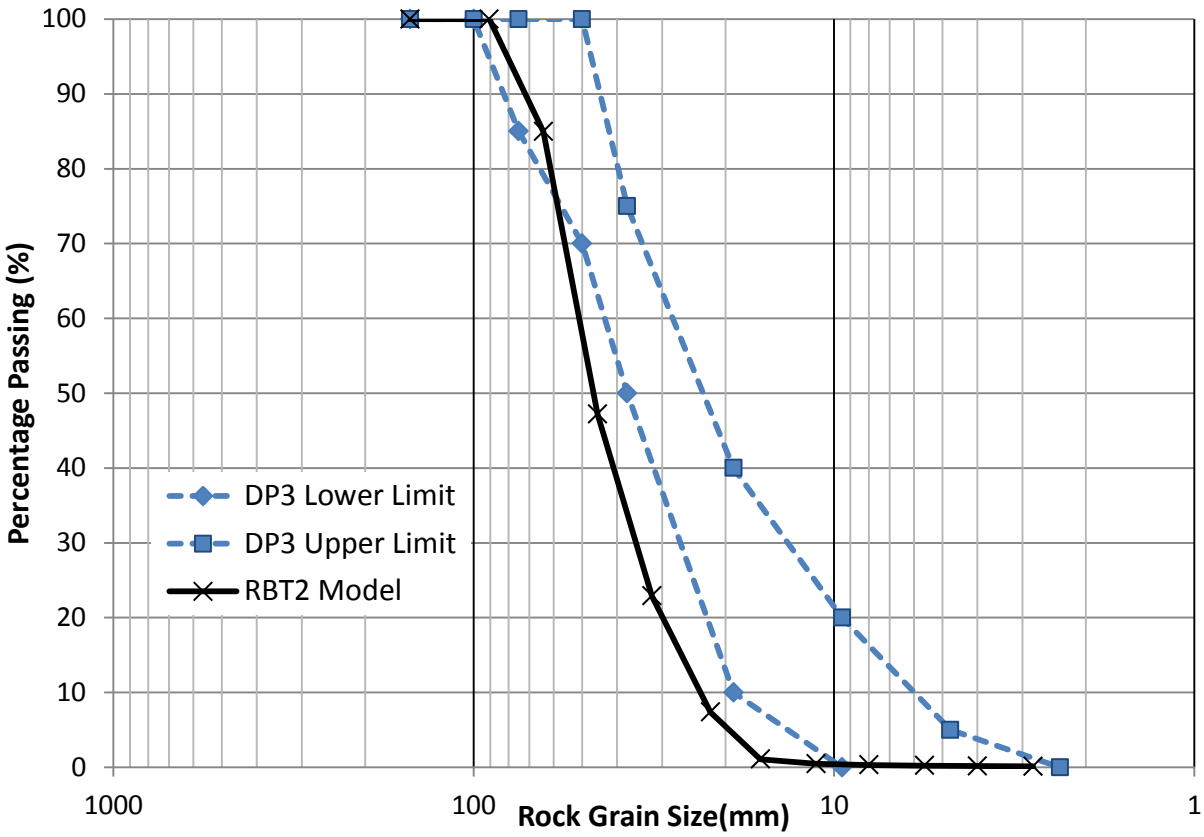

Figure 5. **Rock gradation used in physical model and gradation used previously in Deltaport Berth 3 (DP3).**

[1] A grain size distribution table was provided to NHC by Geoff Cooper, KCB.

2.3 TEST CONDITIONS

Four tests were conducted: three under constant water level (steady-state condition) and one under variable water level (unsteady-state condition). For the steady-state condition tests, the flow through both V-notches was recorded and four water levels were measured, one upstream of the dyke and three within the dyke. The unsteady-state test was started at the highest water level and the pumps were turned off to allow the water to drain through the dyke as the water level fell. Measurements of the decreasing upstream water levels and the flow through the downstream V-notch were recorded at regular time intervals.

2.4 TEST RESULTS

The water levels at the upstream side of the dyke and the corresponding unit seepage discharge q [$m^3/s/m$] through the dyke for the three steady-steady experiments are summarised in **Figure 6**, where H [m] is the water depth upstream, h [m] the water depth downstream and L [m] the seepage length (Casagrande 1937). These measured variables can be related to permeability k [m/s] through Dupuit's equation:

$$q = k\frac{(H_i - h)^2}{2L}$$

Equation 1. Dupuit's equation (referenced in Fetter 2001).

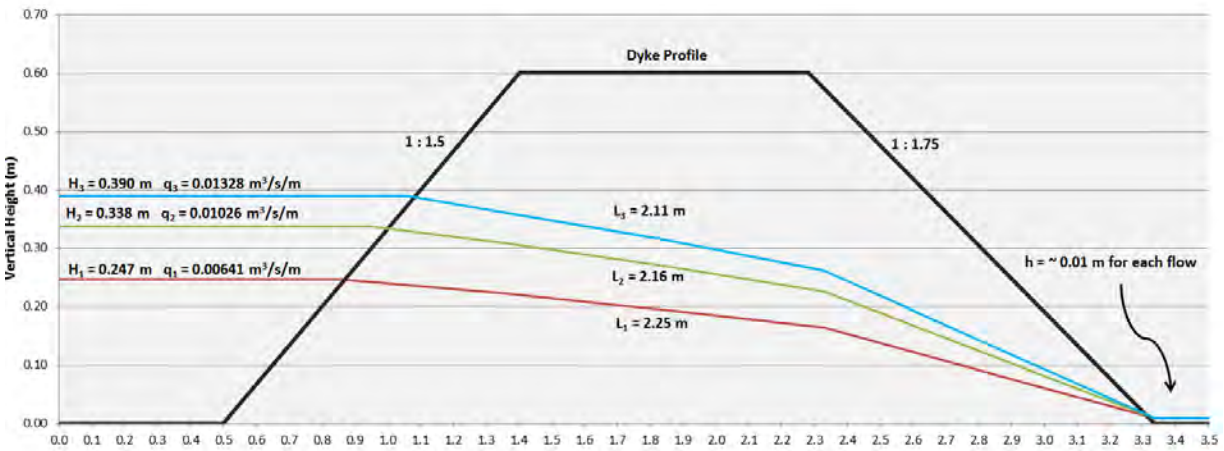

Figure 6. Water levels and discharges measured along dyke profile.

Based on Dupuit's equation (**Equation 1**), if q is plotted against $(Hi - h)^2/2L$ for each test, the slope of the best-fit line will be the average permeability. This is shown in **Figure 7** where $H = (Hi - h)$. The best fit permeability was found to be k = 0.45 m/s (rounded from 0.446 m/s to report the appropriate significant figures).

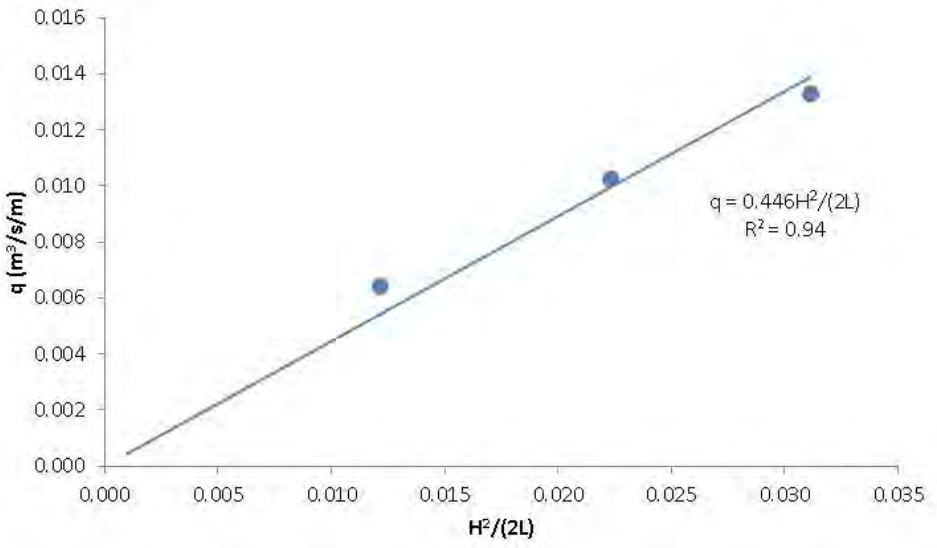

Figure 7. Average permeability k = 0.446 m/s from fitting experimental data.

Results for the unsteady state test are not reported here, but discussed below.

2.5 Discussion of Flume Test Results

The permeability of the rock during the three steady-state tests varied between 0.40 and 0.50 m/s, with an average value of 0.45 m/s (**Figure 7**). The permeability values apparently increased with decreasing water depth. As water depth became smaller than 0.1 m, permeability values became unrealistically high. It is believed that this was caused by water flowing through the larger voids between the flat flume bottom and the first layer of rocks. Although small cut-off walls (wood strips) were installed at the bottom to minimise this issue (**Figure 4**) it was not completely solved for small water depths, hence the unsteady flow results that were mainly measurements with small water depths were discarded. The measurements made under steady-state conditions have high water depths and are less sensitive to bottom flow effects.

The maximum instantaneous seepage unit discharges under tidal flow, computed by two-dimensional numerical modelling along the toe of the containment dyke (see **Section 3**) are shown in **Figure 10** as a function of dyke permeability. The highest seepage flow was found for k = 0.1 m/s. The permeability measured in the physical model is shown also in **Figure 10**. According to these preliminary measurements, the rock tested in the physical model would result in a maximum seepage flow of approximately q = 0.003 m^3/m/s if it were used to build the RBT2 containment dyke.

The final permeability of the causeway containment dyke could be slightly lower than that measured in the physical model because of a variety of factors:

- Incidental compaction of the dyke during construction may reduce its permeability;
- Similar to DP3, the dyke core material may use a finer gradation (**Figure 5**);
- Possible settling of fine sediment transported by tidal currents inside the voids of the rock; and
- The sandy foundation of the dyke and much higher water depths will be free from the bottom flow effects experienced in the physical model.

If the permeability of the containment dyke were in fact slightly smaller, approaching k = 0.1 m/s, it could lead to very high seepage flows according to **Figure 10**.

3 DYKE SEEPAGE FLOW

The pervious containment dyke will transmit water into the expansion area between the dyke and existing causeway during a rising tide, and allow this temporarily-stored water to seep out towards the tidal flats during a dropping tide. **Figure 8** shows a schematic diagram of the seepage flow through the pervious containment dyke during a dropping tide. At the completion of each section of dyke (CD1 and CD2), the area between the existing causeway and the containment dyke will be filled with sand, and therefore, will no longer represent a volume available for storage of seawater.

Water levels on the tidal flat (h_1) vary continuously with time following the tidal water levels and there will be periods of time when water levels in the expansion area (h_2) become larger than those on the tidal flat ($h_2 > h_1$). When this occurs, seepage flow (q) from the expansion area will discharge onto the tidal flat. When the tidal flat becomes dry ($h_1 \approx 0$), seepage flows onto the tidal flat could generate bed shear stresses high enough to erode the bed and cause erosion channels, as was observed during the construction of DP3 (Hemmera et al. 2008).

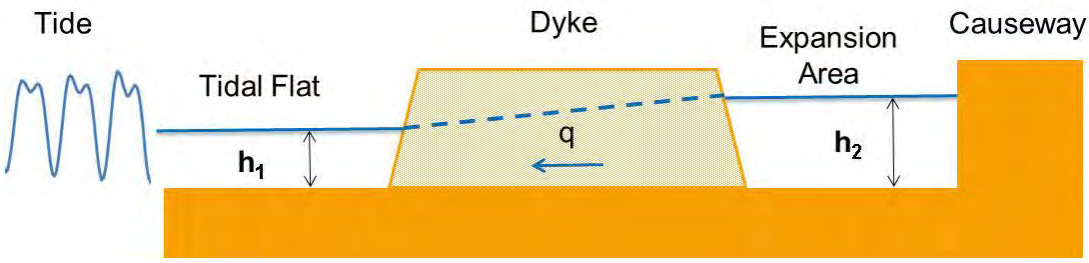

Figure 8. Schematic of seepage flow through containment dyke and onto tidal flat.

Flow through the containment dyke will occur at varying rates and at different times along the length of the dyke. **Figure 9** shows a typical tide cycle with large swings between high and low tides as well as a longitudinal profile along the seaward toe of the dyke. The location of the dyke is shown in **Figure 3**, which also illustrates that the tidal flats slope laterally away from the causeway as well as having an overall slope to seaward.

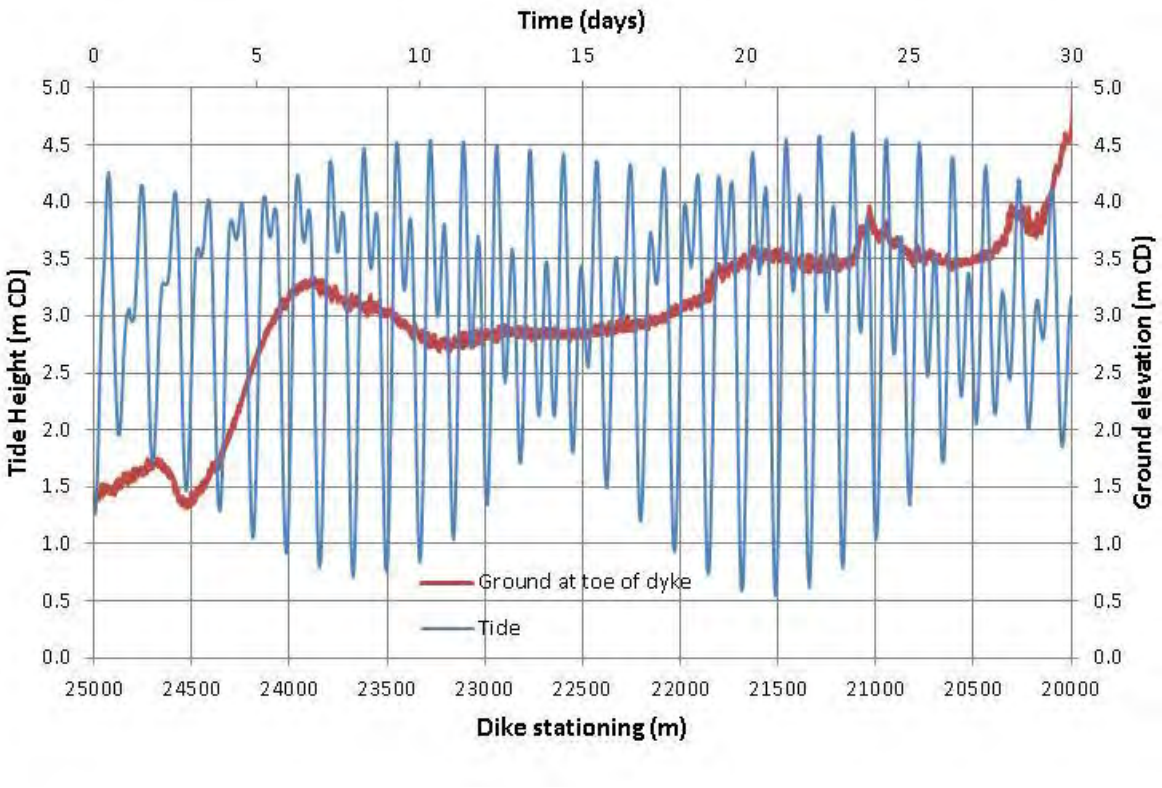

Figure 9. Typical tide levels and longitudinal bed profile along seaward toe of containment dyke.

Water levels (h_2 and h_1) change continuously in both space and time due to tidal forcing, the influence of local topography, as well as the dyke's geometry and permeable properties. Because the dyke alignment is mainly perpendicular to the tidal direction, water levels and hence seepage flows would exhibit strong spatial variability along its length, added to the temporal variability of the tides. This leads to complex interactions of the surface flow on the tidal flat and causeway expansion area with the seepage flow through the dyke core. This problem is considered unique and a methodology to deal with it is not readily available in the technical literature. Hence, the following general approach was used to quantify the discharge of water through the dyke:

1. Apply a depth-averaged two-dimensional (2D) surface/ground-water flow model to compute water levels at both sides of the dyke (h_2 and h_1) during a typical 15-day tidal period. The 2D model output includes hourly water levels along the dyke every 100 m apart; and

2. Use the water levels predicted by the 2-D model to compute the time series (hydrograph) of seepage discharges over time q(t) draining onto the tidal flat.

When computing groundwater, River2D assumes a constant hydraulic transmissivity T [m^2/s] everywhere, which is an approach better suited for confined aquifers of constant depth. Because the dyke behaves more like an unconfined aquifer with varying water levels, using permeability K [m/s] is probably more representative. The two parameters can be related by T = KH, where H [m] is the average water surface elevation (measured from zero datum). Based on the average tidal water levels it can be assumed that H ≈ 3.0 m, which provides an approximate conversion equation to estimate the corresponding permeability value K ≈ T/3. All the numerical computations of seepage flows were carried out using transmissivity, but are reported using the more familiar concept of permeability. This also allows comparing with the dyke's core permeability measured in the physical model (**Section 2**).

Figure 10 shows the maximum instantaneous seepage flow onto the tidal flat predicted by River2D for various transmissivity/permeability values of the dyke's core material. The permeability measured in the physical model (**Section 2**) for a 4" finer gravel, believed to be representative of the future dyke's core material, was found to be approximately K = 0.45 ± 0.05 m/s for a head difference (h_2 - h_1) between 0.24 and 0.38 m. For such a range of measured permeability values, maximum seepage flows were estimated to be roughly 54 ± 6% of those predicted for a permeability K = 0.23 m/s (T = 0.64 m^2/s) and lying between 0.003 and 0.004 $m^3/s/m$.

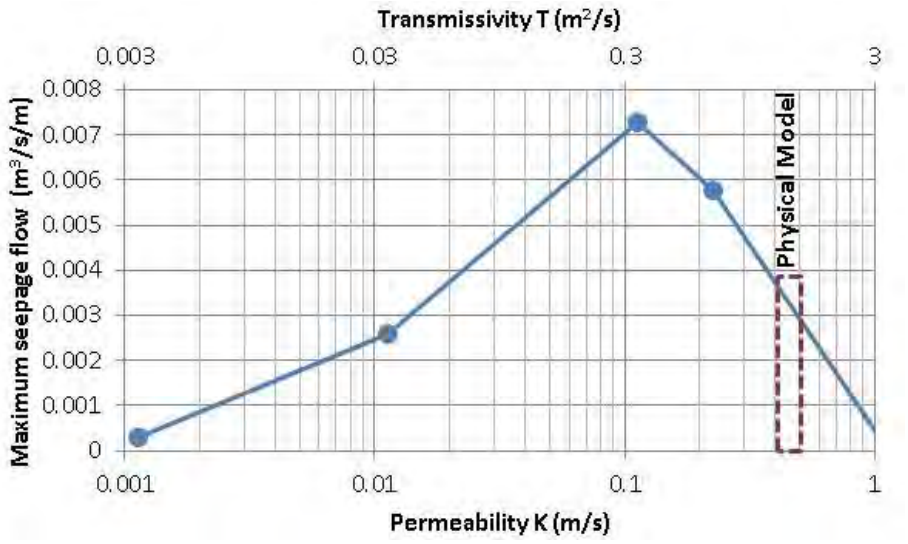

Figure 10. Maximum instantaneous seepage flow computed by River2D for entire dyke and permeability measured in physical model.

Water levels predicted by River2D for K = 0.23 m/s were used to compute the hourly seepage hydrographs every 100 m along the dyke whenever there was a positive water head gradient towards the tidal flat ($h_2 > h_1$) and the expansion area contained surface water ($h_2 > 0$). These hydrographs were scaled down by a factor of 0.54 to represent the expected discharges for K = 0.45 m/s.

4 TIDAL FLAT EROSION

4.1 CRITICAL BED SHEAR STRESS ON THE TIDAL FLAT

Erosion of the tidal flat is expected when flows high enough to produce significant sediment transport occur for sufficiently long periods of time to induce the formation of erosion channels. Experience from DP3 construction demonstrates that such conditions are easily met when seepage flow from a containment dyke drains into a dry tidal flat (**Figure 2**). The precise prediction of scour is very difficult, but it is highly dependent on the bed shear stress generated by the flow.

Although the overall seaward slope of the tidal flats (the direction parallel to the causeway) is very gentle, the bed slope measured in the direction perpendicular to the causeway is about one order of magnitude steeper. Seepage flow from the dyke will flow mainly along this steeper slope. Relevant features of the tidal flat adjacent to the containment dyke are summarised in **Table 1**.

Table 1. Relevant features of the tidal flat adjacent to the containment dyke.

Feature	Abbreviation	Value	Units
Average bed slope	S	0.004	m/km
Grain size diameter	D	0.1	mm
Critical shear stress	τ_{cr}	0.12	Pa

The assumed critical shear stress for initiation of grain motion shown in **Table 1** is for loose sand with D = 0.1 mm (Julien 1995) and ignores the potential cohesive effects of biofilm or the presence of a clay fraction in the sediment mixture.

Shear stress, τ, caused by the flow of water with density, ρ, of depth, h, and with a slope, S, can be represented by **Equation 2**.

$$\tau = \rho g h S$$

Equation 2. Shear stress relation.

Rearranging **Equation 2** to solve for the water depth to move the sand grains as: $h = \tau/\rho g S$ = (0.12)/(9.8x1000x0.004) = 0.003 m = 3 mm. The corresponding flow velocity is in the order of V = 0.1 m/s[2]. The critical discharge per unit length of dyke (unit discharge) that would need to seep through the dyke in order to reach that flow velocity and depth is:

$$q_{cr} = Vh = (0.1 \text{ m/s})(0.003 \text{ m}) = 0.0003 \text{ m}^3\text{/s/m} = 0.3 \text{ L/s/m}$$

[2] Assuming roughness height k_s = 0.3 mm and Darcy-Weisbach friction factor f = 0.08 (because flow is not fully turbulent, Manning's or Chezy's equations are not applicable).

This simple analysis indicates that if a seepage discharge of 0.3 litres/second or larger seeps through one metre of dyke length, it would be able to move and erode the fine sand on the tidal flat. Since such a discharge is not particularly high, scouring of the tidal flat seems very likely. The analysis assumes that a uniform sheet of flow 3 mm deep will develop over an ideal flat bed. In reality, since the bed is not flat, flow will concentrate along deeper paths, incising small channels and further increasing the shear stress and the erosion potential. Prior experience of this effect during the construction of DP3 indicates that concentration of flow occurs very rapidly and that individual channels coalesce to form larger channels within several metres of the toe of the dyke (**Figure 2**).

However, even if sediment starts moving, sediment transport rates can be too low to produce significant scour. It could be argued that areas of the tidal flat that at present do not exhibit visible scour could be used to provide guidance to assess the potential for scour. **Figure 11** and **Figure 12** show the statistical distribution of shear stress computed by the Strait of Georgia Telemac-3D numerical model for the existing conditions and the future conditions (with the Project) respectively, for 2012. The 90% percentile bed shear in the plot represents values that were only exceeded 10% of the time in 2012 and are probably the most representative for scour prediction. The numerical results show that under existing conditions (**Figure 11**), the area where the proposed dyke will be located experiences shear stress values up to 0.27 Pa without evidence of significant scour. The Project does not seem to increase those values in the area of concern (**Figure 12**). Therefore, it could be argued that shear stresses higher than 0.3 Pa are needed for significant scour to occur.

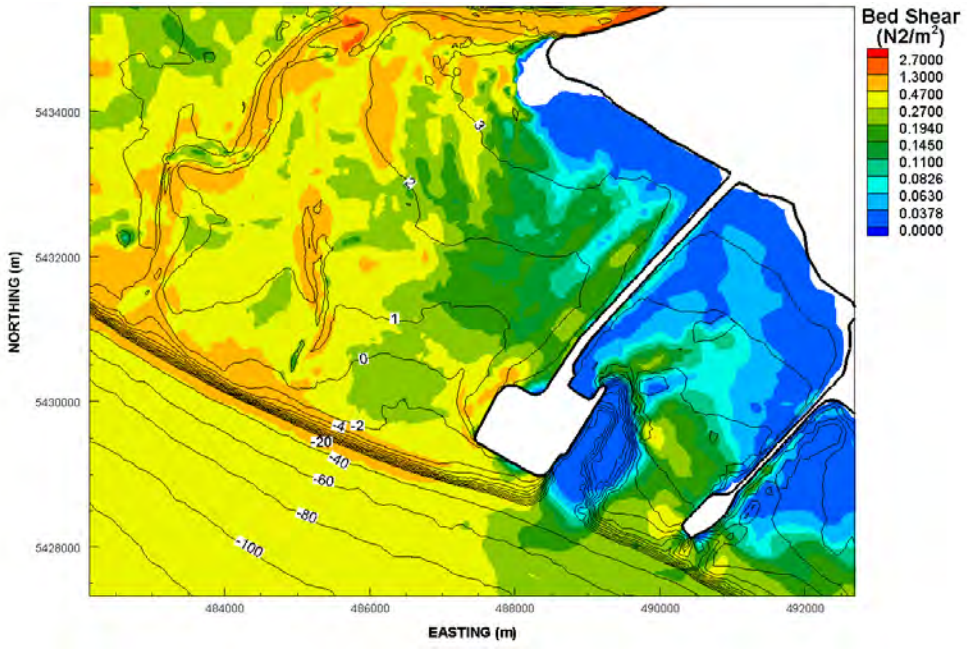

Figure 11. Distribution of the 90th percentile bed shear stress on the tidal flat predicted for the existing conditions for the year 2012.

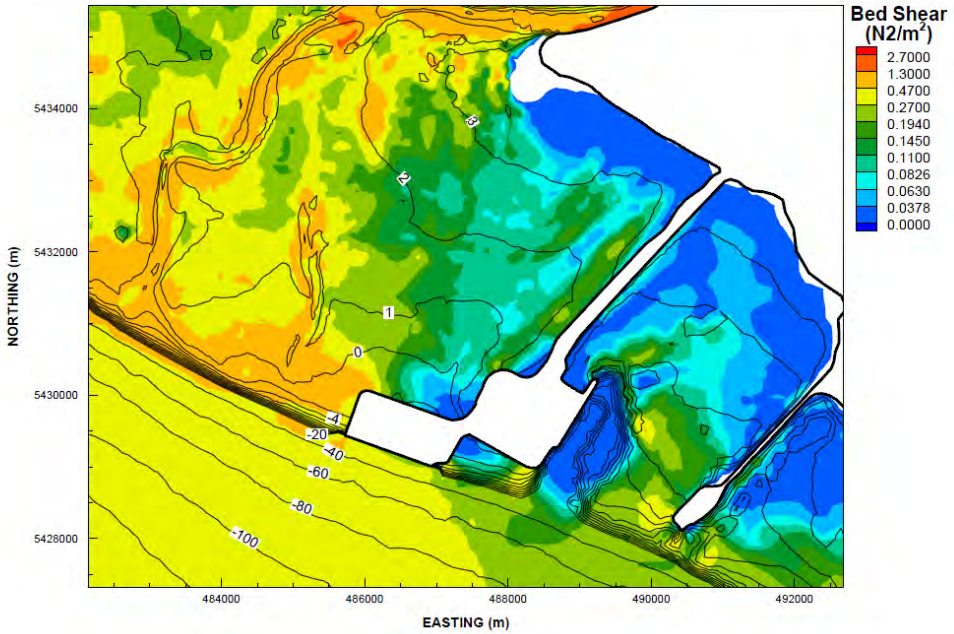

Figure 12. Distribution of the 90th percentile bed shear stress on the tidal flat predicted for the future (with Project) condition for the year 2012.

Figure 13 shows the predicted relationship between bed shear stress and seepage flow through the dyke draining on to the dry tidal flat (the bed slope is 4 m/km). Plotted in the figure are the values of seepage flow needed to both initiate incipient sediment motion and exceed 0.3 Pa, compared with the expected seepage flow for K = 0.45 m/s (**Figure 10**) which would generate shear stresses in the order of 0.4 to 0.5 Pa. Even if the tidal flat were stable at 0.3 Pa, as suggested from **Figure 12**, the expected seepage flows will exceed that value likely leading to bed scour. Another way to look at potential scour is by estimating the corresponding sediment transport rates.

For reference, **Figure 13** also shows the dimensionless sediment transport rate computed using the Engelund-Hansen equation. In relative terms, it shows that an increase in shear stress from 0.12 Pa to 0.3 Pa increases sediment transport 20 times, and increasing shear stress further to 0.5 Pa will increase transport rates 80 times. All these analyses consider sheet surface flow over a perfectly flat bed, once scour channels form and coalesce, both shear stress and sediment transport rates will increase. Although very approximate, the previous estimates seem to corroborate the observation from DP3 (Hemmera et al. 2008).

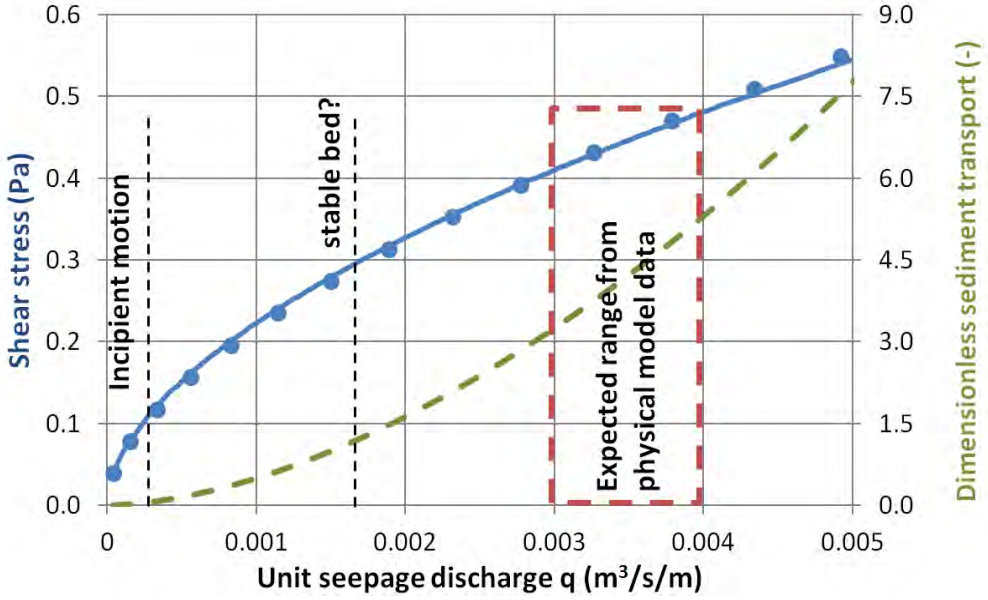

Figure 13. Changes in shear stress and sediment transport on tidal flat as a function of unit seepage discharge through containment dyke.

4.2 ESTIMATING POTENTIAL EROSION EXTENTS FROM SEEPAGE FLOWS

A simple methodology is applied to estimate the potential extents of erosion on the tidal flats from seepage flows where the following conditions must occur to cause erosion:

i. tidal recession has exposed the sediments at the seaward toe of the containment dyke (condition T2 or T3 in **Figure 14**; and

ii. seepage flow from the dyke is greater than 0.0018 m^3/s/m (based on **Figure 13**).

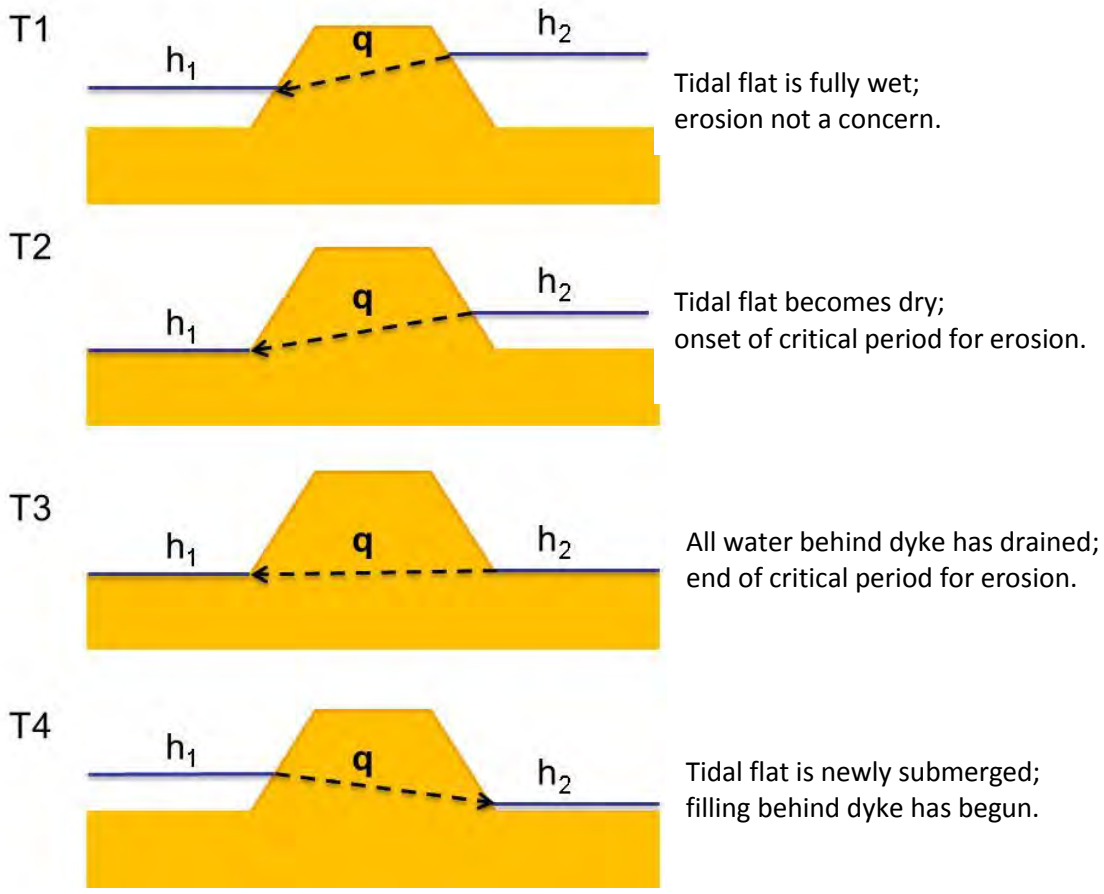

Figure 14. Changes in water levels and seepage flow during a partial tide cycle.

In general, the tidal flat elevation recedes seawards in elevation by 0.004 m/m from the toe of the dyke. Tide height can thus be converted to a lateral distance of tidal flat exposure. When conditions i. and ii. (above) are both met, the difference in elevation of the toe of the dyke to the level of the tide is projected across the tidal flat to provide the extent (i.e., length) of impact of the seepage flow (**Figure 15**). This extent can be converted to tidal flat area by averaging the calculated extents at each of the seepage flow locations which are spaced 100 m apart.

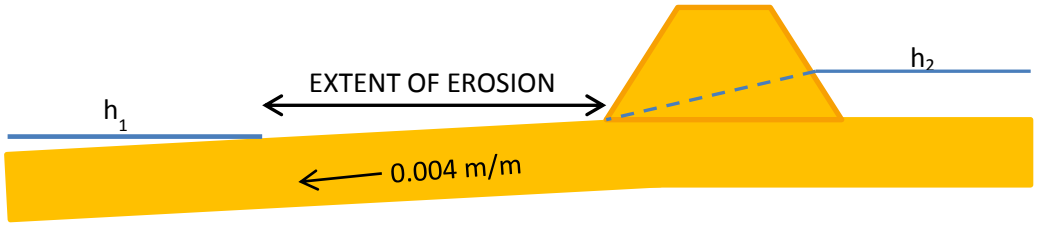

Figure 15. Estimating potential erosion extents from seepage flows.

Previous observations during DP3 construction show that erosion on the tidal flat from seepage flows occurs by concentrating into channels (**Figure 2**). Aerial photo imagery from 2007 corresponding to the immediate post-DP3 construction period, and recent Google Earth imagery were used to estimate the tidal flat area affected by erosion channels associated with DP3 construction. Tidal channels developed from the toe of the dyke and extended to the average low tide line. Of the zone that developed channels, approximately 19% of the surface area was occupied by the channels and associated deposition areas. A similar relative area of erosion channels is anticipated for the exposed tidal flat adjacent to dykes CD1 and CD2.

Based on the experience at DP3, the erosion channel will be active only until the expansion area between the dyke and the causeway is filled with sediment, at which point seepage flow is reduced to near zero. Unlike the inter-causeway area at DP3, the channels on the north side of the causeway will be temporary because over time, coastal processes will redistribute sediments and the channels will fill in. It is also possible that coastal processes will redistribute sediments periodically during the construction phase, but accounting for this is less conservative as it is not possible to reliably predict the occurrence of wind events that would generate sufficiently large waves within the relatively short time periods of CD1 and CD2 dyke construction.

The timing of unit seepage flow rates can be analysed at each station spaced 100 m along the causeway dyke to compare the critical flow rates with tide height and tidal flat exposure. The results are illustrated graphically in **Figure 16**, which shows the extent of channel formation during the CD1 and CD2 construction periods. Assuming that 19% of the area between the toe of the dyke and the red line in **Figure 16** is occupied by channels and associated deposition zones, the total area of temporary disturbance can be estimated as 14.5 ha for dyke CD1 and 8.5 ha for dyke CD2.

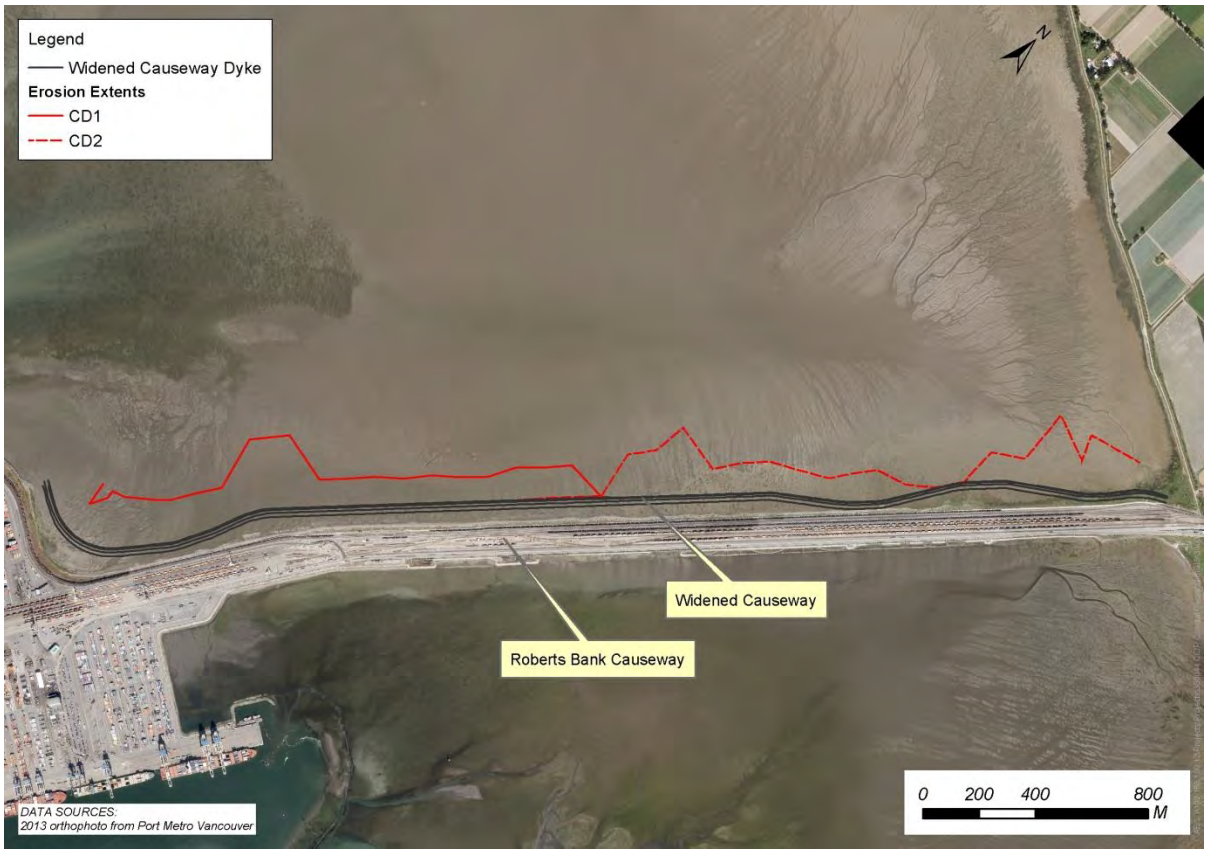

Figure 16. Estimated lateral extents of erosion and channel formation due to unmitigated seepage flows from dykes CD1 and CD2.

5 REFERENCES

Casagrande, A. 1937. Seepage through dams. Journal of the New England Water Works Association 51:131–172.

Fetter, C. W. 2001. Applied Hydrogeology. Fourth Edition. Prentice Hall, New Jersey.

Hemmera, NHC, and Precision. 2008. Deltaport Third Berth Adaptive Management Strategy 2007 Annual Report. Report prepared by Hemmera Envirochem Inc., Northwest Hydraulics Consultants and Precision Identification for Port Metro Vancouver, Vancouver, BC.

Julien, P. Y. 1995. Erosion and Sedimentation. Cambridge, Cambridge.

Steffler, P., and J. Blackburn. 2002. Two-Dimensional Depth Averaged Model of River Hydrodynamics and Fish Habitat: Introduction to Depth Averaged Modelling and User's Manual. University of Alberta.

APPENDIX 9.5-B

Rationale for Exclusion of Other Certain and Reasonably Foreseeable Projects in the Cumulative Change Assessment of Coastal Geomorphology

This page is intentionally left blank

Appendix 9.5-B Rationale for Exclusion of Other Certain and Reasonably Foreseeable Projects in the Cumulative Change Assessment of Coastal Geomorphology

The assessment included consideration of an interaction between predicted Project-related changes to coastal geomorphology and similar changes potentially resulting from other certain and reasonably foreseeable projects and activities. The rationale for exclusion of each certain and reasonably foreseeable project and activity identified in **Table 8-8 Project and Activity Inclusion List**, from the assessment of cumulative change for coastal geomorphology is presented in **Table 9.5-B**.

Table 9.5-B Rationale for Exclusion of Other Certain and Reasonably Foreseeable Projects in the Cumulative Change Assessment of Coastal Geomorphology

Other Certain and Reasonably Foreseeable Project or Activity	Rationale for Exclusion
Project	
BURNCO Aggregate Project, Gibsons, B.C.	No potential for cumulative interaction due to distant location from Roberts Bank.
Centerm Terminal Expansion, Vancouver, B.C.	No potential for cumulative interaction due to distant location from Roberts Bank.
Fraser Surrey Docks Direct Coal Transfer Facility, Surrey, B.C.	No potential for cumulative interaction due to distant location from Roberts Bank.
Gateway Pacific Terminal at Cherry Point and associated BNSF Railway Company Rail Facilities Project, Blaine, Washington	No potential for cumulative interaction due to distant location from Roberts Bank.
Gateway Program – North Fraser Perimeter Road Project, Coquitlam, B.C.	Not relevant to this IC assessment due to land-based nature of project.
George Massey Tunnel Replacement Project, Richmond and Delta, B.C.	Project is potentially relevant to this IC through the potential release of sandy sediments during construction from removal of existing tunnel or changes to riverbed morphology and sediment re-distribution. Due to the preliminary stage of this project, publicly available information is limited, but it is assumed that mitigation will be implemented to minimise potential downstream effects. Although this project may cause a short-term release of sediments, they are not expected to be entrained on Roberts Bank, and therefore a cumulative interaction is not anticipated.
Kinder Morgan Pipeline Expansion Project, Strathcona County, Alberta to Burnaby, B.C.	No potential for cumulative interaction due to distant location from Roberts Bank.

Other Certain and Reasonably Foreseeable Project or Activity	Rationale for Exclusion
Lehigh Hanson Aggregate Facility, Richmond, B.C.	Project relevant to this IC through potential sedimentation effects during berthing infrastructure construction; however, any change from this project is likely to be negligible (unmeasurable) relative to RBT2 scale of influence at Roberts Bank.
Lions Gate Wastewater Treatment Plant Project, District of North Vancouver, B.C.	No potential for cumulative interaction due to distant location from Roberts Bank.
North Shore Trade Area Project – Western Lower Level Route Extension, West Vancouver, B.C.	Not relevant to this IC assessment due to land-based nature of project.
Pattullo Bridge Replacement Project, New Westminster and Surrey, B.C.	Not relevant to this IC assessment due to the fact that this is primarily a land-based project and the project is distant from Roberts Bank
Southlands Development, Delta, B.C.	Not relevant to this IC assessment due to land-based nature of project.
Vancouver Airport Fuel Delivery Project, Richmond, B.C.	Potentially relevant to this IC, but any influence or change to the physical environment from this project is likely to be negligible (unmeasurable) relative to the RBT2 scale of influence at Roberts Bank.
Woodfibre LNG Project, Squamish, B.C.	No potential for cumulative interaction due to distant location from Roberts Bank.
Activity	
Incremental Road Traffic Associated with RBT2	Not relevant to this IC assessment due to land-based nature of activity.
Incremental Rail Traffic Associated with RBT2	Not relevant to this IC assessment due to land-based nature of activity.
Incremental Marine Vessel Traffic Associated with RBT2	Potentially relevant to this marine IC, but changes to the physical environment from vessel transiting and berthing activities are not anticipated.